Experimental Models of Demonstration Pit Lakes: Evaluating Long-Term Effects on Water Quality, Biogeochemical Processes, and Metagenomic Profiles in Oil Sands Tailings

by

Akeem Olawale Bello

A thesis submitted in partial fulfillment of the requirements for the degree of

Doctor of Philosophy

in

Environmental Science

Department of Civil and Environmental Engineering
University of Alberta

ABSTRACT

Bitumen extraction from oil sands reserves in northern Alberta, Canada, has already disturbed large expanse of land and created huge volume of tailings as wastes. The pore water of a tailing contains high concentrations of dissolved organic and inorganic compounds that adversely affect living organisms because of their toxicity upon exposure. Tailings comprises sand, silt, clay, unrecovered bitumen, and oil sands process-affected water (OSPW) and are temporarily being stored in settling basins known as tailing ponds in compliance with the zero-effluent discharge policy in Alberta. To this end, Permanent Aquatic Storage Structure (PASS) technology has been deployed to enhance the dewatering of tailings in demonstration pit lakes (DPL) by adding a coagulant (alum) and a flocculant (polyacrylamide, PAM). It is yet to be understood, however, how these additions would impact the capping water quality and whether their dissociation could affect nutrient biogeochemical cycling leading to unwanted emissions of gases. Therefore, changes in water quality with regards to dissolved organics and polymer additives were investigated along with biogeochemical processes and the likely genes.

DPL models (75.4L) containing 22.6L of tailings and capped with 45.2L of lake water were established to investigate the fate of dissolved organics and polymer additives during long term storage of tailings in DPL under different oxygen conditions (oxic vs anoxic). Tailings settling resulted in 13.8 ± 0.14 cm of consolidation under oxic condition compared to 16.4 ± 0.71 cm under anoxic condition. Considerable flux of dissolved organics from the underlying tailings into the capping water was observed, resulting in an increase in the concentration of dissolved organic carbon, DOC in oxic and anoxic conditions by 5 – 37% and 19 – 72% respectively. Advective flux of DOC decreased gradually, ranging from 0.52 $g/m^2/d$ to 0.11 $g/m^2/d$ under oxic condition and from 0.65 $g/m^2/d$ to 0.13 $g/m^2/d$ under anoxic condition. Residual polymer additives present in the

PASS-treated tailings were initially released into the capping water, with concentrations ranging from 1.13 mg/L in oxic conditions and 0.845 mg/L in anoxic conditions, before being slowly biodegraded over time to 0.123 mg/L in oxic conditions and 0.085 mg/L in anoxic conditions.

To study if the addition of alum and PAM as PASS tailings treatment strategy affects microbial community structures and natural biogeochemical cycles leading to unwanted changes in water quality over time, smaller systems (20.4L) containing 6.7L of tailings and capped with 13.4L of lake water were established. One set of columns, termed treatment groups, were subjected to different temperature regimes of 5 °C, 20 °C, 25 °C, and 8 °C each lasting 2 months. The other set of columns, termed control groups, were operated at constant temperature of 22 °C. Tailings settling resulted in the release of porewater followed by increased DOC, chemical oxygen demand, and naphthenic acids and a decrease in turbidity. Temperature variations significantly affected dissolved oxygen and conductivity but did not alter microbial communities significantly, which were dominated by organisms involved in sulfur, carbon, nitrogen, and iron cycling. Analysis of biogas in headspace revealed that methane was not produced, but production of hydrogen sulfide was evident. Likely, sulfate reduction inhibited methanogenesis in model pit lakes.

Finally, metagenomic analyses were conducted to investigate the microbial biogeochemical cycling in the 20.4L DPL models. Results revealed that bacterial communities dominated the model pit lake columns, with significant variations in abundance and composition between tailings and capping water. Biogeochemical cycling of carbon, sulfur, and nitrogen was prominent in both tailings and capping water. Carbon cycling accounted for 52-60%, sulfur cycling for 16-19%, and nitrogen cycling for 24-28% across all columns. Functional gene analysis further predicted genes for essential processes of nutrient cycling. The most prevalent processes were Wood-Ljungdahl Pathway and methanotrophy for carbon cycling, sulfite reduction and thiosulfate

oxidation for sulfur cycling and, denitrification and dissimilatory nitrate reduction to ammonium for nitrogen cycling. Temperature variations did not affect nutrient cycling in tailings and capping water and there were no significant differences observed in the overall processes between the tailings and capping water indicating microbial resilience.

In summary, this dissertation demonstrates that PASS treatment technology has the potential to promote the development of DPL into a self-sustaining ecosystem with resilient microbial communities and functional biogeochemical cycling while minimizing unwanted gas production.

PREFACE

The research presented in this thesis is an original work designed, planned, performed, and interpreted by me under the supervision of Dr. Mohamed Gamal El-Din. I conducted most of the experiments, data analysis, and preparation of the manuscripts. Some researchers in Dr. Gamal El-Din's Research Group also contributed to sample analysis and edition of manuscripts and were therefore co-authors of the manuscripts submitted and/or prepared for submission for publication. Contributions to each chapter are detailed as follows:

Chapter 2 will be submitted to Water Research as "Foroogh Mehravaran, Akeem O. Bello, Muhammad Arslan, Xiaoying Fan, and Mohamed Gamal El-Din. Demonstration Pit Lake Research & Monitoring Program for Evaluating the Permanent Aquatic Storage Structure Technology (PASS) & Closure Management for Generating a Self-Sustaining Ecosystem". Foroogh Mehravaran and I carried out the experiment, sample analysis, data analysis and manuscript write up. Dr. Muhammad Arslan contributed to supervision, research planning, training, manuscript review and editing. Dr. Xiaoying Fan contributed to sample provision and manuscript review. Dr. Mohamed Gamal El-Din contributed to the supervision, review and approval of the manuscript, and funding acquisition.

Chapter 3 has been submitted to ACS Sustainable Resource Management as "Akeem O. Bello, Muhammad Arslan, Xiaoying Fan, and Mohamed Gamal El-Din. Biogeochemical Processes in Oil Sands Tailings and Capping Water: Permanent Aquatic Closure at Demonstration Pit Lake". Dr. Muhammad Arslan contributed to supervision, training, bioinformatic analysis, manuscript review and editing. Dr. Xiaoying Fan contributed to sample provision and manuscript review. Dr. Mohamed Gamal El-Din contributed to the supervision, review and approval of the manuscript, and funding acquisition.

Chapter 4 will be submitted to Environmental Microbiology as “Akeem O. Bello; Muhammad Arslan, Jochen A. Muller, and Mohamed Gamal El-Din. Metagenomic elucidation of microbial biogeochemical cycling in a model oil sands tailings pit lake system”. Dr. Muhammad Arslan contributed to supervision, bioinformatic analysis, manuscript review and editing. Dr. Jochen A. Muller contributed to supervision, training, and manuscript review. Dr. Mohamed Gamal El-Din contributed to the supervision, review and approval of the manuscript, and funding acquisition.

DEDICATION

To my lovely wife who has always believed in me. Thank you for your unwavering love, support and understanding.

To my wonderful children, you were the reason I could continue to work harder.

To my family and friends, thank you for bearing with me. Your understanding and support went a long way.

To my beloved parents, whose love and prayers kept me going.

To Allah Almighty, for the gift of life.

ACKNOWLEDGEMENTS

I would like to first express my gratitude to my supervisor, Dr. Mohamed Gamal El-Din, for his guidance, supervision, and financial support. I really appreciate the wonderful opportunity provided by Dr. Gamal El-Din, allowing me to work collaboratively with both local and international researchers and gain a valuable experience in the field of wastewater treatment. The structure of his research group enabled easy access to practical experimental knowledge and research advancement.

My immeasurable gratitude goes to the program manager in Dr. Gamal El-Din's research group, Dr. Pamela Chelme-Ayala, for her unbelievable support and encouragement at every stage of my research. Her unwavering dedication and willingness to help every student regardless of their trouble was an inspiration to me.

I would like to thank Dr. Muhammad Arslan for his contribution towards my research. He was always available to answer all my questions. His understanding on microbial ecology and bioremediation techniques was an inspired me greatly. He opened my eyes to the field of bioinformatics and data science. I am forever thankful for his help. The assistance of Dr. Ahmed Mohamed during plotting of variations in microbial communities is highly appreciated.

My profound thanks go to Dr. Jochen A. Muller for his supervision while I was Karlsruhe Institute of Technology, Institute for Biological Interfaces 5 (IBG 5), Germany under the sponsorship of Mitacs Globalink Research. I also appreciate the efforts of Dr. Anne-Kristin Kaster, Director of IBG-5 and members of IBG-5 such as Jasmin Kubetzki, David Thiele, Nico Mühling, Julia Münch, Sagarika Chakraborty, Maximiano Cassal, Drs. Islam Khattab, Gunnar Sturm, Mohammad Mojarrad, Habibu Aliyu, Florian Lenk, and John Vollmers for making my research stay in the center worthwhile.

My gratitude also goes to the postdoctoral fellows and colleagues in Dr. Gamal El-Din's research group for their help when needed. I sincerely appreciate the efforts of Dr. Soliu Ganiyu, Dr. Monsuru Suara, Dr. Yaqub Jomaa and Dr. Foroogh Mehravaran. My appreciation also goes to the laboratory technicians of the department of Civil and Environmental Science for their technical support.

I would like to acknowledge the financial support of the University of Alberta's Future Energy Systems research initiative, supported by the Canada First Research Excellence Fund, the Natural Sciences and Engineering Research Council of Canada (NSERC) Senior Industrial Research Chair (IRC) in Oil Sands Tailings Water Treatment.

Finally, I would like to express my sincere appreciation to my family and friends for their unwavering love and support throughout my academic journey.

Table of Contents

Contents

ABSTRACT ii

PREFACE v

DEDICATION vii

ACKNOWLEDGEMENTS viii

Table of Contents x

List of figures xiv

List of tables xviii

List of Abbreviation xix

CHAPTER 1 INTRODUCTION AND RESEARCH OBJECTIVES 1

1.1 Background 1

1.1.1 Alberta Oil sands 1

1.1.2 Permanent Aquatic Storage Structure (PASS) Treatment 2

1.1.3 Biogeochemical Processes During Long-Term Tailings Management and PASS-Treated Tailings 4

1.1.4 Laboratory-scale EPLs 6

1.2 Research Scope and Objectives 6

1.3 Hypotheses 8

1.4 Thesis organization 9

1.5 References 10

CHAPTER 2 EMPLOYING PERMANENT AQUATIC STORAGE STRUCTURE TECHNOLOGY TO REDUCE DISSOLVED ORGANICS TRANSPORT FROM TAILINGS DEPOSITS TO CAP WATER: DEMONSTRATION PIT LAKE 13

2.1 Introduction 13

2.2 Materials and Methods 15
2.2.1 Characterization of capping water samples and oil sands tailings 15
2.2.2 Set up of laboratory DPL 17
2.2.3 Assessment of dewatering and consolidation behavior of PASS-treated tailings 19
2.2.4 Assessment of gas production potential 20
2.2.5 Physicochemical analysis 21
2.2.6 Mass flux calculation 21
2.3 Results and discussion 24
2.3.1 Settling and consolidation behavior of PASS-treated tailings 24
2.3.2 Fate of dissolved organics 26
2.3.3 Fate of polymer additives 31
2.3.4 Gas production 33
2.4 Conclusion 34
2.5 References 34
CHAPTER 3 BIOGEOCHEMICAL PROCESSES IN OIL SANDS TAILINGS AND CAPPING WATER AT DEMONSTRATION PIT LAKE 37
3.1 Introduction 37
3.2 Materials and Methods 40
3.2.1 Bench-scale column setup and operation 40
3.2.2 Physico-chemical parameters 41
3.2.3 Biogenic gas analyses 42
3.2.4 Microbial Community Analyses 42
3.3 Results 44
3.3.1 Physicochemical characteristics and measurement of biogenic gases 44
3.3.2 Background bacterial community composition 48

3.3.3 Bacterial diversity of PASS-treated pit lake 51
3.3.4 Temporal/temperature changes on biogeochemical cycles of pit lakes containing PASS-treated tailings 51
3.3.4.1 Sulfur cycling 51
3.3.4.2 Carbon cycling 54
3.3.4.3 Iron cycling 57
3.3.4.4 Nitrogen cycling 59
3.3.5 Patterns of temporal changes in bacterial community structures 62
3.3.6 Active bacterial communities 67

3.4 Discussion 69
3.4.1 Changes in physicochemical properties of capping water 69
3.4.2 Diversity of bacterial communities in PASS-treated pit lakes 72
3.4.3 Temporal changes on biogeochemical cycles of PASS-treated pit lakes 73
3.4.3.1 Sulfur cycling 73
3.4.3.2 Carbon cycling 75
3.4.3.3 Iron cycling 77
3.4.3.4 Nitrogen cycling 78
3.4.4 Patterns of temporal changes in overall bacterial community structures 80
3.3.5 Implications for pit lake ecosystem stability and sustainability 81
3.5 Conclusion 83
3.6 References 84
CHAPTER 4 METAGENOMIC ELUCIDATION OF MICROBIAL BIOGEOCHEMICAL CYCLING IN A MODEL OIL SANDS TAILINGS PIT LAKE SYSTEM 95
4.1 Introduction 95
4.2 Materials and Methods 97

4.2.1 Oil sands model pit lake samples 97
4.2.2 DNA extraction and Library preparation 98
4.2.3 Metagenome analysis 98
4.2.4 Biogeochemical cycling analysis 99
4.3 Results 100
4.3.1 Sequencing, de novo assembly, and bins generation 100
4.3.2 Taxonomic estimation of metagenome-assembled genomes in model pit lakes 100
4.3.3 Processes/mechanisms of biogeochemical cycling in model pit lakes 106
4.3.4 Functional genes for biogeochemical cycling in model pit lakes 111
4.3.4.1 Carbon cycle 112
4.3.4.2 Sulfur cycle 116
4.3.4.3 Nitrogen cycle 118
4.4 Discussion 121
4.4.1 Microbial diversity in model pit lakes 121
4.4.2 Biogeochemical cycling in model pit lakes: processes and functional genes 123
4.5 Corroborating 16S rRNA amplicon sequencing with metagenomic sequencing 127
4.6 Conclusions 128
4.7 References 128
CHAPTER 5 GENERAL CONCLUSIONS AND RECOMMENDATIONS 137
5.1 Thesis overview 137
5.2 Conclusions 139
5.3 Recommendations 141
BIBLIOGRAPHY 143
APPENDIX 164

List of figures

Figure 2.1: Aerial view of Lake Miwasin showing DPL location 15

Figure 2.2**: (A)** Pit lake model **(B)** Lake Miwasin DO profile 2020 (C) DO profile under oxic condition (D) DO profile under anoxic condition..... 18

Figure 2.3: Batch Settling test of tailings showing consolidation of tailings over 3 months 19

Figure 2.4: Serum bottle experiment showing tailings and capping water incubated at 25°C 20

Figure 2.5: (A) Settling rate in oxic columns (B) Settling rate in anoxic columns (C) comparison of settling rate in oxic, anoxic and batch columns to observe the effect of water capping on natural settling on PASS-treated tailings..... 25

Figure 2.6: Changes in concentrations of (A) COD in oxic and anoxic columns, (B) DOC in oxic and anoxic columns, (C) AEF in oxic and anoxic columns and (D) NAs in oxic and anoxic columns. Different letters indicate "significant difference" while same letters indicate "no significant difference" at $\alpha = 0.05$. COD = chemical oxygen demand; DOC = dissolved organic carbon; AEF = acid extractable fractions; NAs = naphthenic acids 27

Figure 2.7: (A) Fate of dissolved organics in Oxic condition (B) Fate of dissolved organics in Anoxic condition..... 29

Figure 2.8: (A) Mass flux of DOC in Oxic condition (B) Mass flux of DOC in Anoxic condition (C) Mass flux of NAs in Oxic condition (D) Mass flux of NAs in Anoxic condition..... 30

Figure 2.9: Changes in concentrations of (A) PAM over a 2-year period in, (B) AMD over an 18-month period, (C) TKN over a 2-year period, and (D) Ammonia over a 2-year period in oxic and anoxic columns. Different letters indicate "significant difference" while same letters indicate "no significant difference" at $\alpha = 0.05$. PAM = polyacrylamide; AMD = acrylamide; TKN = total kjeldahl nitrogen; NH_3 = ammonia..... 32

Figure 3.1: Laboratory experimental set up showing the column dimension and arrangement of sampling ports 40
Figure 3.2: Lake Miwasin Temperature Profiles: 2019 & 2020 indicating different temperatures observed at certain depths and months 41
Figure 3.3: Off-gas production during the experimental period. Methane was not detected 48
Figure 3.4: Krona plot for taxonomic abundance of (A) top of capping water, (B) bottom of capping water, (C) top of tailings, and (D) bottom of tailings 50
Figure 3.5: Alpha diversity between (A) tailings and capping water (B) treatment and control groups of capping water (C) treatment and control groups of tailings and Principal coordinate analysis (PCoA) illustrating similarities between (A) tailings and capping water (B) treatment and control groups of capping water (C) treatment and control groups of tailings 52
Figure 3.6: Top 10 microbial communities involved in sulfur cycling in (A) Capping water of treatment groups (B) Capping water of control groups (C) Tailings of treatment groups (D) Tailings of control groups 54
Figure 3.7: Top 10 microbial communities involved in carbon cycling in (A) Capping water of treatment groups (B) Capping water of control groups (C) Tailings of treatment groups (D) Tailings of control groups 56
Figure 3.8: Top 10 microbial communities involved in iron cycling in (A) Capping water of treatment groups (B) Capping water of control groups (C) Tailings of treatment groups (D) Tailings of control groups 59
Figure 3.9: Top 10 microbial communities involved in nitrogen cycling in (A) Capping water of treatment groups (B) Capping water of control groups (C) Tailings of treatment groups (D) Tailings of control groups 61

Figure 3.10: Top sulfur-cycling genera with distinct correlation in capping water and tailings .. 63
Figure 3.11: Top carbon-cycling genera with distinct correlation in capping water and tailings. 64
Figure 3.12: Top iron-cycling genera with distinct correlation in capping water and tailings 65
Figure 3.13: Top nitrogen-cycling genera with distinct correlation in capping water and tailings 66
Figure 3.14: Heatmap showing the top active bacterial communities (RNA). CB = control bottom; CT = control top; TB = treatment bottom; TT = treatment top; _WS = winter start; _WE = winter end; _SP = spring; _SU =summer; _F = fall 68
Figure 3.15: Temporal changes in physico-chemical parameters in (A) treatment, and (B) control. DOC: dissolved organic carbon, COD: chemical oxygen demand, TKN: total Kjeldahl nitrogen, DO: dissolved oxygen, NTU: Nephelometric Turbidity Units, NO2+NO3-N: nitrite and nitrate-nitrogen, NAs: naphthenic acids 72
Figure 3.16: Schematic diagram of biogeochemical cycles in pit lake containing PASS-treated tailings showing (A) Sulfur cycling in treatment columns (B) Sulfur cycling in control columns 75
Figure 3.17: Schematic diagram of biogeochemical cycles in pit lake containing PASS-treated tailings showing (A) Carbon cycling in treatment columns (B) Carbon cycling in control columns 77
Figure 3.18: Schematic diagram of biogeochemical cycles in pit lake containing PASS-treated tailings showing (A) Iron cycling in treatment columns (B) Iron cycling in control columns..... 78
Figure 3.19: Schematic diagram of biogeochemical cycles in pit lake containing PASS-treated tailings showing (A) Nitrogen cycling in treatment columns (B) Nitrogen cycling in control columns 80

Figure 4.1: Principal coordinate analysis of model pit lakes 102

Figure 4.2: Taxonomy of tailings and capping water in temperature-constant and temperature-modified columns at (A) domain level and (B) phylum level. Taxonomy was estimated with Anvi'o anvi-estimate-scg-taxonomy 104

Figure 4.3: Heatmap of the most abundant bacteria genera in model pit lake systems 105

Figure 4.4: Krona plot of nutrient cycling processes in TC 107

Figure 4.5: Krona plot of nutrient cycling processes in TT 108

Figure 4.6: Krona plot of nutrient cycling processes in WC 109

Figure 4.7: Krona plot of nutrient cycling processes in WT 110

Figure 4.8: (A) Carbon cycling processes and functional genes. A = methanotrophy; B = Wood-Ljungdahl pathway; C = Serine pathway (B) Sulfur cycling processes and functional genes. A = thiosulfate oxidation; B = sulfate reduction; C = sulfite reduction; D = sulfite oxidation; E = sulfide oxidation; F = sulfur reduction; G = thiosulfate reduction (C) Nitrogen cycling processes and functional genes 125

Figure A1: (A) Fate of PAM in Oxic columns (B) Mass flux of PAM in Oxic columns (C) Fate of PAM in Anoxic columns (D) Mass flux of PAM in Anoxic columns. PAM = polyacrylamide… 177

Figure A2: Rarefraction curve comparing species richness in tailings against capping water ... 178

Figure A3: Rarefraction curve comparing species richness in control columns against treatment columns 179

Figure A4: FastQC plot showing adapter content before trimming with Trimmomatic and fastp 180

Figure A5: FastQC plot showing adapter content after trimming with Trimmomatic and fastp 181

List of tables

Table 2.1: Initial concentrations of capping water and tailings (mean ± standard deviation) 16

Table 2.2: Mass Flux calculations of DOC in oxic condition 23

Table 2.3: Mass Flux calculations of DOC in anoxic condition 23

Table 2.4: concentrations of selected parameters in the porewater of PASS-treated tailings 28

Table 3.1: Summary statistics and Mann-Whitney U test results for physicochemical parameters of treatment and control columns (means ± standard deviation) 45

Table 3.2**:** Two-way ANOVA summary of selected parameters 46

Table 4.1: Nutrient cycling processes predicted in model pit lakes 111

Table 4.2: Functional genes for carbon cycling and their percent expression in model pit lakes 114

Table 4.3: Functional genes for sulfur cycling and their percent expression in model pit lakes .117

Table 4.4: Functional genes for nitrogen cycling and their percent expression in model pit lakes 119

Table A1: Average of microbial abundance for sulfur biogeochemical cycling over the experimental period 164

Table A2: Average of microbial abundance for carbon biogeochemical cycling over the experimental period 167

Table A3: Average of microbial abundance for iron biogeochemical cycling over the experimental period 169

Table A4: Average of microbial abundance for nitrogen biogeochemical cycling over the experimental period 171

Table A5: Concentrations of elements in capping water and tailings 173

Table A6: CheckM2 bin quality report 174

List of Abbreviation

AEF	Acid Extractable Fraction
AMD	Acrylamide
Anammox	Anaerobic ammonium oxidation
ANOVA	Analysis of Variance
ANR	Assimilatory Nitrate Reduction
BLASTN	Basic Local Alignment Search Tool for Nucleotides
BML	Base Mine Lake
CBB	Calvin-Benson-Bassham cycle
COD	Chemical Oxygen Demand
CONCOCT	Clustering cONtigs with COverage and ComposiTion
COPCs	Contaminants of Potential Concerns
COSIA	Canada's Oil Sands Innovation Alliance
CPR	Candidate Phyla Radiation
DO	Dissolved Oxygen
DOC	Dissolved Organic Carbon
DNA	DeoxyriboNucleic Acid
DNRA	Dissimilatory Nitrate Reduction to Ammonium
DPL	Demonstrated Pit Lake
EPLs	End Pit Lakes
FASP	Formaldehyde Assimilation - Serine Pathway
FFT	Fluid Fine Tailings
FT-IR	Fourier Transform Infrared Spectroscopy

GC-TCD	Gas Chromatography-Thermal Conductivity Detector
GTDB	Genome Taxonomy DataBase
HGT	Horizontal Gene Transfer
HMMs	Hidden Markov Models
HPLC	High Performance Liquid Chromatography
IBC totes	Intermediate Bulk Containers
ICP-MS	Inductively Coupled Plasma-Optical Emission Spectrometry
IBG	Institute of Bio- and Geosciences
IC	Ion Chromatography
KEGG	Kyoto Encyclopedia of Genes and Genomes
KIT	Karlsruhe Institute of Technology
MAGs	Metagenome-Assembled Genomes
NADH	Nicotinamide Adenine Dinucleotide
NADPH	Nicotinamide Adenine Dinucleotide Phosphate
NAs	Naphthenic Acids
NCBI	National Center for Biotechnology Information
ORFs	Open Reading Frames
OSPW	Oil Sands Process Water
OTUs	Operational Taxonomic Units
PAM	Polyacrylamide
PASS	Permanent Aquatic Storage Structure
PCoA	Principal Coordinate Analysis
PERMANOVA	PERmutational Multivariate ANalysis Of VAriance

PPP	Pentose Phosphate Pathway
QIIME	Quantitative Insights Into Microbial Ecology
RNA	RiboNucleic Acid
SOB	Sulfur-Oxidizing Bacteria
SRB	Sulfate-Reducing Bacteria
TC	Tailings-Control
TCA	TriCarboxylic Acid cycle
TKN	Total Kjeldahl Nitrogen
TN	Total Nitrogen
TOC	Total Organic Carbon
TT	Tailings-Treatment
UBA	Uncultivated Bacteria and Archaea
UPL	Upper Pit Lake
UPLC-TOF-MS	Ultra-Performance Liquid Chromatography Time-Of-Flight Mass Spectrometry
VOCs	Volatile Organic Compounds
WC	Water-Control
WT	Water-Treatment
XRD	X-Ray Diffraction

CHAPTER 1 INTRODUCTION AND RESEARCH OBJECTIVES

1.1 Background

1.1.1 Alberta Oil sands

The Alberta oil sands, located in the northeastern part of the Canadian province of Alberta, contain one of the largest reserves of bitumen in the world. Bitumen, a highly viscous form of petroleum, is extracted through surface mining and in-situ techniques (Natural Resources Canada, 2022). As of 2020, Alberta's oil sands production had reached 3 million barrels per day, with projections to potentially double within the next decade (Alberta Energy Regulator, 2020). This industry has driven significant industrial growth and job creation, contributing substantially to the local and national economy. However, the environmental and health implications of bitumen extraction are a growing concern. The process consumes substantial water resources, with estimates indicating that up to 4.4 barrels of water are required to produce a single barrel of oil. Additionally, the industry generates large volumes of tailings, a byproduct of bitumen extraction that includes toxic substances like naphthenic acids and petroleum hydrocarbons. The release of pollutants during extraction can have toxic impacts on local ecosystems and human populations. For instance, elevated levels of heavy metals and hydrocarbons have been detected in nearby water bodies, posing risks to aquatic life, and potentially affecting human health (The Royal Society of Canada, 2010).

Balancing the economic benefits of bitumen extraction with the need for environmental protection and sustainability is essential for the future of Alberta's oil sands industry. In this regard, tailings management is crucial and challenging as they retain a high-water content and exhibit low shear strength, complicating their stabilization and reclamation. As of recent reports, Alberta's oil

sands industry has accumulated over 1.3 billion cubic meters of FFT, stored in expansive tailings ponds that cover approximately 220 square kilometers (Kuznetsov et al., 2023). These ponds pose significant environmental risks, including the potential for contamination of surface and groundwater with toxic substances such as naphthenic acids, heavy metals, and hydrocarbons (Allen, 2008). Alberta's oil sands industry is actively pursuing various tailings management and reclamation strategies to address the environmental challenges posed by tailings. Two prominent approaches are end pit lakes (EPLs) and capped soft deposits. EPLs are engineered water bodies formed by placing tailings in open pits, which are then covered with a layer of water. This method aims to create stable aquatic ecosystems over time. The primary objective of EPLs is to evolve into self-sustaining aquatic ecosystems that integrate with the surrounding landscape, receiving surface and groundwater inputs while discharging water downstream. Currently, there are plans for 23 EPLs in northern Alberta, with the aim of these becoming permanent fixtures in reclaimed-mine landscapes (Syncrude, 2019). A notable example is Base Mine Lake (BML), a full-scale demonstration EPL developed by Syncrude in 2012, which includes approximately 45 meters of FFT covered by 9 meters of water. The long-term geochemical stability and ecological viability of EPLs however remain under investigation (Siddique et al., 2012; Yu, 2019).

1.1.2 Permanent Aquatic Storage Structure (PASS) Treatment

The Permanent Aquatic Storage Structure (PASS) pretreatment of tailings is an innovative approach in Alberta's oil sands industry that aims to enhance the stability and environmental sustainability of tailings deposits. PASS involves treating tailings with coagulants, such as alum, and flocculants, like polyacrylamide (PAM), through in-line flocculation. This process enhances the settling and consolidation of fine tailings, resulting in a denser and more stable material suitable for deposition in decommissioned pits, facilitating long-term aquatic closure. The primary

objective of PASS is to create stable aquatic environments capable of supporting diverse ecosystems. By enhancing the physical properties of tailings, PASS reduces risks associated with traditional storage methods, such as fluid fine tailings (FFT) that have low shear strength and high water content, thereby minimizing the likelihood of resuspension (Alberta Energy Regulator, 2022).

Suncor Energy is leading the implementation of PASS, with notable projects including the commercial-scale Upper Pit Lake (UPL) and the Demonstration Pit Lake scale (DPL) also known as Lake Miwasin. These initiatives aim to showcase the feasibility and effectiveness of PASS in managing tailings while reducing environmental impacts (Environmental Defence, 2022). Suncor's PASS method involves treating tailings with potash alum and PAM to facilitate quicker dewatering and consolidation, which allows for the creation of more stable deposits. This not only aids in environmental management but also helps in reducing the area needed for tailings storage, thus mitigating land disturbance (Government of Alberta, 2024). For PASS treatment, 1200 ppm of alum ($KAl(SO_4)_2 \cdot 12H_2O$) was added alongside 1500 g/tonne clay of anionic PAM. Alum dissociates in water into into aluminum ions (Al^{3+}) and sulfate ions (SO_4^{2-}) as follows:

$$KAl(SO_4)_2 \cdot 12H_2O \longrightarrow K^+ + Al^{3+} + 2SO_4^{2-} + 12H_2O$$

Al^{3+} forms a series of polyvalent hydroxide complexes such as:

$$Al^{3+} + OH^- \rightleftharpoons Al(OH)^{2+}$$

$$7Al^{3+} + 17OH^- \rightleftharpoons Al_7(OH)_{17}^{4+}$$

$$13Al^{3+} + 34OH^- \rightleftharpoons Al_{13}(OH)_{34}^{5+}$$

These aluminum species adsorb to the surfaces of the suspended negative colloids, thereby destabilizing the colloidal particles and allowing them to aggregate together. Subsequently, PAM

forms bridges with the larger aggregates known as "flocs" until they become heavy enough to settle out of the water under the influence of gravity (Crittenden et al., 2012).

The implementation of PASS also addresses the long-term ecological impact by potentially transforming reclaimed tailings ponds into functional aquatic ecosystems. However, the Alberta Energy Regulator has emphasized the need for further research and demonstration projects to fully understand the long-term stability and ecological effects of PASS before it can be widely approved and implemented (Alberta Energy Regulator, 2022). The large-scale demonstration at Base Mine Lake (BML), established by Syncrude in 2013, serves as a crucial case study. BML covers approximately 800 hectares and includes around 45 meters of FFT topped with 9 meters of water, demonstrating the practical application of PASS on a large scale (Environmental Defence, 2022).

Despite its promise, PASS technology faces challenges and requires continuous monitoring and validation. Ensuring the safety and stability of these aquatic systems is paramount, especially considering concerns about their potential impact on local vegetation, fish, and wildlife. Additionally, gaining the acceptance of Indigenous communities, who rely on traditional land use, remains a significant consideration. The successful implementation of PASS as a standard tailing's management strategy will depend on addressing these ecological and social factors effectively.

1.1.3 Biogeochemical Processes During Long-Term Tailings Management and PASS-Treated Tailings

Long-term management of oil sands tailings involves complex biogeochemical processes that significantly impact their stability and environmental sustainability, with carbon and sulfur cycling playing critical roles. In the context of PASS-treated tailings, which use coagulants like alum and flocculants such as polyacrylamide (PAM), these cycles are particularly influential.

Sulfur cycling is a critical biogeochemical process in tailings management, especially in environments treated with alum. In the anoxic zones of tailings ponds, sulfate-reducing bacteria (SRB) utilize sulfate as an electron acceptor, producing hydrogen sulfide (H_2S) in the process (Warren et al., 2016). This H_2S can then react with ferrous iron to form insoluble iron sulfides (FeS), effectively immobilizing heavy metals and reducing their mobility in the environment (Siddique et al., 2019). However, the production of H_2S can pose long-term challenges for water quality and sustainability. H_2S can oxidize to form sulfuric acid (H_2SO_4), leading to acidification of the water, which can have detrimental effects on aquatic ecosystems and complicate tailings reclamation efforts (Siddique et al., 2014). The presence of alum in PASS-treated tailings influences sulfur cycling by modifying the chemical environment, thus promoting conditions favorable for SRB activity (Foght et al., 2017). While the precipitation of FeS aids in stabilizing tailings and reducing sulfate concentrations, which mitigates some environmental concerns, the potential for acid generation through H_2SO_4 formation must be carefully managed. Sulfuric acid production can lower the pH of water bodies, increasing the solubility of heavy metals and potentially leading to the release of toxic elements into the environment. This acidification process can impair water quality and pose significant risks to achieving long-term sustainability of reclaimed tailings ponds (Bordenave et al., 2010).

These biogeochemical processes underscore the importance of microbial activity in transforming and stabilizing tailings. The use of PASS technology may help improve the environmental performance of tailings deposits. However, continuous monitoring and research are essential to fully understand the long-term impacts of these processes and to optimize tailings management strategies for sustainability and ecological compatibility.

1.1.4 Laboratory-scale EPLs

EPLs are engineered water bodies formed in the pits left after mining and extraction activities and are often used as a permanent disposal method for tailings and other mine wastes. The effectiveness and sustainability of EPLs are typically assessed through laboratory-scale experiments (laboratory EPLs) and field studies (field EPLs) (COSIA, 2020). The differences between these two approaches can significantly impact the observed results and their implications for large-scale implementation. If planned properly, laboratory EPLs can provide empirical data to validate predictions made from numerical models and can refine models for future validation of field EPLs (McCullough and Vandenberg, 2020). Laboratory EPLs are usually limited by factors such as scale and complexity, environmental conditions, hydrological dynamics, ecological interactions, and time frame (COSIA, 2020; McCullough and Vandenberg, 2020; Syncrude, 2021). Laboratory EPLs provide a controlled environment for studying specific processes, offering insights that can inform the management and design of field EPLs. However, field EPLs, with their larger scale and environmental complexity, present a more accurate representation of real-world conditions. The differences between the two highlight the importance of using both approaches to understand and manage EPLs effectively. Laboratory studies help in hypothesis testing and mechanistic understanding, while field studies validate these findings in natural settings, ensuring the ecological sustainability and success of EPLs in long-term mine reclamation efforts (McCullough and Vandenberg, 2020).

1.2 Research Scope and Objectives

The overall objective of this research was to evaluate the effect of PASS technology on reclamation of oil sands tailings. To achieve this, two different sets of laboratory-based DPL

columns were established to answer specific questions related to tailings long-term reclamation efforts. These specific questions are presented below as three main objectives:

Objective 1: Assessment of the long-time impacts of PASS technology on the transport of dissolved organics and polymer additives under different oxygen conditions (oxic vs anoxic conditions), achieved by

- Characterizing the settling and consolidation of PASS-treated tailings over time.
- Monitoring capping water quality including the effect of dissolved oxygen differences on spatial and temporal variations and trajectories of dissolved organics and polymer additives over a two-year period.
- Characterizing the geochemical properties of PASS-treated tailings and assess the long-term impacts of PASS-treatment on the development of the lake ecosystem.
- Assessing the effect of PASS-treatment technology on the release of greenhouse gases such as carbon dioxide and methane and the possibility of generating other unwanted gases such as hydrogen sulfide.

Objective 2: Investigation of the effects of temperature on water quality parameters and underlying biogeochemical processes in PASS-treated DPL, achieved by

- Assessing the biogeochemical processes occurring in PASS-treated tailings and capping water in the presence of alum and PAM.
- Investigating the microbial communities involved in the biogeochemical cycling.
- Analyzing the effects of temperature changes on biogeochemical processes in tailing deposits and water column during long-term storage.

Objective 3: Metagenomic analysis of microbial biogeochemical cycling of PASS-treated DPL, achieved by:

- Recovering metagenome-assembled genomes (MAGs) from PASS-treated capping water and tailings.
- Predicting the functional genes and assessing the metabolic processes involved in biogeochemical cycling found in PASS-treated capping water and tailings.
- Estimating the effect of temperature variations on the predicted functional genes and metabolic processes.

1.3 Hypotheses

PASS technology was developed to enhance the dewatering of tailings. However, the addition of alum and PAM could create unique conditions within the pit lake ecosystem. Furthermore, temperature changes during seasonal transitions might also influence the behavior of alum and PAM. Understanding how PASS technology impacts the lake ecosystem is crucial for achieving a self-sustaining ecosystem. Therefore, this research focused on studying various aspects of PASS technology's effects on the pit lake ecosystem. The following hypotheses were tested against the research's objectives:

- Assessment of the long-time impacts of PASS technology on the transport of dissolved organics and polymer additives under different oxygen conditions

  Hypothesis: Dissolved oxygen levels significantly affect the spatial and temporal variations and trajectories of dissolved organics and polymer additives in the capping water.
- Investigation of the effects of temperature on water quality parameters and underlying biogeochemical processes in PASS-treated DPL

  Hypothesis 1: The addition of alum and PAM in PASS technology significantly influences the biogeochemical processes occurring within the ecosystem.

Hypothesis 2: Temperature changes affect the biogeochemical processes in PASS-treated tailings and capping water.

Hypothesis 3: There will be significant differences in microbial community compositions of PASS-treated tailings and capping water caused by temperature variations.

- Objective 3: Metagenomic analyses of microbial biogeochemical cycling of PASS-treated DPL

  Hypothesis 1: MAGs recovered from PASS-treated capping water and tailings will reveal distinct microbial communities.

  Hypothesis 2: The functional genes and metabolic processes will be reflective of their specific microenvironment.

  Hypothesis 3: Temperature variations will impact the abundance and activity of functional genes and metabolic processes.

1.4 Thesis organization

This thesis consists of five chapters, starting with introduction and ending with conclusion. Chapter 1 provides a general introduction including the research background, objectives, hypotheses, and research significance. Chapter 1 covers a brief review of Alberta oil sands, PASS technology and biogeochemical processes.

Chapter 2 focuses on the establishment of DPL models with initial characterizations of lake water and tailings. This was done to establish the baseline concentrations of selected water quality parameters before the lake water was used to cap the tailings. The settling behavior of tailings without capping water was then assessed for 3 months while tailings with capping water was assessed for 24 months. The gas production potential was later evaluated using 120-mL air-tight serum bottles.

Chapter 3 investigates the effects of seasonality and changes in temperature on lake water chemistry and microbial community structure using a 20.4L columns containing 6.7L of tailings and capped with 13.4L of lake water. The treatment groups were subjected to different temperature regimes representing winter (5 °C), spring (20 °C), summer (25 °C) and fall (8 °C) with each lasting a period of 2 months. The control groups were set up at laboratory temperature of 22 °C. The physicochemical parameters of both treatment and control groups were measured at the beginning of the experiment and at the end of each temperature regime. Furthermore, bacterial communities were analyzed in both tailings and lake water for treatment and control groups.

Chapter 4 focuses on the metagenomic analysis of the tailings and capping water samples previously obtained from Chapter 3. Libraries were prepared for paired-end sequencing on an Illumina NexSeq 550. Raw sequence data obtained were quality-checked and low-quality reads and adaptor sequences removed before they were co-assembled into contigs. The contigs were later reconstructed into MAGs before being analyzed for biogeochemical cycling.

Chapter 5 summarizes the major findings and conclusions of the thesis. Furthermore, recommendations for future work that arise from this thesis are also outlined in this chapter.

1.5 References

Alberta Energy Regulator, 2022. Tailings [WWW Document]. Provid. Inf. URL https://www.aer.ca/providing-information/by-topic/tailings (accessed 11.20.23).

Alberta Energy Regulator, 2020. ST98 Alberta Energy Outlook, Alberta Energy Regulator.

Allen, E.W., 2008. Process water treatment in Canada's oil sands industry: I. Target pollutants and treatment objectives. J. Environ. Eng. Sci. 7, 123–138. https://doi.org/10.1139/S07-038

Bordenave, S., Kostenko, V., Dutkoski, M., Grigoryan, A., Martinuzzi, R.J., Voordouw, G., 2010.

Relation between the activity of anaerobic microbial populations in oil sands tailings ponds and the sedimentation of tailings. Chemosphere 81, 663–668. https://doi.org/10.1016/j.chemosphere.2010.07.058

Canada's Oil Sands Innovation Alliance (COSIA), 2020. 2019 Water Mining Research Report. https://cosia.ca/sites/default/files/attachments/COSIA_2019_Mining Research Summary Report_Final.pdf

Crittenden, J.C., Trussell, R., Hand, D., Howe, J.K., Tchobanoglous, G., 2012. MWH's Water Treatment: Principles and Design, Third. ed. John Wiley & Sons, Inc., Hoboken, New Jersey.

Environmental Defence, 2022. 50 Years of Sprawling Tailings.

Foght, J.M., Gieg, L.M., Siddique, T., 2017. The microbiology of oil sands tailings: Past, present, future. FEMS Microbiol. Ecol. 93, 1–22. https://doi.org/10.1093/femsec/fix034

Government of Alberta, 2024. Oil sands tailings and mine water.

Kuznetsov, P., Wei, K., Kuznetsova, A., Foght, J., Ulrich, A., Siddique, T., 2023. Anaerobic Microbial Activity May Affect Development and Sustainability of End-Pit Lakes: A Laboratory Study of Biogeochemical Aspects of Oil Sands Mine Tailings. ACS ES T Water 3, 1039–1049. https://doi.org/10.1021/acsestwater.2c00505

McCullough, C.D., Vandenberg, J., 2020. Studying Mine Pit Lake Systems Across Multiple Scales. Mine Water Environ. 39, 173–194. https://doi.org/10.1007/s10230-020-00678-7

Natural Resources Canada, 2022. Energy Fact Book 2022–2023, Natural Resources Canada.

Siddique, T., Kuznetsov, P., Kuznetsova, A., Arkell, N., Young, R., Li, C., Guigard, S., Underwood, E., Foght, J.M., 2014. Microbially-accelerated consolidation of oil sands tailings. Pathway I: Changes in porewater chemistry. Front. Microbiol. 5, 1–11.

https://doi.org/10.3389/fmicb.2014.00106

Siddique, T., Penner, T., Klassen, J., Nesbø, C., Foght, J.M., 2012. Microbial communities involved in methane production from hydrocarbons in oil sands tailings. Environ. Sci. Technol. 46, 9802–9810. https://doi.org/10.1021/es302202c

Siddique, T., Stasik, S., Shahimin, M.F.M., Wendt-Potthoff, K., 2019. Microbial Communities in Oil Sands Tailings: Their Implications in Biogeochemical Processes and Tailings Management, Microbial Communities Utilizing Hydrocarbons and Lipids: Members, Metagenomics and Ecophysiology. Springer Nature Switzerland AG 2019. https://doi.org/10.1007/978-3-030-14785-3

Syncrude, 2019. Base Mine Lake Monitoring and Research Summary Report: Results from 2013-2018

Syncrude, 2021. 2021 Pit Lake Monitoring and Research Report (Base Mine Lake Demonstration Summary: 2012-2020)

The Royal Society of Canada, 2010. The Royal Society of Canada Expert Panel: Environmental and Health Impacts of Canada's Oil Sands Industry: Report, The Royal Society of Canada.

Warren, L.A., Kendra, K.E., Brady, A.L., Slater, G.F., 2016. Sulfur Biogeochemistry of an Oil Sands Composite Tailings Deposit. Front. Microbiol. 6, 1–14. https://doi.org/10.3389/fmicb.2015.01533

Yu, X., 2019. Improving cap water quality in an oil sands end pit lake with microbial applications. University of Alberta.

CHAPTER 2 EMPLOYING PERMANENT AQUATIC STORAGE STRUCTURE TECHNOLOGY TO REDUCE DISSOLVED ORGANICS TRANSPORT FROM TAILINGS DEPOSITS TO CAP WATER: DEMONSTRATION PIT LAKE

2.1 Introduction

Extracting bitumen from naturally occurring oil sands by open-pit oil sands mining generates tailings wastes. The volume of tailings generated varies depending on a number of factors such as the quality of the oil sands, and the processes and technologies used during bitumen extraction (Alberta Energy Regulator, 2022). More than 1.3 billion cubic meters of tailings have been stored in temporary storage known as tailings ponds (Cossey et al., 2021; White and Liber, 2020). One method of permanent reclamation of tailings that has been proposed by oil sands operators is the creation of end-pit lakes (EPL), which are projected to develop into self-sustaining aquatic ecosystems (White and Liber, 2020).

EPL is formed by placing untreated or treated tailings in a mined-out pit, which is then covered with a mixture of oil sands process water (OSPW) and freshwater (Syncrude, 2019). EPL has been used globally by mining industries. However, the first full-scale EPL for oil sands industry was base mine lake (BML), which was established in December 2012. BML contained 1.16 billion barrels of untreated tailings covered with 365 million barrels of freshwater and OSPW covering a total area of 8 km^2 (COSIA, 2021; Syncrude Canada Ltd., 2019; White and Liber, 2020). Several studies have been carried out to assess the performance of BML. The results of these studies showed that the capping water quality improved over time, however, movement of organic and inorganic constituents from tailings into the capping water also occurred (Cossey et al., 2021;

Syncrude, 2019). Furthermore, methane cycling was prominent, increasing rapidly with depth over the upper 1 m to 3 m of tailings (Albakistani et al., 2022; Syncrude, 2019). In Canada, Alberta and Saskatchewan provinces account for about 70% of methane emissions from the oil and gas sector, primarily from the production and processing of crude oil and natural gas. Recently, Government of Canada has established the national regulations to reduce methane emissions from the oil and gas sector by 40-45% by 2025 (Government of Canada, 2018). Therefore, efforts to reduce methane production from EPL is of paramount importance.

Lake Miwasin is a demonstration pit lake (DPL) that was established in 2016 and uses the new Permanent Aquatic Storage Structure (PASS) treatment technology for tailings. PASS technology uses an inline treatment process where coagulant (alum) and flocculant (polyacrylamide, PAM) are added to accelerate the natural attenuation of pollutants over time (COSIA, 2021). The addition of alum and PAM is expected to help the settling of suspended fine particles, thereby enhancing consolidation (Alberta Energy Regulator, 2022). However, the effect of PASS-treatment on transport of dissolved organics from the underlying tailings as well as the effect on the overall capping water quality requires further investigation.

In this research therefore, a laboratory DPL was established to:

- Characterize the geochemical properties of PASS-treated tailings and assess the long-term impacts of PASS-treatment on the development of the lake ecosystem.
- Monitor capping water quality including spatial and temporal variations and trajectories of dissolved organics and polymer additives over a two-year period.
- Assess the effect of PASS-treatment technology on the release of greenhouse gases such as carbon dioxide and methane and the possibility of generating other unwanted gases such as hydrogen sulfide.

2.2 Materials and Methods

2.2.1 Characterization of capping water samples and oil sands tailings

The capping water and oil sands tailings used in this study were obtained from Lake Miwasin pit lake operated by Suncor Energy Ltd., Alberta, Canada (coordinates: 476543 E, 6304902 N) (Figure 2.1) and shipped to University of Alberta using separate 275-gallon IBC totes for capping water and tailings. The samples were later transferred to the laboratory, where they were used to set up laboratory-based pit lake models.

Figure 2.1: Aerial view of Lake Miwasin showing DPL location

The capping water was made up of 43% lake water and 57% oil sands process water (OSPW). Initial characterizations of lake water were carried out to establish the baseline of selected water quality parameters and monitor changes in water chemistry over time. Concentration of dissolved organics was determined by measuring chemical oxygen demand (COD), dissolved organic carbon (DOC), acid extractable fractions (AEF), and naphthenic acids (NAs), while polymer additives were measured through polyacrylamide (PAM), acrylamide

(ADM), ammonia, and total Kjeldahl nitrogen (TKN). The pH and conductivity of the capping water were also recorded. Additionally, the initial characterization of PASS-treated tailings was conducted by determining its composition, mineral content, organic matter, and organic carbon content (Table 2.1).

Table 2.1: Initial concentrations of capping water and tailings (mean ± standard deviation)

Parameter	**Value**
Capping water	
COD (mg/L)	98.05 ± *0.35*
DOC (mg/L)	38.305 ± *0.219*
AEF (mg/L)	23.135 ± *1.843*
NAs (mg/L)	2.71 ± *0.04*
PAM (mg/L)	< 0.1
Acrylamide (mg/L)	0.14 ± *0.01*
Ammonia (mg/L)	< 0.1
TKN (mg/L)	2.785 ± *0.417*
pH	8.12 ± *0.05*
Tailings	
Tailings composition (wt%):	
Fine solids	47.32 ± 0.24
Water	52.21 ± 0.28
Bitumen	0.47 ± 0.16
Mineral composition (wt%) ± 2.6:	
Quartz	47.7
Kaolinite	29.9
Muscovite	15.6
Microcline	5.7
Natural mineral form of TiO_2	1.2
Organic matter (wt%)	12.66 ± 0.78
Organic carbon (wt%):	
Total organic carbon	8.1 ± 0.4
Dissolved organic carbon	1.15 ± 0.20

2.2.2 Set up of laboratory DPL

Pit lake models were established to mimic the conditions of Lake Miwasin and were operated for a period of two years to investigate the performance of PASS treatment technology. To this end, eight vertical columns of 2.4 m height, 0.2 m in diameter, and having sample ports at 0.2 m intervals were filled with one-part tailings and two-part capping water to form tailings to capping water of ratio 1:2 (Figure 2.2A). Efforts were made to establish oxygen gradient representing oxic and anoxic conditions in each column, however, the DO profile reported for Lake Miwasin ranged between 10 mg/L to 0 mg/L (Figure 2.2B), which was difficult to be generated within the columns. Hence, six columns were operated under oxic conditions ranging from 9 mg/L to 6 mg/L (Figure 2.2C) while the remaining two columns were maintained under anoxic conditions ranging from 1 mg/L to 0 mg/L (Figure 2.2D). For oxic columns, pure oxygen was added at the top of the capping water using a stone aerator to establish the DO gradient (top: 10 mg/L, middle: 8mg/L, bottom: 6 mg/L); while for anoxic columns, nitrogen gas was added at the bottom of the water section using similar stone aerator to keep the DO of the whole water below 1.0 mg/L. Apart from DO measurement and optimization, conductivity and ORP were measured on a weekly basis. Water samples were taken from the top, middle, and bottom of the oxic columns, and from the middle of the anoxic columns at regular intervals for analysis of physicochemical parameters such as chemical oxygen demand (COD), dissolved organic carbon (DOC), acid extractable fractions (AEF), naphthenic acids (NAs), polyacrylamide, acrylamide, TKN, ammonia, and toxicity.

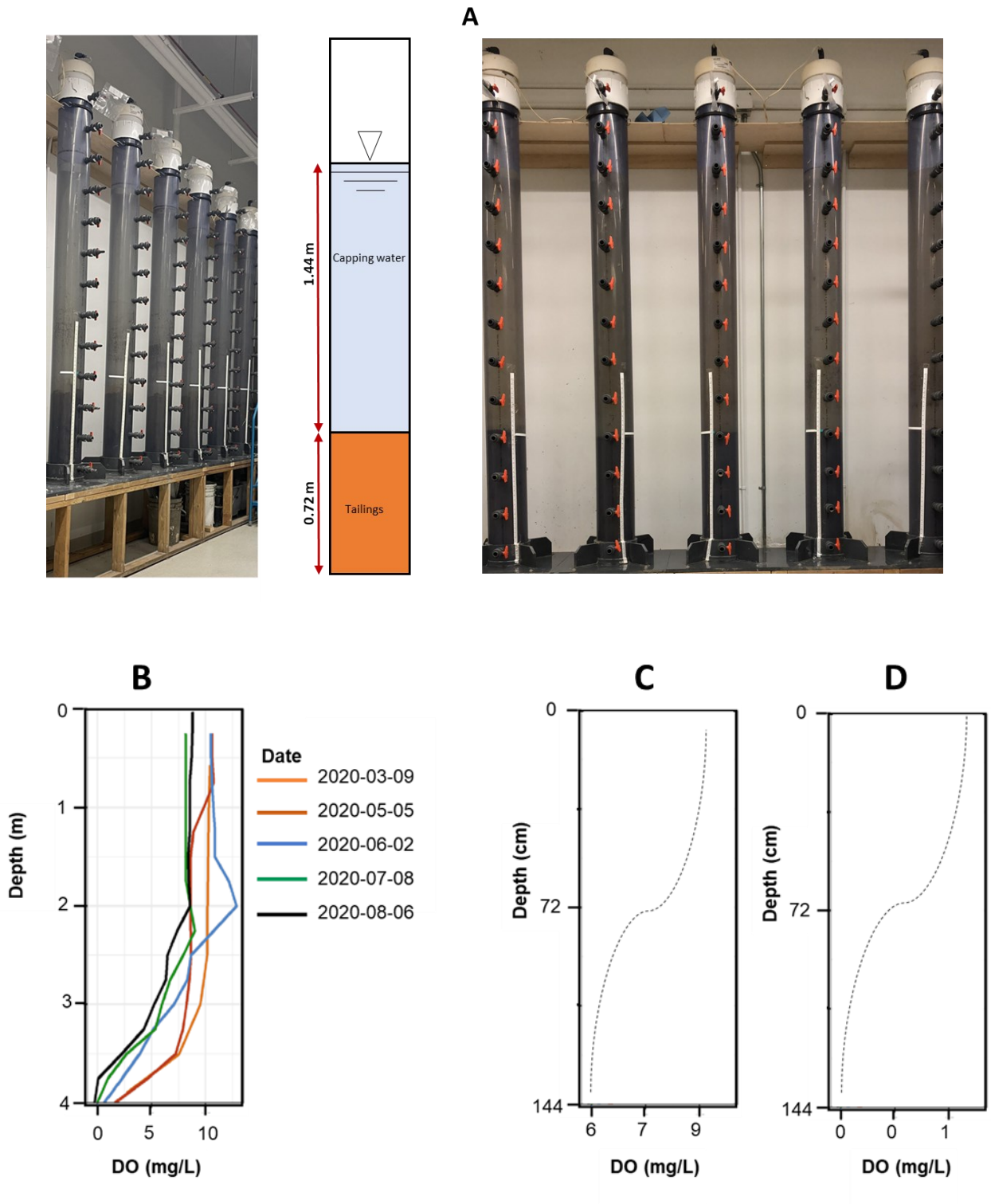

Figure 2.2**: (A)** Pit lake model **(B)** Lake Miwasin DO profile 2020 (C) DO profile under oxic condition (D) DO profile under anoxic condition

2.2.3 Assessment of dewatering and consolidation behavior of PASS-treated tailings

The settling behavior of tailings was assessed for 3 months using batch experiment with columns having internal diameters of 3.5 inches and 7.0 inches. Briefly, graduated cylinders were filled with tailings, covered up and allowed to naturally settle. The position of the consolidated tailings on the graduated cylinders was then measured and recorded at different time intervals to determine the settling rate (Figure 2.3). At the end of the batch settling experiment, pore water was expressed out of the PASS-treated tailings due to tailings self-weight consolidation. This pore water was collected and analyzed for selected parameters. Furthermore, the settling behavior of the laboratory DPL under the influence of capping water was observed and recorded over time for comparison.

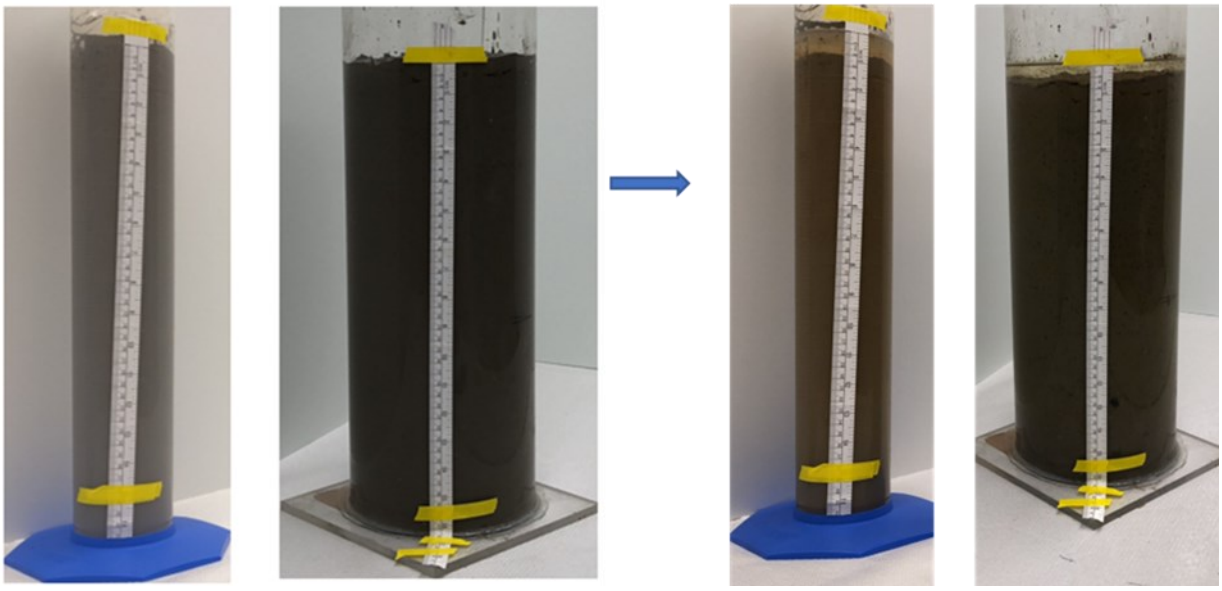

Figure 2.3: Batch Settling test of tailings showing consolidation of tailings over 3 months

2.2.4 Assessment of gas production potential

The gas production of the laboratory columns was initially assessed using air bags attached to the topmost sample ports of the columns. However, due to the likelihood of the gas production being affected by the weekly optimization and sampling, the gas production potential was further evaluated using air-tight serum bottles. In each bottle, 30 mL of tailings and 60 mL of capping water were combined, maintaining a 1:2 ratio, and leaving adequate headspace for gas collection. The bottles were left untouched and incubated at 25°C over a period of 10 weeks (Figure 2.4). The bottles were divided into two groups, one group representing oxic condition (without nitrogen gas added) and the other group simulating anoxic conditions (with nitrogen gas added). Gas was collected from the headspace in the serum bottles using a 0.5 mL syringe and manually introduced into Agilent 7890B Gas Chromatography-Thermal Conductivity Detector (GC-TCD) instrument. The samples were re-analyzed with the GC after 2 months to confirm if there was any change in gas production. The hydrogen sulfide production was measured using The Acrulog™ H_2S Gas Monitor data-logger.

Figure 2.4: Serum bottle experiment showing tailings and capping water incubated at 25°C

2.2.5 Physicochemical analysis

Dissolved oxygen (DO) concentration and conductivity were monitored by using a YSI Professional Plus handheld multi-parameter water quality meter (Yellow Springs Instrument Company, USA). pH was measured by using Accumet Research AR20 pH/conductivity meter (Fisher-Scientific). COD, Ammonia, TKN, nitrite (NO_2^-), and nitrate (NO_3^-) were analyzed using Hach® Water Quality Test Kits and their concentrations were determined by using DR 3900 spectrophotometer (HACH, Germany). The concentrations of AEF, DOC, NAs, PAM (and acrylamide), and microtoxicity were determined using Fourier transform infrared (FT-IR) spectroscopy (Spectrum 100, PerkinElmer Ltd, Bucks, UK), TOC analyzer (Shimadzu), ultraperformance liquid chromatography time-of-flight mass spectrometry (UPLC-TOF-MS), high performance liquid chromatography (HPLC) with UV multiple wavelength detector (Agilent 1100), and Microtox 500 Analyzer (AZUR Environmental, Carlsbad, CA, USA) respectively.

2.2.6 Mass flux calculation

The fluxes of dissolved organics from the tailings into the capping water can be understood as chemical mass transfer driven by (i) vertical one-dimensional advection-dispersion due to tailings settlement and dewatering advection and (ii) diffusion due to concentration gradients between the tailings and capping water (Crittenden et al., 2012; Dompierre et al., 2017). Thus, the mass flux can be described by the following equation:

$$J_\alpha = v * C \qquad (2.1)$$

$$J_d = - D_o * dC/dz \qquad (2.2)$$

Where J_α = mass flux of dissolved organics due to advection, g/m^2/d

v = fluid velocity in direction of concentration gradient, where v = Q/A, m^3/m^2/d (m/d)

C = average concentration of dissolved organics, mg/L

J_d = mass flux of dissolved organics due to diffusion, g/m^2/d

D_o = diffusion coefficient of dissolved organics, m^2/d

z = distance in direction of concentration gradient, m

The negative sign in Eq. 2.2 arises because the flux was from regions of high concentration to low concentration. thus, positive flux is in the direction of a negative concentration gradient (dC/dz). The combination of Eq. 2.1 and Eq. 2.2 gives the overall mass flux due to both advection and diffusion (Eq. 2.3).

$$J = J_\alpha + J_d = v * C - D_o * dC/dz \qquad (2.3)$$

The diffusion coefficient of solutes in liquid typically ranges between ~10^{-10} to 10^{-9} m^2/s (Crittenden et al., 2012) and for BML, it ranged from 7.8 x 10^{-10} to 6.6 x 10^{-10} m^2/s (Dompierre et al., 2017). Thus, some values within this range were chosen for D_o, diffusion coefficient. Furthermore, the porewater velocity for BML was found to be in the range of 0 to 1.4 x 10^{-7} m/s (Dompierre et al., 2017). Therefore, some values within this range were selected for v, fluid velocity. Using Eq. 2.3 with the selected values for v and D_o, the overall flux for selected dissolved organics was calculated (Table 2.2 and Table 2.3).

Table 2.2: Mass Flux calculations of DOC in oxic condition

Day	Depth	Jα (v*C)	Jd (-Do*dC/dz)	Jα(g/m^2/d)	Jd(g/m^2/d)
Week #1	144	5.98652E-06	-2.48253E-07	0.517235	-0.02145
Month #1	145.4	4.58708E-06	-3.19293E-07	0.396324	-0.02759
Month #2	146.15	3.82133E-06	5.76191E-07	0.330163	0.049783
Month #3	146.6	3.40647E-06	-1.2166E-08	0.294319	-0.00105
Month #4	147.35	2.85314E-06	8.16987E-08	0.246511	0.007059
Month #5	149	3.14555E-06	-1.41944E-06	0.271776	-0.12264
Month #6	149.6	2.28225E-06	2.16987E-07	0.197186	0.018748
Month #7	151.85	1.8502E-06	-2.79419E-08	0.159857	-0.00241
Month #8	153.4	1.5086E-06	-4.70362E-07	0.130343	-0.04064
Month #9	154	9.996E-07	2.11602E-08	0.086365	0.001828
Month #10	155	4.91792E-07	3.63043E-07	0.042491	0.031367
Month #11	155.15	2.16792E-06	5.57138E-07	0.187308	0.048137
Month #12	155.85	1.68213E-06	6.09E-08	0.145336	0.005262
Month #15	157.35	1.3066E-06	-2.3E-07	0.11289	-0.01987

Table 2.3: Mass Flux calculations of DOC in anoxic condition

Day	Depth	Jα (v*C)	Jd (-Do*dC/dz)	Jα(g/m^2/d)	Jd(g/m^2/d)
Week #1	144	7.5467E-06	-6.95314E-07	0.652035	-0.060075
Month #1	145.75	5.50125E-06	-5.68517E-08	0.475308	-0.004912
Month #2	147.25	4.8591E-06	8.63444E-08	0.419826	0.00746
Month #3	148.15	4.3118E-06	3.22674E-09	0.37254	0.000279
Month #4	150.3	3.53465E-06	1.19898E-07	0.305394	0.010359
Month #5	152.4	3.7695E-06	-6.42921E-07	0.325685	-0.055548
Month #6	153.8	0.000002811	9.5112E-07	0.24287	0.082177
Month #7	154.3	2.6388E-06	-1.53833E-06	0.227992	-0.132912
Month #8	154.75	1.79085E-06	4.18333E-07	0.154729	0.036144
Month #9	155.8	0.000001108	1.91197E-07	0.095731	0.016519
Month #10	157.35	5.263E-07	6.27867E-07	0.045472	0.054248
Month #11	157.65	0.00000258	9.85857E-08	0.222912	0.008518
Month #12	158.35	1.9632E-06	3.92E-07	0.16962	0.033869
Month #15	158.8	1.4775E-06	-7.33125E-09	0.127656	-0.000633

2.3 Results and discussion

2.3.1 Settling and consolidation behavior of PASS-treated tailings

The settling of the treated tailings which was initially at 72cm mark (interface height) of the DPL columns (Figure 2.2A) was observed over time. There was a gradual consolidation of the water-capped treated tailings over time in both oxic and anoxic columns. Specifically, the interface height in oxic columns was reduced by 13.8 cm ± 0.14 (Figure 2.5A) whereas it was reduced by 16.4 cm ± 0.71 in anoxic columns (Figure 2.5B). This indicated higher dewatering in anoxic columns which might further be reflected in the concentration of contaminants found in the capping water of oxic and anoxic columns. The slight difference in settling rate between the oxic and anoxic columns might be due to differences in solid contents of the tailings. When compared over a three month-period with batch columns that were not water-capped, the ratio of the interface height (interface ratio) was 0.959 ± 0.017, 0.964 ± 0.0059, 0.942 ± 0.0088 for batch columns, oxic columns and anoxic columns respectively (Figure 2.5C). Further, ANOVA (Analysis of Variance) revealed that the there was no significant difference between the settling rate in oxic, anoxic and batch columns (p-value = 0.508613). This suggested that water capping did not significantly affect the rate of consolidation of PASS-treated tailings. It has been demonstrated that the addition of alum and PAM in PASS treatment enhanced dewatering of tailings (Cossey et al., 2022; Liu et al., 2018). Additionally, the mineral composition of PASS-treated tailings (Table 2.1) suggested a combination of improved hydraulic conductivity due to high quartz content and decrease hydraulic conductivity due to clay minerals (Liu et al., 2018).

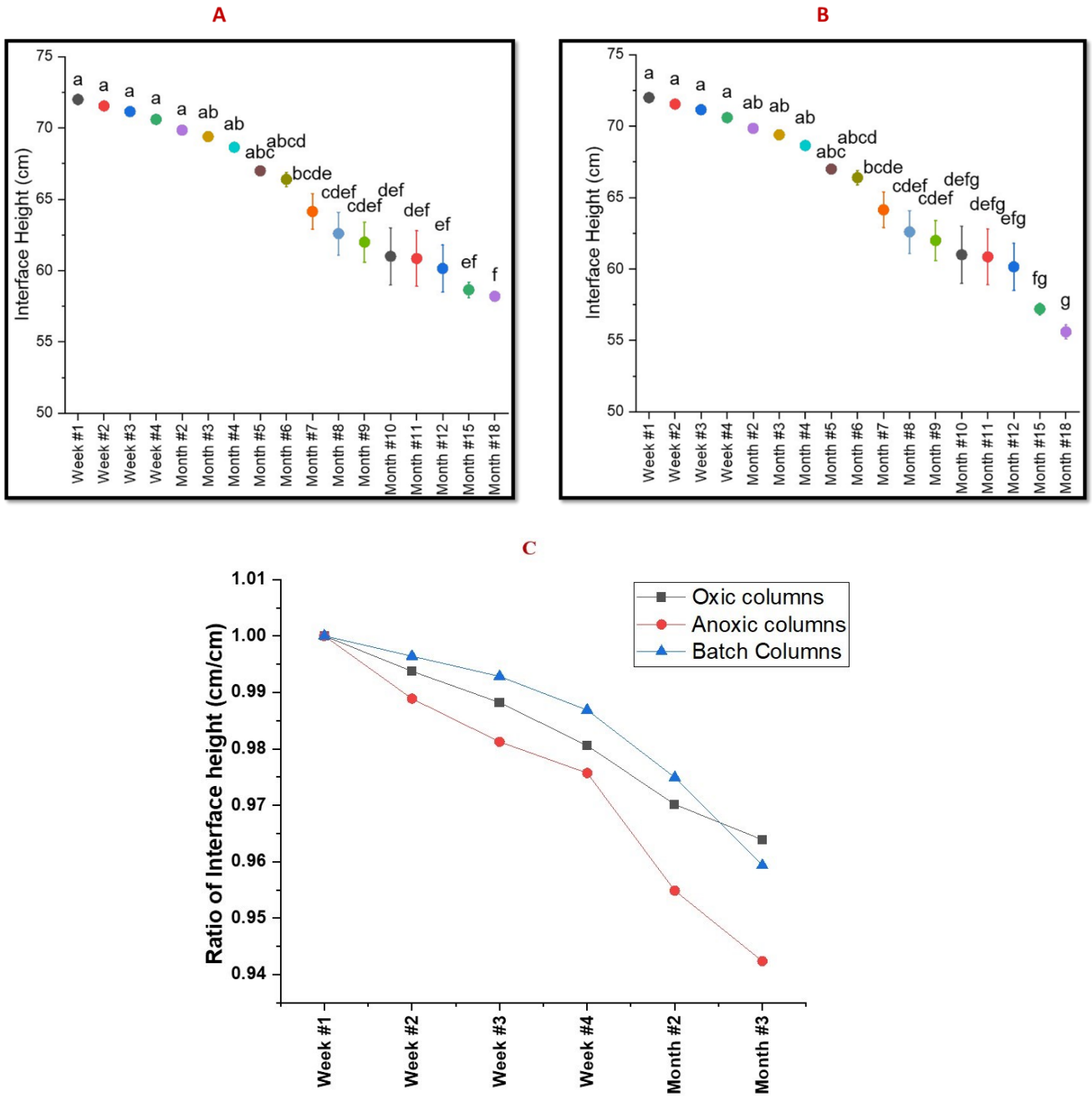

Figure 2.5: (A) Settling rate in oxic columns (B) Settling rate in anoxic columns (C) comparison of settling rate in oxic, anoxic and batch columns to observe the effect of water capping on natural settling on PASS-treated tailings

2.3.2 Fate of dissolved organics

The fate of dissolved organics was determined by measuring the concentrations of surrogate parameters including COD, DOC, AEF, and NAs in the capping water of both oxic and anoxic columns and comparing them to the background concentrations. Specifically, the concentration of COD increased by approximately 150% in oxic columns and 173% in anoxic columns during the first week. This later decreased by about 111% under oxic condition and 59% under anoxic condition by the end of one month. Subsequently, there was an increase of about 13% - 25% in COD concentrations in oxic columns and about 40% - 61% in anoxic columns over the experimental period (Figure 2.6A). The very high increase in COD concentration during the first week was likely due to initial mixing of tailings with the capping water during the establishment of the experimental columns. Measurement of filtered samples showed a relatively low concentration increase. For example, DOC showed an increase in concentration in the range of approximately 5% - 37% in oxic columns as against an increase of approximately 19% - 72% in anoxic columns (Figure 2.6B). Similarly, AEF measurement, revealed a concentration range covering a decrease of 14% to an increase of 7.5% in oxic condition as against an increase of about 4% - 31% in anoxic condition (Figure 2.6C). Additionally, NAs revealed an initial increase in concentration up to about 63% before a gradual decrease of about 18% in oxic columns as compared to an increase between the range of 38% - 110% in anoxic columns (Figure 2.6D). Overall, an initial increase to the background concentrations of dissolved organics was observed in the capping water of both oxic and anoxic columns (with anoxic columns having higher increases), which then stabilized over time before decreasing towards the end of the experimental period.

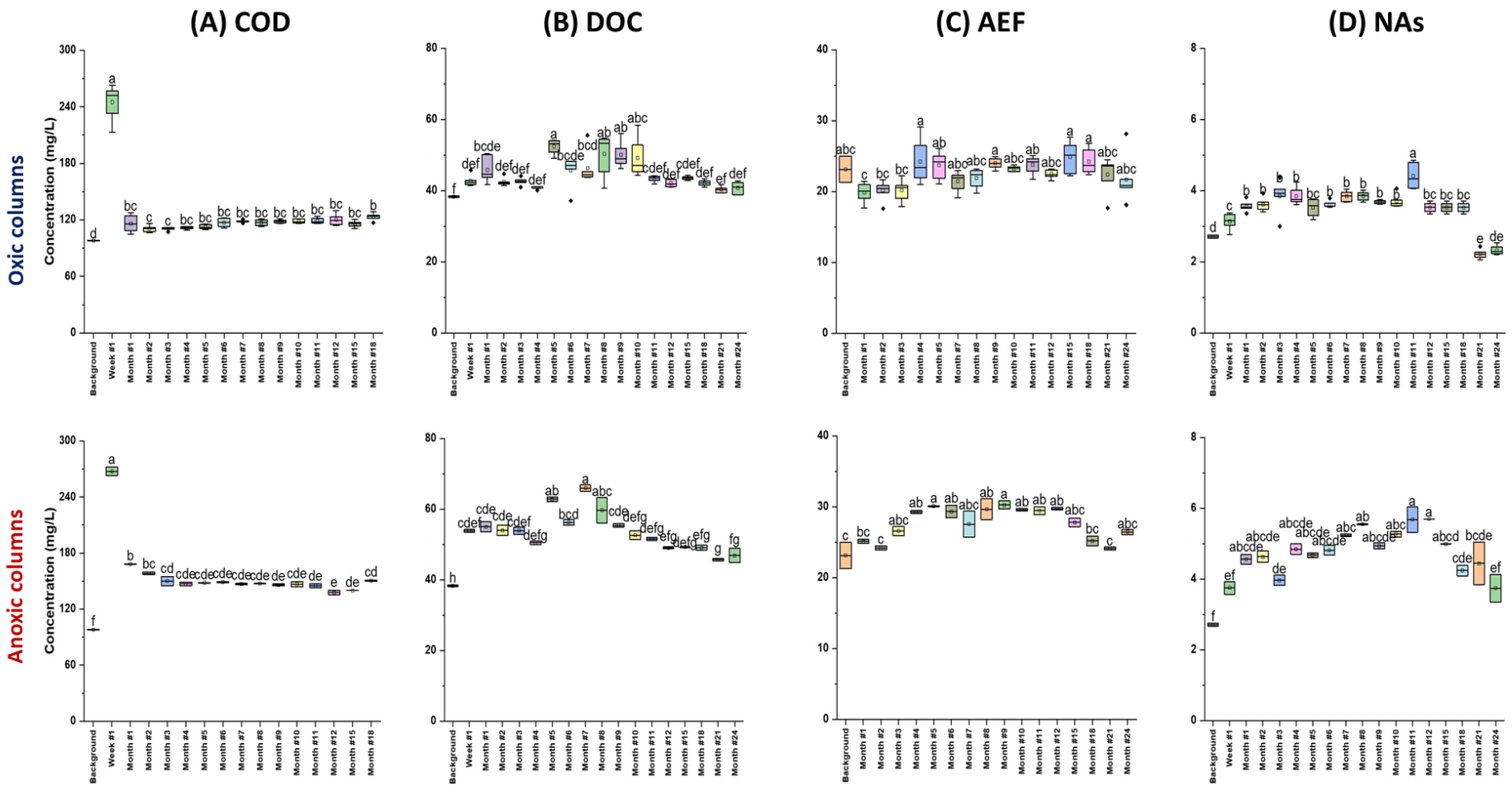

Figure 2.6: Changes in concentrations of (A) COD in oxic and anoxic columns, (B) DOC in oxic and anoxic columns, (C) AEF in oxic and anoxic columns and (D) NAs in oxic and anoxic columns. Different letters indicate "significant difference" while same letters indicate "no significant difference" at $\alpha = 0.05$. COD = chemical oxygen demand; DOC = dissolved organic carbon; AEF = acid extractable fractions; NAs = naphthenic acids

The analysis of the porewater released after tailings settling revealed significantly higher concentrations of dissolved organics compared to background concentrations in the capping water (Table 2.4). This suggested that dissolved organics in tailings porewater was likely being released into the capping water during tailings consolidation through advection-diffusion processes (COSIA, 2021; Dompierre et al., 2017). Furthermore, the concentrations of dissolved organics were higher in anoxic columns (Figure 2.7B) than in oxic conditions (Figure 2.7A), which was in line with the higher settling rates observed in anoxic columns.

Table 2.4: concentrations of selected parameters in the porewater of PASS-treated tailings

Parameter	**Value**
COD (mg/L)	618 ± *42.42*
DOC (mg/L)	86.7 ± *0.42*
NAs (mg/L)	21.23 ± *0.1*
Ammonia (mg/L)	3.35 ± *0.1*
TKN (mg/L)	7.99 ± *0.41*
NO_3+NO_2-N	7.75 ± *0.47*
Total-N	15.7 ± *0.87*
pH	8.38 ± *0.04*

The mass flux plots of advection and diffusion fluxes further revealed high advective flux of dissolved organics which reduced gradually overtime whereas diffusive flux was consistently low. For instance, the advective flux for DOC decreased from 0.52 g/m^2/d to 0.11 g/m^2/d in oxic columns (Figure 2.8A) and from 0.65 g/m^2/d to 0.13 g/m^2/d in anoxic columns (Figure 2.8B). On the other hand, the advective flux for NAs decreased from 0.038 g/m^2/d to 0.009 g/m^2/d in oxic columns (Figure 2.8C) and from 0.045 g/m^2/d to 0.013 g/m^2/d in anoxic columns (Figure 2.8D).

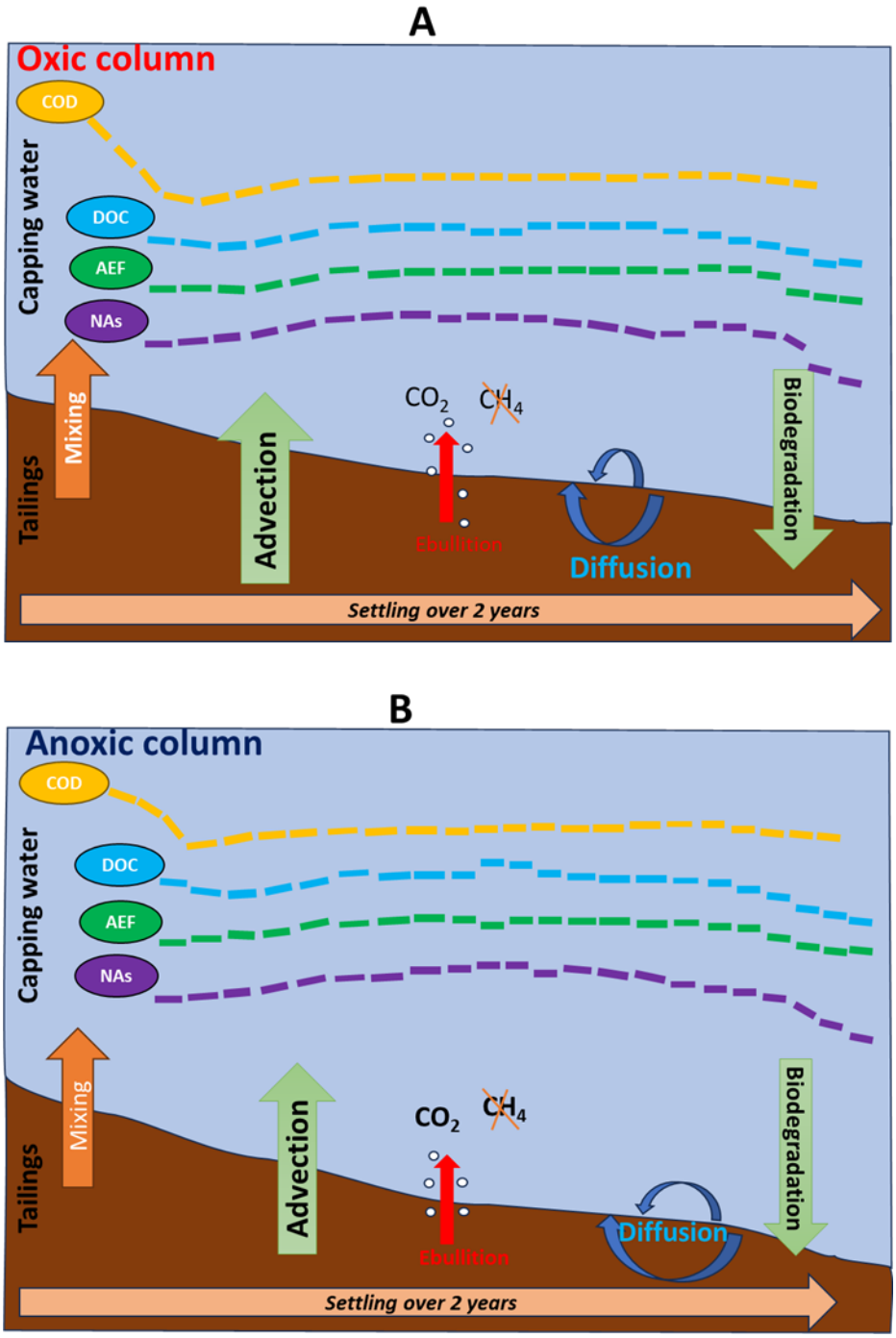

Figure 2.7: (A) Fate of dissolved organics in Oxic condition (B) Fate of dissolved organics in Anoxic condition

This further showed that advective flux was the dominant mass transport process with diffusion likely playing a role as settling reduced drastically towards the later months (Cossey et al., 2021). It could then be inferred that the observed decrease in concentrations of dissolved organics during the later months was likely due to consumption of less toxic and easily degradable organics such as short chain hydrocarbons and carboxylic acids, by the indigenous microbial communities (Syncrude, 2021).

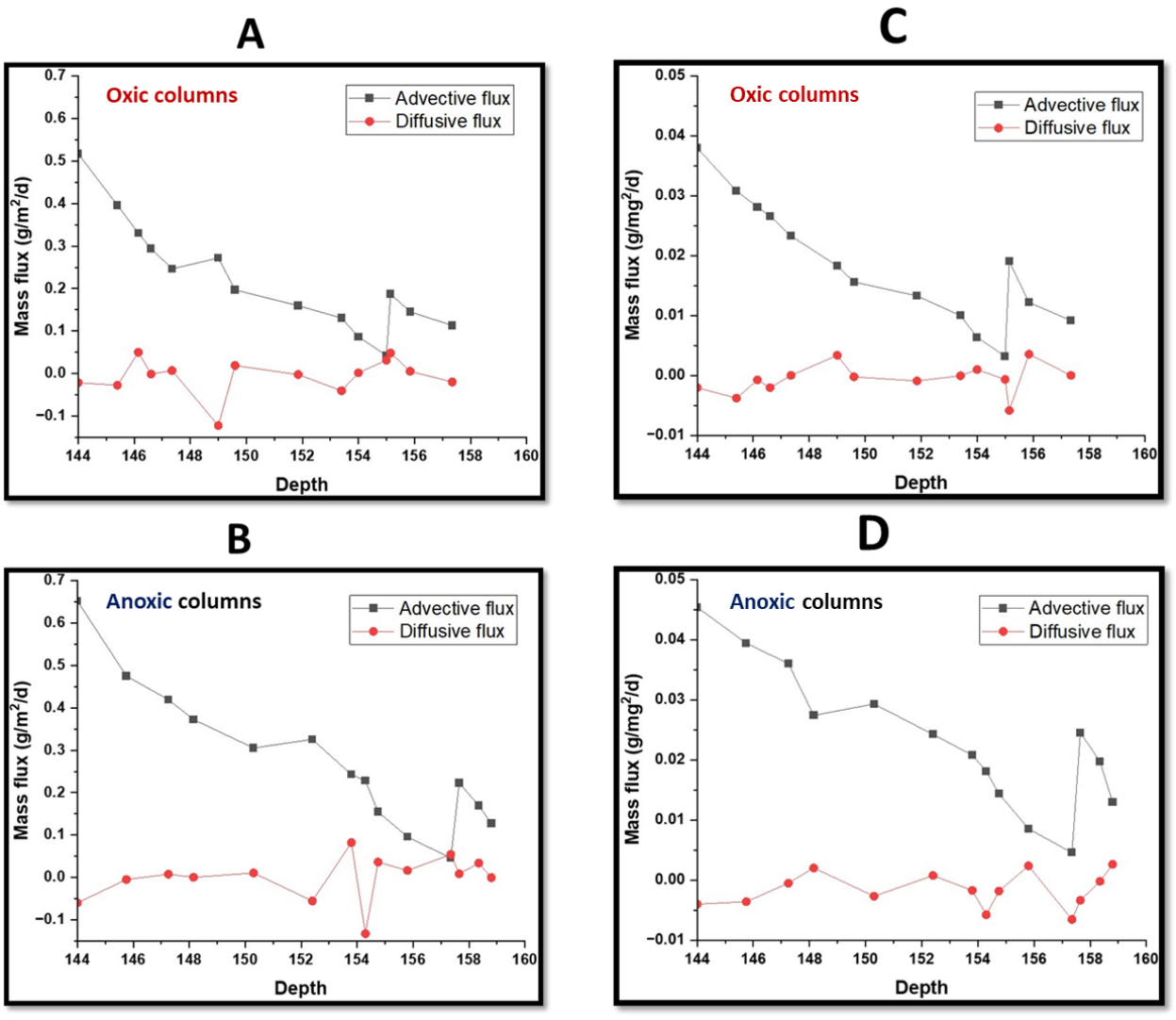

Figure 2.8: (A) Mass flux of DOC in Oxic condition (B) Mass flux of DOC in Anoxic condition (C) Mass flux of NAs in Oxic condition (D) Mass flux of NAs in Anoxic condition

2.3.3 Fate of polymer additives

The fate of polymer additives was assessed by measuring the concentrations of PAM, ADM, TKN and NH_3 in the capping water of oxic and anoxic columns and comparing the concentrations to the background concentrations of the capping water. The average background concentration of PAM in the capping water was initially below the detection limit of 0.1 mg/L, but later increased to an average of 1.13 mg/L in oxic columns and 0.845 mg/L in anoxic columns after a week of column establishment. Thereafter, there was a significant decrease in PAM concentration over time in both columns. Specifically, the average PAM concentration was in the range 1.13 mg/L to 0.123 mg/L in oxic columns and 0.845 mg/L to 0.085 mg/L in anoxic columns (Figure 2.9A). This suggested that residual PAM present in the PASS-treated tailings was initially released into the water cap during the first week before being biodegraded slowly over time. Previous studies have reported the ability of bacteria to utilize PAM as nitrogen and carbon sources (Guezennec et al., 2015).

On the other hand, the average background concentration of AMD in the capping water was 0.14 mg/L but later increased after addition to the columns before decreasing overtime in both oxic and anoxic columns. Specifically, the average AMD concentrations ranged between 0.95 mg/L to 0.18 mg/L in oxic columns and between 1.75 mg/L to 0.22 mg/L in anoxic columns (Figure 2.9B). Additionally, average AMD concentrations were lower than those of PAM in oxic columns but higher in the anoxic columns suggesting that PAM and AMD behaved differently under these conditions. The results of TKN revealed an average background concentration of 2.79 mg/L which increased to 3.9 mg/L after a week of column establishment in oxic columns before decreasing significantly to 0.7 mg/L. Then, the concentration increased significantly before stabilizing until

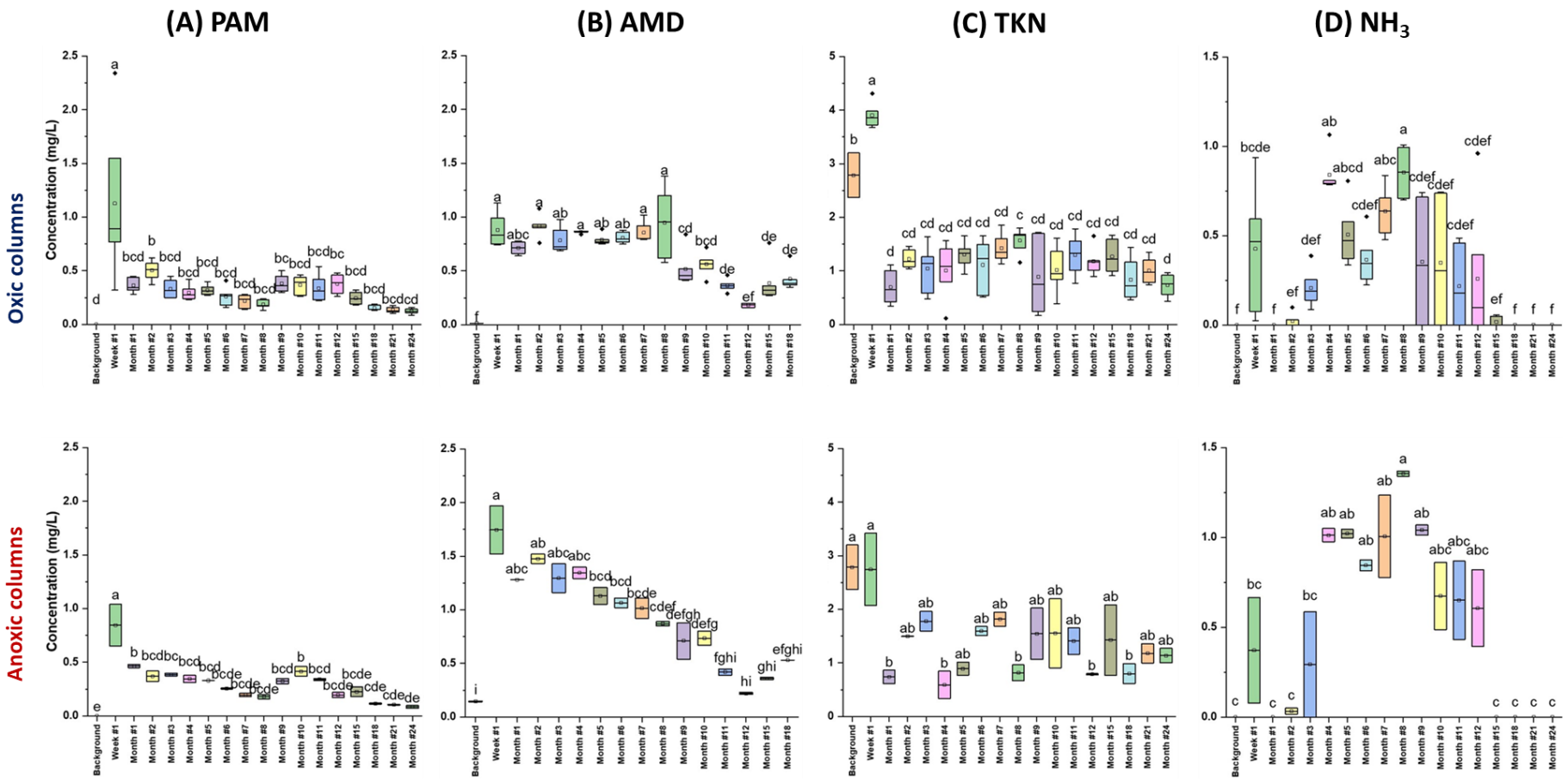

Figure 2.9: Changes in concentrations of (A) PAM over a 2-year period in, (B) AMD over an 18-month period, (C) TKN over a 2-year period, and (D) Ammonia over a 2-year period in oxic and anoxic columns. Different letters indicate "significant difference" while same letters indicate "no significant difference" at $\alpha = 0.05$. PAM = polyacrylamide; AMD = acrylamide; TKN = total kjeldahl nitrogen; NH_3 = ammonia

the last month when it significantly reduced. In anoxic columns, the average background concentration (2.79 mg/L) did not change significantly after a week of column establishment (2.74 mg/L) but later decreased significantly to 0.74 mg/L before demonstrating an upward trend in concentration increase (Figure 2.9C). The results of NH_3 revealed an upward trend in average concentrations in oxic columns (ranging from 0.0 mg/L to 0.85 mg/L) and anoxic columns (ranging from 0.0 mg/L to 1.36 mg/L) for a period of 8 months before significantly decreasing until no NH_3 was detectable towards the end of the experimental period (Figure 2.9D). This suggested that there was an initial increase in NH_3 production over a period of 8 months likely due PAM and AMD biodegradation. It has been previously reported that the biodegradation of PAM and ADM by bacteria through the hydrolysis of amide group produces NH_3 (Guezennec et al., 2015; Joshi and Abed, 2017).

Overall, the addition of PAM, which was produced through polymerization of AMD, during PASS treatment resulted in the presence of residual AMD in the tailings due to incomplete polymerization (Guezennec et al., 2015). These results suggested that there was a flux of PAM and residual AMD into the capping water, and this was later degraded into organic nitrogen and ammonia nitrogen as indicated by an increase in PAM and AMD concentrations as compared to their background concentrations (Figure A1). After the release into the capping water, PAM decreased by about 89% and 90% in oxic and anoxic columns respectively whereas AMD decreased by approximately 51% and 70% under the same condition.

2.3.4 Gas production

The analysis of gases focused on the presence and detection of greenhouse gases (CH_4 and CO_2) and H_2S. The results of gas analysis using GC-TCD with capacity to detect CH_4, CO_2 and H_2 revealed the presence of only CO_2 at 100% while CH_4 and H_2 were undetected in all the samples. CO_2 concentration in the headspace was in the range of 1.02 to 2.15 mole% in oxic condition whereas it was in the range of 5.28 to 6.50 mole% in anoxic condition after 10 weeks of incubation. These results suggested that CO_2 was the

prominent gas produced by PASS treatment technology and at a low rate. Contrary to BML where CH_4 and CO_2 were actively being produced at high rate from the untreated underlying tailings (Kuznetsov et al., 2023), PASS treatment resulted in low production of CO_2 and no detection of CH_4.

2.4 Conclusion

The EPL is still being evaluated for permanent reclamation of oil sands tailings and PASS treatment technology is the recent attempt at demonstrating the effectively of EPL for sustainable tailings reclamation. PASS treatment technology, developed by Suncor Energy, has demonstrated the ability to enhance dewatering and consolidation of tailings. Despite the high concentration of dissolved organics measured in the pore water of tailings, there were relatively low increases in concentrations of the measured dissolved organic constituents in capping water when compared to the initial background concentrations. A detailed analysis of mass flux demonstrated the ability of PASS treatment technology to limit the fluxes of dissolved organics into the overlying capping water over time. Furthermore, there was also low fluxes of the added PAM and residual AMD from the tailings into the capping water. Additionally, there was low production of CO_2, while CH_4 was not detected. The results of this laboratory study show that PASS treatment technology has the capacity to create a self-sustaining EPL system for tailings reclamation.

2.5 References

Albakistani, E.A., Nwosu, F.C., Furgason, C., Haupt, E.S., Smirnova, A. V., Verbeke, T.J., Lee, E.S., Kim, J.J., Chan, A., Ruhl, I.A., Sheremet, A., Rudderham, S.B., Lindsay, M.B.J., Dunfield, P.F., 2022. Seasonal Dynamics of Methanotrophic Bacteria in a Boreal Oil Sands End Pit Lake. Appl. Environ. Microbiol. 88. https://doi.org/10.1128/aem.01455-21

Alberta Energy Regulator, 2022. Tailings [WWW Document]. Provid. Inf. URL

https://www.aer.ca/providing-information/by-topic/tailings (accessed 11.20.23).

Canada's Oil Sands Innovation Alliance (COSIA), 2021. Pit Lakes: A surface mining perspective, Tailings Environmental Priority Area (EPA).

Cossey, H.L., Batycky, A.E., Kaminsky, H., Ulrich, A.C., 2021. Geochemical stability of oil sands tailings in mine closure landforms. Minerals 11. https://doi.org/10.3390/min11080830

Cossey, H.L., Kaminsky, H., Ulrich, A.C., 2022. Evaluating the long-term behaviour and viability of an oil sands tailings management and reclamation strategy, in: AB Fourie, M Tibbett & G Boggs (eds), M.C. 2022 (Ed.), Proceedings of the International Conference on Mine Closure. Australian Centre for Geomechanics, Perth, pp. 307–320. https://doi.org/10.36487/ACG_repo/2215_19

Crittenden, J.C., Trussell, R., Hand, D., Howe, J.K., Tchobanoglous, G., 2012. MWH's Water Treatment: Principles and Design, Third. ed. John Wiley & Sons, Inc., Hoboken, New Jersey.

Dompierre, K.A., Barbour, S.L., North, R.L., Carey, S.K., Lindsay, M.B.J., 2017. Chemical mass transport between fluid fine tailings and the overlying water cover of an oil sands end pit lake. Water Resour. Res. 5, 4725–4740. https://doi.org/10.1002/2016WR020112

Government of Canada, 2018. Technical Backgrounder: Federal methane regulations for the upstream oil and gas sector [WWW Document]. Environ. Clim. Chang. Canada. URL https://www.canada.ca/en/environment-climate-change/news/2018/04/federal-methane-regulations-for-the-upstream-oil-and-gas-sector.html (accessed 10.21.22).

Guezennec, A.G., Michel, C., Bru, K., Touze, S., Desroche, N., Mnif, I., Motelica-Heino, M., 2015. Transfer and degradation of polyacrylamide-based flocculants in hydrosystems: A review. Environ. Sci. Pollut. Res. 22, 6390–6406. https://doi.org/10.1007/s11356-014-3556-6

Joshi, S.J., Abed, R.M.M., 2017. Biodegradation of Polyacrylamide and Its Derivatives. Environ. Process.

4, 463–476. https://doi.org/10.1007/s40710-017-0224-0

Kuznetsov, P., Wei, K., Kuznetsova, A., Foght, J., Ulrich, A., Siddique, T., 2023. Anaerobic Microbial Activity May Affect Development and Sustainability of End-Pit Lakes: A Laboratory Study of Biogeochemical Aspects of Oil Sands Mine Tailings. ACS ES T Water 3, 1039–1049. https://doi.org/10.1021/acsestwater.2c00505

Liu, D., Edraki, M., Berry, L., 2018. Investigating the settling behaviour of saline tailing suspensions using kaolinite, bentonite, and illite clay minerals. Powder Technol. 326, 228–236. https://doi.org/10.1016/j.powtec.2017.11.070

Syncrude, 2019. Base Mine Lake Monitoring and Research Summary Report: Results from 2013-2018.

Syncrude, 2021. 2021 Pit Lake Monitoring and Research Report (Base Mine Lake Demonstration Summary: 2012-2020).

White, K.B., Liber, K., 2020. Chronic Toxicity of Surface Water from a Canadian Oil Sands End Pit Lake to the Freshwater Invertebrates Chironomus dilutus and Ceriodaphnia dubia. Arch. Environ. Contam. Toxicol. 78, 439–450. https://doi.org/10.1007/s00244-020-00720-3

CHAPTER 3 BIOGEOCHEMICAL PROCESSES IN OIL SANDS TAILINGS AND CAPPING WATER AT DEMONSTRATION PIT LAKE

3.1 Introduction

Alberta's oil sands in Canada are the 4th largest proven crude oil reserves in the world (165.4 billion barrels) after Venezuela, Saudi Arabia, and Iran, with crude bitumen production estimated at around 2.8 million barrels per day in 2017 (Alberta Government, 2022). Bitumen production is achieved either via surface mining (20%) or *in situ* extraction (80%) (Alberta Government, 2022). Surface mining of bitumen leads to the generation of large volumes of waste known as oil sands tailings. These tailings comprise sand, silt, clay, unrecovered bitumen, water, and organics and inorganics (Alberta Energy Regulator, 2022). More than 1.3 billion cubic meters of tailings have been stored in tailings ponds, covering over 88 square kilometers of land (Cossey et al., 2021; White and Liber, 2020).

Pit lakes has been proposed as a sustainable solution for the permanent reclamation of tailings (White and Liber, 2020). It is formed by placing tailings in an open pit covered with a mixture of OSPW and freshwater, termed capping water (Syncrude, 2019). Hence, using pit lakes could be used to manage tailings, trap sediments, and provide water treatment thereby improving capping water quality over time (COSIA, 2021). Base Mine Lake (BML) was the first full-scale pit lake established in 2012 to test its effectiveness for Canadian oil sands mines reclamation. In BML, methane production from underlying untreated tailings was high (Syncrude, 2019) coupled with the release of porewater having high concentrations of contaminants of potential concerns (COPCs) into the capping water (Dompierre and Barbour, 2016). In 2016, *Suncor Energy* used a new tailings treatment technology known as Permanent Aquatic Storage Structure (PASS) and

established a demonstration pit lake (DPL) which was later named Lake Miwasin. PASS technology uses an inline treatment process where flocculant (polyacrylamide, PAM) is added to improve tailings dewatering at accelerated rates, and coagulant (alum) is added to improve tailings expressed water quality. It is also expected that the treatment would immobilize the contaminants in tailings which could, because of PASS treatment, further improve the quality of capping water during long-term storage as a PL function (COSIA, 2021).

Currently, research is being carried out to investigate the impact of PASS treatment technology for biomonitoring, ecotoxicological, and reclamation of oil sands tailings. For example, Lillico et al. (2022) successfully established sensitive biomarkers for toxicity studies at pilot-scale DPL models. Accordingly, Choo-yin, (2021) examined the bioactivity of two OSPW sources collected from Lake Miwasin and concluded that each OSPW sample contained bioactive constituents. However, outcomes related to reclamation and biogeochemical cycling of nutrients and transport of dissolved organics in Lake Miwasin are largely unknown and are being investigated by Lake Miwasin monitoring programs. Particularly, it is crucial to investigate the effect of alum and PAM on biogeochemical processes in tailings as well as in the capping water. This is because alum and PAM can influence microbial sulfur and nitrogen cycling respectively, by affecting the composition and activities of various microbial populations thereby creating a system that may negatively affect other forms of life and causing microbial imbalance (Robinson et al., 2018). Also, it is previously established that in a water-capped tailings technology, tailings will continue to dewater overtime due to self-weight consolidation, thereby releasing contaminants through advective and diffusive transport of porewater constituents into the overlying water (Dompierre and Barbour, 2016; Syncrude, 2019). This has also been observed for PASS-treated tailings. Nevertheless, how the advective and diffusive transport of contaminants is regulated by

seasonal temperature variations has yet to be established for Lake Miwasin. Alberta's continental climate not only contributes to significant seasonal fluctuations in pit lake temperatures, leading to stratification and turnover, but also influences biotic activity, including the distribution and metabolic functions of a diverse array of microbes across varying redox conditions within tailings ponds, which are integral to the biogeochemical cycling of organics and nutrients (Foght et al., 2017; Chen et al., 2013; Siddique et al., 2020).

Many forms of tailings (e.g., diluent affected tailings) are known as significant sources of methane (CH_4) and volatile organic compounds (VOCs), contributing to the overall budget of greenhouse gases. This investigation delineates the mechanisms through which the incorporation of alum into tailings, facilitated by the PASS treatment, enhances sulfate reduction which may inhibit methanogenesis and fosters the microbial oxidation of any resultant CH_4, thus reducing its atmospheric release. Additionally, this study also investigates the potential for sulfate introduction via alum leading to the formation of hydrogen sulfide (H_2S)-emitting aquatic systems. To this end, our research comprehensively examines: (i) the biogeochemical processes occurring in PASS-treated tailings and capping water in the presence of alum and PAM, (ii) the shift in microbial community compositions over the experimental period (iii) the effects of temperature changes on biogeochemical processes in tailing deposits and water column during long-term storage. We postulated that PASS treatment could influence the biogeochemical cycles and subsequently impact the gases production at DPL.

3.2 Materials and Methods

3.2.1 Bench-scale column setup and operation

To investigate the effects of seasonality and changes in temperature on lake water chemistry and microbial community structure, a bench-scale column (height: 48 inches, internal diameter: 5.75 inches) was established (Figure 3.1). These columns were then filled with tailings and lake water in ratio 1:2, with sampling ports established at different locations for lake water and tailings sample collections. The top of the column was sealed but connected with an airbag for gases collection. The column setup was in duplicates for treatment and control columns. The treatment columns were subjected to different temperature regimes representing winter (5 °C), spring (20 °C), summer (25 °C) and fall (8 °C) as reported in prior Lake Miwasin's water column temperature profiles (Figure 3.2).

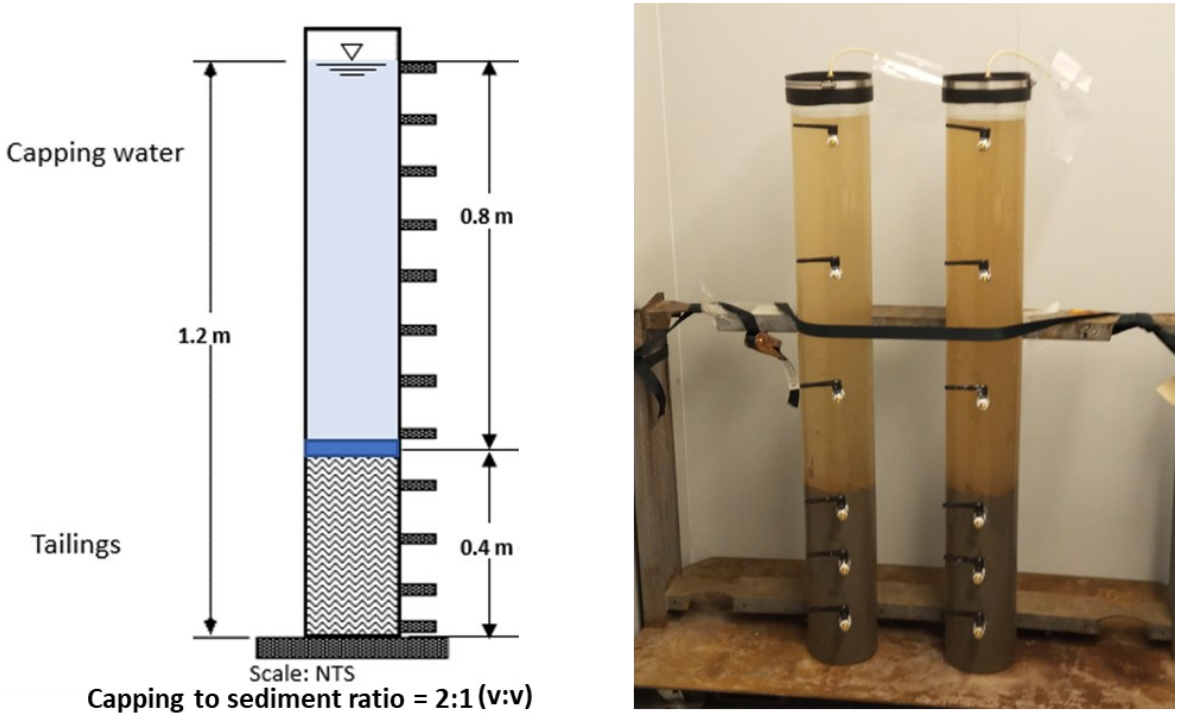

Figure 3.1: Laboratory experimental set up showing the column dimension and arrangement of sampling ports

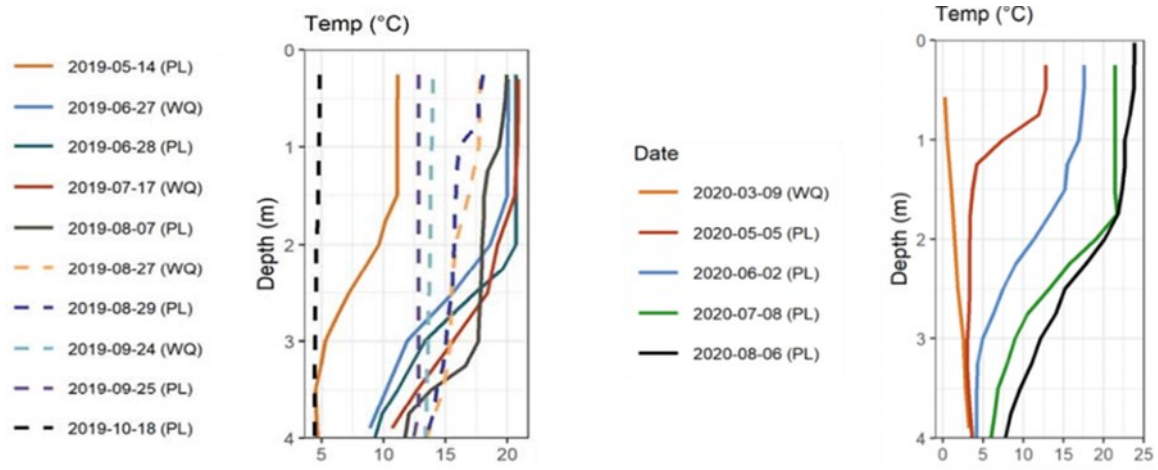

Figure 3.2: Lake Miwasin Temperature Profiles: 2019 & 2020 indicating different temperatures observed at certain depths and months

Each treatment regime (winter, spring, summer, and fall) lasted for a period of 2 months and samples were collected at the beginning and end of each treatment regime. The control column was set up at laboratory temperature of 22 °C. The tailings samples were stored at -80 °C until analysis while the lake water samples were filtered using 0.45micron filter papers which were then stored at -80 °C until analysis.

3.2.2 Physicochemical parameters

The physicochemical parameters of both treatment and control columns were measured at the beginning of the experiment and at the end of each temperature regime using standard analytical techniques and protocols. Water quality parameters such as pH, conductivity, and dissolved oxygen (DO) were measured using YSI Pro Plus multi-parameter instrument. Parameters such as total kjeldahl nitrogen (TKN), nitrite-nitrogen and nitrate-nitrogen (NO_2-N+NO_3-N), and chemical oxygen demand (COD) were measured using Hach® Water Quality Test Kits. Turbidity, dissolved organic carbon (DOC), and naphthenic acids (NAs) were measured using T-100

handheld Oakton Turbidimeter, Shimadzu TOC analyzer and ultraperformance liquid chromatography time-of-flight mass spectrometry (UPLC-TOF-MS) respectively. Dissolved metals, sulfur (S), and phosphorus (P) were measured at the end of the experiment using Thermo iCAP6300 Duo (N. America) inductively coupled plasma-optical emission spectrometer (ICP-OES).

3.2.3 Biogenic gas analyses

Gas production was assessed using gas chromatography (Agilent 7890A, Agilent Technologies, USA). However, due to the likelihood of the gas production being affected by sample collection, the gas production potential of the model pit lake system was further evaluated using air-tight serum bottles. In each bottle, 30 mL of tailings and 60 mL of capping water were combined, maintaining a 1:2 ratio, and leaving adequate headspace for gas collection. The bottles were left untouched and incubated at 25°C and 37°C over a period of 10 weeks. Gas was collected from the headspace in the serum bottles using a 0.5 mL syringe and manually introduced into Gas Chromatography-Thermal Conductivity Detector (GC-TCD) instrument for detection of methane, carbon dioxide, nitrogen and hydrogen gas. The samples were re-analyzed with the GC after 2 months to confirm if there was any change in gas production. Hydrogen sulfide production was measured using The Acrulog™ H_2S Gas Monitor data-logger (Sapkota, 2022).

3.2.4 Microbial Community Analyses

Total and active bacterial communities were analyzed in both tailings and lake water. To this end, samples were taken from the top and bottom of tailings and lake water samples. For the analysis of total bacterial communities, DNA was extracted using DNeasy PowerSoil Kits (Qiagen Inc., USA) for tailings, and DNeasy Blood & Tissue Kits (Qiagen Inc., USA) for lake water

following manufactural instructions. For active communities, RNA was extracted from tailings samples using RNeasy Extraction Kits (Qiagen Inc., USA), followed by reverse transcription and cDNA synthesis using Reverse Transcription Kits (Qiagen Inc., USA). Thereafter, 16S rRNA amplicon sequencing was carried out to investigate the microbial communities. The sequencing was performed with an Illumina MiSeq instrument by targeting the V3-V4 hypervariable region at Applied Genomics Core facility, University of Alberta, Canada. For library preparation, 341F and 785R primers were used as standard primers (Thijs et al., 2017). QIIME2 microbiome analysis pipeline (Core 2020.2 distribution) was then used to process the raw reads (Bolyen et al., 2019). To this end, DADA2 was used for quality control (Callahan et al., 2016) and identical reads were clustered together as operational taxonomic units (OTUs) and alpha and beta diversity analyses were carried out. For alpha diversity, Shannon diversity index (H) and Chao1 richness estimator indices were computed to study the overall diversity and richness within each temperature regime. For beta diversity analysis, principal coordinate analysis (PCoA) was performed to compare the composition of bacterial communities (diversity patterns) between treatment and control columns. Following diversity analysis, Naïve Bayes classifier, which was already trained on SILVA rRNA database (v 138), was used for taxonomic assignments (Arslan and Gamal El-Din, 2021). Profiles were then collapsed to the different taxonomic levels such as phylum, class, order, family, genus, and species. For visualization purpose, taxonomy-assigned OTU table was imported into the R computational language where ‘Ampvis2’ and ‘Krona’ web browsers were used to make plots and perform diversity analyses (Ondov et al., 2011; Arslan et al., 2022).

3.3 Results

3.3.1 Physicochemical characteristics and measurement of biogenic gases

The mean conductivity in treatment columns ranged from 1436.75 µS/cm to 2336.75 µS/cm over the experimental periods. In control columns, the average conductivity was between 2002.25 µS/cm to 2364 µS/cm over the course of the experimental. Notably, there were significant differences in mean conductivity between treatment and control on days 60 and 240, aligning with periods of substantial temperature variation (Two-way ANOVA, F-value = 325.95, p-value = 4.79E-28) (Table 3.1 and Table 3.2). Likewise, the average DO concentrations ranged between 4.0 mg/L to 9.35 mg/L in treatment columns whereas the mean DO concentrations in control columns were between 2.75 mg/L and 6.05 mg/L over the experimental periods. Consequently, significant differences in mean DO levels between the treatment and control groups were observed on days 60 and 240, coinciding with periods of notable temperature differences (p-value = 3.05E-14) (Table 3.1 and Table 3.2). Similarly, the average sulfate concentrations ranged between 112.30 mg/L to 136.82 mg/L in treatment columns whereas the mean sulfate concentrations in control columns were between 112.29 mg/L and 126.29 mg/L over the experimental periods. As a result, there were significant differences in mean sulfate levels between the treatment and control groups on days 60 and 240, corresponding to periods of huge temperature differences (p-value = 0.00143) (Table 3.1 and Table 3.2).

On the other hand, the average concentrations of DOC in treatment columns were between 42.24 mg/L and 60.92 mg/L which were not significantly different from the mean DOC concentrations ranging between 42.43 mg/L and 56.75 mg/L in control columns (F-value = 0.99, p-value = 0.32) (Table 3.1 and Table 3.2). Similarly, there were no significant differences in mean

values of COD (p-value = 0.39), turbidity (p-value = 0.41), TKN (p-value = 0.68), NO_2+NO_3-N (p-value = 0.82), pH (p-value = 0.60), and NAs (p-value = 0.45) between the treatment and control columns (Table 3.1 and Table 3.2). While the mean COD, DOC, turbidity, TKN, NO_2+NO_3-N, pH and NAs of treatment columns were not significantly different from those of the control columns (Table 3.1), they were significantly different overtime. COD (p-value = 4.16E-18), DOC (p-value = 7.22E-15), TKN (p-value = 3.55E-12) and NAs (p-value = 1.48E-10) increased over time whereas turbidity (p-value = 0.00133), NO_2+NO_3-N (p-value = 3.22E-25), and pH (p-value = 3.65E-13) decreased over time (Table 3.2).

Production of biogenic gases (methane, carbon dioxide, nitrogen, oxygen, hydrogen, and hydrogen sulfide) was further examined to elucidate methanogenic and sulfidogenic metabolism of hydrocarbons and alum within tailings.

Table 3.1: Summary statistics and Mann-Whitney U test results for physicochemical parameters of treatment and control columns (means ± standard deviation)

	Parameters	Treatment[a]	Control[b]	*U-value*	*p*-value
Day 1	Conductivity (µS/cm)	1489.75 ± 11.89	2002.25 ± 9.15	**0**	**0.00094**
	DO (mg/L)	7.78 ± 0.29	6.05 ± 0.22	**0**	**0.00094**
	DOC (mg/L)	43.23 ± 3.87	45.56 ± 4.51	12	0.38
	COD (mg/L)	209.17 ± 8.64	204.33 ± 3.88	9.5	0.2
	Turbidity (NTU)	34.74 ± 18.56	18.65 ± 0.91	10	0.23
	TKN (mg/L)	1.21 ± 0.37	1.15 ± 0.55	17	0.94
	NO_2+NO_3-N (mg/L)	0.56 ± 0.06	0.56 ± 0.03	17	0.94
	pH	8.34 ± 0.01	8.29 ± 0.04	**3**	**0.02**
	NAs (mg/L)	2.95 ± 0.23	2.95 ± 0.23	18	0.94
	SO_4^{2-} (mg/L)	112.30 ± 3.41	112.29 ± 3.40	18	0.94
Day 60	Conductivity (µS/cm)	1436.75 ± 90.36	2278.25 ± 218	**0**	**0.00094**
	DO (mg/L)	9.35 ± 1.24	2.75 ± 1.82	**0**	**0.00094**
	DOC (mg/L)	42.24 ± 1.53	42.45 ± 1.32	16	0.81
	COD (mg/L)	147.17 ± 3.19	147.83 ± 10.65	18	0.94
	Turbidity (NTU)	4.55 ± 4.39	2.59 ± 3.37	11	0.3
	TKN (mg/L)	0.02 ± 0.06	0.1 ± 0.12	11.5	0.34
	NO_2+NO_3-N (mg/L)	0.43 ± 0.02	0.44 ± 0.02	13	0.47
	pH	8.12 ± 0.07	7.98 ± 0.11	5.5	0.055
	NAs (mg/L)	3.55 ± 0.27	3.58 ± 0.27	16	0.81
	SO_4^{2-} (mg/L)	123.37 ± 1.71	120.0 ± 0.38	**0**	**0.0051**
Day 120	Conductivity (µS/cm)	2215.5 ± 100.61	2364 ± 153.92	16	0.1
	DO (mg/L)	4.18 ± 1.31	2.93 ± 1.86	16	0.1
	DOC (mg/L)	44.72 ± 2.63	42.43 ± 2.96	9	0.17
	COD (mg/L)	283.17 ± 62.42	278.17 ± 70.88	16	0.81

	Turbidity (NTU)	12.49 ± 8.69	18.3 ± 24.65	12	0.38
	TKN (mg/L)	0.96 ± 1.4	1.37 ± 0.8	13	0.47
	NO_2+NO_3-N (mg/L)	0.38 ± 0.03	0.4 ± 0.02	10.5	0.26
	pH	7.67 ± 0.27	7.65 ± 0.24	15	0.69
	NAs (mg/L)	3.75 ± 0.34	3.77 ± 0.4	18	0.94
	SO_4^{2-} (mg/L)	137.38 ± 15.92	130.0 ± 9.45	9	0.17
Day 180	Conductivity (µS/cm)	2336.75 ± 22.19	2303.75 ± 119.28	32	0.96
	DO (mg/L)	4.0 ± 0.43	4.03 ± 1.23	32	0.96
	DOC (mg/L)	46.31 ± 1.57	45.46 ± 2.53	10.5	0.26
	COD (mg/L)	359.5 ± 45.25	353.5 ± 42.94	17	0.94
	Turbidity (NTU)	14.63 ± 9.75	17.35 ± 20.99	15	0.69
	TKN (mg/L)	2.55 ± 0.58	2.44 ± 0.78	14	0.58
	NO_2+NO_3-N (mg/L)	0.34 ± 0.01	0.34 ± 0.01	10.5	0.3
	pH	7.78 ± 0.16	7.81 ± 0.21	13	0.47
	NAs (mg/L)	4.15 ± 0.38	3.96 ± 0.4	13.5	0.52
	SO_4^{2-} (mg/L)	131.49 ± 4.84	124.02 ± 4.24	9	0.17
Day 240	Conductivity (µS/cm)	1579.25 ± 21.18	2193 ± 40.29	**0**	**0.00094**
	DO (mg/L)	6.75 ± 0.12	4.35 ± 0.86	**0**	**0.00094**
	DOC (mg/L)	60.92 ± 7.22	56.75 ± 4.73	8	0.13
	COD (mg/L)	290.17 ± 4.45	300.5 ± 24.15	18	0.94
	Turbidity (NTU)	12.52 ± 3.63	8.33 ± 6.42	8	0.13
	TKN (mg/L)	2.3 ± 0.07	2.32 ± 0.47	12	0.38
	NO_2+NO_3-N (mg/L)	0.37 ± 0.01	0.36 ± 0.01	4.5	**0.04**
	pH	7.78 ± 0.03	7.84 ± 0.18	12	0.38
	NAs (mg/L)	4.49 ± 0.56	4.24 ± 0.4	10	0.23
	SO_4^{2-} (mg/L)	136.82 ± 4.91	126.29 ± 0.61	**0**	**0.0051**

a. The treatment columns were at 10°C on day 1; 5°C between days 1-60; 20°C between days 61-120; 25°C between days 121-180; and 8°C between days 181-240.

b. The control columns were operated at 22°C throughout the experimental period.

The mean values were compared by nonparametric Mann–Whitney U-tests with two-tailed hypothesis at $\alpha = 0.05$. Significant differences are highlighted in bold. DOC: dissolved organic carbon, COD: chemical oxygen demand, TKN: total Kjeldahl nitrogen, DO: dissolved oxygen, NTU: Nephelometric Turbidity Units, NO_2+NO_3-N: nitrite and nitrate-nitrogen, NAs: naphthenic acids.

Table 3.2**:** Two-way ANOVA summary of selected parameters

Parameters	Source of variation	df	Sum of Squares	Mean Square	F Value	P Value
DOC	Temperature	1	13.68993	13.68993	0.98898	0.32478
	Days	4	2177.67697	544.41924	39.32961	**7.2226E-15**
	Interaction	4	72.90291	18.22573	1.31665	0.27663
	Model	9	2264.26981	251.58553	18.17489	**6.3871E-13**
	Error	50	692.12387	13.84248		
	Corrected Total	59	2956.39367			
COD	Temperature	1	1152.81667	1152.81667	0.73635	0.39493
	Days	4	360473.26667	90118.31667	57.56189	**4.15856E-18**
	Interaction	4	9544.6	2386.15	1.52412	0.20943
	Model	9	371170.68333	41241.18704	26.34227	**5.04495E-16**
	Error	50	78279.5	1565.59		
	Corrected Total	59	449450.18333			
Turbidity	Temperature	1	112.83331	112.83331	0.68417	0.41208
	Days	4	3453.80969	863.45242	5.23561	**0.00133**

	Interaction	4	851.06438	212.76609	1.29012	0.28651
	Model	9	4417.70737	490.85637	2.97635	**0.00649**
	Error	50	8245.9511	164.91902		
	Corrected Total	59	12663.65847			
TKN	Temperature	1	0.07073	0.07073	0.16744	0.68415
	Days	4	46.98002	11.745	27.8048	**3.54823E-12**
	Interaction	4	0.48564	0.12141	0.28742	0.88478
	Model	9	47.53638	5.28182	12.50404	**4.21817E-10**
	Error	50	21.12046	0.42241		
	Corrected Total	59	68.65684			
NO_2+NO_3-N	Temperature	1	4.00167E-5	4.00167E-5	0.05498	0.81558
	Days	4	0.35774	0.08944	122.87193	**3.22945E-25**
	Interaction	4	0.0026	6.48975E-4	0.8916	0.47594
	Model	9	0.36038	0.04004	55.01212	**7.56873E-23**
	Error	50	0.03639	7.27877E-4		
	Corrected Total	59	0.39677			
NAs	Temperature	1	0.09224	0.09224	0.58983	0.4461
	Days	4	13.8363	3.45908	22.1202	**1.47666E-10**
	Interaction	4	0.19828	0.04957	0.31699	0.86528
	Model	9	14.12682	1.56965	10.03762	**1.30386E-8**
	Error	50	7.81882	0.15638		
	Corrected Total	59	21.94563			
pH	Temperature	1	0.00704	0.00704	0.27433	0.60276
	Days	4	3.25588	0.81397	31.71027	**3.64634E-13**
	Interaction	4	0.06788	0.01697	0.66114	0.6219
	Model	9	3.33081	0.37009	14.41777	**3.90313E-11**
	Error	50	1.28345	0.02567		
	Corrected Total	59	4.61426			
Conductivity	Temperature	1	3471944.45	3471944.45	325.94799	**4.78515E-28**
	Days	4	4517117.8	1129279.45	106.01736	**6.13466E-29**
	Interaction	4	2010490.8	502622.7	47.18649	**3.56135E-19**
	Model	9	9999553.05	1111061.45	104.30704	**5.92143E-37**
	Error	50	745628.5	10651.83571		
	Corrected Total	59	1.07452E7			
DO	Temperature	1	114.242	114.242	90.50407	**3.04873E-14**
	Days	4	126.547	31.63675	25.06307	**6.68077E-13**
	Interaction	4	101.193	25.29825	20.04162	**4.92614E-11**
	Model	9	341.982	37.998	30.10254	**1.07122E-20**
	Error	50	88.36	1.26229		
	Corrected Total	59	430.342			
SO_4^{2-}	Temperature	1	496.08437	496.08437	11.3992	**0.00143**
	Days	4	3570.92336	892.73084	20.51347	**<0.0001**
	Interaction	4	201.77326	50.44332	1.1591	0.34006
	Model	9	4268.781	474.309	10.89883	**<0.0001**
	Error	50	2175.9621	43.51924		
	Corrected Total	59	6444.7431			

Significant p-value is in Bold letter.

The findings revealed that, in both the control and treatment groups, the headspace gases composition included carbon dioxide (0.43% for the control versus 0.30% for the treatment), nitrogen (76.2% for the control versus 75.2% for the treatment), and oxygen (20.6% for the control versus 20.7% for the treatment) (Figure 3.3). Notably, methane and hydrogen sulfide were not detected (below detection limit) in either the control or treatment groups of the 20.4L columns, however hydrogen sulfide was detected in the serum bottles.

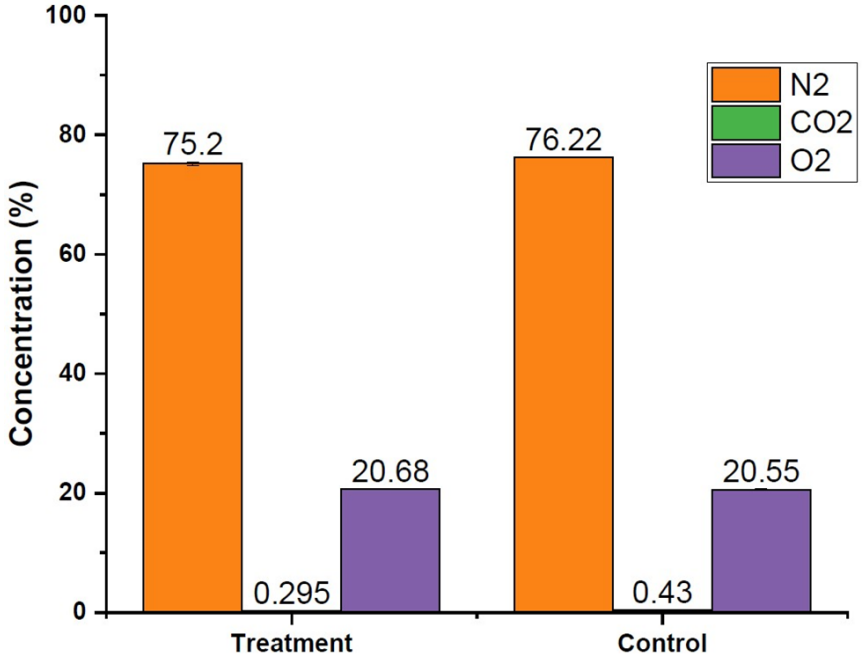

Figure 3.3: Off-gas production during the experimental period. Methane was not detected

3.3.2 Background bacterial community composition

Capping Water: Proteobacteria made up more than 50% of the bacterial community, followed by Actinobacteriota, Verrucomicrobiota, Bacteriodota and Cyanobacteria. At genus level, the bacteria communities were made up of mostly aerobes and facultative anaerobes. The most abundant genus was the sulfur oxidizing *Sulfuritalea*, followed by *Sporichthya*. Photosynthetic cyanobacteria were

represented by the abundance of *Cyanobium gracile* PCC 6307. We also noted the abundance of genera involved in hydrocarbon degradation, represented by *Sphingobium*, *Oceanibaculum*, *Caulobacter*, *Brevundimonas* and *Xanthobacter*. There was also an abundance of members of Ilumatobacteraceae represented by CL500–29 marine group; *Luteolibacter*; *Prosthecobacter*, Sporichthyaceae hgcl-clade and many genera of Candidate Phyla Radiation (CPR) such as *Candidatus Aquirestis* (Figure 3.4A and Figure 3.4B).

Tailings: The taxonomic composition and abundance of bacteria did not vary significantly between the top and bottom of the tailings. At phylum level, Proteobacteria was the most abundant, followed by Chloroflexi, Bacteriodota, Desulfobacterota, Patescibacteria and Firmicutes. At genus level, the most abundant OTU was uncultured Anaerolineaceae, followed by sulfur-oxidizing bacteria (such as *Sulfuritalea*, *Thiobacillus*, and *Sulfuricurvum*), and sulfate-reducing bacteria (such as *Desulfurivibrio*, *Desulfatirhabdium* and many unassigned members of Desulfobacteraceae, Desulfosarcinaceae, Desulfobulbaceae, Desulfocapsaceae and Desulfuromonadaceae). In addition, many genera belonging to the CPR such as *Ca. Moranbacteria* and *Ca. Dojkabacteria* were also found (Figure 3.4C and Figure 3.4D).

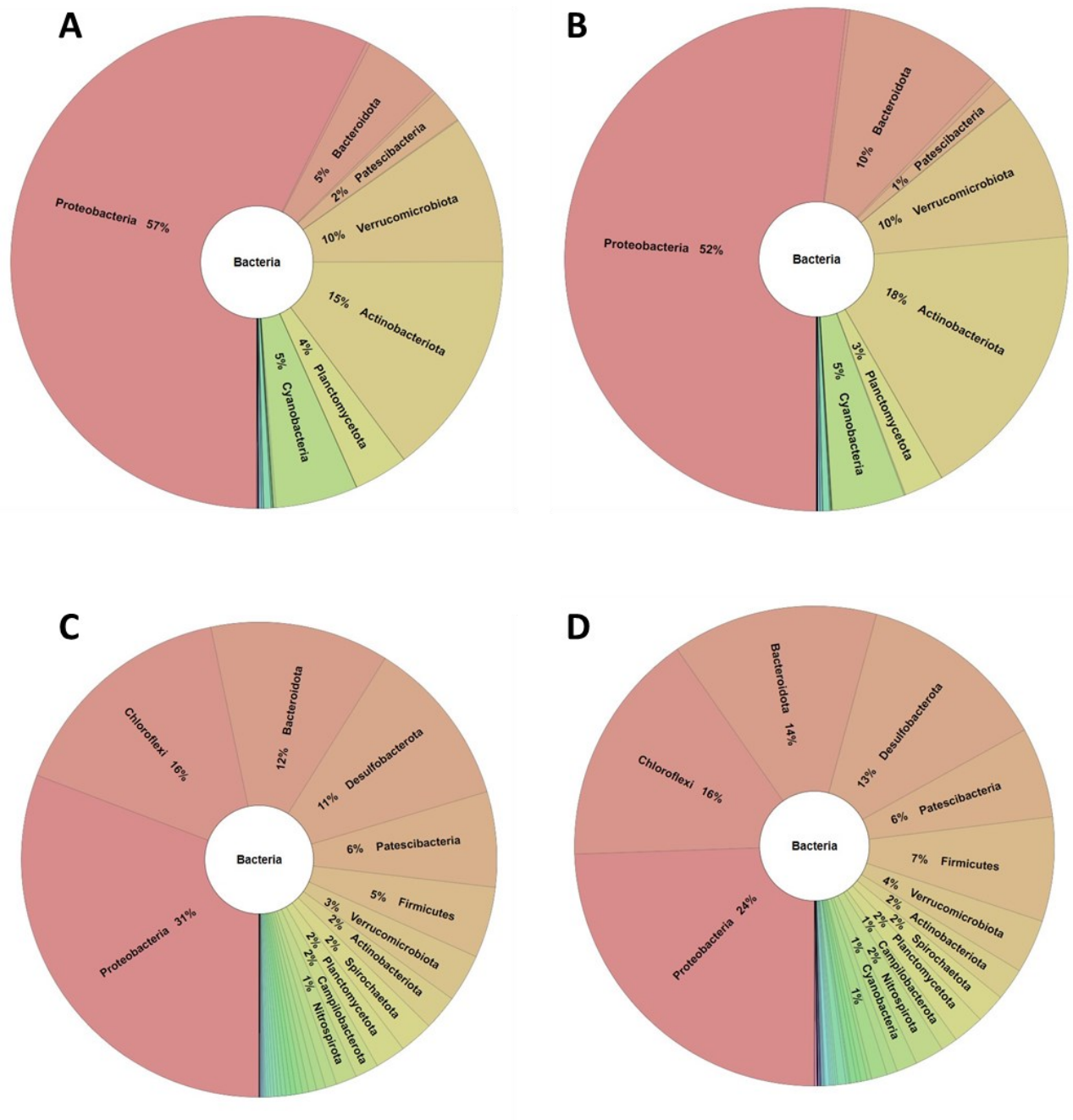

Figure 3.4: Krona plot for taxonomic abundance of (A) top of capping water, (B) bottom of capping water, (C) top of tailings, and (D) bottom of tailings

3.3.3 Bacterial diversity of PASS-treated pit lake

Alpha and beta diversity analyses were carried out to compare the diversity between capping water and tailings, as well as between treatment and control groups of capping water and tailings. The Shannon diversity index indicated a significant difference in bacterial communities between tailings and capping water (Mann-Whitney, p-value = 3.89E-17), but no significant differences between treatment and control groups in either capping water (p-value = 1.0) or tailings (p-value = 0.22) (Figure 3.5 A-C). For beta diversity, the Bray-Curtis Index revealed significant dissimilarity between tailings and capping water communities (PERMANOVA, p-value = 0.001), while treatment and control groups showed no significant differences in either capping water (p-value = 0.21) or tailings (p = 0.45) (Figure 3.5 D-F). Species richness ranged between 100 and 620 in tailings whereas it ranged between 80 and 400 in capping water (Figure A2). On the other hand, species richness ranged between 80 and 620 in control whereas it ranged between 80 and 580 in treatment (Figure A3).

3.3.4 Temporal/temperature changes on biogeochemical cycles of pit lakes containing PASS-treated tailings

3.3.4.1 Sulfur cycling

In this study, high sulfur concentration (103.5 mg/L in treatment and 112.5 mg/L in control) could effectively drive the sulfur cycle in the capping water. Specifically, water of both treatment and control columns were dominated by the sulfur-oxidizing bacteria (SOB), *Sulfuritalea*. The abundance of *Sulfuritalea* in the treatment columns initially increased from an average of 13.1% on day 1 to 35.5% on day 120, subsequently declining to 18.2% by day 240. In addition, there were very low abundances of other SOBs (including *Immundisolibacter*, *Thiobacillus* and

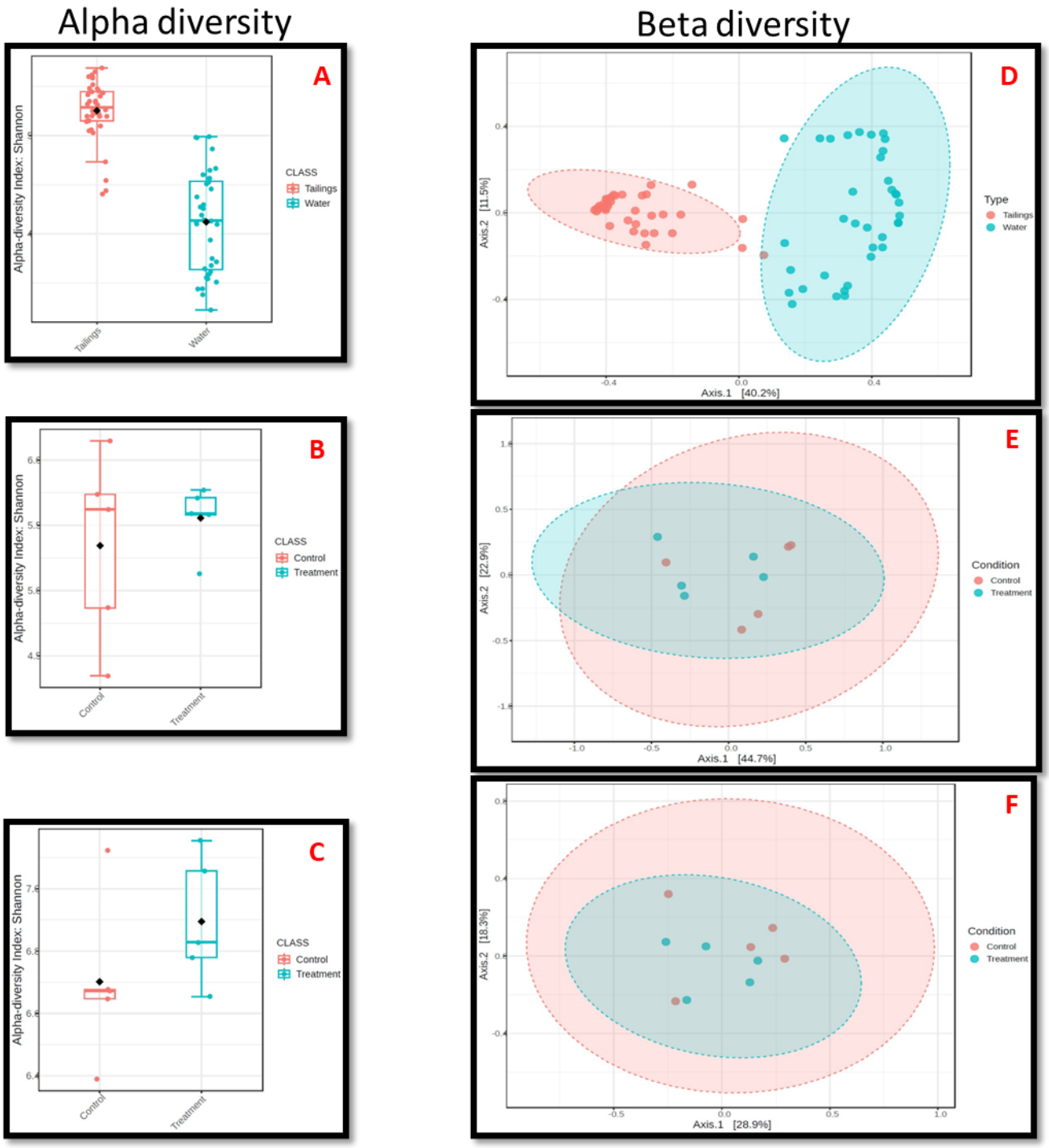

Figure 3.5: Alpha diversity between (A) tailings and capping water (B) treatment and control groups of capping water (C) treatment and control groups of tailings and Principal coordinate analysis (PCoA) illustrating similarities between (D) tailings and capping water (E) treatment and control groups of capping water (F) treatment and control groups of tailings

Sulfuricurvum) and sulfate-reducing bacteria (SRB) (including *Desulfovirga* and *Desulfovibrio*) ranging from 0% to 2.1% over the course of the experiment (Figure 3.6A). Conversely, in the control columns, the abundance of *Sulfuritalea* initially rose from an average of 18.3% on day 1 to 37.9% on day 60, before gradually dropping to 3.2% by the end of the experiment. Additionally, there were low abundance of other SOBs, for example *Chlorobium* which increased from 0% on day 120 to 2.4% on day 240 and *Immundisolibacter* which increased 0.1% to 1.2% over the experimental period. Furthermore, the abundances of SRBs such as *Desulfurivibrio*, *Desulfatiglans*, *Desulfovirga* were in the range of 0% and 0.7% over the course of the experiment (Figure 3.6B).

The microbial community structures in the tailings exhibited significant differences from those in the capping water. The tailings of treatment columns were dominated by both SOBs (such as *Sulfuritalea* ranging from 5.3% to 5.8% and *Thiobacillus* ranging from 2.4% to 1.7%) and SRBs (such as *Desulfatiglans* ranging from 0.7% to 8.1% and *Desulfurivibrio* ranging from 1.6% to 3.3%) over the experimental period (Figure 3.6C). In contrast, the microbial community in the tailings of control columns exhibited a different compositional abundance as revealed by the SOBs *Chlorobium* ranging from 0.0% to 18.6% on day 180 before dropping to 7.7% on day 240; *Sulfuritalea* ranging from 6.9% to 2.5%; and *Thiobacillus* ranging from an average of 2.1% to 1.1% over the experimental period. Furthermore, there was considerable abundance of SRBs such as *Desulfatiglans* which increased from 0.4% to 14.4%, and *Desulfurivibrio* which increased from 1.3% to 4.5% (Figure 3.6D).

Overall, SOBs and SRBs constituted averages of about 98% and 1% respectively of the total sulfur cycling communities in treatment columns of capping water whereas SOBs and SRBs made up averages of about 94% and 5% respectively in the control columns over the experimental

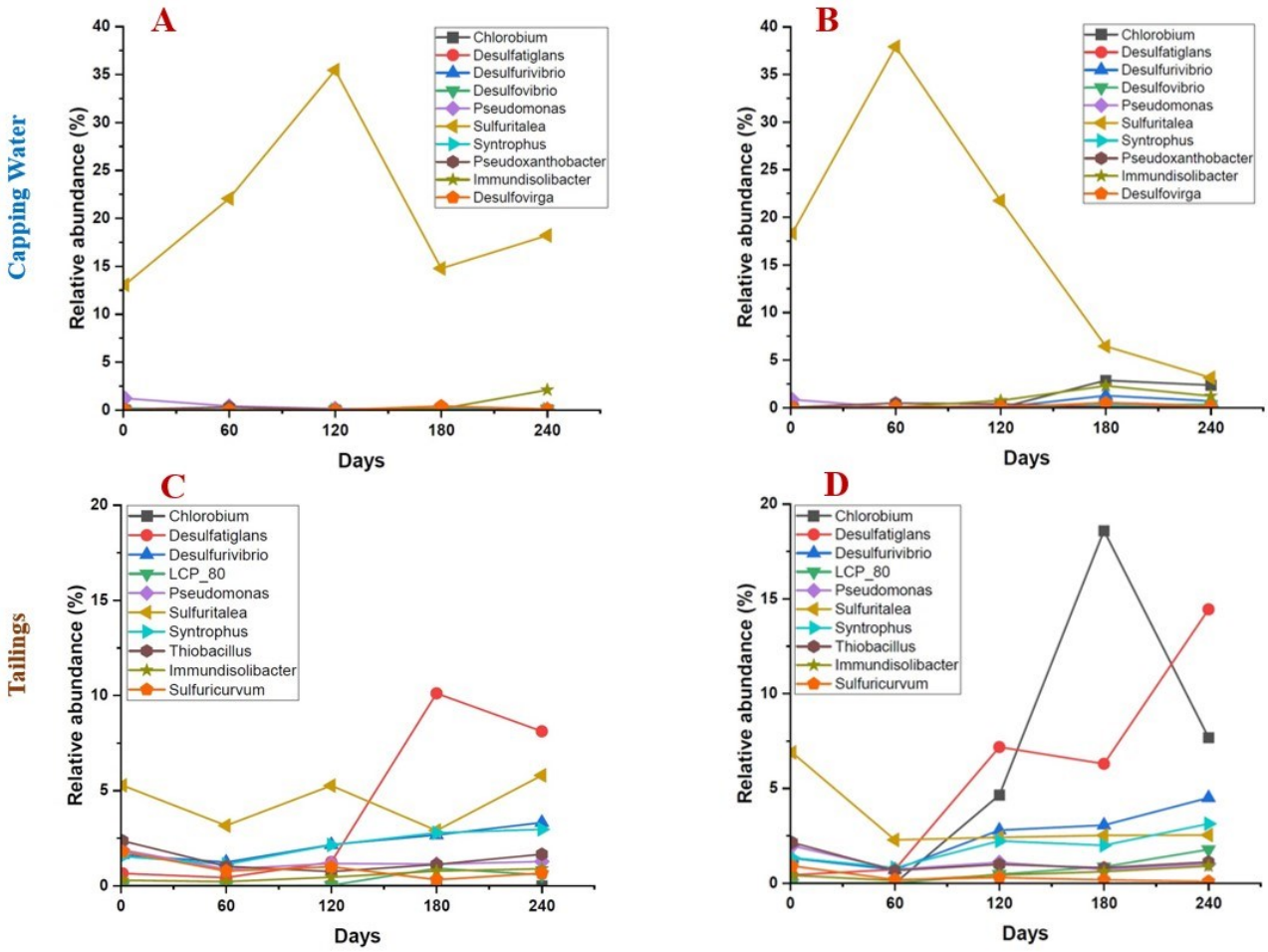

Figure 3.6: Top 10 microbial communities involved in sulfur cycling in (A) Capping water of treatment groups (B) Capping water of control groups (C) Tailings of treatment groups (D) Tailings of control groups

period. In contrast, SOBs and SRBs constituted approximately 33% and 43% respectively of the total assigned sulfur cycling communities in tailings of treatment columns, whereas SOBs and SRBs accounted for roughly 43% and 38% respectively in the control columns (Table A1).

3.3.4.2 Carbon cycling

Total carbon concentration was found to be 141.7 mg/L for control and 153.7 mg/L for treatment groups. Hence, capping water of treatment columns was dominated by organic

compound-degrading bacteria, some of which increased in abundance over the experimental period whereas others decreased in abundance over the same period. Specifically, there was an increase in abundance of *Brevundimonas* (from 0.9% to 6.2%), *Xanthobacter* (from 0.8% to 9.0%) and *Magnetospirillum* (from 0% to 2.5%) whereas there was a decrease in abundance of *Sphingobium* (from 0.95% to 0.92%), *Oceanibaculum* (from 1.5% to 0.08%) and *Pseudomonas* (from 1.2% to 0.02%). Furthermore, carbon-fixing Cyanobacteria, *Cyanobium gracile* PCC 6307 was abundant initially but decreased overtime (from 4.6% to 0.07%). In addition, there was an increase in abundance of methanotrophs such as *Methylovulum* (from 0% to 4.6%) and *Methyloversatilis* (from 0.3% to 0.9%) (Figure 3.7A). In contrast, the control columns of the capping water displayed different abundances for these bacteria over the same period. Specifically, there was an increase in *Brevundimonas* (from 1.0% to 5.4%), *Xanthobacter* (from 0.9% to 6.8%), and *Magnetospirillum* (from 0.06% to 0.9%) whereas there was a decrease in *Sphingobium* (from 2.9% to 1.7%), *Oceanibaculum* (2.2% to 0.01%), and *Pseudomonas* (from 0.8% to 0.1%). Meanwhile, *Cyanobium gracile* PCC 6307 decreased from 4.6% to 0%, whereas *Methyloversatilis* and *Methylovulum* increased from 0.3% to 1.5%, and from 0% to 1.1% respectively (Figure 3.7B).

For tailings, total carbon content was 7.9 mg/kg for control and 7.81 mg/kg for treatment columns. Hence, tailings of treatment columns were abundantly enriched with syntrophic bacteria *Syntrophus*, increasing from 1.5% to 3.0% over the experimental period. Furthermore, there was an abundance of *Pseudomonas* (from 1.9% to 1.3%) and methanotrophs such as *Methylotenera* (from 0.29% to 0.27%), *Methyloversatilis* (from 0.2% to 0.4%). There was low abundance of organic compound-degrading bacteria, however, a huge spike in the abundance of *Magnetospirillum* was observed on day 60 followed by a sharp decrease by day 180. In the tailings of control columns, *Syntrophus* was equally enriched (from 1.3% to 3.1%). Additionally, there was

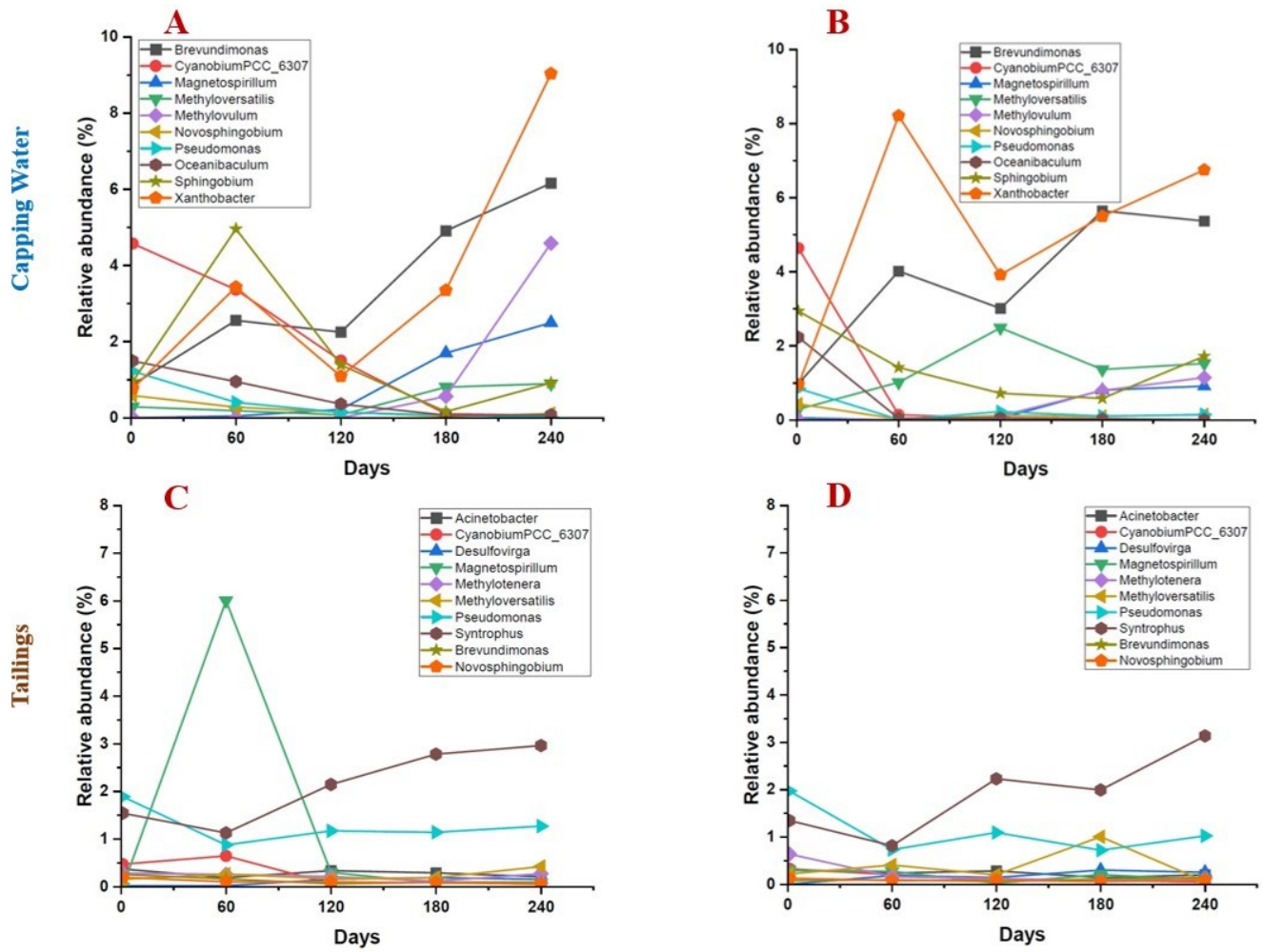

Figure 3.7: Top 10 microbial communities involved in carbon cycling in (A) Capping water of treatment groups (B) Capping water of control groups (C) Tailings of treatment groups (D) Tailings of control groups

abundance of *Pseudomonas* (from 2.0% to 1.0%), methanotrophs including *Methylotenera* (from 0.6% to 0.1%) and *Methyloversatilis* (from 0.2% to 0.1%), and *Magnetospirillum* (from 0.3% to 0.1%) (Figure 3.7C and Figure 3.7D). Notably, both tailings of treatment and control columns showed a very low abundance (0.1%) of methane-producing archaea, *Methanolobus* (Table A2). This observation aligns with the biogenic gas data, which indicated an absence of methane production in the columns. Collectively over the experimental period, approximately 76% and 80% of the assigned carbon cycling communities in capping water were organic compound

degraders in treatment columns and control columns respectively. Additionally, about 13% and 10% of the assigned carbon cycling communities in treatment columns were carbon fixers and methanotrophs respectively while approximately 5% and 15% of the assigned carbon communities in control columns were carbon fixers and methanotrophs respectively. Conversely, in tailings of treatment columns, about 79%, 9% and 2% of the assigned carbon cycling communities were organic compound degraders, methanotrophs and carbon fixers respectively whereas approximately 69%, 17% and 1% of the assigned carbon cycling communities in control columns were organic compound degraders, methanotrophs and carbon fixers respectively. In addition, approximately 0.2% and 1.6% of the assigned carbon cycling communities were methanogens in treatment and control columns respectively (Table A2).

3.3.4.3 Iron cycling

Throughout the experimental period from day 1 to day 240 in capping water, the abundance of Iron II oxidizing bacteria (Fe(II) oxidizers) and Iron III reducing bacteria (Fe(III) reducers) exhibited significant variations between the treatment and control columns. Specifically, in the treatment columns, considerable changes were observed in the abundance of Fe(II) oxidizers, including *Ferritrophicum* (from 0.0% to an average of 4.0%), *Sediminibacterium* (from 0.5% to 0.6%), *Acidovorax* (from 1.2% to 0.7%), *Pseudomonas* (from 1.2% to 0.02%), *Magnetospirillum* (from 0.0% to 2.5%), and *Hydrogenophaga* (from 0.31% to 0.29%). Additionally, Fe(III) reducers in the treatment columns included *Rhodoferax* (from 0.24% to 0.27%) and *Geobacter* (from 0.0% to 0.2%) (Figure 3.8A). These results contrasted with the abundances in the control columns, having *Ferritrophicum* (from 0.0% to 0.4%), *Sediminibacterium* (from 0.3% to 1.9%), *Acidovorax* (from 1.2% to 0.1%), *Pseudomonas* (from 0.8% to 0.1%), *Magnetospirillum* (from 0.1% to 0.9%),

Hydrogenophaga (from 0.4% to 0.1%), *Rhodoferax* (from 0.2% to 0.04%), and *Geobacter* (from 0.02% to 0.1%) (Figure 3.8B).

In tailings, high iron concentration was recorded, i.e. 32.2 mg/kg in treatment and 34.1 mg/kg in the control. As such, the treatment columns revealed the presence of Fe(II) oxidizers including, *Acidovorax* (from 1.3% to 0.4%), *Pseudomonas* (from 1.9% to 1.3%), *Thiobacillus* (from 2.4% to 1.7%), *Ferritrophicum* (from 0.06% to 1.2%), *Hydrogenophaga* (from 0.8% to 0.4%), and *Magnetospirillum* (from 0.0% to 0.1%, but with high abundance of 6.0% on day60). Additionally, there were Fe(III) reducers such as *Geothermobacter* (from 1.5% to 1.6%), and *Rhodoferax* (from 1.0% to 1.0%) (Figure 3.8C). Conversely, the control columns of tailings revealed the presence of *Acidovorax* (from 1.5% to 0.3%), *Pseudomonas* (from 2.0% to 1.0%), *Thiobacillus* (from 2.1% to 1.1%), *Ferritrophicum* (from 0.02% to 0.06%, with abundance of 1.0% on day180), *Hydrogenophaga* (from 0.5% to 0.2%), *Magnetospirillum* (from 0.3% to 0.1%), *Geothermobacter* (from 1.1% to 1.1%), and *Rhodoferax* (from 0.5% to 0.5%) (Figure 3.8D).

Overall, approximately 94% and 4% of the assigned iron cycling communities in treatment columns of capping water were Fe-oxidizers and Fe-reducers respectively over the experimental periods whereas about 94% and 6% of the assigned iron cycling communities in control columns were Fe-oxidizers and Fe-reducers respectively. Conversely, 65% and 28% of the assigned iron cycling communities in treatment columns of tailings were Fe-oxidizers and Fe-reducers respectively while about 59% and 34% of the assigned iron cycling communities in control columns were Fe-oxidizers and Fe-reducers respectively (Table A3).

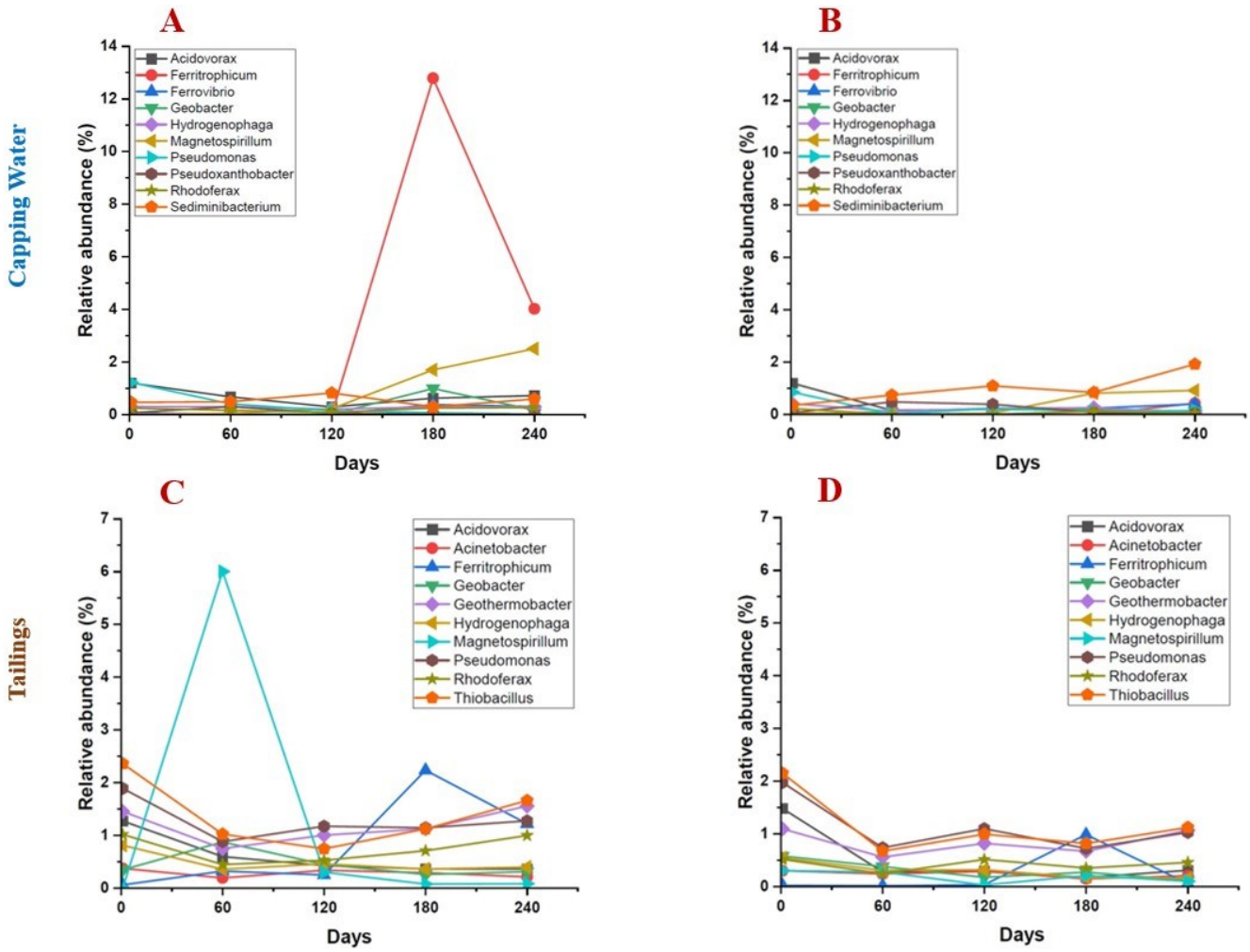

Figure 3.8: Top 10 microbial communities involved in iron cycling in (A) Capping water of treatment groups (B) Capping water of control groups (C) Tailings of treatment groups (D) Tailings of control groups

3.3.4.4 Nitrogen cycling

Total nitrogen (TN) concentration in capping water was recorded to be 0.98 mg/L in control and 2.76 mg/L in treatment columns. Nitrogen-fixing bacterial genera exhibited notable abundance in early days of column's operation, both in the treatment and control columns of the capping water. Specifically, the treatment columns featured copious amounts of cyanobacteria up to day 120 but decreased later. This included *Cyanobium gracile* PCC 6307 (from 4.6% to 0.07%), members of the family Obscuribacteraceae (from 0.4% to 0.3%), members of the order Vampirovibrionales (0.02% to 0.1%), *Azospirillum* (from 0.6% to 0.01%) and *Novispirillum* (from

0.4% to 0.01%). In contrast, the control columns had *Cyanobium gracile* PCC 6307 (decreasing from 4.6% to 0.0%), members of the family Obscuribacteraceae (increasing from 0.12% to 0.13%), members of the order Vampirovibrionales (increasing from 0.005% to 0.1%), *Azospirillum* (decreasing from 0.9% to 0.1%), *Niveispirillum* (increasing from 0.4% to 0.2%), *Magnetospirillum* (increasing from 0.06% to 0.9%), and *Pseudomonas* (decreasing from 0.8% to 0.1%) as the most abundant phylotypes (Figure 3.9A and Figure 3.9B). Furthermore, there was the presence of *Acinetobacter*, known for nitrification-denitrification in control columns (Table A4).

In tailings, TN concentration was recorded to be 11 mg/kg for control and 10 mg/kg for the treatment group. As such, treatment and control columns harbored a significant proportion of nitrogen-associated bacteria. Notably, the treatment columns revealed high abundance of *Pseudomonas* (from 1.9% to 1.3%), *Thauera* (from 1.6% to 1.7%), and *Thiobacillus* (from 2.4% to 1.7%) as well as a low abundance of *Magnetospirillum* (from 0.0% to 0.1%, though there was a relatively high abundance of 6.0% on day60). Furthermore, there was a relatively low abundance *Cyanobium gracile* PCC 6307 (from 0.5% to 0.05%) and *Rhizobium* (from 0.4% to 0.2%) as well as the nitrifying-denitrifying *Acinetobacter* (from 0.4% to 0.2%) (Figure 3.9C). In contrast, the control columns revealed abundant presence of *Thiobacillus* (from 2.1% to 1.1%), *Pseudomonas* (from 2.0% to 1.0%), and *Thauera* (from 1.0% to 1.2%). Additionally, there was relatively low abundance of *Magnetospirillum* (from 0.3% to 0.1%), *Acinetobacter* (from 0.3% to 0.2%), *Cyanobium gracile* PCC 6307 (from 0.3% to 0.05%), and *Rhizobium* (from 0.5% to 0.04%) (Figure 3.9D)

The overall average abundances of the assigned nitrogen cycling communities in the capping water of treatment columns over the experimental period were approximately 61%, 29% and 0.3% respectively for nitrogen fixers, denitrifying bacteria, and nitrifying bacteria whereas the

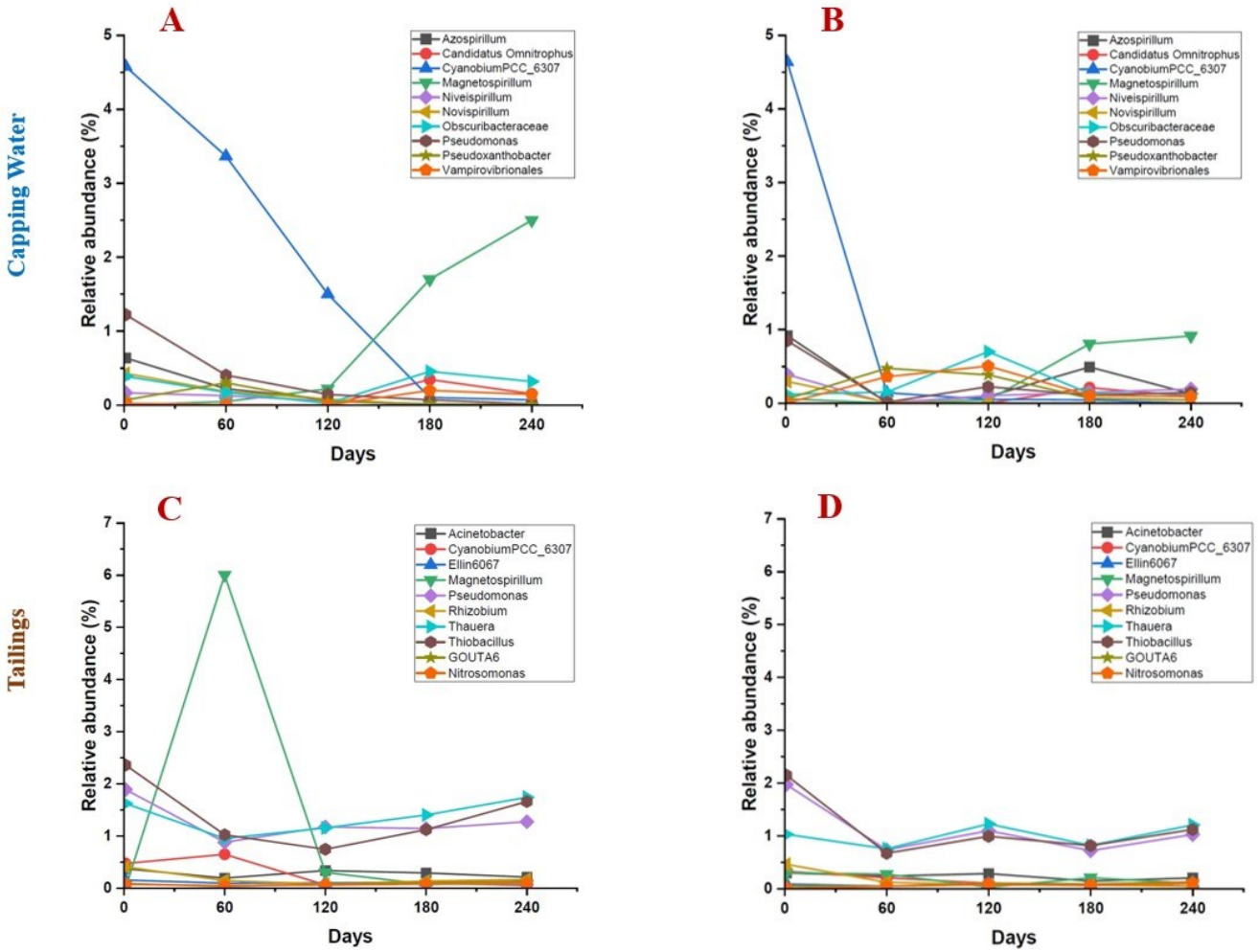

Figure 3.9: Top 10 microbial communities involved in nitrogen cycling in (A) Capping water of treatment groups (B) Capping water of control groups (C) Tailings of treatment groups (D) Tailings of control groups

average abundances were respectively about 64%, 27% and 3% in control columns. In contrast, the average abundances in tailings were approximately 4%, 67%, and 4% respectively for nitrogen fixers, denitrifying bacteria, and nitrifying bacteria in treatment columns while the average abundances were approximately 2%, 66%, and 4% respectively for nitrogen fixers, denitrifying bacteria, and nitrifying bacteria in treatment columns (Table A4).

3.3.5 Patterns of temporal changes in bacterial community structures

The Pearson r correlation analysis revealed temporal shifts in the abundance of genera involved in sulfur, carbon, iron, and nitrogen cycling throughout the experimental period. For sulfur cycling, there were 20 genera with positive correlations with time and 5 genera with negative correlations in capping water, while tailings had 8 genera with positive correlations and 17 genera with negative correlations (Figure 3.10). For carbon cycling, capping water showed 10 positive and 14 negative correlations, whereas tailings presented 11 positive and 14 negative correlations (Figure 3.11). In iron cycling, there were equal numbers of positive and negative correlations (10 each) in capping water, compared to 15 positive and 10 negative correlations in tailings (Figure 3.12). For nitrogen cycling, 12 positive and 10 negative correlations were found in capping water, in contrast to 17 positive and 8 negative correlations in tailings (Figure 3.13).

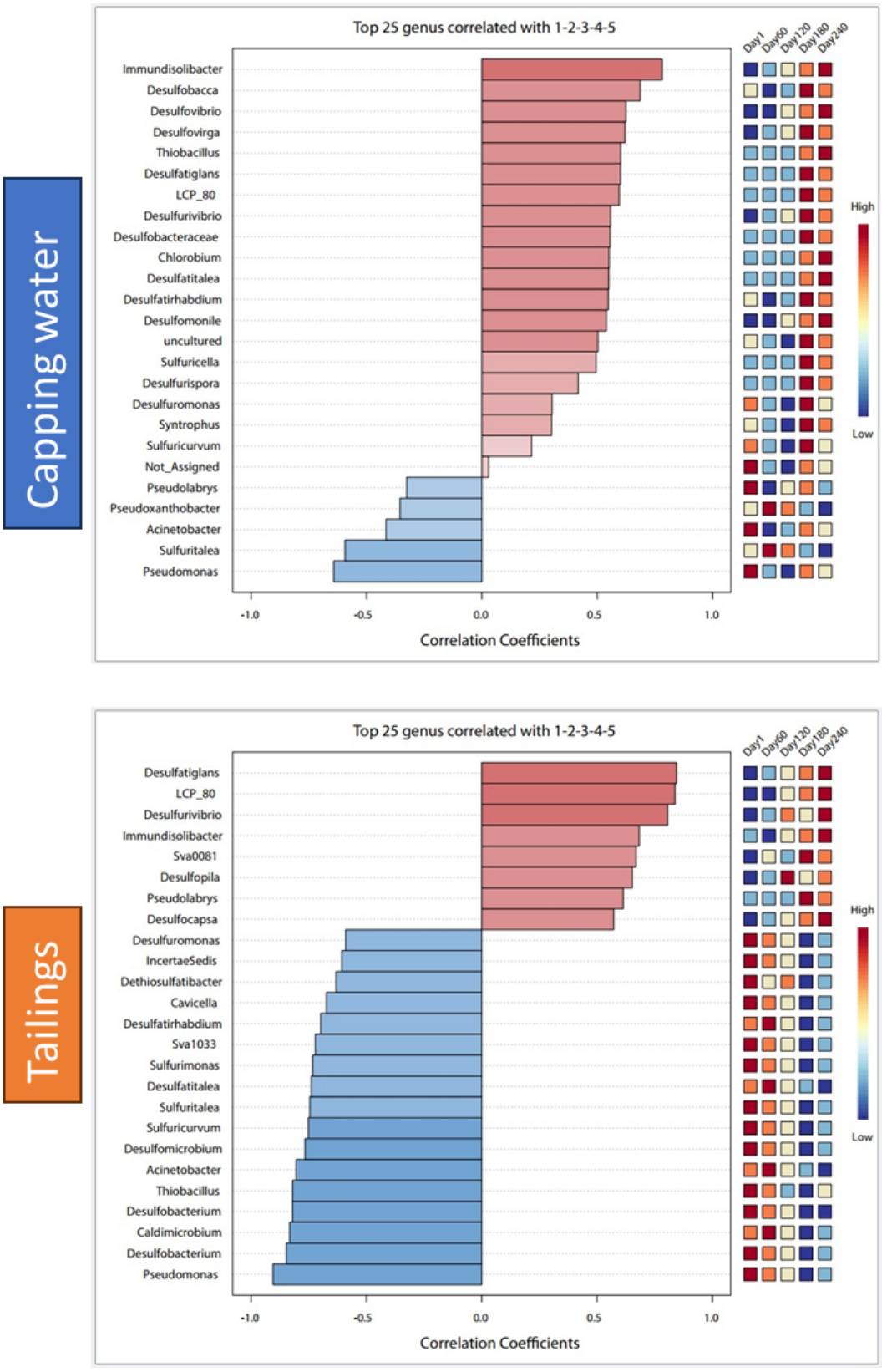

Figure 3.10: Top sulfur-cycling genera with distinct correlation in capping water and tailings

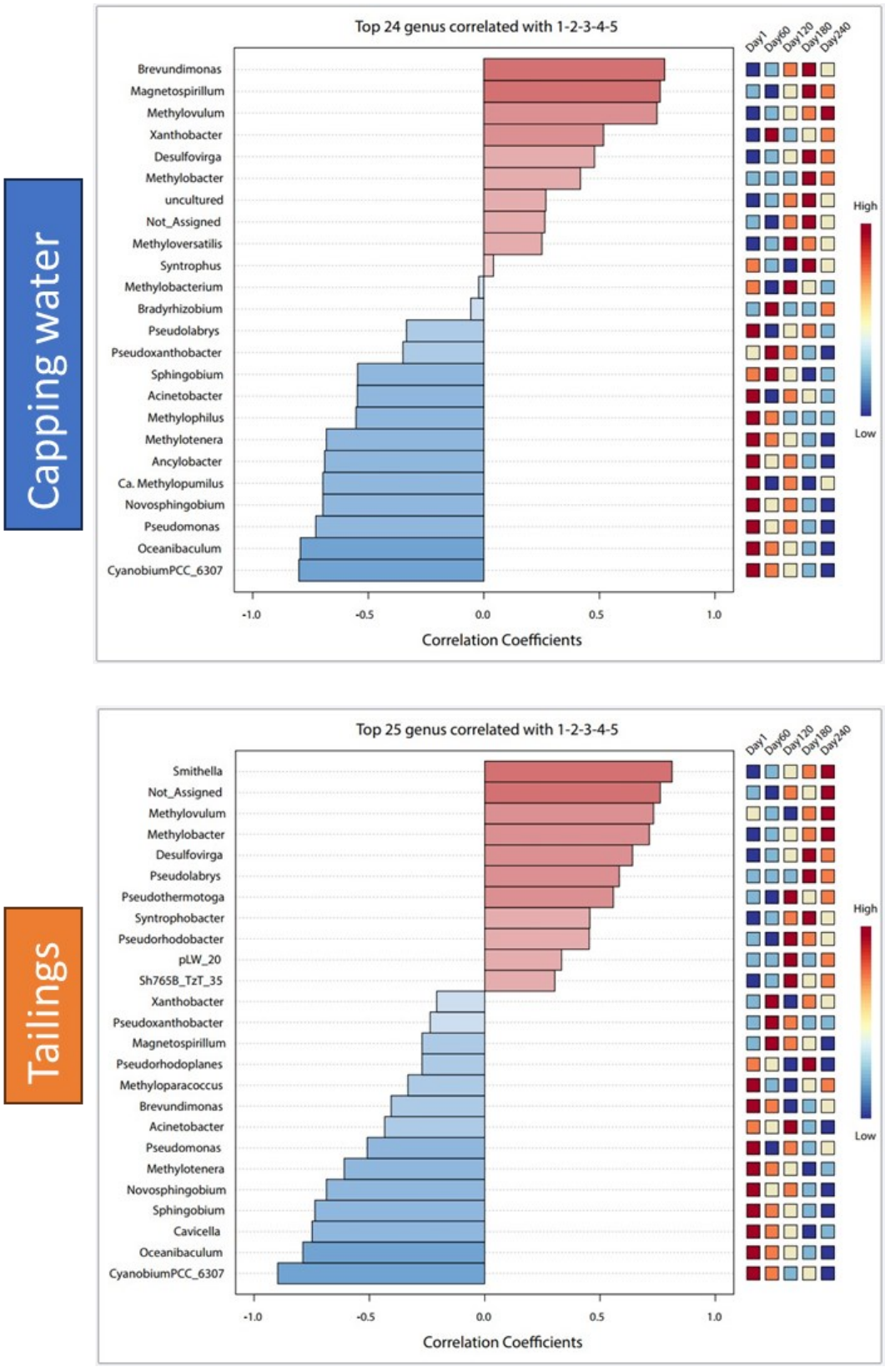

Figure 3.11: Top carbon-cycling genera with distinct correlation in capping water and tailings

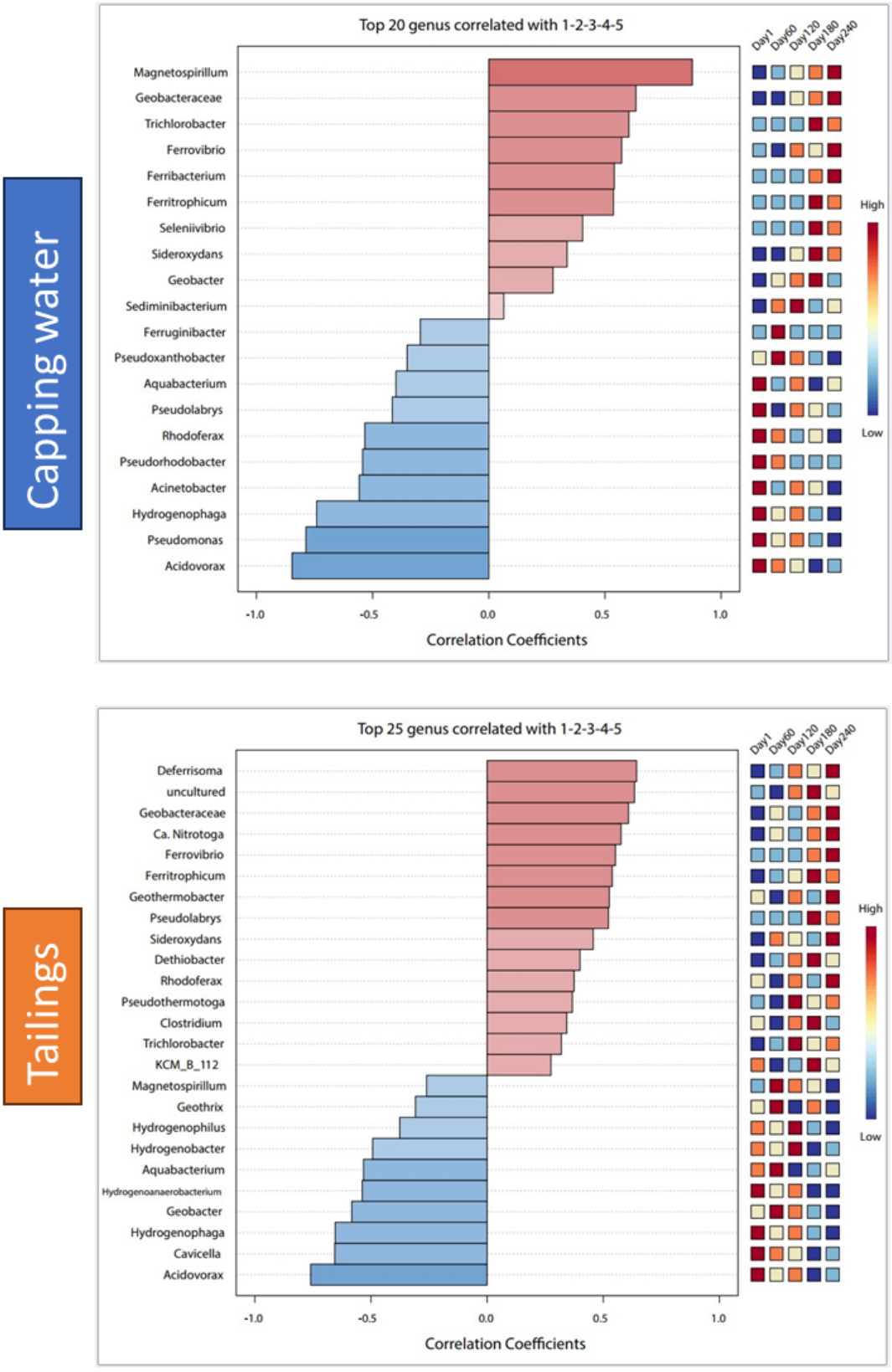

Figure 3.12: Top iron-cycling genera with distinct correlation in capping water and tailings

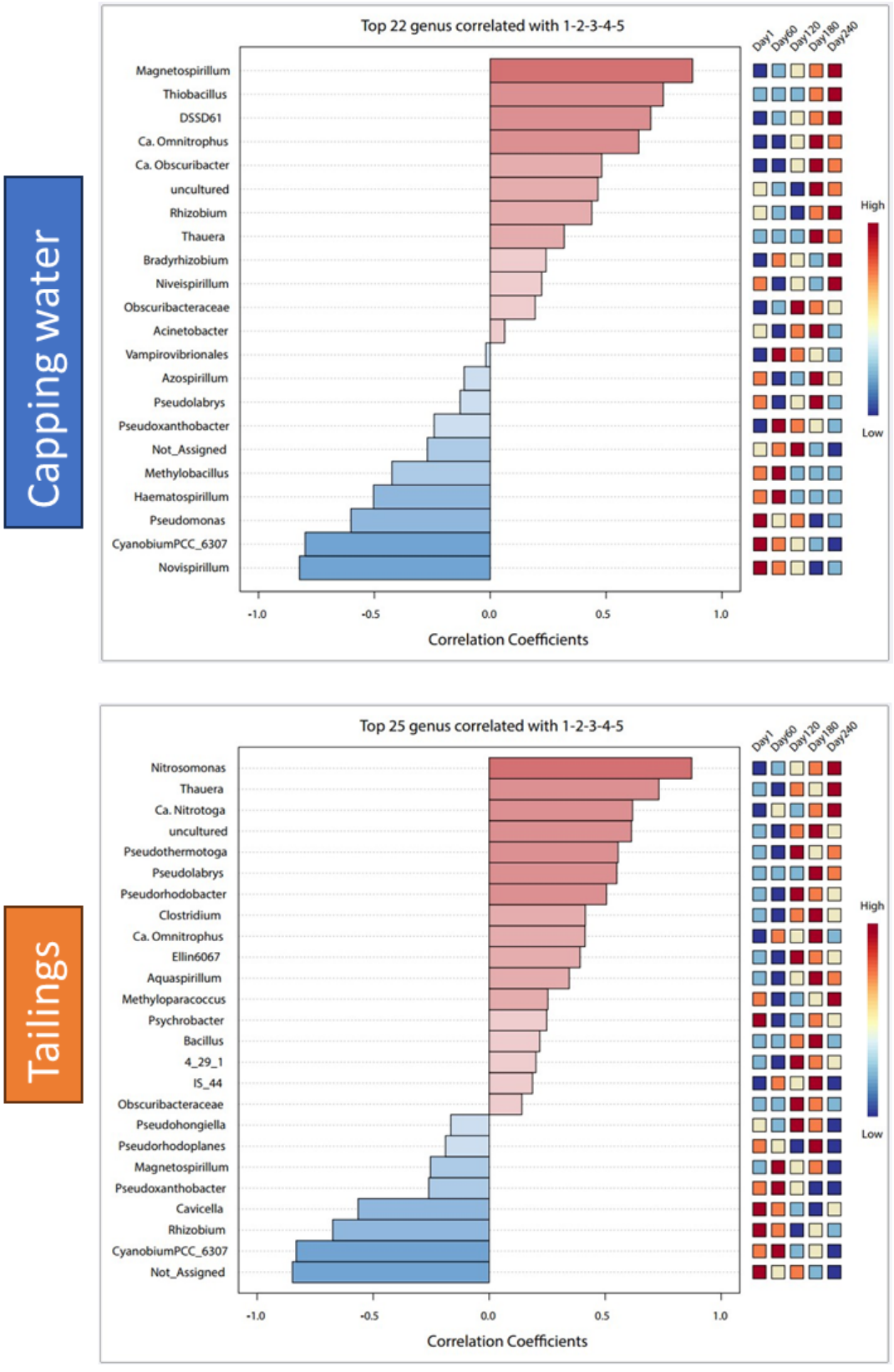

Figure 3.13: Top nitrogen-cycling genera with distinct correlation in capping water and tailings

3.3.6 Active bacterial communities

To identify the actively transcribing bacteria, c-DNA from extracted RNA where sequenced. The results showed that key sulfur genera such as *Desulfatiglans, Sulfuritalea, Thiobacillus, Synthrophus, Desulfatirhabdium, Desulfurivibrio* and *Chlorobium* were likely responsible for the observed sulfur cycling processes. Similarly, genera that were actively responsible for the cycling of carbon, iron and nitrogen were abundant (Figure 3.14). The active bacterial communities were different in abundance between treatment and control groups, however no specific pattern could be discerned. For example, the abundance of *Desulfatiglans* in bottom tailings of control column was reduced from 50.8% to 0%, then was enriched to 32.4% before being reduced to 0% at the end. Meanwhile in bottom tailings of treatment column, it was reduced from 43.2% to 3.8%, then enriched to 15.7% before being reduced to 2% at the end of the end. The other genera showed a similar pattern in abundance distribution.

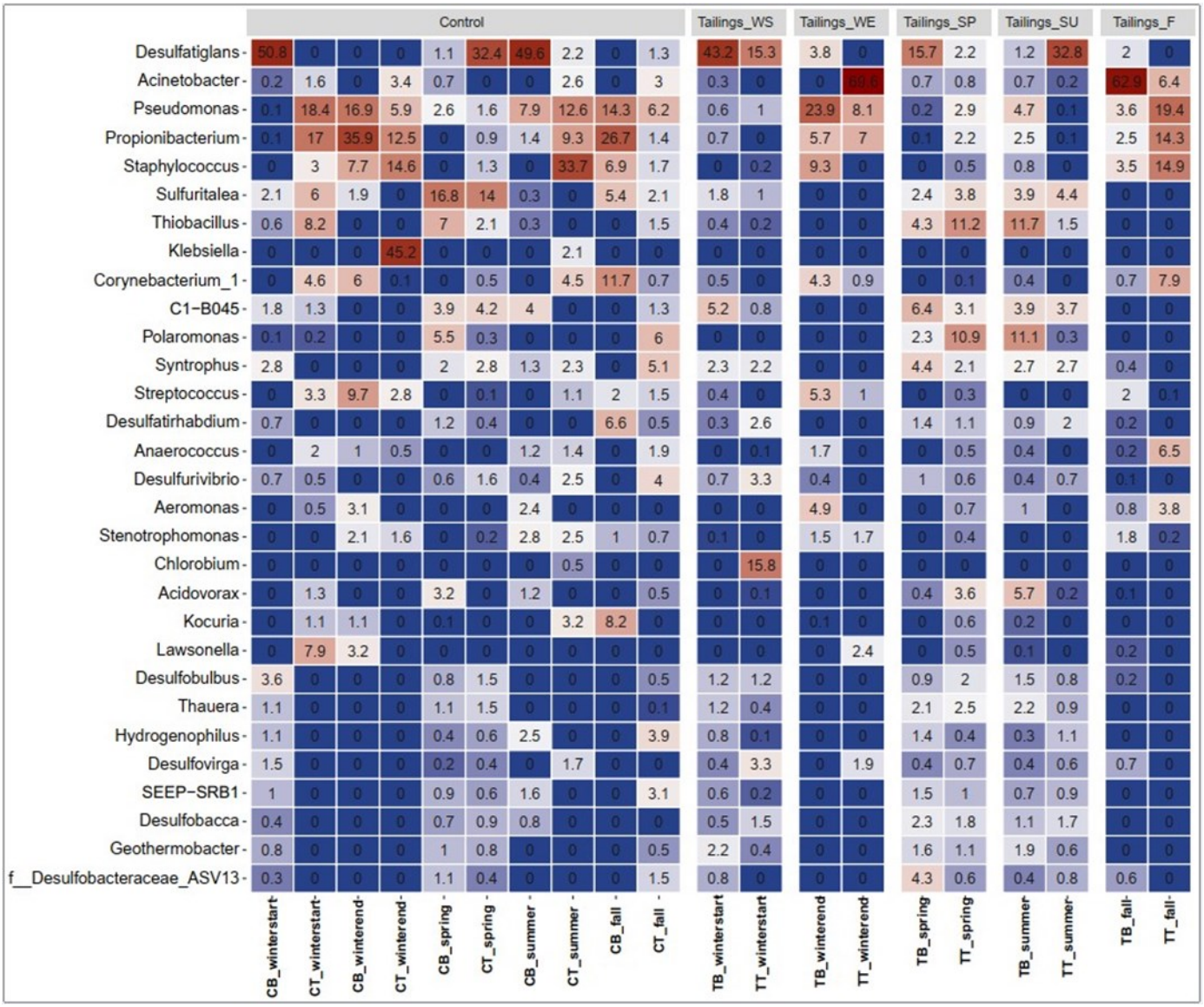

Figure 3.14: Heatmap showing the top active bacterial communities (RNA). CB = control bottom; CT = control top; TB = treatment bottom; TT = treatment top; _WS = winter start; _WE = winter end; _SP = spring; _SU =summer; _F = fall

3.4 Discussion

3.4.1 Changes in physicochemical properties of capping water

Evaluation of the physicochemical characteristics of capping water (Table 3.1) revealed notable increments in the concentrations of dissolved organics. Specifically, there were elevations in the concentrations of DOC, COD and NAs when compared to background water concentration (Table 2.1). This increase in concentrations indicated that there was transfer of porewater containing dissolved organics from the underlying tailings into the capping water due to advective chemical fluxes driven by tailings consolidation (Cossey et al., 2021; Dompierre et al., 2017). Furthermore, the results of DO, conductivity, and sulfate concentrations (Table 3.1) showed significant differences between treatment and control columns. Specifically, the DO had an inverse relationship with temperature due to poor oxygen solubility. It has been established that DO in a pit lake directly influences biogeochemical processes and fate of organics in the system by dictating the nature of microbial communities and the processes they favor (Chen et al., 2013; Vandenberg et al., 2011). For example, aerobic microbial communities dominate oxygen-rich environments, facilitating processes like nitrification and organic matter decomposition. Whereas in oxygen-poor environments, anaerobic microbial communities thrive, leading to processes like sulfate reduction, denitrification and methanogenesis (Albakistani et al., 2022; Alewell et al., 2006). In this study, due to low mixing, both oxic and anoxic conditions were developed in the capping water, thus supporting the development of both aerobic bacteria and facultative anaerobic bacteria. In contrast, conductivity exhibited a positive correlation with temperature, diminishing during periods of lower temperatures in treatment columns and subsequently rising as temperatures increased. Traditionally, conductivity has served as a broad indicator of water quality, reflecting the concentration of ionic species in water (Hayashi, 2004). High conductivity often indicates

elevated levels of salts and nutrients, which can influence microbial community composition by favoring halotolerant or halophilic microorganisms (Ayayee et al., 2024). Specific ions contributing to conductivity, such as sulfate, chloride, and metals, can have distinct effects on microbial communities which could potentially influence nutrient cycling (Muyzer and Stams, 2008). The combined effect of DO and conductivity can create complex habitats where different microbial communities coexist. For instance, highly conductive and anoxic environments, could create specific niches for sulfate-reducing and methanogenic microbial communities, contributing to unique biogeochemical cycles (Bell et al., 2022; Wolfe and Wilkin, 2017). In our system, both oxic and anoxic microenvironments co-existed, thus supporting different microbial communities. PASS technology involved the addition of alum, which on dissociation, would release sulfate ions into the water column. At lower temperatures, the dissociation of alum and the solubility of sulfate in water are generally reduced resulting in fewer sulfate ions being released from the alum into the water column (Stumm and Morgan, 1996). Furthermore, the activity of SRB decreases at lower temperatures, reducing the rate of sulfate reduction to hydrogen sulfide thereby leading to an accumulation of sulfate in the water column (Muyzer and Stams, 2008). Conversely, higher temperatures increase the dissociation rate of alum, leading to more sulfate ions being released into the water column (Stumm and Morgan, 1996). Also, the metabolic rates of microorganisms, including SRBs increase at higher temperature, leading to more rapid sulfate reduction and potentially lower sulfate concentrations in the water column if conditions favor microbial sulfate reduction (Muyzer and Stams, 2008).

Meanwhile, there were no significant changes between treatment and control columns for DOC, COD, TKN, NO_2+NO_3-N, pH, NAs, and turbidity (Table 3.1), suggesting that temperature variations did not exert a pronounced effect on the advective movement of dissolved organics and

suspended particles. This could be attributed to the nature of the experimental columns which permitted little turbulence and no flow, thus resulting in limited temperature effect on settling (Lau, 1994). The short timeline of two months for each temperature period might also play a role, thus future research might need to consider longer timeline. Interestingly, there were temporal changes in these parameters in both treatment and control columns, indicating a shift over time. Specifically, there was an upward trend in COD, DOC, NAs, and TKN over time, while turbidity, NO_2+NO_3-N, and pH exhibited a declining pattern (Figure 3.15). This suggested a continual release of dissolved organics into the capping water from the underlying tailings (Dompierre et al., 2017). Moreover, TKN results revealed an initial concentration decrease followed by an increase, indicating the utilization of residual organic nitrogen and ammonia nitrogen by microbial communities before the degradation of PAM to nitrogenous compounds, likely in this scenario, through hydrolysis of amide groups by amidase enzymes (Li et al., 2023; Nyyssölä and Ahlgren, 2019). Conversely, the decline in turbidity was likely a result of the agglomeration of suspended particles in the capping water caused by alum and PAM (Gonçalves et al., 2019). Meanwhile, reduction in NO_2+NO_3-N was probably attributable to denitrification, leading to the production of nitrogen gas (Seitzinger et al., 2006). The observed pH decrease could be attributed to the transformation of dissolved organics into organic acids (e.g., acetate) via fermentation or microbial oxidation of sulfur compounds resulting in acidification (Arslan and Gamal El-Din, 2021; Vigneron et al., 2021). Additionally, it could be linked to the reaction of carbon dioxide, produced during the biodegradation of dissolved organics, with water, forming carbonic acid (Cossey et al., 2021; West et al., 2001).

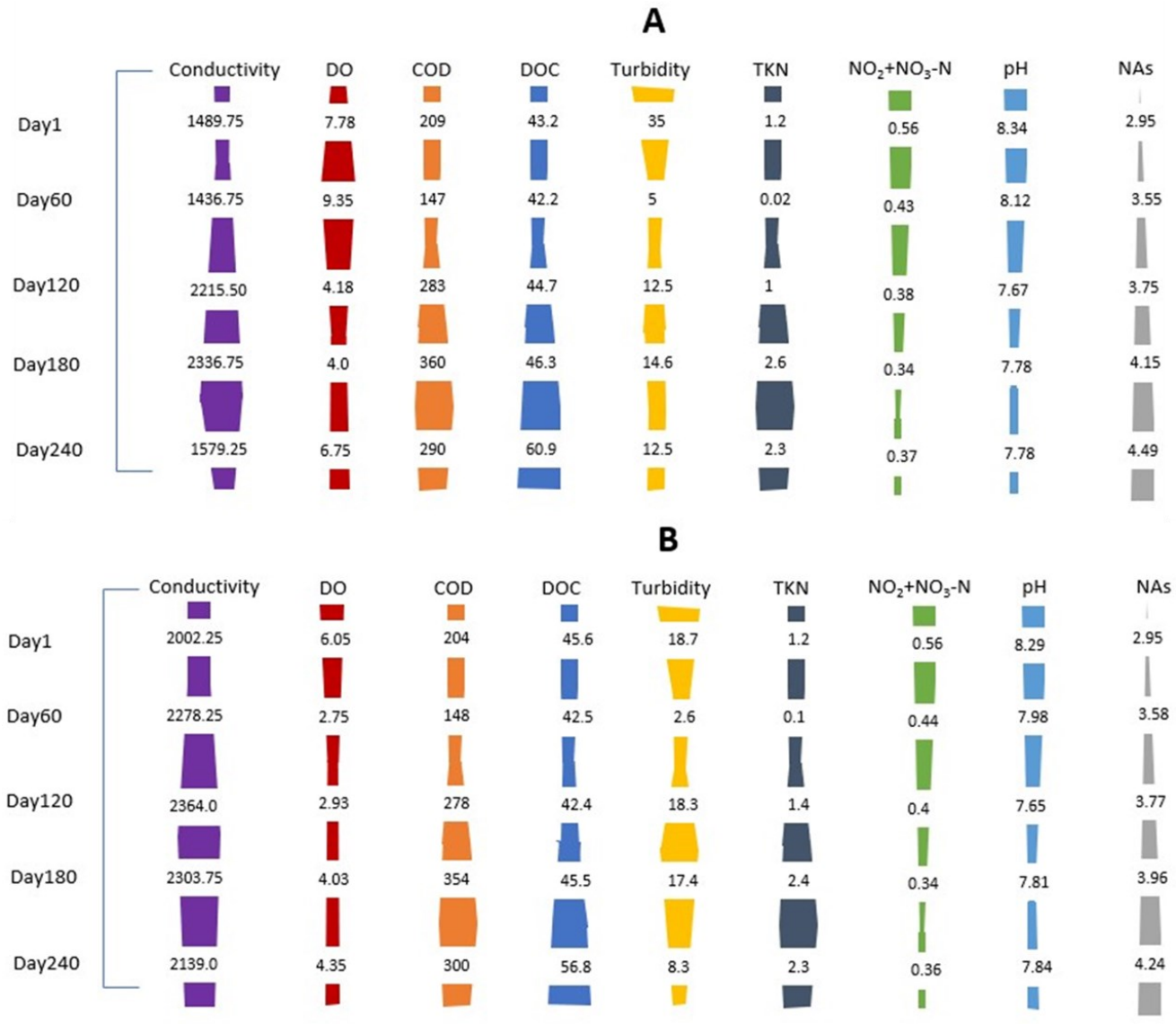

Figure 3.15: Temporal changes in physico-chemical parameters in (A) treatment, and (B) control. DOC: dissolved organic carbon, COD: chemical oxygen demand, TKN: total Kjeldahl nitrogen, DO: dissolved oxygen, NTU: Nephelometric Turbidity Units, NO2+NO3-N: nitrite and nitrate-nitrogen, NAs: naphthenic acids

3.4.2 Diversity of bacterial communities in PASS-treated pit lakes

The examination of the diversity of bacteria community structures within PASS-treated pit lakes has revealed distinct differences between the capping water and tailings. This could be attributed to the inherent differences in physical and chemical properties between capping water and tailings microenvironment of pit lakes. Previous studies have shown that different habitats

exhibit different levels of alpha, beta, and gamma diversity of bacteria (Walters and Martiny, 2020). Interestingly, temperature changes in both the capping water and tailings did not significantly affect bacterial diversity, suggesting that these microenvironments harbor stable and resilient bacterial communities capable of withstanding temperature fluctuations between the treatment and control groups (Shade et al., 2012). Additionally, the diversity analysis indicated a high diversity index in PASS-treated pit lakes. For instance, the Shannon diversity index (H) typically ranges between 1.5 and 3.5 for most ecological settings, with higher H values indicating a higher degree of biogeochemical cycling (Arslan and Gamal El-Din, 2021). In this study, H was ≥3.5 in both capping water and tailings, aligning with the observed high levels of biogeochemical cycles (see Chapter 3.4.3). While there were differences in species richness between capping water and tailings (Figure A2) and between treatment and control groups (Figure A3), not all samples reached a plateau. This suggested that there was an under-sampling of some samples however, this was likely due to the nature of tailings. Environmental structures are known to affect species richness (Junkins et al., 2022), and DNA extraction for oil sands tailings has been very challenging (Foght, 2015).

3.4.3 Temporal changes on biogeochemical cycles of PASS-treated pit lakes

3.4.3.1 Sulfur cycling

Alum, which was added during PASS treatment as coagulant, is subject to dissociation upon contact with water, thereby forming aluminium hydroxide flocs which enhance tailings settling (Jessen et al., 2022). This would also introduce sulfate into the system which could alter microbial community structure, function, and thus ecological outcomes by enhancing sulfur cycling (Jessen et al., 2022). The analysis of phylotypes known for sulfur cycling in treatment

columns and control columns (Figure 3.6A-D) revealed the presence of varying abundances of SOB and SRB in both treatment and control columns. Specifically, the capping water of both treatment and control columns was dominated by SOB, *Sulfuritalea*, the abundance of which decreased overtime in both columns at different rate. Furthermore, other SOBs such as *Immundisolibacter*, *Thiobacillus*, and *Sulfuricurvum* in treatment columns and, *Chlorobium* and *Immundisolibacter* in control columns were present at different low abundances, suggesting the influence of temperature. Moreover, SRBs such as *Desulfovirga* and *Desulfovibrio*, were observed in both treatment and control columns, indicating that high sulfur oxidation and low sulfate reduction were occurring concurrently. Although differences in microbial abundances were noted between treatment and control columns, no discernible pattern of temperature effects on bacterial community structures could be discerned. Comparatively, the microbial community structures in the tailings exhibited significant differences from those in the capping water. In treatment columns, *Sulfuritalea*, *Desulfatiglans*, and *Desulfurivibrio* dominated, with varying abundances over the experimental period. Conversely, control columns had a different composition, featuring the abundance of *Desulfatiglans*, *Chlorobium*, *Sulfuritalea*, and *Desulfurivibrio*. The observed variations in microbial composition underscored the influence of temperature on tailings microbial communities, however no apparent temperature-related patterns were evident in the bacterial community structures. The sulfur cycling was likely initiated by abundant SRBs such as *Desulfatiglans*, *Desulfurivibrio*, and *Desulfuromonas* found in tailings which utilized sulfate as terminal electron acceptor and dissolved organics as electron donor to produce sulfide or sulfur (Holmer and Storkholm, 2001; Liamleam and Annachhatre, 2007). The sulfide might then be oxidized by facultative anaerobes such as *Thiobacillus*, *Sulfuricurvum*, and *Sulfurimonas*, while sulfur might be oxidized by *Sulfuritalea* and *Immundisolibacter* to produce sulfate. Some

facultative autotrophic denitrifying bacteria such as *Pseudomonas* had also been reported to utilize sulfide as electron donors for denitrification (Guo et al., 2013). This shows that a complete sulfur cycling involving reductive and oxidative processes was occurring within PASS treated tailings (Figure 3.16A and Figure 3.16B).

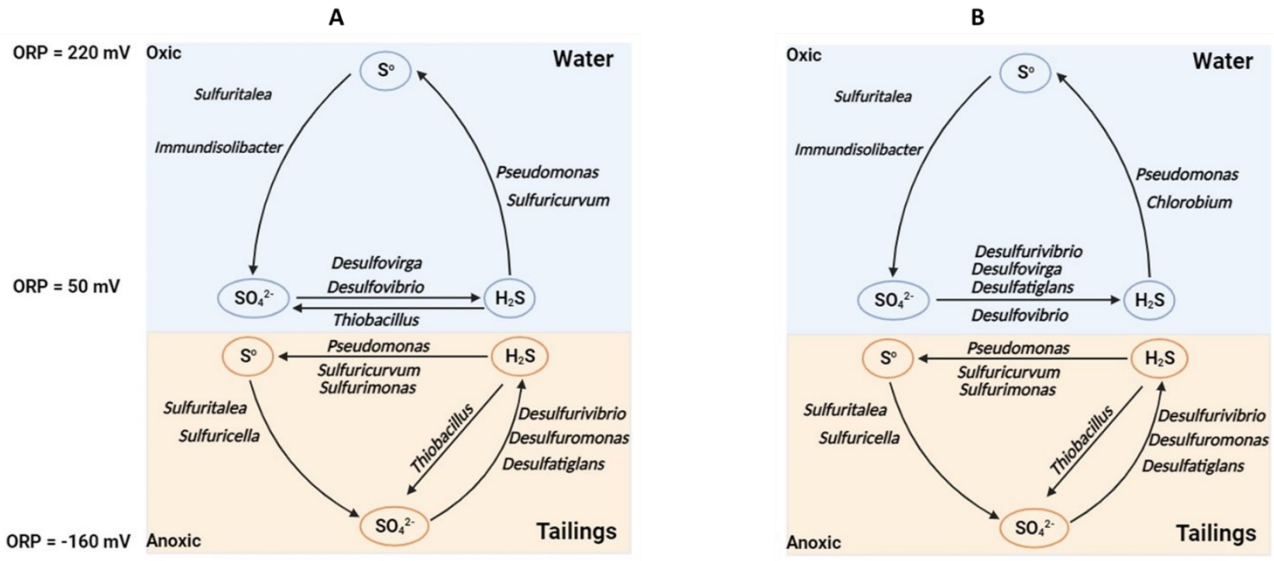

Figure 3.16: Schematic diagram of biogeochemical cycles in pit lake containing PASS-treated tailings showing (A) Sulfur cycling in treatment columns (B) Sulfur cycling in control columns

3.4.3.2 Carbon cycling

Elevated concentrations of dissolved organics were observed in the capping water of both treatment and control columns, which indicated the availability of organic compounds through advective transfer from the underlying tailings. Analysis of phylotypes involved in carbon cycling revealed varying abundances of organic compound-degrading bacteria such as *Xanthobacter*, *Brevundimonas*, *Magnetospirillum*, *Oceanibaculum*, and *Sphingobium* in capping water of both treatment (Figure 3.7A) and control columns (Figure 3.7B) suggesting that their abundances were affected by temperature variations. In addition, methanotrophs such as *Methyloversatilis*,

Methylovulum, and *Methylotenera* equally had varied abundances in capping water. They were probably selected due to availability of carbon-1 compounds such as methane, originally produced in the tailings but which later bubbled up in water column (Arslan et al., 2021). The metabolic action of organic compounds-degrading bacteria and methanotrophs would likely produce CO_2 which could be fixed by *Cyanobium PCC_6307* and other cyanobacteria in the capping water (Allaf and Peerhossaini, 2022). Furthermore, SRBs which were abundant in tailings, are known to use sulfate as electron acceptor for the degradation of organic compounds (Li et al., 2018) into organic intermediates which could then the utilized by the abundant *Syntrophus*. Though gas analysis revealed the absence of methane gas (Figure 3.3), methanogens represented by *Methanolobus*, and methanotrophs were present at comparatively low abundance in tailings. This indicated that high sulfate reduction and low methanogenesis were likely co-existing (Sela-Adler et al., 2017). It is possible that anaerobic oxidation of methane was likely being carried out by methanotrophs, which is important for carbon cycling (Cabrol et al., 2020) (Figure 3.17A and Figure 3.17B). Interestingly, sulfur cycling, nitrogen cycling, and iron cycling have steps that require the oxidation of organics to intermediate compounds or CO_2 and therefore play important roles in carbon cycling (Li et al., 2012).

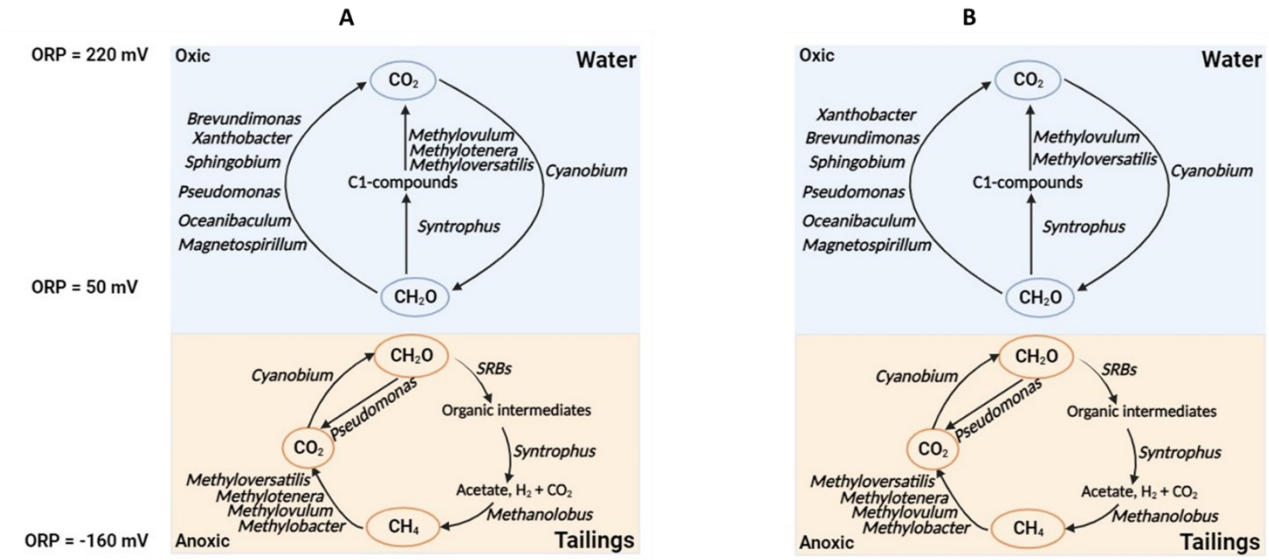

Figure 3.17: Schematic diagram of biogeochemical cycles in pit lake containing PASS-treated tailings showing (A) Carbon cycling in treatment columns (B) Carbon cycling in control columns

3.4.3.3 Iron cycling

The process of iron cycling involves the reduction of Fe(III) to Fe(II) and the subsequent re-oxidation of Fe(II) to Fe(III) (Siddique et al., 2019). Analysis of phylotypes related to iron cycling revealed significant differences in abundances between the treatment and control columns (Figure 3.8A-D). In capping water, there was a notable prevalence of Fe(II) oxidizers such as *Ferritrophicum*, *Sediminibacterium*, *Acidovorax*, *Pseudomonas*, *Magnetospirillum*, and *Hydrogenophaga*, compared to Fe(III) reducers like *Geobacter* and *Rhodoferax*. Conversely, the tailings exhibited high abundances of both Fe(II) oxidizers and Fe(III) reducers, with presence of *Geothermobacter* and *Deferrisoma* in addition to *Geobacter* and *Rhodoferax* found in the capping water. This discrepancy in the abundance patterns of Fe(II) oxidizers and Fe(III) reducers suggests active iron cycling, involving both oxidation and reduction of iron, in capping water and tailings (Figure 3.18A and Figure 3.18B). The elemental analysis results further support these

observations, indicating Fe deposits of 32.18 mg/kg and 34.06 mg/kg in the tailings from the treatment and control columns, respectively (Table A5). Interestingly, previous research has highlighted the interconnectedness of the biogeochemical cycle, specifically linking the iron cycle to sulfur, carbon, and nitrogen cycles through the processes of Fe(II) oxidation and Fe(III) reduction (Otte et al., 2018).

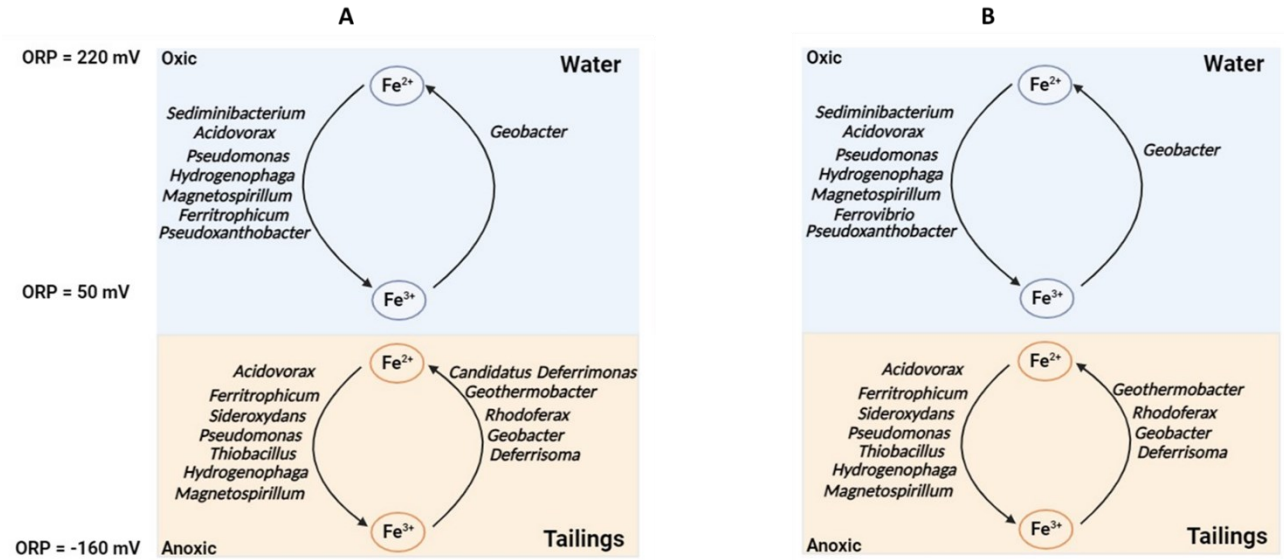

Figure 3.18: Schematic diagram of biogeochemical cycles in pit lake containing PASS-treated tailings showing (A) Iron cycling in treatment columns (B) Iron cycling in control columns

3.4.3.4 Nitrogen cycling

PAM is known to degrade gradually over time, with minimal likelihood of causing environmental issues beyond the lake's confines (Xiong et al., 2018). Acrylamide, a monomer of PAM, is readily biodegradable, ensuring low concentrations within the lake ecosystem, as observed in the previous chapter (Figure 2.9). PAM addition during PASS treatment could produce nitrogenous intermediates upon degradation which would promote nitrogen cycling (Intrinsik Corp., 2022). The introduction of PAM may have further promoted the biodegradation of other

organic compounds through a process that transitions from ammonification to nitrification in the oxygen-rich capping water, and ultimately to denitrification within the tailings, involving microorganisms such as *Thauera* and *Magnetospirillum*. This finding corroborates with the abundance of *Thauera* and *Magnetospirillum* in the system.

Phylotypes known for nitrogen fixation, nitrification and denitrification were found in the capping water and tailings of treatment and control columns. The capping water of both treatment and control columns were dominated by nitrogen-fixing bacterial genera but with distinct abundances for each experimental column (Figure 3.9A-B). Given that ample fixed nitrogen was present, the nitrogen fixing bacteria were observed to rapidly decline over time, suggesting that further nitrogen fixation was unlikely to be taking place (Vitousek and Howarth, 1991). Furthermore, *Magnetospirillum* which has been reported to be capable of both nitrogen fixation due to the presence of nitrogenase enzyme (Bazylinski et al., 2000) and denitrification by using dissolved organics as electron donor and nitrate as electron acceptor (Shinoda et al., 2005) was of higher abundance in the treatment column of capping water.

In tailings, *Thauera*, *Thiobacillus* and *Pseudomonas* were the dominant phylotypes, but with distinct abundances in treatment and control columns (Figure 3.9C-D). These phylotypes have been reported to carry out denitrification under both oxic and anoxic conditions (Li et al., 2022; Takaya et al., 2003). Additionally, *Acinetobacter* known to be capable of both nitrification and denitrification (Zhao et al., 2021) was equally abundant in treatment and control columns. Interestingly, *Acinetobacter* and *Pseudomonas* species isolated from soil and dewatered sludge have been reported to be capable of degrading PAM through deamination of the amide group (Joshi and Abed, 2017). These results collectively suggest that the addition of PAM during PASS

treatment likely promoted nitrogen cycling through nitrification, denitrification, and nitrogen fixation (Figure 3.19A and Figure 3.19B).

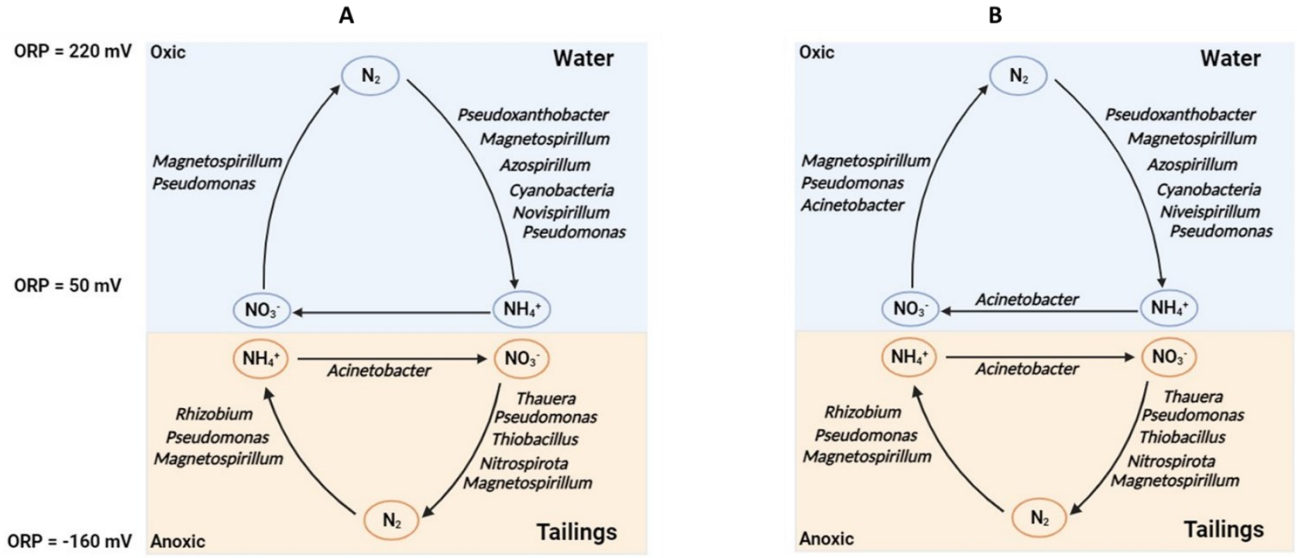

Figure 3.19: Schematic diagram of biogeochemical cycles in pit lake containing PASS-treated tailings showing (A) Nitrogen cycling in treatment columns (B) Nitrogen cycling in control columns

3.4.4 Patterns of temporal changes in bacterial community structures

The bacterial communities in capping water and tailings changed overtime with some genera increasing in abundance while some decreased in abundance. In capping water, the number of sulfur-cycling genera with increased abundance overtime was considerably higher than the number of genera that decreased (20 positive correlations vs 5 negative correlations) suggesting stable or cooperative interactions among SOBs and SRBs. In contrast, the abundance of greater number of sulfur-cycling genera decreased overtime compared to the number that were enriched (17 negative correlations vs 8 positive correlations) indicating competition or environmental stress affecting sulfur cycling processes (Li et al., 2021). On the other hand, the number of carbon-cycling bacteria that were enriched and the number that decreased overtime were nearly equal in both capping water and tailing, indication a balance in the interactions of the carbon-cycling

bacteria (Ren et al., 2022). The number of iron-cycling bacteria that were enriched was equal to the number that decreased overtime in capping water, however, higher number were enriched in tailings. This suggested that iron oxidation and reduction occurred at similar rate and competed against each other (Ionescu et al., 2015). Almost equal number of nitrogen-cycling bacteria were enriched and reduced overtime in capping water, however, higher number were enriched in tailings. This indicated that denitrification and nitrification likely occurred at similar rate but with limited nitrogen fixation (Vitousek and Howarth, 1991).

3.4.5 Implications for Pit Lake Ecosystem Stability and Sustainability

Understanding the biogeochemical processes occurring in model pit lakes provide crucial insights into the stability and sustainability of pit lake systems. In pit lakes having tailings treated with sulfate-containing coagulants such as gypsum and alum, sulfur cycling is promoted. Principally, the sulfur cycle involves complex biochemical processes where sulfur species are transformed through oxidation, reduction, disproportionation or putative comproportionating by taxonomically diverse microorganisms (Vigneron et al., 2021). Interestingly, the sulfur cycle is associated with other cycles such as carbon and nitrogen cycles. For instance, SRBs typically outcompete methanogenic microorganisms such as primary and secondary fermenters, homoacetogens, and methanogens for substrates, thus diverting anaerobic carbon mineralization away from methanogenesis to carbon dioxide production (Holowenko et al., 2000). Additionally, SRBs are also known to grow in syntrophic association with hydrogen-scavenging methanogens or can themselves constitute the hydrogen-scavenging partner in syntrophic associations (Pester et al., 2012). On the other hand, the sulfur and nitrogen cycles could interact with one another through competition for labile organic carbon between nitrate-reducing bacteria and SRBs, or through

nitrate reduction coupled to sulfur oxidation thereby consuming nitrate and producing sulfate (Gu et al., 2012).

Overall, the actions of SRBs could lead to high production of toxic H_2S, and acidification of upper water layers during sulfide oxidation (Koizumi et al., 2005; Siddique et al., 2019). This may turn the entire water layer into an extreme environment where only SRBs and other anaerobes could survive but the overall system could not support other forms of life such as chemolithoautotrophs or organisms involve in primary production (Meier et al., 2012). In this study, while sulfur cycling was prominent, carbon, nitrogen and iron cycling were equally developed suggesting the co-occurrence of different microbial communities in PASS-treated tailings. Furthermore, the transport of dissolved organics from the underlying tailings into the capping water due to advective chemical fluxes highlights the importance of understanding subsurface chemical interactions.

Temperature is considered as one of the most important factors affecting microbial communities and variations in temperature can affect community-level dynamics (Lin et al., 2017; Zander et al., 2017). Additionally, temperature variations are known to affect the physicochemical properties of aquatic systems (De Stasio et al., 2009; Li et al., 2013). Hence, understanding the response of pit lakes to seasonal temperature changes is important towards proper management of pit lake ecosystems. Our findings showed that temperature changes did not significantly impact the pit lake parameters other than dissolved oxygen and conductivity, indicating stability in the chemical environment of the model pit lake. Furthermore, the microbial communities in both tailings and capping water showed resistance to temperature variations, suggesting robust microbial populations capable of maintaining ecological functions across a range of temperatures (Zhu et al., 2019).

The findings in this dissertation also revealed temporal changes in physicochemical parameters of capping water, highlighting the dynamic nature of the pit lake environment. These changes could be driven by a combination of seasonal variations, biological activity, and ongoing chemical reactions in the system (España et al., 2005). Understanding these temporal dynamics is important for predicting long-term changes in pit lake chemistry and implementing effective management strategies. The synergized development of sulfur, carbon, nitrogen, and iron cycling indicates a complex and interconnected microbial ecosystem. Efficient cycling of these elements is essential for nutrient availability, primary productivity, and overall ecosystem stability (Falkowski et al., 2008).

3.5 Conclusion

The concentration of dissolved organics in the capping water of DPL increased due to advective chemical fluxes from the underlying PASS-treated tailings. Notably, temperature variations did not impact these fluxes or the concentration of other measured parameters in the capping water, except for dissolved oxygen, conductivity, and sulfate concentrations. However, there was a temporal change in the physicochemical parameters of capping water. The examination of bacterial community structures revealed distinct compositions in tailings and capping water that are resistant to temperature variations within the system. The addition of alum and PAM during PASS treatment likely played a role in shaping the bacterial community structures of tailings and capping water. Furthermore, biogeochemical analysis revealed that the abundances of these communities changed with temperature variation, though without a discernible pattern. Furthermore, a synergized development of sulfur, carbon, nitrogen, and iron biogeochemical cycling was observed. Interestingly, there was limited gas production. This study highlights the

dynamic nature of microbial communities in engineered ecosystems, offering valuable insights for the design and optimization of such systems for environmental management of oil sands tailings.

3.6 References

Albakistani, E.A., Nwosu, F.C., Furgason, C., Haupt, E.S., Smirnova, A. V., Verbeke, T.J., Lee, E.S., Kim, J.J., Chan, A., Ruhl, I.A., Sheremet, A., Rudderham, S.B., Lindsay, M.B.J., Dunfield, P.F., 2022. Seasonal Dynamics of Methanotrophic Bacteria in a Boreal Oil Sands End Pit Lake. Appl. Environ. Microbiol. 88. https://doi.org/10.1128/aem.01455-21

Alberta Energy Regulator, 2022. Tailings [WWW Document]. Provid. Inf. URL https://www.aer.ca/providing-information/by-topic/tailings (accessed 11.20.23).

Alberta Government, 2022. Oil Sands: Facts and Statistics [WWW Document]. Gov. Alberta. URL https://www.alberta.ca/oil-sands-facts-and-statistics.aspx (accessed 1.26.22).

Alewell, C., Paul, S., Lischeid, G., Küsel, K., Gehre, M., 2006. Characterizing the redox status in three different forested wetlands with geochemical data. Environ. Sci. Technol. 40, 7609–7615. https://doi.org/10.1021/es061018y

Allaf, M.M., Peerhossaini, H., 2022. Cyanobacteria: Model Microorganisms and Beyond. Microorganisms 10. https://doi.org/10.3390/microorganisms10040696

Arslan, M., Gamal El-Din, M., 2021. Bacterial diversity in petroleum coke based biofilters treating oil sands process water. Sci. Total Environ. 782, 146742. https://doi.org/10.1016/j.scitotenv.2021.146742

Arslan, M., Müller, J.A., Gamal El-Din, M., 2021. Aerobic naphthenic acid-degrading bacteria in

petroleum-coke improve oil sands process water remediation in biofilters: DNA-stable isotope probing reveals methylotrophy in Schmutzdecke. Sci. Total Environ. 151961. https://doi.org/10.1016/j.scitotenv.2021.151961

Ayayee, P.A., Custer, G.F., Tronstad, L.M., van Diepen, L.T.A., 2024. Unveiling salinity-driven shifts in microbial community composition across compartments of naturally saline inland streams. Hydrobiologia 851, 2627–2639. https://doi.org/10.1007/s10750-024-05479-5

Bazylinski, D.A., Dean, A.J., Schüler, D., Phillips, E.J.P., Lovley, D.R., 2000. N2-dependent growth and nitrogenase activity in the metal-metabolizing bacteria, Geobacter and Magnetospirillum species. Environ. Microbiol. 2, 266–273. https://doi.org/10.1046/j.1462-2920.2000.00096.x

Bell, E., Lamminmäki, T., Alneberg, J., Qian, C., Xiong, W., Hettich, R.L., Frutschi, M., Bernier-Latmani, R., 2022. Active anaerobic methane oxidation and sulfur disproportionation in the deep terrestrial subsurface. ISME J. 16, 1583–1593. https://doi.org/10.1038/s41396-022-01207-w

Bolyen, E., Rideout, J.R., Dillon, M.R., Bokulich, N.A., Abnet, C.C., Al-Ghalith, G.A., Alexander, H., 2019. Reproducible, interactive, scalable and extensible microbiome data science using QIIME 2. Nat. Biotechnol. 37, 852–857. https://doi.org/http://dx.doi.org/10.1038/s41587-019-0209-9

Cabrol, L., Thalasso, F., Gandois, L., Sepulveda-Jauregui, A., Martinez-Cruz, K., Teisserenc, R., Tananaev, N., Tveit, A., Svenning, M.M., Barret, M., 2020. Anaerobic oxidation of methane and associated microbiome in anoxic water of Northwestern Siberian lakes. Sci.

Total Environ. 736. https://doi.org/10.1016/j.scitotenv.2020.139588

Callahan, B.J., McMurdie, P.J., Rosen, M.J., Han, A.W., Amy Jo A Johnson, and S.P.H., 2016. DADA2: High resolution sample inference from Illumina amplicon data. Nat Methods. 13, 581–583. https://doi.org/10.1038/nmeth.3869

Canada's Oil Sands Innovation Alliance (COSIA), 2021. Pit Lakes: A surface mining perspective, Tailings Environmental Priority Area (EPA).

Chen, M., Walshe, G., Chi Fru, E., Ciborowski, J.J.H., Weisener, C.G., 2013. Microcosm assessment of the biogeochemical development of sulfur and oxygen in oil sands fluid fine tailings. Appl. Geochemistry 37, 1–11. https://doi.org/10.1016/j.apgeochem.2013.06.007

Choo-yin, Y., 2021. Monitoring Macrophage Immune Gene Expression Profiles as an Early Indicator System for Examining the Bioactivity of Oil Sands Process Affected Waters. University of Alberta.

Cossey, H.L., Batycky, A.E., Kaminsky, H., Ulrich, A.C., 2021. Geochemical stability of oil sands tailings in mine closure landforms. Minerals 11. https://doi.org/10.3390/min11080830

De Stasio, B.T., Golemgeski, T., Livingstone, D.M., 2009. Temperature as a Driving Factor in Aquatic Ecosystems. Encycl. Inl. Waters 690–698. https://doi.org/10.1016/B978-0-12-819166-8.00062-1

Dompierre, K.A., Barbour, S.L., 2016. Characterization of physical mass transport through oil sands fluid fine tailings in an end pit lake: A multi-tracer study. J. Contam. Hydrol. 189, 12–26. https://doi.org/10.1016/j.jconhyd.2016.03.006

Dompierre, K.A., Barbour, S.L., North, R.L., Carey, S.K., Lindsay, M.B.J., 2017. Chemical mass transport between fluid fine tailings and the overlying water cover of an oil sands end pit lake. Water Resour. Res. 5, 4725–4740. https://doi.org/10.1002/2016WR020112

España, J.S., Pamo, E.L., Santofimia, E., Aduvire, O., Reyes, J., Barettino, D., 2005. Acid mine drainage in the Iberian Pyrite Belt (Odiel river watershed, Huelva, SW Spain): Geochemistry, mineralogy and environmental implications. Appl. Geochemistry 20, 1320–1356. https://doi.org/10.1016/j.apgeochem.2005.01.011

Falkowski, P.G., Fenchel, T., Delong, E.F., 2008. The microbial engines that drive earth's biogeochemical cycles. Science (80-.). 320, 1034–1039. https://doi.org/10.1126/science.1153213

Foght, J.M., 2015. Microbial metagenomics of oil sands tailings ponds: Small bugs, big data. Genome 58, 507–510. https://doi.org/10.1139/gen-2015-0146

Gonçalves, J., Baldovi, A.A., Chyoshi, B., Zanata, L., Salcedo, A.M., Subtil, E.L., Coelho, L.H.G., 2019. Effect of aluminum sulfate and cationic polymer addition in the mixed liquor of a submerged membrane bioreactor (SMBR): Sludge characteristics and orthophosphate removal in batch experiments. Brazilian J. Chem. Eng. 36, 693–703. https://doi.org/10.1590/0104-6632.20190362s20180128

Gu, C., Laverman, A.M., Pallud, C.E., 2012. Environmental controls on nitrogen and sulfur cycles in surficial aquatic sediments. Front. Microbiol. 3, 1–11. https://doi.org/10.3389/fmicb.2012.00045

Guo, H., Chen, C., Lee, D.J., Wang, A., Ren, N., 2013. Sulfur-nitrogen-carbon removal of

Pseudomonas sp. C27 under sulfide stress. Enzyme Microb. Technol. 53, 6–12. https://doi.org/10.1016/j.enzmictec.2013.04.002

Holmer, M., Storkholm, P., 2001. Sulphate reduction and sulphur cycling in lake sediments: A review. Freshw. Biol. 46, 431–451. https://doi.org/10.1046/j.1365-2427.2001.00687.x

Holowenko, F.M., MacKinnon, M.D., Fedorak, P.M., 2000. Methanogens and sulfate-reducing bacteria in oil sands fine tailings waste. Can. J. Microbiol. 46, 927–937. https://doi.org/10.1139/w00-081

Intrinsik Corp., 2022. Environmental fate and behaviour of anionic polyacrylamides in oil sands tailings management: A state of knowledge synthesis. Albert.

Ionescu, D., Heim, C., Polerecky, L., Thiel, V., De Beer, D., 2015. Biotic and abiotic oxidation and reduction of iron at circumneutral pH are inseparable processes under natural conditions. Geomicrobiol. J. 32, 221–230. https://doi.org/10.1080/01490451.2014.887393

Jessen, G.L., Chen, L.X., Mori, J.F., Nelson, T.E.C., Slater, G.F., Lindsay, M.B.J., Banfield, J.F., Warren, L.A., 2022. Alum Addition Triggers Hypoxia in an Engineered Pit Lake. Microorganisms 10. https://doi.org/10.3390/microorganisms10030510

Joshi, S.J., Abed, R.M.M., 2017. Biodegradation of Polyacrylamide and Its Derivatives. Environ. Process. 4, 463–476. https://doi.org/10.1007/s40710-017-0224-0

Junkins, E.N., McWhirter, J.B., McCall, L.-I., Stevenson, B.S., 2022. Environmental structure impacts microbial composition and secondary metabolism. ISME Commun. 2, 1–10. https://doi.org/10.1038/s43705-022-00097-5

Koizumi, Y., Kojima, H., Fukui, M., 2005. Potential sulfur metabolisms and associated bacteria within anoxic surface sediment from saline meromictic Lake Kaiike (Japan). FEMS Microbiol. Ecol. 52, 297–305. https://doi.org/10.1016/j.femsec.2004.11.009

Lau, Y.L., 1994. Temperature effect on settling velocity and deposition of cohesive sediments: Influence de la témperature sur la vitesse de chute et le dépôt de sédiments cohesifs. J. Hydraul. Res. 32, 41–51. https://doi.org/10.1080/00221689409498788

Li, H.Y., Xu, J., Xu, R.Q., 2013. The effect of temperature on the water quality of lake. Adv. Mater. Res. 821–822, 1001–1004. https://doi.org/10.4028/www.scientific.net/AMR.821-822.1001

Li, J., How, Z.T., Gamal El-Din, M., 2023. Aerobic degradation of anionic polyacrylamide in oil sands tailings: Impact factor, degradation effect, and mechanism. Sci. Total Environ. 856, 159079. https://doi.org/10.1016/j.scitotenv.2022.159079

Li, M., Fang, A., Yu, X., Zhang, K., He, Z., Wang, C., Peng, Y., Xiao, F., Yang, T., Zhang, W., Zheng, X., Zhong, Q., Liu, X., Yan, Q., 2021. Microbially-driven sulfur cycling microbial communities in different mangrove sediments. Chemosphere 273, 128597. https://doi.org/10.1016/j.chemosphere.2020.128597

Li, X., Lan, S. ming, Zhu, Z. ping, Zhang, C., Zeng, G. ming, Liu, Y. guo, Cao, W. cheng, Song, B., Yang, H., Wang, S. fan, Wu, S. hua, 2018. The bioenergetics mechanisms and applications of sulfate-reducing bacteria in remediation of pollutants in drainage: A review. Ecotoxicol. Environ. Saf. 158, 162–170. https://doi.org/10.1016/j.ecoenv.2018.04.025

Li, Y., Liu, L., Wang, H., 2022. Mixotrophic denitrification for enhancing nitrogen removal of

municipal tailwater: Contribution of heterotrophic/sulfur autotrophic denitrification and bacterial community. Sci. Total Environ. 814, 151940. https://doi.org/10.1016/j.scitotenv.2021.151940

Li, Y., Yu, S., Strong, J., Wang, H., 2012. Are the biogeochemical cycles of carbon, nitrogen, sulfur, and phosphorus driven by the "FeIII-FeII redox wheel" in dynamic redox environments? J. Soils Sediments 12, 683–693. https://doi.org/10.1007/s11368-012-0507-z

Liamleam, W., Annachhatre, A.P., 2007. Electron donors for biological sulfate reduction. Biotechnol. Adv. 25, 452–463. https://doi.org/10.1016/j.biotechadv.2007.05.002

Lillico, D.M.E., Hussain, N.A.S., Choo-Yin, Y.Y., Qin, R., How, Z.T., El-Din, M.G., Stafford, J.L., 2022. Using immune cell-based bioactivity assays to compare the inflammatory activities of oil sands process-affected waters from a pilot scale demonstration pit lake. J. Environ. Sci. https://doi.org/10.1016/j.jes.2022.07.018

Lin, Y. Te, Jia, Z., Wang, D., Chiu, C.Y., 2017. Effects of temperature on the composition and diversity of bacterial communities in bamboo soils at different elevations. Biogeosciences 14, 4879–4889. https://doi.org/10.5194/bg-14-4879-2017

Meier, J., Piva, A., Fortin, D., 2012. Enrichment of sulfate-reducing bacteria and resulting mineral formation in media mimicking pore water metal ion concentrations and pH conditions of acidic pit lakes. FEMS Microbiol. Ecol. 79, 69–84. https://doi.org/10.1111/j.1574-6941.2011.01199.x

Muyzer, G., Stams, A.J.M., 2008. The ecology and biotechnology of sulphate-reducing bacteria. Nat. Rev. Microbiol. 6, 441–454. https://doi.org/10.1038/nrmicro1892

Nyyssölä, A., Ahlgren, J., 2019. Microbial degradation of polyacrylamide and the deamination product polyacrylate. Int. Biodeterior. Biodegrad. 139, 24–33. https://doi.org/10.1016/j.ibiod.2019.02.005

Otte, J.M., Harter, J., Laufer, K., Blackwell, N., Straub, D., Kappler, A., Kleindienst, S., 2018. The distribution of active iron-cycling bacteria in marine and freshwater sediments is decoupled from geochemical gradients. Environ. Microbiol. 20, 2483–2499. https://doi.org/10.1111/1462-2920.14260

Pester, M., Knorr, K.H., Friedrich, M.W., Wagner, M., Loy, A., 2012. Sulfate-reducing microorganisms in wetlands - fameless actors in carbon cycling and climate change. Front. Microbiol. 3, 1–19. https://doi.org/10.3389/fmicb.2012.00072

Ren, L., Jensen, K., Porada, P., Mueller, P., 2022. Biota-mediated carbon cycling—A synthesis of biotic-interaction controls on blue carbon. Ecol. Lett. 25, 521–540. https://doi.org/10.1111/ele.13940

Robinson, J., Mills, J., Breed, M., 2018. Walking Ecosystems in Microbiome-Inspired Green Infrastructure: An Ecological Perspective on Enhancing Personal and Planetary Health. Challenges 9, 40. https://doi.org/10.3390/challe9020040

Seitzinger, S., Harrison, J.A., Böhlke, J.K., Bouwman, A.F., Lowrance, R., Peterson, B., Tobias, C., Van Drecht, G., 2006. Denitrification across landscapes and waterscapes: A synthesis. Ecol. Appl. 16, 2064–2090. https://doi.org/10.1890/1051-0761(2006)016[2064:DALAWA]2.0.CO;2

Sela-Adler, M., Ronen, Z., Herut, B., Antler, G., Vigderovich, H., Eckert, W., Sivan, O., 2017.

Co-existence of methanogenesis and sulfate reduction with common substrates in sulfate-rich estuarine sediments. Front. Microbiol. 8, 1–11. https://doi.org/10.3389/fmicb.2017.00766

Shade, A., Peter, H., Allison, S.D., Baho, D.L., Berga, M., Bürgmann, H., Huber, D.H., Langenheder, S., Lennon, J.T., Martiny, J.B.H., Matulich, K.L., Schmidt, T.M., Handelsman, J., 2012. Fundamentals of microbial community resistance and resilience. Front. Microbiol. 3, 1–19. https://doi.org/10.3389/fmicb.2012.00417

Shinoda, Y., Akagi, J., Uchihashi, Y., Hiraishi, A., Yukawa, H., Yurimoto, H., Sakai, Y., Kato, N., 2005. Anaerobic degradation of aromatic compounds by Magnetospirillum strains: Isolation and degradation genes. Biosci. Biotechnol. Biochem. 69, 1483–1491. https://doi.org/10.1271/bbb.69.1483

Siddique, T., Stasik, S., Shahimin, M.F.M., Wendt-Potthoff, K., 2019. Microbial Communities in Oil Sands Tailings: Their Implications in Biogeochemical Processes and Tailings Management, Microbial Communities Utilizing Hydrocarbons and Lipids: Members, Metagenomics and Ecophysiology. Springer Nature Switzerland AG 2019. https://doi.org/10.1007/978-3-030-14785-3

Stumm, W., & Morgan, J. J. (1996). Aquatic Chemistry: Chemical Equilibria and Rates in Natural Waters. Wiley-Interscience

Syncrude, 2019. Base Mine Lake Monitoring and Research Summary Report: Results from 2013-2018.

Takaya, N., Catalan-Sakairi, M.A.B., Sakaguchi, Y., Kato, I., Zhou, Z., Shoun, H., 2003.

Aerobic denitrifying bacteria that produce low levels of nitrous oxide. Appl. Environ. Microbiol. 69, 3152–3157. https://doi.org/10.1128/AEM.69.6.3152-3157.2003

Thijs, S., De Beeck, M.O., Beckers, B., Truyens, S., Stevens, V., Van Hamme, J.D., Weyens, N., Vangronsveld, J., 2017. Comparative evaluation of four bacteria-specific primer pairs for 16S rRNA gene surveys. Front. Microbiol. 8, 1–15. https://doi.org/10.3389/fmicb.2017.00494

Vandenberg, J.A., Lauzon, N., Prakash, S., Salzsauler, K., 2011. Use of water quality models for design and evaluation of pit lakes. Mine Pit Lakes Clos. Manag. 63–81.

Vigneron, A., Cruaud, P., Culley, A.I., Couture, R.M., Lovejoy, C., Vincent, W.F., 2021. Genomic evidence for sulfur intermediates as new biogeochemical hubs in a model aquatic microbial ecosystem. Microbiome 9, 1–14. https://doi.org/10.1186/s40168-021-00999-x

Vitousek, P.M., Howarth, R.W., 1991. Nitrogen limitation on land and in the sea: How can it occur? Biogeochemistry 13, 87–115. https://doi.org/10.1007/BF00002772

Walters, K.E., Martiny, J.B.H., 2020. Alpha-, beta-, and gamma-diversity of bacteria varies across habitats. PLoS One 15, 1–17. https://doi.org/10.1371/journal.pone.0233872

West, K.N., Wheeler, C., McCarney, J.P., Griffith, K.N., Bush, D., Liotta, C.L., Eckert, C.A., 2001. In situ formation of alkylcarbonic acids with CO2. J. Phys. Chem. A 105, 3947–3948. https://doi.org/10.1021/jp003846y

White, K.B., Liber, K., 2020. Chronic Toxicity of Surface Water from a Canadian Oil Sands End Pit Lake to the Freshwater Invertebrates Chironomus dilutus and Ceriodaphnia dubia. Arch.

Environ. Contam. Toxicol. 78, 439–450. https://doi.org/10.1007/s00244-020-00720-3

Wolfe, A.L., Wilkin, R.T., 2017. Evidence of Sulfate-Dependent Anaerobic Methane Oxidation within an Area Impacted by Coalbed Methane-Related Gas Migration. Env. Sci Technol. 51, 1901–1909. https://doi.org/10.1021/acs.est.6b03709

Xiong, B., Loss, R.D., Shields, D., Pawlik, T., Hochreiter, R., Zydney, A.L., Kumar, M., 2018. Polyacrylamide degradation and its implications in environmental systems. npj Clean Water 1. https://doi.org/10.1038/s41545-018-0016-8

Zander, A., Bersier, L.F., Gray, S.M., 2017. Effects of temperature variability on community structure in a natural microbial food web. Glob. Chang. Biol. 23, 56–67. https://doi.org/10.1111/gcb.13374

Zhao, T., Chen, P., Zhang, Lijie, Zhang, Lei, Gao, Y., Ai, S., Liu, H., Liu, X., 2021. Heterotrophic nitrification and aerobic denitrification by a novel Acinetobacter sp. TAC-1 at low temperature and high ammonia nitrogen. Bioresour. Technol. 339, 125620. https://doi.org/10.1016/j.biortech.2021.125620

Zhu, Y.G., Zhao, Y., Zhu, D., Gillings, M., Penuelas, J., Ok, Y.S., Capon, A., Banwart, S., 2019. Soil biota, antimicrobial resistance and planetary health. Environ. Int. 131, 105059. https://doi.org/10.1016/j.envint.2019.105059

CHAPTER 4 METAGENOMIC ELUCIDATION OF MICROBIAL BIOGEOCHEMICAL CYCLING IN A MODEL OIL SANDS TAILINGS PIT LAKE SYSTEM

4.1 Introduction

Microorganisms are integral to the biogeochemical cycling of nutrients, significantly influencing the flow of energy and matter within ecosystems. Through their interactions with the environment and their role in the mineralization of organic matter, these microorganisms facilitate the circulation of essential nutrients, thereby maintaining ecosystem stability and productivity (Shang et al., 2022). The biochemical transformations of key nutrients such as carbon, nitrogen, and sulfur are governed by a myriad of factors including redox conditions, pH levels, energy availability, nutrient concentrations, and the presence of specific substrates (Paerl and Pinckney, 1996). Variations in any of these environmental parameters can lead to shifts in microbial community structures and functions, potentially enhancing the production of undesirable gaseous by-products such as methane and carbon dioxide from carbon cycling, ammonia from nitrogen cycling, and hydrogen sulfide from sulfur cycling (Herman and Maier, 2009; Shang et al., 2022).

The oil sands industry has recently adopted the use of pit lakes as a sustainable method for managing tailings wastes produced during bitumen extraction (White and Liber, 2020). These pit lakes serve as repositories for tailings and provide a unique environment for studying biogeochemical processes. Research into the biogeochemical cycling within oil sands pit lakes has focused on elucidating the patterns and structures of microbial communities and observing biogeochemical changes over time (Kuznetsov et al., 2023; Siddique et al., 2019). Notably, studies have also aimed to understand the biogeochemical development of sulfur through techniques such

as 16S rRNA amplicon sequencing (Chen et al., 2013; Warren et al., 2016). While this molecular approach offers valuable insights into the composition of microbial communities, it falls short of providing detailed information about their metabolic capabilities and specific roles in nutrient cycling (Li and Li, 2021). To bridge this gap, recent research has turned to metagenomic analysis, a powerful tool that allows for the comprehensive identification of microbial communities and the prediction of their biogeochemical functions (Zhang et al., 2016). Metagenomics involves sequencing the collective genomes of microbial communities, thereby enabling the detection of functional genes involved in various biogeochemical cycles such as carbon, sulfur, nitrogen, and iron cycling (Alfreider et al., 2017; Ayala-Muñoz et al., 2022; Garber et al., 2021; Mosley et al., 2022). This approach not only enhances our understanding of microbial diversity but also provides insights into the metabolic pathways and ecological roles of these microorganisms. The application of metagenomics in studying pit lakes has yielded significant findings. For instance, Ayala-Muñoz et al., (2022) employed a combination of amplicon sequencing, metagenomics and metatranscriptomics to taxonomically resolve the contributions of microbial communities to carbon, sulfur, iron, and nitrogen cycling. Furthermore, the integration of metagenomic data with other omics approaches, such as metatranscriptomics and metaproteomics, has the potential to provide a more holistic view of microbial activities and their contributions to biogeochemical cycles. By examining gene expression and protein production in conjunction with genetic potential, researchers can gain deeper insights into the dynamic processes governing nutrient cycling in complex ecosystems like oil sands pit lakes (Ayala-Muñoz et al., 2020).

In this chapter, a metagenomic approach was utilized to investigate the microbial biogeochemical cycling within a newly established demonstration pit lake (DPL) using laboratory-based pit lake models. These models involved the strategic capping of tailings with water and the

creation of separate columns subjected to modified seasonal temperature variations, alongside other columns maintained at a constant temperature. We hypothesized that altering the temperature would exert a selection pressure, thereby inducing changes in microbial community structures and their functional gene predictions. By examining these controlled environmental conditions, we aimed to elucidate the adaptive responses and functional capabilities of the microbial communities involved in nutrient cycling within the DPL.

4.2 Materials and Methods

4.2.1 Oil sands model pit lake samples

The oil sands pit lake samples used in this chapter comprised of tailings and capping water that were collected from a laboratory pit lake model which was established using tailings and capping water collected from a DPL in Canada. The tailings samples were stored at -20 ^{o}C while the water samples were filtered using a 0.45 µm filter before the filter papers were stored at -20 ^{o}C. The frozen samples were then shipped to Department of Microbial Genetics and Biotechnology (IBG-5), Karlsruhe Institute of Technology (KIT), Germany, where they were stored at -20 ^{o}C upon arrival. There were 40 samples in total, separated into four categories of 10 samples each, collected from a laboratory pit lake system under two different temperature conditions. These categories were: (i) tailings-control (TC, which were samples from tailings of temperature-constant columns), (ii) tailings-treatment (TT, which were samples from tailings of temperature-modified columns), (iii) water-control (WC, which were samples from capping water of temperature-constant columns) and (iv) water-treatment (WT, which were samples from capping water of temperature-modified columns).

4.2.2 DNA extraction and Library preparation

DNA was extracted using DNeasy PowerSoil Kits (Qiagen Inc., USA) for tailings samples, and DNeasy Blood & Tissue Kits (Qiagen Inc., USA) for water samples following manufactural instructions. Libraries were prepared using the NEBNext UltraTM II FS DNA Library Prep Kit (New England BioLabs) following the manufacturer's protocols. Briefly, the library preparation was divided into 6 steps namely:

(i) DNA fragmentation and end repair: Input DNA was enzymatically fragmented, and the ends were repaired to create blunt or 3'-A overhangs.

(ii) Adaptor Ligation: Pre-prepared adaptors were ligated to the DNA fragments. This step prepared the DNA for amplification and sequencing.

(iii) Clean-up of adaptor-ligated DNA: Post-ligation clean-up was carried out to remove non-ligated adaptors and excess enzymes using AMPure XP beads.

(iv) PCR Enrichment: The adaptor-ligated DNA was amplified using PCR to increase the quantity of DNA suitable for sequencing. NEBNext Ultra II Q5 Master Mix and Universal primer were employed.

(v) Clean-up of PCR reaction: PCR product was cleaned up using AMPure XP beads.

(vi) Assessment of library quality: Library qualities were evaluated using the Agilent High Sensitivity DNA Kit on the Agilent 2100 Bioanalyzer instrument (Agilent Technologies).

4.2.3 Metagenome analysis

Prepared libraries were pooled for paired-end sequencing on an Illumina NexSeq 550. Raw sequence data quality was checked using FastQC v0.12.1 (Andrews, 2010) and MultiQC v1.14 (Ewels et al., 2016) before low-quality reads and adaptor sequences were removed using a

combination of Trimmomatic v.0.39 (Bolger et al., 2014) and fastp v0.23.2 (Chen et al., 2018). Two approaches were employed for the assembly of the trimmed samples. The first approach involved the co-assembly of all samples whereas the second approach involved dividing the trimmed short reads into the four categories of TC, TT, WC and WT. The sample reads were then co-assembled into contigs accordingly using MegaHit v1.2.9 (Li et al., 2015) followed by subsequent mapping of short reads from individual samples back to the contigs they belonged using Bowtie2 v2.3.5 (Langmead and Salzberg, 2012) and SAMtools v1.9 (Danecek et al., 2021). The metagenome assemblies and reads were then reconstructed into metagenome bins using MetaBAT2 (Kang et al., 2019), CONCOCT (Alneberg et al., 2014) and MaxBin2 (Wu et al., 2016) in MetaWRAP v1.3.2 (Uritskiy et al., 2018). The generated bins were refined using MetaWRAP bin-refinement module, then dereplicated and cleaned of contamination using dRep v3.4.3 (Olm et al., 2017) and MDMcleaner v0.8.3 (Vollmers et al., 2022) respectively before being quality-checked by CheckM2 (Chklovski et al., 2023). The cleaned bins were then imported into Anvi'o v7.1 (Eren et al., 2015) for metagenomic workflow where identification of open reading frames (ORFs) was done using Prodigal (Hyatt et al., 2010). Furthermore, processing of functional and taxonomic annotations for ORFs, searching contigs for hidden Markov model (HMM) profiles, and gene annotations from NCBI's Clusters of Orthologous Groups and Kyoto Encyclopedia of Genes and Genomes (KEGG) were carried out on Anvi'o v7.1.

4.2.4 Biogeochemical cycling analysis

Analysis of biogeochemical cycling was done for each of the categories using Metascan (Cremers et al., 2022). Metascan was set up as per the author's github instruction (https://github.com/gcremers/metascan) and run on co-assembled contigs (unbinned core assemblies) of TC, TT, WC, and WT to generate biogeochemical cycling genes for each category.

Briefly, the Metascan analysis was initiated with gene calling using Prodigal and the recovered rRNA gene sequences were compared against a local NCBI non-redundant database using BLASTN. Subsequent gene annotation is performed using hmmsearch against each of the seven subsets of the key genes representing important nutrient cycles of Nitrogen, Methane, Carbon fixation, Hydrogenases, C1 (methylotrophy) molecules, Sulfur, and Oxidative phosphorylation; and one miscellaneous subset of metal cycling (Cremers et al., 2022).

4.3 Results

4.3.1 Sequencing, de novo assembly, and bins generation

Following DNA extraction and library preparation, metagenomic DNA was subjected to Illumina NextSeq sequencing. Short DNA sequences ranging between 2.1 million and 9.7 million were obtained, but with more than 97% adapter contamination. After trimming with Trimmomatic and fastp, high-quality sequence reads, between 1.9 million and 9.0 million with zero percent adapter contamination, were obtained (Figure A1 and Figure A2). After bin refinement with MetaWRAP, a total of 113 bins accounting for 367,636,671 nucleotides were generated. These bins had completeness within 60% - 100%, contamination within 0% - 13%, N50 in the range of 2,124 – 911,438, genome size between 598.67Kb - 7.95Mb, and GC content within 31% - 71% (Table A6).

4.3.2 Taxonomic estimation of metagenome-assembled genomes in model pit lakes

The results of principal coordinate analysis (PCoA) revealed two distinct clusters representing microbial communities in capping water and tailings (Figure 4.1A). A deeper look into these clusters revealed similarities and differences between WC and WT of capping water as well as TC and TT of tailings (Figure 4.1B). Exploring the clusters further showed that top and

bottom samples of capping water were dispersed whereas the top and bottom samples of tailings were aggregated separately (Figure 4.1C and Figure 4.1D).

Taxonomy estimation following The Genome Taxonomy Database (GTDB; https://gtdb.ecogenomic.org) revealed the dominance of bacteria in both tailings and capping water of temperature-constant and temperature-modified columns. In tailings, TC was comprised of 93% bacteria and 7% unknown domain whereas TT was 100% bacteria. In capping water, WC was made up of 97% bacteria and 3% unknown domain while WT was comprised of 89% bacteria and 11% unknown domain (Figure 4.2A). The bacterial phyla were distinctively different between the columns in terms of abundance and composition. The most abundant phyla in TC were Proteobacteria (34%), Patescibacteria (18), Chloroflexota (14%), Bacteroidota (11%), and Desulfobacterota (13%) whereas the abundant phyla in TT were Proteobacteria (48%),

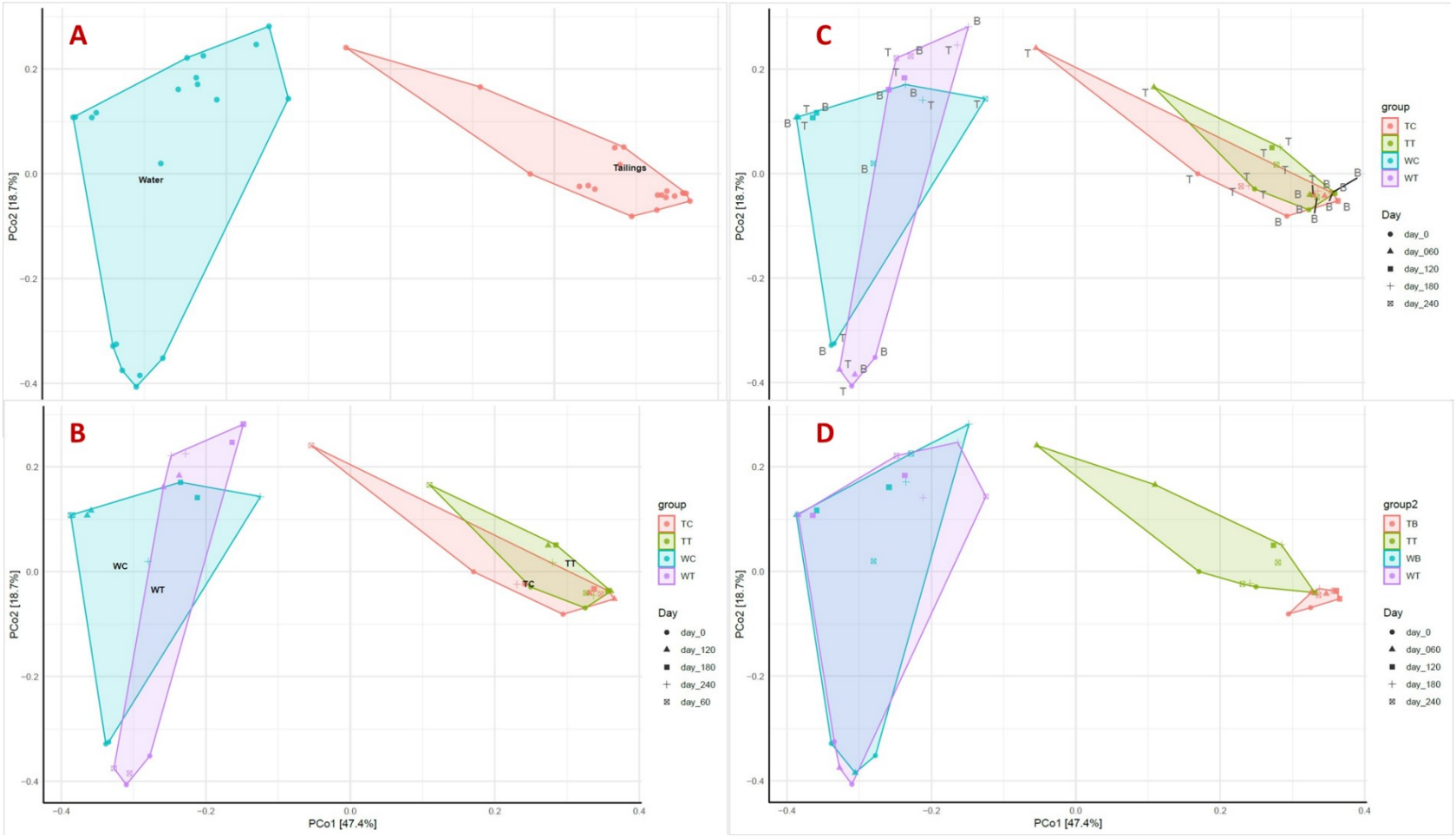

Figure 4.1: Principal coordinate analysis of model pit lakes

Bdellovibrionota (18%), Patescibacteria (13), Chloroflexota (10%), and Desulfobacterota (8%). On the other hand, the most abundant phyla in WC were Proteobacteria (75%), Planctomycetota (9%), Patescibacteria (4%), Acidobacteriota (4%) and Actinomycetota (3%) while the most abundant phyla in WT were Proteobacteria (80%), Actinomycetota (8%), Acidobacteriota (6%), and Chlamydiota (2%) (Figure 4.2B). At genus level, the bacterial communities were significantly different between the tailings and capping water (Figure 4.3). The most abundant bacterial genera in TC were members of Uncultivated Bacteria and Archaea (UBA) including *UBA2259* (7%); *UBA5623* (6%); *UBA4096* (5%); *UBA12087* (4%); *UBA6170* (4%). Additionally, important genera known for nutrient cycling such as *Rugosibacter*, *Chlorobium*, *Immundisolibacter*, *Brevundimonas*, and *Acidovorax*, were relatively abundant. Conversely, the five most abundant bacterial genera in TT were *UBA4096* (18%); *Stutzerimonas* (15%); *Rugosibacter* (12%); *UBA2259* (10%); and *UBA6170* (10%). On the other hand, the five most abundant bacterial genera in WC were *Rugosibacter* (22%); *Brevundimonas* (11%); *CAIJLX01* (8%); *Hyphomonas* (4%); and *Immundisolibacter* (4%). Meanwhile, the most abundant bacterial genera in WT were *Rugosibacter* (21%); *Brevundimonas* (11%); JAGXQV01 (10%); *UBA2020* (10%); *Planktophila* (6%).

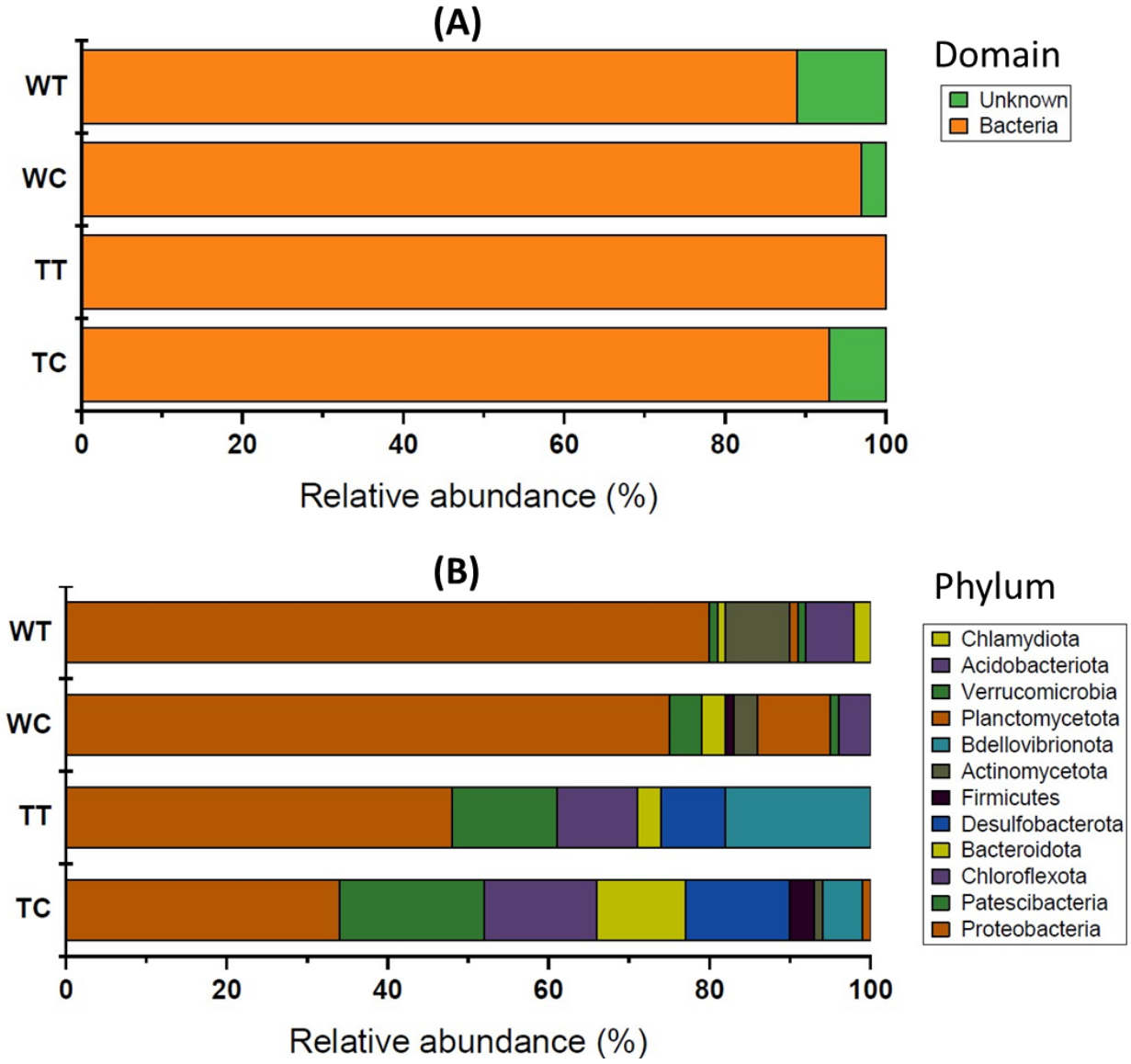

Figure 4.2: Taxonomy of tailings and capping water in temperature-constant and temperature-modified columns at (A) domain level and (B) phylum level. Taxonomy was estimated with Anvi'o anvi-estimate-scg-taxonomy

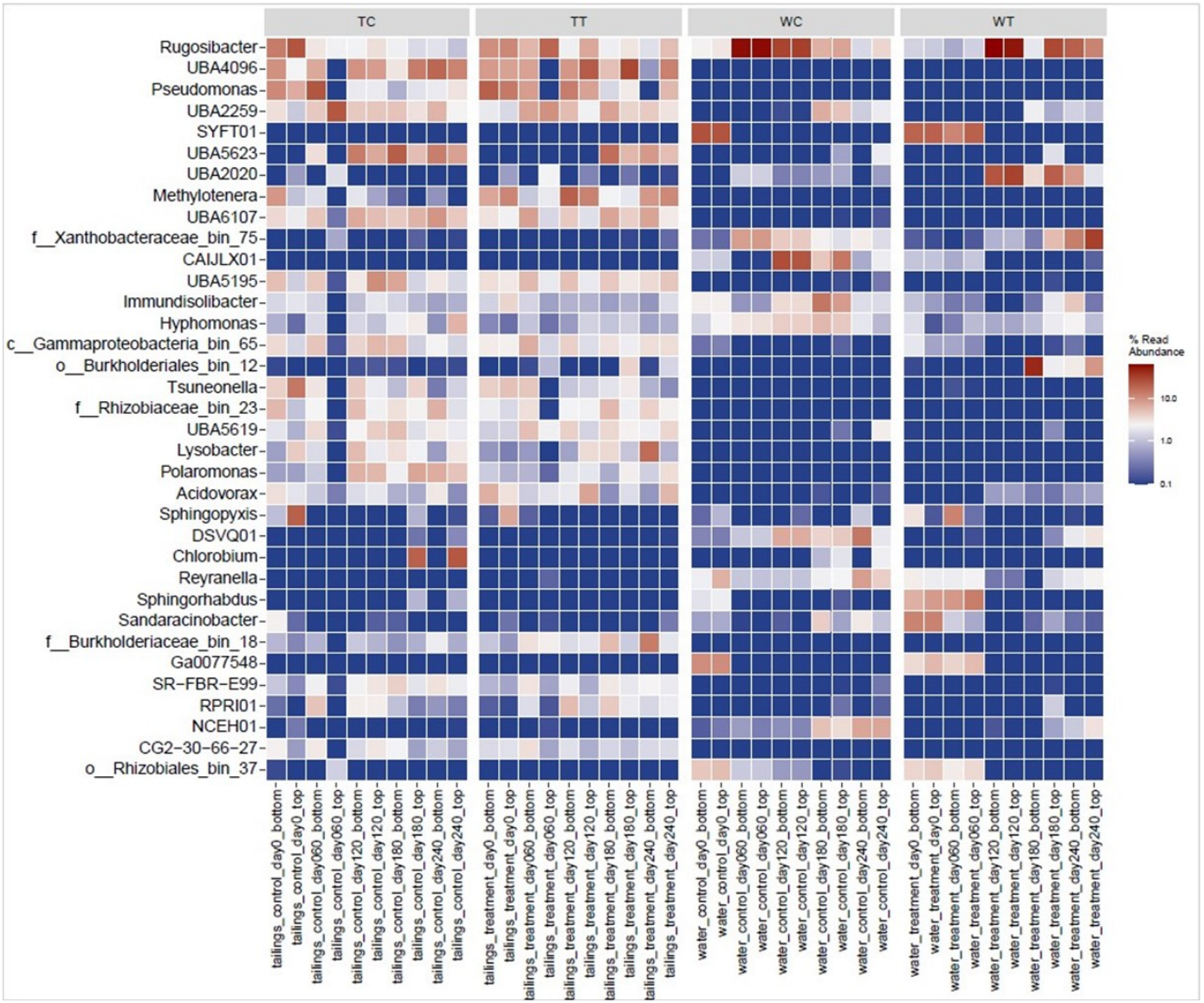

Figure 4.3: Heatmap of the most abundant bacteria genera in model pit lake systems

4.3.3 Processes/mechanisms of biogeochemical cycling in model pit lakes

As explained in section 4.2.4, the nutrient cycling analysis was separately carried out for each of TC, TT, WC, and WT using Metascan. The results of the analyses revealed the occurrence of carbon, sulfur, and nitrogen cycling in the model pit lakes. In TC, carbon cycling accounted for 60%, with sulfur cycling accounting for 16.5%, while nitrogen cycling accounted for 23.5% (Figure 4.4). Meanwhile, in TT carbon cycling, sulfur cycling, and nitrogen cycling accounted for 52.4%, 19.3%, and 28.3% respectively (Figure 4.5). On the other hand, in WC carbon cycling, sulfur cycling, and nitrogen cycling accounted for 58%, 17%, and 25% respectively (Figure 4.6). Comparatively, in WT carbon cycling, sulfur cycling, and nitrogen cycling accounted for 59%, 16% and 25% respectively (Figure 4.7). Each of these nutrient cycles was differently influenced by specific processes. For example, the most prominent carbon cycling processes in model pit lakes were Methanotrophy, Formaldehyde assimilation via serine pathway, Wood-Ljungdahl pathway, Citric Acid cycle, and Oxidative phosphorylation. For sulfur cycling, the most prominent processes include Sulfite reduction and Thiosulfate oxidation whereas the most prominent nitrogen cycling processes include Nitrite oxidation, Denitrification and Dissimilatory nitrate reduction to ammonium (DNRA). Table 4.1 summarizes the processes found in model pit lakes along with their percentages.

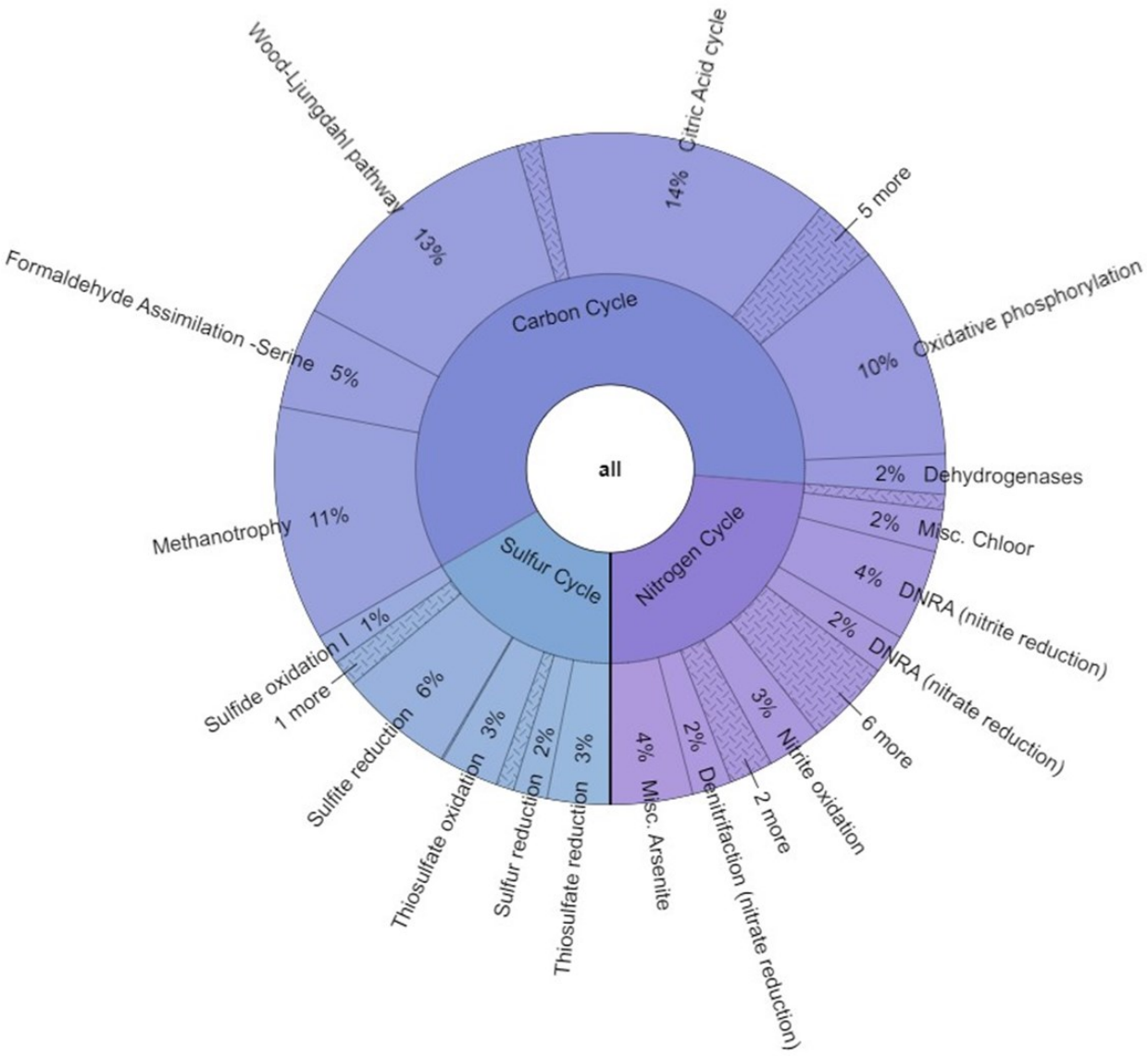

Figure 4.4: Krona plot of nutrient cycling processes in TC

Figure 4.5: Krona plot of nutrient cycling processes in TT

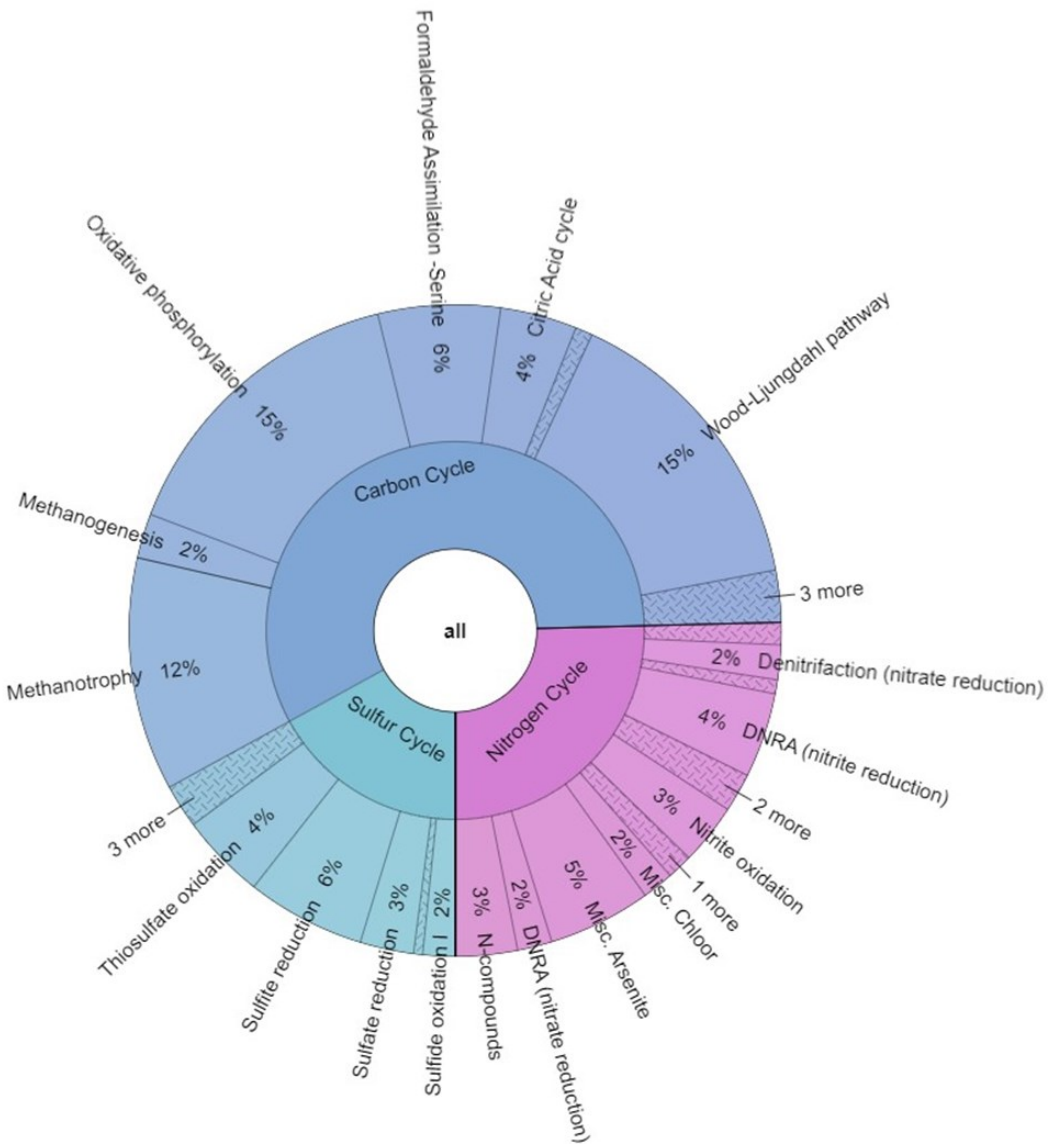

Figure 4.6: Krona plot of nutrient cycling processes in WC

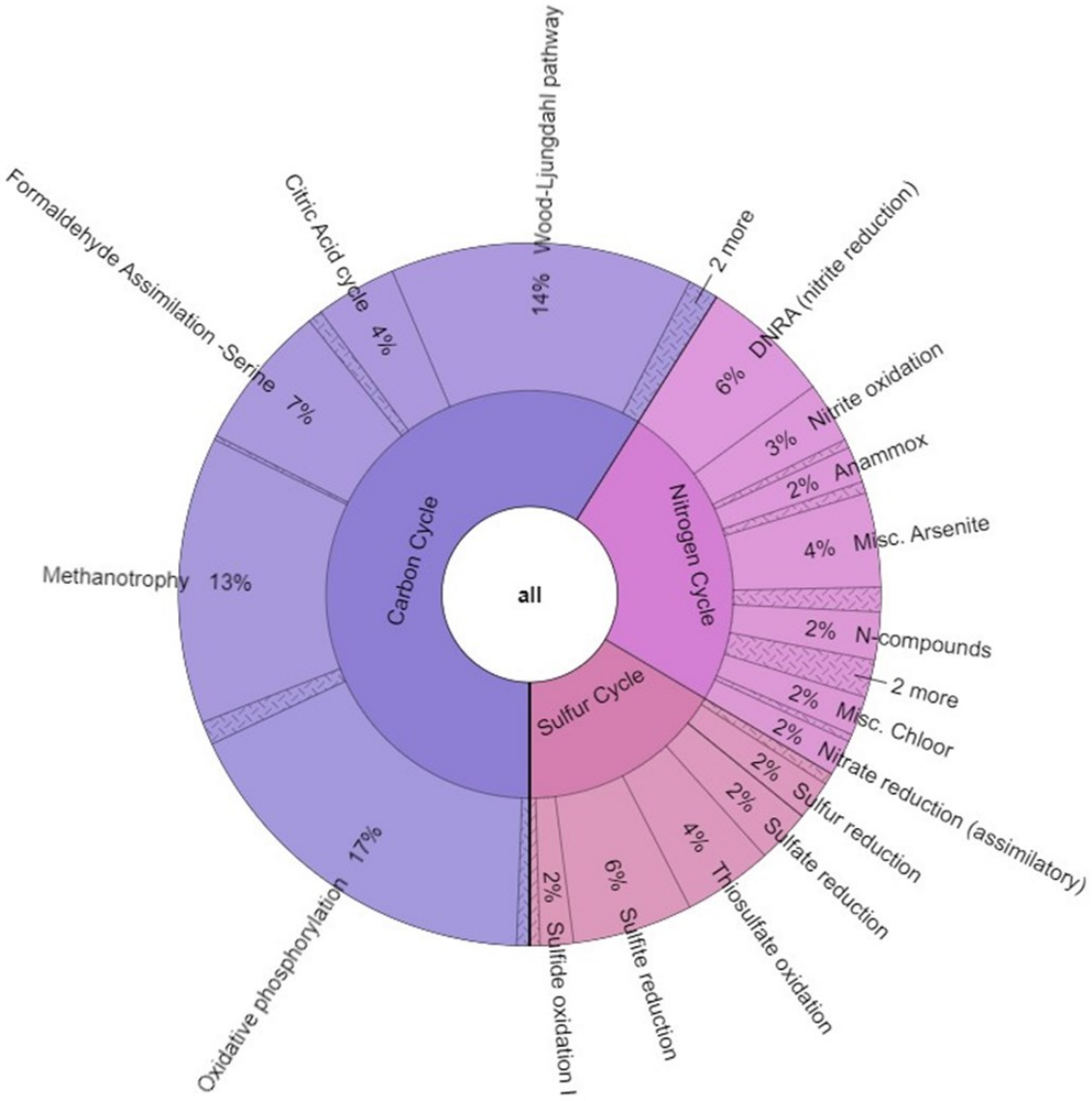

Figure 4.7: Krona plot of nutrient cycling processes in WT

Table 4.1: Nutrient cycling processes predicted in model pit lakes

Processes	TC (%)	TT (%)	WC (%)	WT (%)	**
Carbon cycling					
Methanotrophy	11.7	11.0	13.0	14.0	**
Formaldehyde assimilation - serine	5.0	5.0	6.0	7.0	**
Wood-Ljungdahl pathway	13.0	11.0	15.0	14.0	**
Calvin cycle	1.0	1.0	0.7	0.7	
Citric Acid cycle	14.0	10.0	4.0	4.0	**
Methanogenesis	1.0	0.5	2.0	0.6	**
Oxidative phosphorylation	10.0	10.0	15.0	17.0	**
Sulfur cycling					
Sulfide oxidation	1.0	1.0	2.0	2.0	**
Sulfate reduction	1.0	2.0	3.0	2.0	**
Sulfite reduction	6.0	6.0	6.0	6.0	
Thiosulfate oxidation	3.0	4.0	4.0	4.0	**
Sulfite oxidation	0.9	1.0	0.8	0.5	**
Sulfur reduction	2.0	3.0	1.0	2.0	**
Thiosulfate reduction	3.0	2.0	0.4	0.5	**
Nitrogen cycling					
Nitrogen fixation	1.0	2.0	0.6	0.07	**
Ammonium oxidation	0.1	0.4	0.0	0.07	**
Nitrite oxidation	3.0	3.0	3.0	3.0	
Anammox	0.7	0.8	1.0	2.0	**
Assimilatory nitrate reduction	0.7	0.8	1.0	2.0	**
Denitrification	3.9	6.5	3.0	2.0	**
Dissimilatory nitrate reduction to ammonium	6.0	7.0	6.0	7.0	**
N-compounds	0.9	1.0	3.0	2.0	**

** Significant difference based on statistical tests (ANOVA, post-hoc tests), indicating differences between conditions (TC, TT, WC, WT)

4.3.4 Functional genes for biogeochemical cycling in model pit lakes

The functional genes for biogeochemical cycling for tailings (TC and TT) and capping water (WC and WT) were analyzed based on the prevailing processes/mechanisms for each of the three nutrient cycles observed in the model pit lake columns. For carbon cycle, the prevailing processes were Methanotrophy, Formaldehyde assimilation via the serine pathway, Wood-Ljungdahl pathway, Calvin cycle, Citric acid cycle (TCA cycle), Methanogenesis, and Oxidative phosphorylation. Meanwhile, the prevailing mechanisms for sulfur cycle were Sulfide oxidation, Sulfate reduction, Sulfite reduction, Thiosulfate oxidation, Sulfite oxidation, Sulfur reduction, and

Thiosulfate reduction. Finally, the prevailing processes for nitrogen cycles were Nitrogen fixation, Ammonium oxidation, Nitrite oxidation, Anammox, Assimilatory nitrate reduction (ANR), Denitrification, Dissimilatory nitrate reduction to ammonium (DNRA), and N-compounds.

4.3.4.1 Carbon cycle

The analysis of functional genes for carbon cycling across TC, TT, WC, and WT conditions revealed the expression levels for various processes (Table 4.2). Methanotrophy showed the highest expression with formate dehydrogenase major subunit (*fdoG*, *fdhF*, *fdwA*), formate dehydrogenase subunit gamma (*fdoI*, *fdsG*), formate dehydrogenase iron-sulfur subunit (*fdoH*, *fdsB*) and S-[hydroxymethyl]glutathione dehydrogenase/alcohol dehydrogenase (*frmA, ADH5, adhC*) at 3% while the least expressed was formate dehydrogenase (*FDH*) at 0.04%. One-way ANOVA indicated no significant difference in expression levels among TC, TT, WC, and WT (F-value = 0.048, p-value = 0.99).

For formaldehyde assimilation via the serine pathway, glycine hydroxymethyltransferase (*glyA*, *SHMT*), malate-CoA ligase subunit beta (*mtkA*) and malate-CoA ligase subunit alpha (*mtkB*) were the most expressed at 2%, with malyl-CoA/(S)-citramalyl-CoA lyase (*mcl*) being the least expressed at 0.04%. ANOVA showed no significant variation among conditions (F-value = 0.19, p-value = 0.90). In the Wood-Ljungdahl pathway, the most expressed genes were aerobic carbon-monoxide dehydrogenase large subunit (*coxL, cutL*) and small subunit (*coxS*) at 5%, while acetyl-CoA decarbonylase/synthase complex subunits delta (*cdhD, acsD*) and gamma (*cdhE, acsC*) were the least expressed at 0.1%. ANOVA results showed no significant difference (F-value = 0.098, p-value = 0.96).

For the Calvin cycle, ribulose-bisphosphate carboxylase large chain (*rbcL*) was the most expressed at 0.6%, and the small chain (*rbcS*) was the least at 0.07%. ANOVA revealed no

significant differences (F-value = 0.70, p-value = 0.58). In TCA cycle, the most expressed genes were 2-oxoglutarate/2-oxoacid ferredoxin oxidoreductase subunit alpha (*korA, oorA, oforA*) and delta (*korD, oorD*) at 3%, while pyruvate ferredoxin oxidoreductase alpha subunit (*porA*), gamma subunit (*porG*), and malyl-CoA/(S)-citramalyl-CoA lyase (*mcl*) were the least at 0.04%. ANOVA showed significant differences (F-value = 4.20, p-value = 0.011).

For methanogenesis, the most expressed gene was 5,6,7,8-tetrahydromethanopterin hydrolyase (*fae*) at 1%, and the least expressed were formylmethanofuran-tetrahydromethanopterin N-formyltransferase (*ftr*) and [methyl-Co(III) methanol-specific corrinoid protein]M methyltransferase (*mtaA*) at 0.04%. ANOVA indicated no significant difference (F-value = 1.70, p-value = 0.20).

Lastly, for oxidative phosphorylation, cytochrome c oxidase subunit I (*coxA, ctaD*) and subunit II (*coxB, ctaC*) were the most expressed at 3%, while cytochrome o ubiquinol oxidase subunit II (*cyoA*), cytochrome c oxidase subunit I+III (*coxAC*), and cytochrome aa3-600 menaquinol oxidase subunit I (*qoxB*) were the least at 0.1%. ANOVA revealed no significant variation (F-value = 1.97, p-value = 0.13).

Table 4.2: Functional genes for carbon cycling and their percent expression in model pit lakes

Processes/mechanisms	Functional genes	Expression (%)			
		TC	TT	WC	WT
Methanotrophy	*fdoG, fdhF, fdwA* (formate dehydrogenase major subunit)	3.0	2.0	2.0	2.0
	fdoI, fdsG (formate dehydrogenase subunit gamma)	3.0	3.0	2.0	2.0
	fdoH, fdsB (formate dehydrogenase iron-sulfur subunit)	2.0	2.0	2.0	3.0
	fdwB (formate dehydrogenase beta subunit)	1.0	2.0	0.4	0.5
	frmA, ADH5, adhC (S-[hydroxymethyl]glutathione dehydrogenase / alcohol dehydrogenase)	1.0	1.0	3.0	3.0
	frmB, ESD, fghA (S-formylglutathione hydrolase)	0.6	0.6	0.5	0.5
	mdh1, mxaF (methanol dehydrogenase [cytochrome c] subunit 1)	0.6	0.8	1.0	0.9
	fdsD (formate dehydrogenase subunit delta)	0.2	0.2	0.4	0.5
	fdhA (formate dehydrogenase [coenzyme F420] alpha subunit)	0.09	0.1	0.2	0.4
	FDH (formate dehydrogenase)	0.04	0.1	0.08	0.07
	mauB (methylamine dehydrogenase heavy chain)	-	-	1.0	0.2
	mauA (methylamine dehydrogenase light chain)	-	-	0.08	0.2
Formaldehyde assimilation -serine	*glyA, SHMT* (glycine hydroxymethyltransferase)	2.0	2.0	2.0	2.0
	mtkA (malate-CoA ligase subunit beta)	1.4	1.0	2.0	2.0
	mtkB (malate-CoA ligase subunit alpha)	1.3	2.0	1.0	2.0
	mcl (malyl-CoA/(S)-citramalyl-CoA lyase)	0.04	0.1	0.5	0.4
Wood-Ljungdahl pathway	*cooF* (anaerobic carbon-monoxide dehydrogenase iron sulfur subunit)	4.0	4.0	3.0	4.0
	fdhA (formate dehydrogenase (NADP+) alpha subunit)	2.0	1.0	0.3	0.6
	coxL, cutL (aerobic carbon-monoxide dehydrogenase large subunit)	2.0	2.0	5.0	3.0
	coxS (aerobic carbon-monoxide dehydrogenase small subunit)	2.0	2.0	5.0	5.0
	cooS, acsA (anaerobic carbon-monoxide dehydrogenase catalytic subunit)	0.8	0.3	-	-
	fdhB (formate dehydrogenase (NADP+) beta subunit)	0.7	0.3	0.2	0.2
	cdhD, acsD (acetyl-CoA decarbonylase/synthase complex subunit delta)	0.5	0.1	-	-
	acsB (acetyl-CoA synthase)	0.4	0.2	-	-
	coxM, cutM (aerobic carbon-monoxide dehydrogenase medium subunit)	0.3	0.6	1.0	0.6
	cdhE, acsC (acetyl-CoA decarbonylase/synthase complex subunit gamma)	0.3	0.1	-	-
Calvin cycle	*rbcL* (ribulose-bisphosphate carboxylase large chain)	0.6	0.5	0.3	0.3
	rbcS (ribulose-bisphosphate carboxylase small chain)	0.3	0.2	0.2	0.07
	PRK, prkB (phosphoribulokinase)	0.2	0.3	0.2	0.3
	korD, oorD (2-oxoglutarate ferredoxin oxidoreductase subunit delta)	3.0	2.0	0.5	0.5
	korA, oorA, oforA (2-oxoglutarate/2-oxoacid ferredoxin oxidoreductase subunit alpha)	3.0	2.0	0.9	0.7
	korB, oorB, oforB (2-oxoglutarate/2-oxoacid ferredoxin oxidoreductase subunit beta)	2.0	1.0	0.7	0.5
	korC, oorC (2-oxoglutarate ferredoxin oxidoreductase subunit gamma)	2.0	1.0	0.2	0.07
	por, nifJ (pyruvate-ferredoxin/flavodoxin oxidoreductase)	1.0	1.0	0.2	0.1

Citric Acid cycle (TCA cycle)	*porD* (pyruvate ferredoxin oxidoreductase delta subunit)	1.0	1.0	0.5	0.9
	porG (pyruvate ferredoxin oxidoreductase gamma subunit)	0.6	0.2	0.04	0.2
	porB (pyruvate ferredoxin oxidoreductase beta subunit)	0.5	0.2	0.08	0.2
	porA (pyruvate ferredoxin oxidoreductase alpha subunit)	0.4	0.2	0.04	0.2
	mcl (malyl-CoA/(S)-citramalyl-CoA lyase)	0.04	0.1	0.5	0.4
	aclA (ATP-citrate lyase alpha subunit)	-	-	0.08	-
Methanogenesis	*cdhD, acsD* (acetyl-CoA decarbonylase/synthase complex subunit delta)	0.5	0.1	-	-
	cdhE, acsC (acetyl-CoA decarbonylase/synthase complex subunit gamma)	0.3	0.1	-	-
	fae (5,6,7,8-tetrahydromethanopterin hydrolyase)	0.09	0.1	1.0	0.3
	mch (methenyltetrahydromethanopterin cyclohydrolase)	0.09	0.1	0.5	0.1
	ftr (formylmethanofuran-tetrahydromethanopterin N-formyltransferase)	0.04	0.1	0.7	0.2
	mtaA ([methyl-Co(III) methanol-specific corrinoid protein]:coenzyme M methyltransferase)	0.04	-	-	-
Oxidative phosphorylation	*cydA* (cytochrome bd ubiquinol oxidase subunit I)	2.0	2.0	2.0	2.0
	ccoP (cytochrome c oxidase cbb3-type subunit III)	2.0	1.0	1.0	2.0
	coxA, ctaD (cytochrome c oxidase subunit I)	1.0	1.0	3.0	3.0
	ccoO (cytochrome c oxidase cbb3-type subunit II)	1.0	0.9	0.9	1.0
	cydB (cytochrome bd ubiquinol oxidase subunit II)	1.0	1.0	2.0	2.0
	coxB, ctaC (cytochrome c oxidase subunit II)	1.0	1.0	3.0	3.0
	ccoN (cytochrome c oxidase cbb3-type subunit I)	0.9	1.0	1.0	1.0
	COX10, ctaB, cyoE (heme o synthase)	0.9	0.8	1.0	2.0
	cyoD (cytochrome o ubiquinol oxidase subunit IV)	0.2	0.3	0.6	0.7
	cyoA (cytochrome o ubiquinol oxidase subunit II)	0.1	0.1	0.6	0.5
	qoxB (cytochrome aa3-600 menaquinol oxidase subunit I)	0.1	0.2	0.5	0.8
	coxAC (cytochrome c oxidase subunit I+III)	0.1	1.0	0.1	-

4.3.4.2 Sulfur cycle

The analysis of functional genes for sulfur cycling across TC, TT, WC, and WT conditions revealed the expression levels for various mechanisms (Table 4.3). Sulfide oxidation was observed with sulfide:quinone oxidoreductase (*sqr*), showing 2% expression in WC and WT, and 1% in TC and TT. Sulfate reduction revealed sulfite reductase (NADPH) hemoprotein beta component (*cysI*) and sulfite reductase (NADPH) flavoprotein alpha component (*cysJ*) expressed at 1% while dissimilatory sulfite reductase alpha subunit (*dsrA*) and dissimilatory sulfite reductase beta subunit (*dsrB*) were least expressed at 0.04%. ANOVA indicated no significant variation (F-value = 0.30, p-value = 0.83). For sulfite reduction, adenylylsulfate kinase (*cysC*) was the most expressed gene at 2%, and adenylylsulfate reductase subunit A (*aprA*) was the least expressed at 0.07%. ANOVA showed no significant variation (F-value = 0.33, p-value = 0.80). In thiosulfate oxidation, sulfur-oxidizing protein SoxX (*soxX*) was the most expressed gene at 1%, while sulfite dehydrogenase subunit SoxC (*soxC*) and sulfur-oxidizing protein SoxA (*soxA*) were the least expressed at 0.2%. ANOVA revealed no significant variation (F-value = 0.85, p-value = 0.48). For sulfite oxidation, the highest gene expression was sulfite dehydrogenase (*E1.8.2.1*) at 0.4%, and the lowest was sulfite oxidase (*SUOX*) at 0.04%. ANOVA indicated no significant variation (F-value = 1.16, p-value = 0.36). In sulfur reduction, cytochrome subunit of sulfide dehydrogenase (*fccA*) was the most expressed gene at 2%, while sulfide dehydrogenase [flavocytochrome c] flavoprotein chain (*fccB*) was the least expressed at 0.1%. ANOVA showed no significant variation (F-value = 0.094, p-value = 0.96). For thiosulfate reduction, thiosulfate reductase/polysulfide reductase chain A (*phsA, psrA*) was the most expressed gene at 2%, and thiosulfate reductase electron transport protein (*phsB*) was the least expressed at 0.08%. ANOVA revealed no significant variation (F-value = 1.29, p-value = 0.39).

Table 4.3: Functional genes for sulfur cycling and their percent expression in model pit lakes

Processes/mechanisms	Functional genes	Expression (%)			
		TC	TT	WC	WT
Sulfide oxidation	*sqr* (sulfide:quinone oxidoreductase)	1.0	1.0	2.0	2.0
Sulfate reduction	*cysI* (sulfite reductase (NADPH) hemoprotein beta component)	0.6	0.8	1.0	1.0
	dsrA (dissimilatory sulfite reductase alpha subunit)	0.3	0.5	0.04	0.1
	dsrB (dissimilatory sulfite reductase beta subunit)	0.2	0.3	0.04	0.07
	cysJ (sulfite reductase (NADPH) flavoprotein alpha component)	0.2	0.3	1.0	0.9
	sir (sulfite reductase [ferredoxin])	0.1	0.2	0.4	0.07
Sulfite reduction	*cysC* (adenylylsulfate kinase)	1.0	2.0	1.0	1.0
	cysD (sulfate adenylyltransferase subunit 2)	0.9	0.9	1.0	1.0
	aprB (adenylylsulfate reductase, subunit B)	0.7	0.7	0.8	0.3
	cysNC (bifunctional enzyme CysN/CysC)	0.7	0.8	1.0	1.0
	cysH (phosphoadenosine phosphosulfate reductase)	0.6	0.8	1.0	0.9
	cysN (sulfate adenylyltransferase subunit 1)	0.5	0.5	0.3	0.5
	sat, met3 (sulfate adenylyltransferase)	0.4	0.4	0.2	0.1
	aprA (adenylylsulfate reductase subunit A)	0.3	0.3	-	0.07
Thiosulfate oxidation	*soxY* (sulfur-oxidizing protein SoxY)	0.6	0.9	0.7	0.7
	soxX (sulfur-oxidizing protein SoxX)	0.6	0.7	1.0	1.0
	soxB (sulfur-oxidizing protein SoxB)	0.5	0.4	0.4	0.4
	soxC (sulfite dehydrogenase subunit SoxC)	0.3	0.2	0.3	0.3
	soxD (S-disulfanyl-L-cysteine oxidoreductase SoxD)	0.3	0.5	0.5	0.5
	soxZ (sulfur-oxidizing protein SoxZ)	0.3	0.5	0.5	0.6
	soxA (sulfur-oxidizing protein SoxA)	0.2	0.4	0.4	0.5
Sulfite oxidation	*E1.8.2.1* (sulfite dehydrogenase)	0.4	0.3	0.2	0.1
	soeA (sulfite dehydrogenase [quinone] subunit SoeA)	0.2	0.3	0.2	0.1
	soeB (sulfite dehydrogenase [quinone] subunit SoeB)	0.1	0.2	0.2	0.07
	soeC (sulfite dehydrogenase [quinone] subunit SoeC)	0.1	0.2	0.2	0.07
	SUOX (sulfite oxidase)	-	-	0.04	0.07
Sulfur reduction	*fccA* (cytochrome subunit of sulfide dehydrogenase)	2.0	2.0	0.9	2.0
	fccB (sulfide dehydrogenase [flavocytochrome c] flavoprotein chain)	0.1	0.3	0.4	0.3
Thiosulfate reduction	*phsA, psrA* (thiosulfate reductase / polysulfide reductase chain A)	2.0	2.0	0.4	0.4
	phsB (thiosulfate reductase electron transport protein)	0.9	0.2	0.08	0.1

4.3.4.3 Nitrogen cycle

The analysis of functional genes for nitrogen cycling across TC, TT, WC, and WT conditions revealed the expression levels for various processes (Table 4.4). For nitrogen fixation, the highest expression was observed with nitrogenase molybdenum-iron protein alpha chain (*nifD*) at 0.9%, and the lowest expression was with nitrogenase delta subunit (*anfG*) at 0.04%. ANOVA indicated significant variations among the conditions (F-value = 5.02, p-value = 0.033).

For ammonium oxidation, the most expressed gene was methane/ammonia monooxygenase subunit A (*pmoA-amoA*) at 0.2%, while the least expressed was methane/ammonia monooxygenase subunit B (*pmoB-amoB*) at 0.07%. Significant differences among conditions were found (ANOVA, F-value = 4.07, p-value = 0.030).

In nitrite oxidation, the highest expression was for assimilatory nitrate reductase catalytic subunit (*nasA*) at 2%, and the lowest was for cytochrome c-type protein NapB (*napB*) and ferredoxin-nitrate reductase (*narB*) at 0.04%. No significant variation was detected (ANOVA, F-value = 0.091, p-value = 0.96). For anammox, the most expressed gene was *nasA* at 2%, and the least was *nasB* at 0.08%. ANOVA revealed no significant differences (F-value = 0.29, p-value = 0.83). For assimilatory nitrate reduction (ANR), *nasA* was again the most expressed at 2%, while *narB* was the least at 0.04%. There was no significant variation (ANOVA, F-value = 0.27, p-value = 0.84).

In denitrification, the highest expression was for nitric oxide reductase subunit B (*norB*) at 1%, and the lowest was for *NapB* at 0.04%. Significant differences were observed (ANOVA, F-value = 4.9, p-value = 0.0059). For dissimilatory nitrate reduction to ammonium (DNRA), nitrite reductase [NADH] small subunit (*nirD*) had the highest expression at 4%, while *NapB* had the lowest at 0.04%. ANOVA showed no significant variation (F-value = 0.039, p-value = 0.99).

Table 4.4: Functional genes for nitrogen cycling and their percent expression in model pit lakes

Processes/mechanisms	Functional genes	Expression (%)			
		TC	TT	WC	WT
Nitrogen fixation	*nifK* (nitrogenase molybdenum-iron protein beta chain)	0.5	0.7	0.2	-
	nifD (nitrogenase molybdenum-iron protein alpha chain)	0.4	0.9	0.2	-
	nifH (nitrogenase iron protein NifH)	0.2	0.6	0.2	0.07
	anfG (nitrogenase delta subunit)	0.04	-	-	-
Ammonium oxidation	*pmoA-amoA* (methane/ammonia monooxygenase subunit B)	-	0.2	-	-
	pmoB-amoB (methane/ammonia monooxygenase subunit B)	0.1	0.1	-	0.07
	pmoC-amoC (methane/ammonia monooxygenase subunit C)	-	0.1	-	-
Nitrite oxidation	*narG, narZ, nxrA* (nitrate reductase / nitrite oxidoreductase alpha subunit)	0.8	0.8	0.6	0.5
	nasA (assimilatory nitrate reductase catalytic subunit)	0.7	0.8	1.0	2.0
	narI, narV (nitrate reductase gamma subunit)	0.6	0.6	0.4	0.3
	narH, narY, nxrB (nitrate reductase / nitrite oxidoreductase beta subunit)	0.3	0.8	0.6	0.2
	napA (periplasmic nitrate reductase NapA)	0.09	0.2	0.08	0.07
	napB (cytochrome c-type protein NapB)	0.04	0.2	-	0.07
	narB (ferredoxin-nitrate reductase)	0.04	-	0.04	-
	nasB (assimilatory nitrate reductase electron transfer subunit)	-	-	0.08	0.1
Anammox	*nasA* (assimilatory nitrate reductase catalytic subunit)	0.7	0.8	1.0	2.0
	nasB (assimilatory nitrate reductase electron transfer subunit)	-	-	0.08	0.1
Assimilatory nitrate reduction	*nasA* (assimilatory nitrate reductase catalytic subunit)	0.7	0.8	1.0	2.0
	narB (ferredoxin-nitrate reductase)	0.04	-	0.04	-
	nasB (assimilatory nitrate reductase electron transfer subunit)	-	-	0.08	0.1
Denitrification	*narG, narZ, nxrA* (nitrate reductase / nitrite oxidoreductase alpha subunit)	0.8	0.8	0.6	0.5
	norB (nitric oxide reductase subunit B)	0.8	1.0	0.4	0.2
	norC (nitric oxide reductase subunit C)	0.6	0.9	0.3	0.4
	narI, narV (nitrate reductase gamma subunit)	0.6	0.6	0.4	0.3
	nosZ (nitrous-oxide reductase)	0.5	0.9	0.2	0.3
	narH, narY, nxrB (nitrate reductase / nitrite oxidoreductase beta subunit)	0.3	0.8	0.6	0.2
	nirK (nitrite reductase [NO-forming])	0.2	0.3	0.08	0.07
	nirS (nitrite reductase (NO-forming) / hydroxylamine reductase)	0.2	0.4	-	0.07
	napA (periplasmic nitrate reductase NapA)	0.09	0.2	0.08	0.07
	napB (cytochrome c-type protein NapB)	0.04	0.2	-	0.07
	nirD (nitrite reductase [NADH] small subunit)	2.0	2.0	3.0	4.0
	nirB (nitrite reductase (NADH) large subunit)	0.8	0.8	0.8	1.0
	narG, narZ, nxrA (nitrate reductase / nitrite oxidoreductase alpha subunit)	0.8	0.8	0.6	0.5
	nrfA (nitrite reductase [cytochrome c-552])	0.7	0.6	0.2	0.07

Dissimilatory nitrate reduction to ammonium (DNRA)	*nrfH* (cytochrome c nitrite reductase small subunit)	0.6	0.9	0.2	0.2
	narI, narV (nitrate reductase gamma subunit)	0.6	0.6	0.4	0.3
	narH, narY, nxrB (nitrate reductase / nitrite oxidoreductase beta subunit)	0.3	0.8	0.6	0.2
	napA (periplasmic nitrate reductase NapA)	0.09	0.2	0.08	0.07
	napB (cytochrome c-type protein NapB)	0.04	0.2	-	0.07
N-compounds	*ureC* (urease subunit alpha)	0.3	0.3	0.9	0.7
	ureB (urease subunit beta)	0.3	0.4	0.3	0.4
	ureA (urease subunit gamma)	0.2	0.3	0.4	0.4
	cynS (cyanate lyase)	0.09	0.2	0.7	0.3
	ureAB (urease subunit gamma/beta)	0.04	-	0.4	0.3
	nthA (nitrile hydratase subunit alpha)	0.04	-	0.4	0.07

For N-compounds, urease subunit alpha (*ureC*) was the most expressed at 0.9%, whereas urease subunit gamma/beta (*ureAB*) and nitrile hydratase subunit alpha (*nthA*) were the least at 0.04%. Significant differences among conditions were found (ANOVA, F-value = 4.59, p-value = 0.013).

4.4 Discussion

4.4.1 Microbial diversity in model pit lakes

The microbial communities in the model pit lakes were distinctively unique between capping water and tailings. Within the tailings (TC and TT) and capping water (WC and WT), there were similarity and differences between the microbial compositions. For the capping water, the top (surface water) and bottom (deeper water) samples are dispersed, indicating that they have a more varied microbial community. For the tailings, the top and bottom samples were aggregated separately, indicating that the microbial communities at different depths in the tailings are more distinct from each other and form separate subclusters. Overall, model pit lakes were dominated by bacteria which vary significantly in abundance and composition between tailings and capping water. The observed differences in abundance and composition are likely driven by a combination of environmental conditions, nutrient availability, microbial interactions, hydrodynamic factors, and microbial physiological adaptations. Specifically, the temperature differences between the temperature-constant (TC, WC) and temperature-modified (TT, WT) columns could influence microbial growth and metabolism as temperature is a critical factor that affects enzyme activity, metabolic rates, and the overall physiological state of microorganisms (Pietikäinen et al., 2005). Furthermore, the physical and chemical properties of tailings and capping water are inherently different. Tailings tends to have lower oxygen levels and higher concentrations of organic matter and nutrients compared to capping water. These differences could lead to variation in microbial composition and abundance and can therefore select distinct microbial communities adapted to

specific conditions (Borer et al., 2018; Grettenberger et al., 2020; Leff et al., 2015). Also, the interface between tailings and capping water can create unique microenvironments that affect microbial communities. The transport of nutrients, oxygen, and other chemicals across this interface can create gradients that favor different microbial taxa (Ki et al., 2018). Additionally, microbial communities are influenced by interactions between different species, including competition for resources and synergistic relationships. The composition and abundance of bacteria can be shaped by these interactions, which may differ between the tailings and capping water due to the distinct environmental pressures and resource availability (Little et al., 2008).

In the model pit lakes, the most abundant phylum in all conditions was Proteobacteria, with 34%, 48%, 75%, and 80% respectively in TC, TT, WC, and WT. The higher relative abundance of Proteobacteria in capping water (WC and WT) suggests that this phylum may thrive better in the more oxygenated and nutrient-diluted environment of the water column. Furthermore, the higher percentage of Proteobacteria in the temperature-modified columns (TT and WT) suggests that these bacteria may be more adaptable or resilient to temperature changes compared to other phyla. Proteobacteria are known for their metabolic versatility and ability to adapt to various environmental conditions. This phylum includes many species that can utilize a wide range of substrates, possess diverse metabolic pathways, and play key roles in the carbon, sulfur, and nitrogen cycle (Kersters et al., 2006). This might explain their dominance across all conditions in the model pit lakes.

While members of Uncultivated Bacteria and Archaea (UBA) dominated the tailings in model pit lake columns at genus level, TT differed from TC by having a very high abundance of *Stutzerimonas* (15%) and *Rugosibacter* (12%). It has been revealed that many bacterial phyla contain abundant UBA genomes. Recently, Parks et al., (2017) recovered about 8,000 UBA

genomes distributed across 76 bacterial phyla and 21 archaeal phyla. *Stutzerimonas* is a new genus recently proposed by Lalucat et al., (2022). *Stutzerimonas* species are chemoorganotroph with aerobic, strictly oxidative, and non-fermentative metabolism. Most species are capable of starch hydrolysis, nitrate reduction and nitrogen fixation (Lalucat et al., 2022). *Rugosibacter* species can use aromatic compounds as sole carbon and energy sources and are closely related to *Sulfuritalea hydrogenivorans* strain sk43H^T, *Denitratisoma sp.* TSA61, *Georgfuchsia toluolica* G5G6^T, *Sulfurisoma sediminicola* BSN1^T, *Denitratisoma oestradiolicum* AcBE2-1^T and *Sterolibacterium denitrificans* ChoI-1S^T suggesting likelyhood of denitrification and sulfur oxidation (Corteselli et al., 2017; Kojima et al., 2022). Meanwhile, the capping water was dominated by *Rugosibacter* (22% in WC and 21% in WT) and *Brevundimonas* (11% in both WC and WT). *Brevundimonas* species have been implicated in hydrocarbon degradation (Ganiyu et al., 2022) and nitrogen cycling (Sun et al., 2019). Additionally, both tailings and capping water featured abundant genera capable of carbon, sulfur, and nitrogen cycling.

4.4.2 Biogeochemical cycling in model pit lakes: processes and functional genes

The biogeochemical cycling of carbon, sulfur and nitrogen was prominent in both tailings and capping water, with carbon cycling accounting for 52 to 60%, sulfur cycling accounting for 16 to 19% and nitrogen cycling accounting for 24 to 28% across all columns. This suggested that there was little difference between tailings and capping water with regards to individual cycling, however carbon cycling was more prominent than the other cycling in the model pit lakes. Likewise, there was no difference in nutrient cycling between temperature-constant and temperature-varied columns of the model pit lakes. While the microbial community structures were significantly different in abundance and composition in model pit lakes, the lack of significant functional differences in biogeochemical cycling could be attributed to a couple of

factors including functional redundancy, horizontal gene transfer (HGT), core microbiomes, and microbial ecosystem stability and resilience. Microbial communities often exhibit functional redundancy, whereby different microbial species carry out the same biogeochemical functions using similar or identical functional genes. Even though the community composition varies, the functional potential remains similar because multiple taxa possess the necessary genes for nutrient cycling (Allison and Martiny, 2008; Louca et al., 2016). In some cases, HGT could spread functional genes across different microbial species, leading to a situation where diverse communities possess a similar suite of genes with similar functional capacities (Frost et al., 2005). Additionally, there could be a core set of microbial taxa present in both tailings and capping water which might not dominate numerically but contribute significantly to the functional gene pool (Shade and Handelsman, 2012). Finally, the pit lake ecosystem might be relatively stable, with biogeochemical processes buffered against community composition changes and could lead to consistent nutrient cycling functions despite microbial diversity variations (Shade et al., 2012).

Analysis of functional genes revealed important processes for nutrient cycling across all model pit lake columns. For carbon cycling, the model pit lake columns displayed two autotrophic pathways (Calvin Cycle and Wood-Ljungdahl Pathway), four heterotrophic pathways (Methanotrophy, Citric Acid Cycle/TCA Cycle, Methanogenesis, and Oxidative phosphorylation), and one mixed-pathway that could involve both autotrophic and heterotrophic processes especially in methylotrophic organisms (Formaldehyde assimilation - Serine pathway, FASP) (Srivastava et al., 2023). These pathways showed the carbon metabolism and the functional genes involved in model pit lakes (Figure 4.8A). Processes involving methanotrophy, Wood-Ljungdahl Pathway, and Oxidative phosphorylation were relatively very high whereas processes involving Calvin Cycle and methanogenesis were relatively very low. Meanwhile, processes involving FASP were

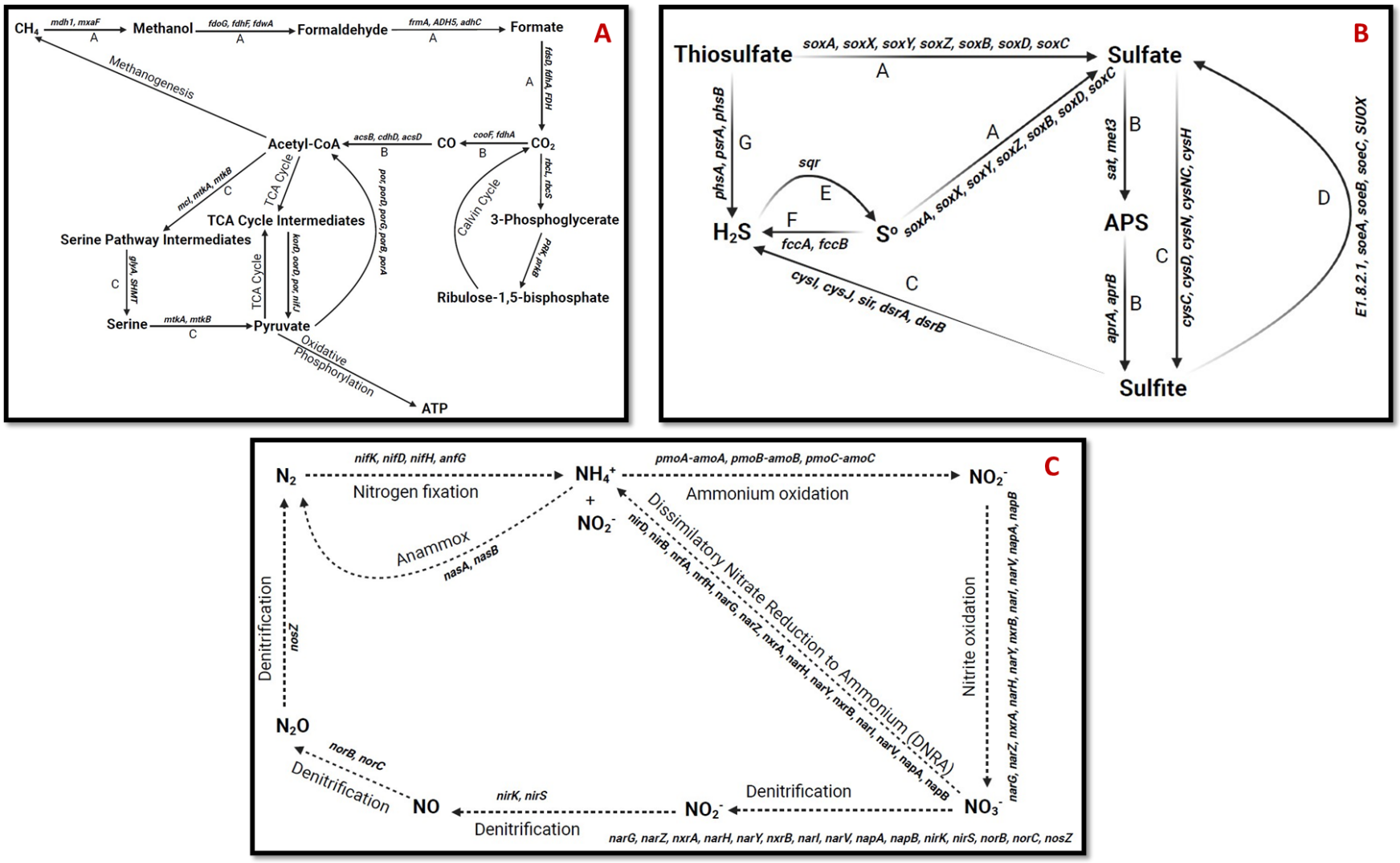

Figure 4.8: (A) Carbon cycling processes and functional genes. A = methanotrophy; B = Wood-Ljungdahl pathway; C = Serine pathway (B) Sulfur cycling processes and functional genes. A = thiosulfate oxidation; B = sulfate reduction; C = sulfite reduction; D = sulfite oxidation; E = sulfide oxidation; F = sulfur reduction; G = thiosulfate reduction (C) Nitrogen cycling processes and functional genes

moderately high and processes involving TCA cycle were relatively very high in tailings and moderately high in capping water. Some important pathways such as pentose phosphate pathway (PPP) that have been shown to be present in acidic pit lake (Ayala-Muñoz et al., 2022) were missing likely because of the differences between the two lakes. Overall, the functional gene analysis provides insight into carbon metabolism of pit lakes and how differences in microbial community structures affect carbon cycling.

For Sulfur cycling, sulfite reduction and thiosulfate oxidation were the processes with highest presence in the model pit lakes and they also had the highest number of expressed functional genes indicating that sulfite and thiosulfate were readily available in model pit lake columns. Sulfite and thiosulfate are important sulfur intermediates that may be reduced to sulfide, oxidized further to sulfate, or disproportionated to form both sulfide and sulfate (Jørgensen et al., 2019). While the other sulfur cycling processes including sulfide oxidation, sulfate reduction, sulfite oxidation, sulfur reduction, and thiosulfate reduction were comparatively low, their presence suggested that complete sulfur cycling was occurring in both tailings and capping water (Figure 4.8B). These processes were equally observed in acidic pit lake though there were some differences in the reported functional genes (Ayala-Muñoz et al., 2022). Most microorganisms found in acidic pit lakes are adapted to extreme acidity, salinity and metal concentrations and this reflects on the functional genes expressed in such pit lakes (Ayala-Muñoz et al., 2020; Sánchez-España, 2024). For nitrogen cycling, denitrification, and dissimilatory nitrate reduction to ammonium (DNRA) were the processes with highest expression in the model pit lakes. Other processes including nitrogen fixation, nitrite oxidation, anammox, assimilatory nitrate reduction, and N-compound were comparatively low (Figure 4.8C). However, expression of nitrogen fixation, ammonium oxidation and denitrification were significantly higher in tailings than capping

water. This was likely due to differences in nitrogen content and redox conditions between tailings and capping water (Feng et al., 2023). Despite this, the overall nitrogen cycling was not significantly different between tailings and capping water. In acidic lakes, dissimilatory nitrate reduction, denitrification, and nitrogen fixation were key processes that contribute to nitrogen cycling (Ayala-Muñoz et al., 2022).

4.5 Corroborating 16S rRNA amplicon sequencing with metagenomics

The 16S rRNA amplicon sequencing conducted in Chapter 3 provided critical insights into the microbial community composition within PASS-treated DPL. This approach allowed for the identification of key taxa present in the system. Comparatively, the metagenome sequencing performed in Chapter 4 yielded a similar microbial profile, with some notable differences. For instance, *Sulfuritalea* was detected in the 16S dataset but not in the metagenomic data, while *Rugosibacter* was identified in the metagenome but absent from the 16S results. These discrepancies could be due to the limitations of each method, such as primer bias in 16S sequencing or lower detection sensitivity in metagenomics for certain low-abundance taxa (Peterson et al., 2021).

Using 16S amplicon sequencing, potential biogeochemical cycles based on the taxonomic composition were inferred, particularly focusing on processes like carbon, sulfur, and nitrogen cycling. However, metagenome sequencing provided deeper insights by directly identifying the functional genes associated with these processes, confirming the involvement of specific microbial taxa in driving these biogeochemical cycles. This allowed for a more detailed understanding of the functional roles played by microbial communities, validating, and expanding on the inferences made from the 16S analysis.

By integrating amplicon sequencing and metagenomics, microbial communities were not only taxonomically resolved but also linked to specific functional pathways, offering a comprehensive picture of their contributions to carbon, sulfur, and nitrogen cycling in the environment. This combined approach enabled a more robust and precise characterization of the microbial ecology and biogeochemical dynamics within the PASS-treated DPL system.

4.6 Conclusions

The metagenomic analysis of nutrient cycling within model pit lake columns has shed light on the taxonomic variations and functional gene differences between tailings and capping water, as well as between columns with constant temperatures and those subjected to seasonal temperature variations. The results reveal notable differences in microbial composition and abundance, alongside variations in the nutrient cycling processes of carbon, sulfur, and nitrogen. While each biogeochemical cycle comprised numerous processes and abundant functional genes, no significant differences were observed in the overall processes between the tailings and capping water thereby indicating a resilient system. This dissertation makes a valuable contribution to our understanding of metagenomic biogeochemical cycling in oil sands pit lakes, highlighting the complex interactions between microbial communities and their environmental conditions.

4.7 References

Alfreider, A., Baumer, A., Bogensperger, T., Posch, T., Salcher, M.M., Summerer, M., 2017. CO2 assimilation strategies in stratified lakes: Diversity and distribution patterns of chemolithoautotrophs. Environ. Microbiol. 19, 2754–2768. https://doi.org/10.1111/1462-2920.13786

Allison, S.D., Martiny, J.B.H., 2008. Resistance, resilience, and redundancy in microbial

communities. Proc. Natl. Acad. Sci. U. S. A. 105, 11512–11519. https://doi.org/10.1073/pnas.0801925105

Alneberg, J., Bjarnason, B.S., De Bruijn, I., Schirmer, M., Quick, J., Ijaz, U.Z., Lahti, L., Loman, N.J., Andersson, A.F., Quince, C., 2014. Binning metagenomic contigs by coverage and composition. Nat. Methods 11, 1144–1146. https://doi.org/10.1038/nmeth.3103

Andrews, S., 2010. FastQC: A quality control tool for high throughput sequence data [WWW Document]. URL http://www.bioinformatics.babraham.ac.uk/projects/fastqc

Ayala-Muñoz, D., Burgos, W.D., Sánchez-España, J., Couradeau, E., Falagán, C., Macalady, J.L., 2020. Metagenomic and metatranscriptomic study of microbial metal resistance in an acidic pit lake. Microorganisms 8, 1–271350. https://doi.org/10.3390/microorganisms8091350

Ayala-Muñoz, D., Macalady, J.L., Sánchez-España, J., Falagán, C., Couradeau, E., Burgos, W.D., 2022. Microbial carbon, sulfur, iron, and nitrogen cycling linked to the potential remediation of a meromictic acidic pit lake. ISME J. 16, 2666–2679. https://doi.org/10.1038/s41396-022-01320-w

Bolger, A.M., Lohse, M., Usadel, B., 2014. Trimmomatic: A flexible trimmer for Illumina sequence data. Bioinformatics 30, 2114–2120. https://doi.org/10.1093/bioinformatics/btu170

Borer, B., Tecon, R., Or, D., 2018. Spatial organization of bacterial populations in response to oxygen and carbon counter-gradients in pore networks. Nat. Commun. 9. https://doi.org/10.1038/s41467-018-03187-y

Chen, M., Walshe, G., Chi Fru, E., Ciborowski, J.J.H., Weisener, C.G., 2013. Microcosm assessment of the biogeochemical development of sulfur and oxygen in oil sands fluid fine tailings. Appl. Geochemistry 37, 1–11. https://doi.org/10.1016/j.apgeochem.2013.06.007

Chen, S., Zhou, Y., Chen, Y., Gu, J., 2018. Fastp: An ultra-fast all-in-one FASTQ preprocessor. Bioinformatics 34, i884–i890. https://doi.org/10.1093/bioinformatics/bty560

Chklovski, A., Parks, D.H., Woodcroft, B.J., Tyson, G.W., 2023. CheckM2: a rapid, scalable and accurate tool for assessing microbial genome quality using machine learning. Nat. Methods 20, 1203–1212. https://doi.org/10.1038/s41592-023-01940-w

Corteselli, E.M., Aitken, M.D., Singleton, D.R., 2017. Rugosibacter aromaticivorans gen. Nov., sp. nov., a bacterium within the family Rhodocyclaceae, isolated from contaminated soil, capable of degrading aromatic compounds. Int. J. Syst. Evol. Microbiol. 67, 311–318. https://doi.org/10.1099/ijsem.0.001622

Cremers, G., Jetten, M.S.M., Op den Camp, H.J.M., Lücker, S., 2022. Metascan: METabolic Analysis, SCreening and ANnotation of Metagenomes. Front. Bioinforma. 2, 1–12. https://doi.org/10.3389/fbinf.2022.861505

Danecek, P., Bonfield, J.K., Liddle, J., Marshall, J., Ohan, V., Pollard, M.O., Whitwham, A., Keane, T., McCarthy, S.A., Davies, R.M., 2021. Twelve years of SAMtools and BCFtools. Gigascience 10, 1–4. https://doi.org/10.1093/gigascience/giab008

Eren, A.M., Esen, O.C., Quince, C., Vineis, J.H., Morrison, H.G., Sogin, M.L., Delmont, T.O., 2015. Anvi'o: An advanced analysis and visualization platformfor 'omics data. PeerJ 2015, 1–29. https://doi.org/10.7717/peerj.1319

Ewels, P., Magnusson, M., Lundin, S., Käller, M., 2016. MultiQC: Summarize analysis results for multiple tools and samples in a single report. Bioinformatics 32, 3047–3048. https://doi.org/10.1093/bioinformatics/btw354

Feng, L., Zhang, Z., Yang, G., Wu, G.Y., Yang, Q., Chen, Q., 2023. Microbial communities and

sediment nitrogen cycle in a coastal eutrophic lake with salinity and nutrients shifted by seawater intrusion. Environ. Res. 225, 115590. https://doi.org/10.1016/j.envres.2023.115590

Frost, L.S., Leplae, R., Summers, A.O., Toussaint, A., 2005. Mobile genetic elements: The agents of open source evolution. Nat. Rev. Microbiol. 3, 722–732. https://doi.org/10.1038/nrmicro1235

Ganiyu, S.O., Arslan, M., Gamal El-Din, M., 2022. Combined solar activated sulfate radical-based advanced oxidation processes (SR-AOPs) and biofiltration for the remediation of dissolved organics in oil sands produced water. Chem. Eng. J. 433, 134579. https://doi.org/10.1016/j.cej.2022.134579

Garber, A.I., Cohen, A.B., Nealson, K.H., Ramírez, G.A., Barco, R.A., Enzingmüller-Bleyl, T.C., Gehringer, M.M., Merino, N., 2021. Metagenomic Insights Into the Microbial Iron Cycle of Subseafloor Habitats. Front. Microbiol. 12. https://doi.org/10.3389/fmicb.2021.667944

Grettenberger, C.L., Mccauley Rench, R.L., Gruen, D.S., Mills, D.B., Carney, C., Brainard, J., Hamasaki, H., Ramirez, R., Watanabe, Y., Amaral-Zettler, L.A., Ohmoto, H., Macalady, J.L., 2020. Microbial population structure in a stratified, acidic pit lake in the Iberian Pyrite Belt. Geomicrobiol. J. 37, 623–634. https://doi.org/10.1080/01490451.2020.1751748

Herman, D.C., Maier, R.M., 2009. Consequences of Biogeochemical Cycles Gone Wild, in: Environmental Microbiology. Academic Press, pp. 319–333.

Hyatt, D., Chen, G.-L., LoCascio, P.F., Land, M.L., Larimer, F.W., Hauser, L.J., 2010. Prodigal: prokaryotic gene recognition and translation initiation site identification. BMC Bioinformatics 11, 119.

Jørgensen, B.B., Findlay, A.J., Pellerin, A., 2019. The biogeochemical sulfur cycle of marine

sediments. Front. Microbiol. 10, 1–27. https://doi.org/10.3389/fmicb.2019.00849

Kang, D.D., Li, F., Kirton, E., Thomas, A., Egan, R., An, H., Wang, Z., 2019. MetaBAT 2: An adaptive binning algorithm for robust and efficient genome reconstruction from metagenome assemblies. PeerJ 2019, 1–13. https://doi.org/10.7717/peerj.7359

Kersters, K., De Vos, P., Gillis, M., Swings, J., Vandamme, P., Stackebrandt, E., 2006. Introduction to the Proteobacteria, in: Dworkin, M., Falkow, S., Rosenberg, E., Schleifer, K., Stackebrandt, E. (Eds.), The Prokaryotes. Springer, New York, NY, pp. 191–201. https://doi.org/10.1128/jb.85.6.1274-1279.1963

Ki, B.M., Huh, I.A., Choi, J.H., Cho, K.S., 2018. Relationship of nutrient dynamics and bacterial community structure at the water–sediment interface using a benthic chamber experiment. J. Environ. Sci. Heal. - Part A Toxic/Hazardous Subst. Environ. Eng. 53, 482–491. https://doi.org/10.1080/10934529.2017.1412191

Kojima, H., Watanabe, M., Miyata, N., Fukui, M., 2022. Sulfuricystis multivorans gen. nov., sp. nov. and Sulfuricystis thermophila sp. nov., facultatively autotropic sulfur-oxidizing bacteria isolated from a hot spring, and emended description of the genus Rugosibacter. Arch. Microbiol. 204, 1–7. https://doi.org/10.1007/s00203-022-03186-0

Kuznetsov, P., Wei, K., Kuznetsova, A., Foght, J., Ulrich, A., Siddique, T., 2023. Anaerobic Microbial Activity May Affect Development and Sustainability of End-Pit Lakes: A Laboratory Study of Biogeochemical Aspects of Oil Sands Mine Tailings. ACS ES T Water 3, 1039–1049. https://doi.org/10.1021/acsestwater.2c00505

Lalucat, J., Gomila, M., Mulet, M., Zaruma, A., García-Valdés, E., 2022. Past, present and future of the boundaries of the Pseudomonas genus: Proposal of Stutzerimonas gen. Nov. Syst. Appl.

Microbiol. 45, 126289. https://doi.org/10.1016/j.syapm.2021.126289

Langmead, B., Salzberg, S.L., 2012. Fast gapped-read alignment with Bowtie 2. Nat. Methods 9, 357–359. https://doi.org/10.1038/nmeth.1923

Leff, J.W., Jones, S.E., Prober, S.M., Barberán, A., Borer, E.T., Firn, J.L., Harpole, W.S., Hobbie, S.E., Hofmockel, K.S., Knops, J.M.H., McCulley, R.L., La Pierre, K., Risch, A.C., Seabloom, E.W., Schütz, M., Steenbock, C., Stevens, C.J., Fierer, N., 2015. Consistent responses of soil microbial communities to elevated nutrient inputs in grasslands across the globe. Proc. Natl. Acad. Sci. U. S. A. 112, 10967–10972. https://doi.org/10.1073/pnas.1508382112

Li, D., Liu, C.M., Luo, R., Sadakane, K., Lam, T.W., 2015. MEGAHIT: An ultra-fast single-node solution for large and complex metagenomics assembly via succinct de Bruijn graph. Bioinformatics 31, 1674–1676. https://doi.org/10.1093/bioinformatics/btv033

Li, W., Li, X., 2021. Metagenome-assembled genomes infer potential microbial metabolism in alkaline sulphidic tailings. Environ. Microbiomes 16, 1–10. https://doi.org/10.1186/s40793-021-00380-3

Little, A.E.F., Robinson, C.J., Peterson, S.B., Raffa, K.F., Handelsman, J., 2008. Rules of engagement: Interspecies interactions that regulate microbial communities. Annu. Rev. Microbiol. 62, 375–401. https://doi.org/10.1146/annurev.micro.030608.101423

Louca, S., Parfrey, L.W., Doebeli, M., 2016. Decoupling function and taxonomy in the global ocean microbiome. Science (80-.). 353, 1272–1277.

Mosley, O.E., Gios, E., Close, M., Weaver, L., Daughney, C., Handley, K.M., 2022. Nitrogen cycling and microbial cooperation in the terrestrial subsurface. ISME J. 16, 2561–2573. https://doi.org/10.1038/s41396-022-01300-0

Olm, M.R., Brown, C.T., Brooks, B., Banfield, J.F., 2017. DRep: A tool for fast and accurate genomic comparisons that enables improved genome recovery from metagenomes through de-replication. ISME J. 11, 2864–2868. https://doi.org/10.1038/ismej.2017.126

Paerl, H.W., Pinckney, J.L., 1996. A mini-review of microbial consortia: Their roles in aquatic production and biogeochemical cycling. Microb. Ecol. 31, 225–247. https://doi.org/10.1007/BF00171569

Parks, D.H., Rinke, C., Chuvochina, M., Chaumeil, P.A., Woodcroft, B.J., Evans, P.N., Hugenholtz, P., Tyson, G.W., 2017. Recovery of nearly 8,000 metagenome-assembled genomes substantially expands the tree of life. Nat. Microbiol. 2, 1533–1542. https://doi.org/10.1038/s41564-017-0012-7

Peterson, D., Bonham, K.S., Rowland, S., Pattanayak, C.W., Klepac-Ceraj, V., Deoni, S.C.L., D'Sa, V., Bruchhage, M., Volpe, A., Beauchemin, J., Wallace, C., Rogers, J., Cano, R., Fernandes, J., Walsh, E., Rhodes, B., Huentelman, M., Lewis, C., De Both, M.D., Naymik, M.A., Carnell, S., Jansen, E., Sadler, J.R., Thapaliya, G., Bonham, K., LeBourgeois, M., Mueller, H.G., Wang, J.L., Zhu, C., Chen, Y., Braun, J., 2021. Comparative Analysis of 16S rRNA Gene and Metagenome Sequencing in Pediatric Gut Microbiomes. Front. Microbiol. 12, 1–13. https://doi.org/10.3389/fmicb.2021.670336

Pietikäinen, J., Pettersson, M., Bååth, E., 2005. Comparison of temperature effects on soil respiration and bacterial and fungal growth rates. FEMS Microbiol. Ecol. 52, 49–58. https://doi.org/10.1016/j.femsec.2004.10.002

Sánchez-España, J., 2024. The Geomicrobiology of Acidic Pit Lakes, in: Staicu, L.C., Barton, L.L. (Eds.), Geomicrobiology: Natural and Anthropogenic Settings. Springer, Cham.

Shade, A., Handelsman, J., 2012. Beyond the Venn diagram: The hunt for a core microbiome. Environ. Microbiol. 14, 4–12. https://doi.org/10.1111/j.1462-2920.2011.02585.x

Shade, A., Peter, H., Allison, S.D., Baho, D.L., Berga, M., Bürgmann, H., Huber, D.H., Langenheder, S., Lennon, J.T., Martiny, J.B.H., Matulich, K.L., Schmidt, T.M., Handelsman, J., 2012. Fundamentals of microbial community resistance and resilience. Front. Microbiol. 3, 1–19. https://doi.org/10.3389/fmicb.2012.00417

Shang, Y., Wu, X., Wang, X., Wei, Q., Ma, S., Sun, G., Zhang, Huanxin, Wang, L., Dou, H., Zhang, Honghai, 2022. Factors affecting seasonal variation of microbial community structure in Hulun Lake, China. Sci. Total Environ. 805, 150294. https://doi.org/10.1016/j.scitotenv.2021.150294

Siddique, T., Stasik, S., Shahimin, M.F.M., Wendt-Potthoff, K., 2019. Microbial Communities in Oil Sands Tailings: Their Implications in Biogeochemical Processes and Tailings Management, Microbial Communities Utilizing Hydrocarbons and Lipids: Members, Metagenomics and Ecophysiology. Springer Nature Switzerland AG 2019. https://doi.org/10.1007/978-3-030-14785-3

Srivastava, A., De Corte, D., Garcia, J.A.L., Swan, B.K., Stepanauskas, R., Herndl, G.J., Sintes, E., 2023. Interplay between autotrophic and heterotrophic prokaryotic metabolism in the bathypelagic realm revealed by metatranscriptomic analyses. Microbiome 11, 1–11. https://doi.org/10.1186/s40168-023-01688-7

Sun, Y., Men, M., Xu, B., Meng, Q., Bello, A., Xu, X., Huang, X., 2019. Assessing key microbial communities determining nitrogen transformation in composting of cow manure using illumina high-throughput sequencing. Waste Manag. 92, 59–67.

https://doi.org/10.1016/j.wasman.2019.05.007

Uritskiy, G. V., DiRuggiero, J., Taylor, J., 2018. MetaWRAP—a flexible pipeline for genome-resolved metagenomic data analysis. Microbiome 6, 1–13. https://doi.org/10.1186/s40168-018-0541-1

Vollmers, J., Wiegand, S., Lenk, F., Kaster, A.K., 2022. How clear is our current view on microbial dark matter? (Re-)assessing public MAG & SAG datasets with MDMcleaner. Nucleic Acids Res. 50, E76. https://doi.org/10.1093/nar/gkac294

Warren, L.A., Kendra, K.E., Brady, A.L., Slater, G.F., 2016. Sulfur Biogeochemistry of an Oil Sands Composite Tailings Deposit. Front. Microbiol. 6, 1–14. https://doi.org/10.3389/fmicb.2015.01533

White, K.B., Liber, K., 2020. Chronic Toxicity of Surface Water from a Canadian Oil Sands End Pit Lake to the Freshwater Invertebrates Chironomus dilutus and Ceriodaphnia dubia. Arch. Environ. Contam. Toxicol. 78, 439–450. https://doi.org/10.1007/s00244-020-00720-3

Wu, Y.W., Simmons, B.A., Singer, S.W., 2016. MaxBin 2.0: An automated binning algorithm to recover genomes from multiple metagenomic datasets. Bioinformatics 32, 605–607. https://doi.org/10.1093/bioinformatics/btv638

Zhang, X., Niu, J., Liang, Y., Liu, X., Yin, H., 2016. Metagenome-scale analysis yields insights into the structure and function of microbial communities in a copper bioleaching heap. BMC Genet. 17, 1–12. https://doi.org/10.1186/s12863-016-0330-4

CHAPTER 5 GENERAL CONCLUSIONS AND RECOMMENDATIONS

5.1 Thesis overview

The mining and extraction of bitumen generate large volumes of waste known as tailings, which consist of sand, silt, clay, oil sands process-affected water (OSPW), and unrecovered bitumen. In Alberta, Canada, bitumen is extracted from oil sands reservoirs through surface mining, which has already disturbed approximately 895 km^2 of land and has created over 1.3 billion m^3 of tailings. The pore water of a tailing contains high concentrations of dissolved organic and inorganic compounds that adversely affect living organisms. Therefore, reclamation and management of tailings are urgently needed. Yet the overall size of the tailings creates enormous geotechnical and environmental challenges. Currently, tailings are temporarily stored in settling basins known as tailing ponds in compliance with the zero-effluent discharge policy in Alberta.

The use of end pit lakes (EPL) has been suggested as one of the methods for permanent reclamation of tailings. However, it is yet to be fully approved for oil sands mining because very little is known about the geochemical stability of these artificial ecosystems. To test the effectiveness of EPL within the Canadian oil sands, Base Mine Lake was established in December 2012 as the first full scale pit lake in the oil sands industry. Lake Miwasin, a recently established demonstrated pit lake (DPL), uses the new Permanent Aquatic Storage Structure (PASS) treatment technology for tailings' treatment. PASS technology uses an inline treatment process where coagulant (alum) and flocculant (polyacrylamide) are added to accelerate the natural dewatering of tailings.

In a bid to assess the effectively of PASS treatment technology on the development of a self-sustaining ecosystem, a laboratory DPL was established. As PASS technology was meant to

enhance tailings dewatering, Chapter 2 of the research first evaluated the settling behavior of PASS-treated tailings. Since the dewatering of tailings would result in the release of dissolved organics present in the tailings into the water cap of DPL, the changes in the water quality of the water cap over time was also evaluated. The effect of different oxygen conditions, oxic vs anoxic, on the water quality was also evaluated. Additionally, the potential of the laboratory DPL to produce gases was evaluated.

The use of alum during PASS treatment could influence microbial sulfur cycle as its dissociation produces electron acceptor for sulfate reducing bacteria (SRBs). The sulfur cycle is connected with other cycles such as carbon, nitrogen and metal cycles, and is tied to both cellular and ecosystem-level processes. Chapter 3 evaluated the microbial community structures of PASS-treated DPL using 16S rDNA sequencing. During the laboratory DPL's operation, bacterial communities involved in the sulfur cycle, carbon cycle and nitrogen cycle were highly abundant. Furthermore, the effect of seasonal temperature changes on the microbial community structures as well as their effects on dissolved organics in the water cap was also investigated.

Chapter 4 further evaluated the microbial community structures and their response to temperature variations using metagenomic approach. In addition, the functional genes analysis was carried out to evaluate the nutrient cycling in PASS-treated DPL and the mechanisms involved in such cycling with a view to constructing metabolic pathways that might explain the processes occuring in Lake Miwasin.

This research provided a comprehensive understanding on PASS-treated DPL and would serve a point of reference for further studies evaluating PASS technology.

5.2 Conclusions

The research presented in this thesis focused on evaluating the effectiveness of PASS technology on oil sands tailings reclamation. The following main conclusions were made based on experimental results and analysis:

Chapter 2: Employing Permanent Aquatic Storage Structure Technology to Reduce Dissolved Organics Transport from Tailings Deposits to Cap Water: Demonstration Pit Lake

- PASS-treated tailings underwent settling overtime with 13.8 ± 0.14 cm of consolidation observed under oxic condition compared to 16.4 ± 0.71 cm under anoxic condition.
- There was considerable flux of dissolved organics, namely COD, DOC, AEF and NAs, from the underlying tailings into the capping.
- There was higher concentration of dissolved organics overtime in capping water under anoxic condition than oxic condition.
- The mass flux calculations of advection and diffusion fluxes revealed high advective flux of dissolved organics which reduced gradually overtime whereas diffusive flux was consistently low.
- The advective flux of DOC decreased from 0.52 $g/m^2/d$ to 0.11 $g/m^2/d$ in oxic condition and from 0.65 $g/m^2/d$ to 0.13 $g/m^2/d$ in anoxic condition.
- The advective flux of NAs decreased from 0.038 $g/m^2/d$ to 0.009 $g/m^2/d$ in oxic condition and from 0.045 $g/m^2/d$ to 0.013 $g/m^2/d$ in anoxic condition.
- Residual polymer additive present in the PASS-treated tailings was initially released into the capping water during the early period before being biodegraded slowly over time.
- PASS treatment resulted in production of CO_2 at low concentration while CH_4 was not detected.

Chapter 3: Biogeochemical Processes in Oil Sands Tailings and Capping Water at Demonstration Pit Lake

- Temperature variations did not exert a pronounced effect on the advective movement of dissolved organics and suspended particles from tailings to capping water.
- Temperature variations significantly affected dissolved oxygen and conductivity.
- The concentrations of COD, DOC, TKN, and NAs increased over time whereas turbidity and pH decreased over time.
- The taxonomic composition and abundance of bacteria varied significantly between tailings and capping water.
- The taxonomic composition and abundance of bacteria did not vary significantly between the top and bottom layers.
- Seasonal temperature variations did not significantly affect microbial diversity in both tailings and capping water.
- Microbial communities were dominated by organisms involved in sulfur, carbon, nitrogen, and iron cycling.
- Biogas analyses revealed that methane was not produced at high rates, but production of hydrogen sulfide was evident.
- Sulfate reduction likely inhibited methanogenesis in model pit lakes.

Chapter 4: Metagenomic elucidation of microbial biogeochemical cycling in a model oil sands tailings pit lake system

- Bacterial communities dominated the model pit lake columns, with significant variations in abundance and composition between tailings and capping water.
- Proteobacteria was the most abundant phylum.

- Biogeochemical cycling of carbon, sulfur, and nitrogen was prominent in both tailings and capping water.
- Carbon cycling accounted for 52-60%, sulfur cycling for 16-19%, and nitrogen cycling for 24-28%.
- The most prominent carbon cycling processes in model pit lakes were Methanotrophy, Formaldehyde assimilation via serine pathway, Wood-Ljungdahl pathway, Citric Acid cycle, and Oxidative phosphorylation.
- The most prominent processes for sulfur cycling include Sulfite reduction and Thiosulfate oxidation.
- The most prominent nitrogen cycling processes include Nitrite oxidation, Denitrification and Dissimilatory nitrate reduction to ammonium.
- Temperature variations did not affect nutrient cycling in tailings and capping water.
- No significant differences were observed in the overall processes between the tailings and capping water.

5.3 Recommendations

Based on the results obtained from this research, the following are the recommendations for future works:

- In this research, the temperature regimes of 5 °C, 20 °C, 25 °C, and 8 °C each lasting 2 months were used, and the results showed that these temperature variations did not have effect in the model pit lake systems. It would be interesting to see if using longer temperature regimes of at least 4 months yield the same or different results. Future research should also consider if using different transition periods, for example, using 20 °C, 25 °C,

8 °C, and 5 °C or 25 °C, 8 °C, 5 °C and 20 °C, or any other combination, would show different results.

- 16S rDNA amplicon sequencing and shotgun metagenomic sequencing have been used to evaluate the performance of PASS technology. Future work should consider metatranscriptomics to further shed light on the activity of environmental populations.
- DNA and RNA extractions were challenging to carry out for tailings owing to its nature, which caused DNA and RNA yield to be very low. Optimizing the currently available extraction methods would go a long way towards helping develop a better extraction protocol.
- Attempts were made to carry out single cell genomics of PASS treated tailings to specifically target microbial dark matters (MDM), however no single cell was detected using an established method for soil and sediment (In-Solution Fluorescence In Situ Hybridization and Fluorescence-Activated Cell Sorting for Single Cell and Population Genome Recovery). It is therefore recommended to develop a working single cell extraction method for tailings.
- The results of sequencing have revealed that microbial communities are capable of successfully proliferate in PASS treated tailings. Targeted repetitive culturing using PASS treated tailings and model NAs should be able to produce culturable microbial communities with capacity to degrade recalcitrant NAs. This would be a worthwhile future endeavor.
- Water quality parameters that are easily tested on the field are recommended to be incorporated into future analysis. An example is Specific Ultraviolet Absorbance (SUVA), which is used to predict how easily organic matter can be removed by coagulation and how likely it is to form disinfection by-products (DBPs) during chlorination.

BIBLIOGRAPHY

Albakistani, E.A., Nwosu, F.C., Furgason, C., Haupt, E.S., Smirnova, A. V., Verbeke, T.J., Lee, E.S., Kim, J.J., Chan, A., Ruhl, I.A., Sheremet, A., Rudderham, S.B., Lindsay, M.B.J., Dunfield, P.F., 2022. Seasonal Dynamics of Methanotrophic Bacteria in a Boreal Oil Sands End Pit Lake. Appl. Environ. Microbiol. 88. https://doi.org/10.1128/aem.01455-21

Alberta Energy Regulator, 2020. ST98 Alberta Energy Outlook, Alberta Energy Regulator.

Alberta Energy Regulator, 2022. Tailings [WWW Document]. Provid. Inf. URL https://www.aer.ca/providing-information/by-topic/tailings (accessed 11.20.23).

Alberta Government, 2022. Oil Sands: Facts and Statistics [WWW Document]. Gov. Alberta. URL https://www.alberta.ca/oil-sands-facts-and-statistics.aspx (accessed 1.26.22).

Alewell, C., Paul, S., Lischeid, G., Küsel, K., Gehre, M., 2006. Characterizing the redox status in three different forested wetlands with geochemical data. Environ. Sci. Technol. 40, 7609–7615. https://doi.org/10.1021/es061018y

Alfreider, A., Baumer, A., Bogensperger, T., Posch, T., Salcher, M.M., Summerer, M., 2017. CO2 assimilation strategies in stratified lakes: Diversity and distribution patterns of chemolithoautotrophs. Environ. Microbiol. 19, 2754–2768. https://doi.org/10.1111/1462-2920.13786

Allaf, M.M., Peerhossaini, H., 2022. Cyanobacteria: Model Microorganisms and Beyond. Microorganisms 10. https://doi.org/10.3390/microorganisms10040696

Allen, E.W., 2008. Process water treatment in Canada's oil sands industry: I. Target pollutants and treatment objectives. J. Environ. Eng. Sci. 7, 123–138. https://doi.org/10.1139/S07-038

Allison, S.D., Martiny, J.B.H., 2008. Resistance, resilience, and redundancy in microbial communities. Proc. Natl. Acad. Sci. U. S. A. 105, 11512–11519. https://doi.org/10.1073/pnas.0801925105

Alneberg, J., Bjarnason, B.S., De Bruijn, I., Schirmer, M., Quick, J., Ijaz, U.Z., Lahti, L., Loman, N.J., Andersson, A.F., Quince, C., 2014. Binning metagenomic contigs by coverage and composition. Nat. Methods 11, 1144–1146. https://doi.org/10.1038/nmeth.3103

Andrews, S., 2010. FastQC: A quality control tool for high throughput sequence data [WWW Document]. URL http://www.bioinformatics.babraham.ac.uk/projects/fastqc

Arslan, M., Gamal El-Din, M., 2021. Bacterial diversity in petroleum coke based biofilters treating oil sands process water. Sci. Total Environ. 782, 146742. https://doi.org/10.1016/j.scitotenv.2021.146742

Arslan, M., Müller, J.A., Gamal El-Din, M., 2021. Aerobic naphthenic acid-degrading bacteria in petroleum-coke improve oil sands process water remediation in biofilters: DNA-stable isotope probing reveals methylotrophy in Schmutzdecke. Sci. Total Environ. 151961. https://doi.org/10.1016/j.scitotenv.2021.151961

Ayala-Muñoz, D., Burgos, W.D., Sánchez-España, J., Couradeau, E., Falagán, C., Macalady, J.L., 2020. Metagenomic and metatranscriptomic study of microbial metal resistance in an acidic pit lake. Microorganisms 8, 1–271350. https://doi.org/10.3390/microorganisms8091350

Ayala-Muñoz, D., Macalady, J.L., Sánchez-España, J., Falagán, C., Couradeau, E., Burgos, W.D., 2022. Microbial carbon, sulfur, iron, and nitrogen cycling linked to the potential remediation of a meromictic acidic pit lake. ISME J. 16, 2666–2679. https://doi.org/10.1038/s41396-022-01320-w

Ayayee, P.A., Custer, G.F., Tronstad, L.M., van Diepen, L.T.A., 2024. Unveiling salinity-driven shifts in microbial community composition across compartments of naturally saline inland streams. Hydrobiologia 851, 2627–2639. https://doi.org/10.1007/s10750-024-05479-5

Bazylinski, D.A., Dean, A.J., Schüler, D., Phillips, E.J.P., Lovley, D.R., 2000. N2-dependent growth and nitrogenase activity in the metal-metabolizing bacteria, Geobacter and Magnetospirillum species. Environ. Microbiol. 2, 266–273. https://doi.org/10.1046/j.1462-2920.2000.00096.x

Bell, E., Lamminmäki, T., Alneberg, J., Qian, C., Xiong, W., Hettich, R.L., Frutschi, M., Bernier-Latmani, R., 2022. Active anaerobic methane oxidation and sulfur disproportionation in the deep terrestrial subsurface. ISME J. 16, 1583–1593. https://doi.org/10.1038/s41396-022-01207-w

Bolger, A.M., Lohse, M., Usadel, B., 2014. Trimmomatic: A flexible trimmer for Illumina sequence data. Bioinformatics 30, 2114–2120. https://doi.org/10.1093/bioinformatics/btu170

Bolyen, E., Rideout, J.R., Dillon, M.R., Bokulich, N.A., Abnet, C.C., Al-Ghalith, G.A., Alexander, H., 2019. Reproducible, interactive, scalable and extensible microbiome data science using QIIME 2. Nat. Biotechnol. 37, 852–857. https://doi.org/http://dx.doi.org/10.1038/s41587-019-0209-9

Bordenave, S., Kostenko, V., Dutkoski, M., Grigoryan, A., Martinuzzi, R.J., Voordouw, G., 2010. Relation between the activity of anaerobic microbial populations in oil sands tailings ponds and the sedimentation of tailings. Chemosphere 81, 663–668. https://doi.org/10.1016/j.chemosphere.2010.07.058

Borer, B., Tecon, R., Or, D., 2018. Spatial organization of bacterial populations in response to oxygen and carbon counter-gradients in pore networks. Nat. Commun. 9. https://doi.org/10.1038/s41467-018-03187-y

Cabrol, L., Thalasso, F., Gandois, L., Sepulveda-Jauregui, A., Martinez-Cruz, K., Teisserenc, R., Tananaev, N., Tveit, A., Svenning, M.M., Barret, M., 2020. Anaerobic oxidation of methane and associated microbiome in anoxic water of Northwestern Siberian lakes. Sci. Total Environ. 736. https://doi.org/10.1016/j.scitotenv.2020.139588

Callahan, B.J., McMurdie, P.J., Rosen, M.J., Han, A.W., Amy Jo A Johnson, and S.P.H., 2016. DADA2: High resolution sample inference from Illumina amplicon data. Nat Methods. 13, 581–583. https://doi.org/10.1038/nmeth.3869

Canada's Oil Sands Innovation Alliance (COSIA), 2020. 2019 Water Mining Research Report. https://cosia.ca/sites/default/files/attachments/COSIA_2019_Mining Research Summary Report_Final.pdf

Canada's Oil Sands Innovation Alliance (COSIA), 2021. Pit Lakes: A surface mining perspective, Tailings Environmental Priority Area (EPA).

Chen, M., Walshe, G., Chi Fru, E., Ciborowski, J.J.H., Weisener, C.G., 2013. Microcosm assessment of the biogeochemical development of sulfur and oxygen in oil sands fluid fine

tailings. Appl. Geochemistry 37, 1–11. https://doi.org/10.1016/j.apgeochem.2013.06.007

Chen, S., Zhou, Y., Chen, Y., Gu, J., 2018. Fastp: An ultra-fast all-in-one FASTQ preprocessor. Bioinformatics 34, i884–i890. https://doi.org/10.1093/bioinformatics/bty560

Chklovski, A., Parks, D.H., Woodcroft, B.J., Tyson, G.W., 2023. CheckM2: a rapid, scalable and accurate tool for assessing microbial genome quality using machine learning. Nat. Methods 20, 1203–1212. https://doi.org/10.1038/s41592-023-01940-w

Choo-yin, Y., 2021. Monitoring Macrophage Immune Gene Expression Profiles as an Early Indicator System for Examining the Bioactivity of Oil Sands Process Affected Waters. University of Alberta.

Corteselli, E.M., Aitken, M.D., Singleton, D.R., 2017. Rugosibacter aromaticivorans gen. Nov., sp. nov., a bacterium within the family Rhodocyclaceae, isolated from contaminated soil, capable of degrading aromatic compounds. Int. J. Syst. Evol. Microbiol. 67, 311–318. https://doi.org/10.1099/ijsem.0.001622

Cossey, H.L., Batycky, A.E., Kaminsky, H., Ulrich, A.C., 2021. Geochemical stability of oil sands tailings in mine closure landforms. Minerals 11. https://doi.org/10.3390/min11080830

Cossey, H.L., Kaminsky, H., Ulrich, A.C., 2022. Evaluating the long-term behaviour and viability of an oil sands tailings management and reclamation strategy, in: AB Fourie, M Tibbett & G Boggs (eds), M.C. 2022 (Ed.), Proceedings of the International Conference on Mine Closure. Australian Centre for Geomechanics, Perth, pp. 307–320. https://doi.org/10.36487/ACG_repo/2215_19

Cremers, G., Jetten, M.S.M., Op den Camp, H.J.M., Lücker, S., 2022. Metascan: METabolic Analysis, SCreening and ANnotation of Metagenomes. Front. Bioinforma. 2, 1–12. https://doi.org/10.3389/fbinf.2022.861505

Crittenden, J.C., Trussell, R., Hand, D., Howe, J.K., Tchobanoglous, G., 2012. MWH's Water Treatment: Principles and Design, Third. ed. John Wiley & Sons, Inc., Hoboken, New Jersey.

Danecek, P., Bonfield, J.K., Liddle, J., Marshall, J., Ohan, V., Pollard, M.O., Whitwham, A., Keane, T., McCarthy, S.A., Davies, R.M., 2021. Twelve years of SAMtools and BCFtools. Gigascience 10, 1–4. https://doi.org/10.1093/gigascience/giab008

De Stasio, B.T., Golemgeski, T., Livingstone, D.M., 2009. Temperature as a Driving Factor in Aquatic Ecosystems. Encycl. Inl. Waters 690–698. https://doi.org/10.1016/B978-0-12-819166-8.00062-1

Dompierre, K.A., Barbour, S.L., 2016. Characterization of physical mass transport through oil sands fluid fine tailings in an end pit lake: A multi-tracer study. J. Contam. Hydrol. 189, 12–26. https://doi.org/10.1016/j.jconhyd.2016.03.006

Dompierre, K.A., Barbour, S.L., North, R.L., Carey, S.K., Lindsay, M.B.J., 2017. Chemical mass transport between fluid fine tailings and the overlying water cover of an oil sands end pit lake. Water Resour. Res. 5, 4725–4740. https://doi.org/10.1002/2016WR020112

Environmental Defence, 2022. 50 Years of Sprawling Tailings.

Eren, A.M., Esen, O.C., Quince, C., Vineis, J.H., Morrison, H.G., Sogin, M.L., Delmont, T.O., 2015. Anvi'o: An advanced analysis and visualization platformfor 'omics data. PeerJ 2015,

1–29. https://doi.org/10.7717/peerj.1319

España, J.S., Pamo, E.L., Santofimia, E., Aduvire, O., Reyes, J., Barettino, D., 2005. Acid mine drainage in the Iberian Pyrite Belt (Odiel river watershed, Huelva, SW Spain): Geochemistry, mineralogy and environmental implications. Appl. Geochemistry 20, 1320–1356. https://doi.org/10.1016/j.apgeochem.2005.01.011

Ewels, P., Magnusson, M., Lundin, S., Käller, M., 2016. MultiQC: Summarize analysis results for multiple tools and samples in a single report. Bioinformatics 32, 3047–3048. https://doi.org/10.1093/bioinformatics/btw354

Falkowski, P.G., Fenchel, T., Delong, E.F., 2008. The microbial engines that drive earth's biogeochemical cycles. Science (80-.). 320, 1034–1039. https://doi.org/10.1126/science.1153213

Feng, L., Zhang, Z., Yang, G., Wu, G.Y., Yang, Q., Chen, Q., 2023. Microbial communities and sediment nitrogen cycle in a coastal eutrophic lake with salinity and nutrients shifted by seawater intrusion. Environ. Res. 225, 115590. https://doi.org/10.1016/j.envres.2023.115590

Foght, J.M., 2015. Microbial metagenomics of oil sands tailings ponds: Small bugs, big data. Genome 58, 507–510. https://doi.org/10.1139/gen-2015-0146

Foght, J.M., Gieg, L.M., Siddique, T., 2017. The microbiology of oil sands tailings: Past, present, future. FEMS Microbiol. Ecol. 93, 1–22. https://doi.org/10.1093/femsec/fix034

Frost, L.S., Leplae, R., Summers, A.O., Toussaint, A., 2005. Mobile genetic elements: The agents of open source evolution. Nat. Rev. Microbiol. 3, 722–732.

https://doi.org/10.1038/nrmicro1235

Ganiyu, S.O., Arslan, M., Gamal El-Din, M., 2022. Combined solar activated sulfate radical-based advanced oxidation processes (SR-AOPs) and biofiltration for the remediation of dissolved organics in oil sands produced water. Chem. Eng. J. 433, 134579. https://doi.org/10.1016/j.cej.2022.134579

Garber, A.I., Cohen, A.B., Nealson, K.H., Ramírez, G.A., Barco, R.A., Enzingmüller-Bleyl, T.C., Gehringer, M.M., Merino, N., 2021. Metagenomic Insights Into the Microbial Iron Cycle of Subseafloor Habitats. Front. Microbiol. 12. https://doi.org/10.3389/fmicb.2021.667944

Gonçalves, J., Baldovi, A.A., Chyoshi, B., Zanata, L., Salcedo, A.M., Subtil, E.L., Coelho, L.H.G., 2019. Effect of aluminum sulfate and cationic polymer addition in the mixed liquor of a submerged membrane bioreactor (SMBR): Sludge characteristics and orthophosphate removal in batch experiments. Brazilian J. Chem. Eng. 36, 693–703. https://doi.org/10.1590/0104-6632.20190362s20180128

Government of Alberta, 2024. Oil sands tailings and mine water.

Government of Canada, 2018. Technical Backgrounder: Federal methane regulations for the upstream oil and gas sector [WWW Document]. Environ. Clim. Chang. Canada. URL https://www.canada.ca/en/environment-climate-change/news/2018/04/federal-methane-regulations-for-the-upstream-oil-and-gas-sector.html (accessed 10.21.22).

Grettenberger, C.L., Mccauley Rench, R.L., Gruen, D.S., Mills, D.B., Carney, C., Brainard, J., Hamasaki, H., Ramirez, R., Watanabe, Y., Amaral-Zettler, L.A., Ohmoto, H., Macalady, J.L., 2020. Microbial population structure in a stratified, acidic pit lake in the Iberian Pyrite Belt.

Geomicrobiol. J. 37, 623–634. https://doi.org/10.1080/01490451.2020.1751748

Gu, C., Laverman, A.M., Pallud, C.E., 2012. Environmental controls on nitrogen and sulfur cycles in surficial aquatic sediments. Front. Microbiol. 3, 1–11. https://doi.org/10.3389/fmicb.2012.00045

Guezennec, A.G., Michel, C., Bru, K., Touze, S., Desroche, N., Mnif, I., Motelica-Heino, M., 2015. Transfer and degradation of polyacrylamide-based flocculants in hydrosystems: A review. Environ. Sci. Pollut. Res. 22, 6390–6406. https://doi.org/10.1007/s11356-014-3556-6

Guo, H., Chen, C., Lee, D.J., Wang, A., Ren, N., 2013. Sulfur-nitrogen-carbon removal of Pseudomonas sp. C27 under sulfide stress. Enzyme Microb. Technol. 53, 6–12. https://doi.org/10.1016/j.enzmictec.2013.04.002

Herman, D.C., Maier, R.M., 2009. Consequences of Biogeochemical Cycles Gone Wild, in: Environmental Microbiology. Academic Press, pp. 319–333.

Holmer, M., Storkholm, P., 2001. Sulphate reduction and sulphur cycling in lake sediments: A review. Freshw. Biol. 46, 431–451. https://doi.org/10.1046/j.1365-2427.2001.00687.x

Holowenko, F.M., MacKinnon, M.D., Fedorak, P.M., 2000. Methanogens and sulfate-reducing bacteria in oil sands fine tailings waste. Can. J. Microbiol. 46, 927–937. https://doi.org/10.1139/w00-081

Hyatt, D., Chen, G.-L., LoCascio, P.F., Land, M.L., Larimer, F.W., Hauser, L.J., 2010. Prodigal: prokaryotic gene recognition and translation initiation site identification. BMC

Bioinformatics 11, 119.

Intrinsik Corp., 2022. Environmental fate and behaviour of anionic polyacrylamides in oil sands tailings management: A state of knowledge synthesis. Albert.

Ionescu, D., Heim, C., Polerecky, L., Thiel, V., De Beer, D., 2015. Biotic and abiotic oxidation and reduction of iron at circumneutral pH are inseparable processes under natural conditions. Geomicrobiol. J. 32, 221–230. https://doi.org/10.1080/01490451.2014.887393

Jessen, G.L., Chen, L.X., Mori, J.F., Nelson, T.E.C., Slater, G.F., Lindsay, M.B.J., Banfield, J.F., Warren, L.A., 2022. Alum Addition Triggers Hypoxia in an Engineered Pit Lake. Microorganisms 10. https://doi.org/10.3390/microorganisms10030510

Jørgensen, B.B., Findlay, A.J., Pellerin, A., 2019. The biogeochemical sulfur cycle of marine sediments. Front. Microbiol. 10, 1–27. https://doi.org/10.3389/fmicb.2019.00849

Joshi, S.J., Abed, R.M.M., 2017. Biodegradation of Polyacrylamide and Its Derivatives. Environ. Process. 4, 463–476. https://doi.org/10.1007/s40710-017-0224-0

Junkins, E.N., McWhirter, J.B., McCall, L.-I., Stevenson, B.S., 2022. Environmental structure impacts microbial composition and secondary metabolism. ISME Commun. 2, 1–10. https://doi.org/10.1038/s43705-022-00097-5

Kang, D.D., Li, F., Kirton, E., Thomas, A., Egan, R., An, H., Wang, Z., 2019. MetaBAT 2: An adaptive binning algorithm for robust and efficient genome reconstruction from metagenome assemblies. PeerJ 2019, 1–13. https://doi.org/10.7717/peerj.7359

Kersters, K., De Vos, P., Gillis, M., Swings, J., Vandamme, P., Stackebrandt, E., 2006.

Introduction to the Proteobacteria, in: Dworkin, M., Falkow, S., Rosenberg, E., Schleifer, K., Stackebrandt, E. (Eds.), The Prokaryotes. Springer, New York, NY, pp. 191–201. https://doi.org/10.1128/jb.85.6.1274-1279.1963

Ki, B.M., Huh, I.A., Choi, J.H., Cho, K.S., 2018. Relationship of nutrient dynamics and bacterial community structure at the water–sediment interface using a benthic chamber experiment. J. Environ. Sci. Heal. - Part A Toxic/Hazardous Subst. Environ. Eng. 53, 482–491. https://doi.org/10.1080/10934529.2017.1412191

Koizumi, Y., Kojima, H., Fukui, M., 2005. Potential sulfur metabolisms and associated bacteria within anoxic surface sediment from saline meromictic Lake Kaiike (Japan). FEMS Microbiol. Ecol. 52, 297–305. https://doi.org/10.1016/j.femsec.2004.11.009

Kojima, H., Watanabe, M., Miyata, N., Fukui, M., 2022. Sulfuricystis multivorans gen. nov., sp. nov. and Sulfuricystis thermophila sp. nov., facultatively autotropic sulfur-oxidizing bacteria isolated from a hot spring, and emended description of the genus Rugosibacter. Arch. Microbiol. 204, 1–7. https://doi.org/10.1007/s00203-022-03186-0

Kuznetsov, P., Wei, K., Kuznetsova, A., Foght, J., Ulrich, A., Siddique, T., 2023. Anaerobic Microbial Activity May Affect Development and Sustainability of End-Pit Lakes: A Laboratory Study of Biogeochemical Aspects of Oil Sands Mine Tailings. ACS ES T Water 3, 1039–1049. https://doi.org/10.1021/acsestwater.2c00505

Lalucat, J., Gomila, M., Mulet, M., Zaruma, A., García-Valdés, E., 2022. Past, present and future of the boundaries of the Pseudomonas genus: Proposal of Stutzerimonas gen. Nov. Syst. Appl. Microbiol. 45, 126289. https://doi.org/10.1016/j.syapm.2021.126289

Langmead, B., Salzberg, S.L., 2012. Fast gapped-read alignment with Bowtie 2. Nat. Methods 9, 357–359. https://doi.org/10.1038/nmeth.1923

Lau, Y.L., 1994. Temperature effect on settling velocity and deposition of cohesive sediments: Influence de la témperature sur la vitesse de chute et le dépôt de sédiments cohesifs. J. Hydraul. Res. 32, 41–51. https://doi.org/10.1080/00221689409498788

Leff, J.W., Jones, S.E., Prober, S.M., Barberán, A., Borer, E.T., Firn, J.L., Harpole, W.S., Hobbie, S.E., Hofmockel, K.S., Knops, J.M.H., McCulley, R.L., La Pierre, K., Risch, A.C., Seabloom, E.W., Schütz, M., Steenbock, C., Stevens, C.J., Fierer, N., 2015. Consistent responses of soil microbial communities to elevated nutrient inputs in grasslands across the globe. Proc. Natl. Acad. Sci. U. S. A. 112, 10967–10972. https://doi.org/10.1073/pnas.1508382112

Li, D., Liu, C.M., Luo, R., Sadakane, K., Lam, T.W., 2015. MEGAHIT: An ultra-fast single-node solution for large and complex metagenomics assembly via succinct de Bruijn graph. Bioinformatics 31, 1674–1676. https://doi.org/10.1093/bioinformatics/btv033

Li, H.Y., Xu, J., Xu, R.Q., 2013. The effect of temperature on the water quality of lake. Adv. Mater. Res. 821–822, 1001–1004. https://doi.org/10.4028/www.scientific.net/AMR.821-822.1001

Li, J., How, Z.T., Gamal El-Din, M., 2023. Aerobic degradation of anionic polyacrylamide in oil sands tailings: Impact factor, degradation effect, and mechanism. Sci. Total Environ. 856, 159079. https://doi.org/10.1016/j.scitotenv.2022.159079

Li, M., Fang, A., Yu, X., Zhang, K., He, Z., Wang, C., Peng, Y., Xiao, F., Yang, T., Zhang, W., Zheng, X., Zhong, Q., Liu, X., Yan, Q., 2021. Microbially-driven sulfur cycling microbial

communities in different mangrove sediments. Chemosphere 273, 128597. https://doi.org/10.1016/j.chemosphere.2020.128597

Li, W., Li, X., 2021. Metagenome-assembled genomes infer potential microbial metabolism in alkaline sulphidic tailings. Environ. Microbiomes 16, 1–10. https://doi.org/10.1186/s40793-021-00380-3

Li, X., Lan, S. ming, Zhu, Z. ping, Zhang, C., Zeng, G. ming, Liu, Y. guo, Cao, W. cheng, Song, B., Yang, H., Wang, S. fan, Wu, S. hua, 2018. The bioenergetics mechanisms and applications of sulfate-reducing bacteria in remediation of pollutants in drainage: A review. Ecotoxicol. Environ. Saf. 158, 162–170. https://doi.org/10.1016/j.ecoenv.2018.04.025

Li, Y., Liu, L., Wang, H., 2022. Mixotrophic denitrification for enhancing nitrogen removal of municipal tailwater: Contribution of heterotrophic/sulfur autotrophic denitrification and bacterial community. Sci. Total Environ. 814, 151940. https://doi.org/10.1016/j.scitotenv.2021.151940

Li, Y., Yu, S., Strong, J., Wang, H., 2012. Are the biogeochemical cycles of carbon, nitrogen, sulfur, and phosphorus driven by the “FeIII-FeII redox wheel” in dynamic redox environments? J. Soils Sediments 12, 683–693. https://doi.org/10.1007/s11368-012-0507-z

Liamleam, W., Annachhatre, A.P., 2007. Electron donors for biological sulfate reduction. Biotechnol. Adv. 25, 452–463. https://doi.org/10.1016/j.biotechadv.2007.05.002

Lillico, D.M.E., Hussain, N.A.S., Choo-Yin, Y.Y., Qin, R., How, Z.T., El-Din, M.G., Stafford, J.L., 2022. Using immune cell-based bioactivity assays to compare the inflammatory activities of oil sands process-affected waters from a pilot scale demonstration pit lake. J.

Environ. Sci. https://doi.org/10.1016/j.jes.2022.07.018

Lin, Y. Te, Jia, Z., Wang, D., Chiu, C.Y., 2017. Effects of temperature on the composition and diversity of bacterial communities in bamboo soils at different elevations. Biogeosciences 14, 4879–4889. https://doi.org/10.5194/bg-14-4879-2017

Little, A.E.F., Robinson, C.J., Peterson, S.B., Raffa, K.F., Handelsman, J., 2008. Rules of engagement: Interspecies interactions that regulate microbial communities. Annu. Rev. Microbiol. 62, 375–401. https://doi.org/10.1146/annurev.micro.030608.101423

Liu, D., Edraki, M., Berry, L., 2018. Investigating the settling behaviour of saline tailing suspensions using kaolinite, bentonite, and illite clay minerals. Powder Technol. 326, 228–236. https://doi.org/10.1016/j.powtec.2017.11.070

Louca, S., Parfrey, L.W., Doebeli, M., 2016. Decoupling function and taxonomy in the global ocean microbiome. Science (80-.). 353, 1272–1277.

McCullough, C.D., Vandenberg, J., 2020. Studying Mine Pit Lake Systems Across Multiple Scales. Mine Water Environ. 39, 173–194. https://doi.org/10.1007/s10230-020-00678-7

Meier, J., Piva, A., Fortin, D., 2012. Enrichment of sulfate-reducing bacteria and resulting mineral formation in media mimicking pore water metal ion concentrations and pH conditions of acidic pit lakes. FEMS Microbiol. Ecol. 79, 69–84. https://doi.org/10.1111/j.1574-6941.2011.01199.x

Mosley, O.E., Gios, E., Close, M., Weaver, L., Daughney, C., Handley, K.M., 2022. Nitrogen cycling and microbial cooperation in the terrestrial subsurface. ISME J. 16, 2561–2573.

https://doi.org/10.1038/s41396-022-01300-0

Muyzer, G., Stams, A.J.M., 2008. The ecology and biotechnology of sulphate-reducing bacteria. Nat. Rev. Microbiol. 6, 441–454. https://doi.org/10.1038/nrmicro1892

Natural Resources Canada, 2022. Energy Fact Book 2022–2023, Natural Resources Canada.

Nyyssölä, A., Ahlgren, J., 2019. Microbial degradation of polyacrylamide and the deamination product polyacrylate. Int. Biodeterior. Biodegrad. 139, 24–33. https://doi.org/10.1016/j.ibiod.2019.02.005

Olm, M.R., Brown, C.T., Brooks, B., Banfield, J.F., 2017. DRep: A tool for fast and accurate genomic comparisons that enables improved genome recovery from metagenomes through de-replication. ISME J. 11, 2864–2868. https://doi.org/10.1038/ismej.2017.126

Otte, J.M., Harter, J., Laufer, K., Blackwell, N., Straub, D., Kappler, A., Kleindienst, S., 2018. The distribution of active iron-cycling bacteria in marine and freshwater sediments is decoupled from geochemical gradients. Environ. Microbiol. 20, 2483–2499. https://doi.org/10.1111/1462-2920.14260

Paerl, H.W., Pinckney, J.L., 1996. A mini-review of microbial consortia: Their roles in aquatic production and biogeochemical cycling. Microb. Ecol. 31, 225–247. https://doi.org/10.1007/BF00171569

Parks, D.H., Rinke, C., Chuvochina, M., Chaumeil, P.A., Woodcroft, B.J., Evans, P.N., Hugenholtz, P., Tyson, G.W., 2017. Recovery of nearly 8,000 metagenome-assembled genomes substantially expands the tree of life. Nat. Microbiol. 2, 1533–1542.

https://doi.org/10.1038/s41564-017-0012-7

Pester, M., Knorr, K.H., Friedrich, M.W., Wagner, M., Loy, A., 2012. Sulfate-reducing microorganisms in wetlands - fameless actors in carbon cycling and climate change. Front. Microbiol. 3, 1–19. https://doi.org/10.3389/fmicb.2012.00072

Peterson, D., Bonham, K.S., Rowland, S., Pattanayak, C.W., Klepac-Ceraj, V., Deoni, S.C.L., D'Sa, V., Bruchhage, M., Volpe, A., Beauchemin, J., Wallace, C., Rogers, J., Cano, R., Fernandes, J., Walsh, E., Rhodes, B., Huentelman, M., Lewis, C., De Both, M.D., Naymik, M.A., Carnell, S., Jansen, E., Sadler, J.R., Thapaliya, G., Bonham, K., LeBourgeois, M., Mueller, H.G., Wang, J.L., Zhu, C., Chen, Y., Braun, J., 2021. Comparative Analysis of 16S rRNA Gene and Metagenome Sequencing in Pediatric Gut Microbiomes. Front. Microbiol. 12, 1–13. https://doi.org/10.3389/fmicb.2021.670336

Pietikäinen, J., Pettersson, M., Bååth, E., 2005. Comparison of temperature effects on soil respiration and bacterial and fungal growth rates. FEMS Microbiol. Ecol. 52, 49–58. https://doi.org/10.1016/j.femsec.2004.10.002

Ren, L., Jensen, K., Porada, P., Mueller, P., 2022. Biota-mediated carbon cycling—A synthesis of biotic-interaction controls on blue carbon. Ecol. Lett. 25, 521–540. https://doi.org/10.1111/ele.13940

Robinson, J., Mills, J., Breed, M., 2018. Walking Ecosystems in Microbiome-Inspired Green Infrastructure: An Ecological Perspective on Enhancing Personal and Planetary Health. Challenges 9, 40. https://doi.org/10.3390/challe9020040

Sánchez-España, J., 2024. The Geomicrobiology of Acidic Pit Lakes, in: Staicu, L.C., Barton, L.L.

(Eds.), Geomicrobiology: Natural and Anthropogenic Settings. Springer, Cham.

Seitzinger, S., Harrison, J.A., Böhlke, J.K., Bouwman, A.F., Lowrance, R., Peterson, B., Tobias, C., Van Drecht, G., 2006. Denitrification across landscapes and waterscapes: A synthesis. Ecol. Appl. 16, 2064–2090. https://doi.org/10.1890/1051-0761(2006)016[2064:DALAWA]2.0.CO;2

Sela-Adler, M., Ronen, Z., Herut, B., Antler, G., Vigderovich, H., Eckert, W., Sivan, O., 2017. Co-existence of methanogenesis and sulfate reduction with common substrates in sulfate-rich estuarine sediments. Front. Microbiol. 8, 1–11. https://doi.org/10.3389/fmicb.2017.00766

Shade, A., Handelsman, J., 2012. Beyond the Venn diagram: The hunt for a core microbiome. Environ. Microbiol. 14, 4–12. https://doi.org/10.1111/j.1462-2920.2011.02585.x

Shade, A., Peter, H., Allison, S.D., Baho, D.L., Berga, M., Bürgmann, H., Huber, D.H., Langenheder, S., Lennon, J.T., Martiny, J.B.H., Matulich, K.L., Schmidt, T.M., Handelsman, J., 2012. Fundamentals of microbial community resistance and resilience. Front. Microbiol. 3, 1–19. https://doi.org/10.3389/fmicb.2012.00417

Shang, Y., Wu, X., Wang, X., Wei, Q., Ma, S., Sun, G., Zhang, Huanxin, Wang, L., Dou, H., Zhang, Honghai, 2022. Factors affecting seasonal variation of microbial community structure in Hulun Lake, China. Sci. Total Environ. 805, 150294. https://doi.org/10.1016/j.scitotenv.2021.150294

Shinoda, Y., Akagi, J., Uchihashi, Y., Hiraishi, A., Yukawa, H., Yurimoto, H., Sakai, Y., Kato, N., 2005. Anaerobic degradation of aromatic compounds by Magnetospirillum strains: Isolation and degradation genes. Biosci. Biotechnol. Biochem. 69, 1483–1491.

https://doi.org/10.1271/bbb.69.1483

Siddique, T., Kuznetsov, P., Kuznetsova, A., Arkell, N., Young, R., Li, C., Guigard, S., Underwood, E., Foght, J.M., 2014. Microbially-accelerated consolidation of oil sands tailings. Pathway I: Changes in porewater chemistry. Front. Microbiol. 5, 1–11. https://doi.org/10.3389/fmicb.2014.00106

Siddique, T., Penner, T., Klassen, J., Nesbø, C., Foght, J.M., 2012. Microbial communities involved in methane production from hydrocarbons in oil sands tailings. Environ. Sci. Technol. 46, 9802–9810. https://doi.org/10.1021/es302202c

Siddique, T., Stasik, S., Shahimin, M.F.M., Wendt-Potthoff, K., 2019. Microbial Communities in Oil Sands Tailings: Their Implications in Biogeochemical Processes and Tailings Management, Microbial Communities Utilizing Hydrocarbons and Lipids: Members, Metagenomics and Ecophysiology. Springer Nature Switzerland AG 2019. https://doi.org/10.1007/978-3-030-14785-3

Srivastava, A., De Corte, D., Garcia, J.A.L., Swan, B.K., Stepanauskas, R., Herndl, G.J., Sintes, E., 2023. Interplay between autotrophic and heterotrophic prokaryotic metabolism in the bathypelagic realm revealed by metatranscriptomic analyses. Microbiome 11, 1–11. https://doi.org/10.1186/s40168-023-01688-7

Stumm, W., & Morgan, J. J. (1996). Aquatic Chemistry: Chemical Equilibria and Rates in Natural Waters. Wiley-Interscience

Sun, Y., Men, M., Xu, B., Meng, Q., Bello, A., Xu, X., Huang, X., 2019. Assessing key microbial communities determining nitrogen transformation in composting of cow manure using

illumina high-throughput sequencing. Waste Manag. 92, 59–67. https://doi.org/10.1016/j.wasman.2019.05.007

Syncrude, 2019. Base Mine Lake Monitoring and Research Summary Report: Results from 2013-2018

Syncrude, 2021. 2021 Pit Lake Monitoring and Research Report (Base Mine Lake Demonstration Summary: 2012-2020)

Takaya, N., Catalan-Sakairi, M.A.B., Sakaguchi, Y., Kato, I., Zhou, Z., Shoun, H., 2003. Aerobic denitrifying bacteria that produce low levels of nitrous oxide. Appl. Environ. Microbiol. 69, 3152–3157. https://doi.org/10.1128/AEM.69.6.3152-3157.2003

The Royal Society of Canada, 2010. The Royal Society of Canada Expert Panel: Environmental and Health Impacts of Canada's Oil Sands Industry: Report, The Royal Society of Canada.

Thijs, S., De Beeck, M.O., Beckers, B., Truyens, S., Stevens, V., Van Hamme, J.D., Weyens, N., Vangronsveld, J., 2017. Comparative evaluation of four bacteria-specific primer pairs for 16S rRNA gene surveys. Front. Microbiol. 8, 1–15. https://doi.org/10.3389/fmicb.2017.00494

Uritskiy, G. V., DiRuggiero, J., Taylor, J., 2018. MetaWRAP—a flexible pipeline for genome-resolved metagenomic data analysis. Microbiome 6, 1–13. https://doi.org/10.1186/s40168-018-0541-1

Vandenberg, J.A., Lauzon, N., Prakash, S., Salzsauler, K., 2011. Use of water quality models for design and evaluation of pit lakes. Mine Pit Lakes Clos. Manag. 63–81.

Vigneron, A., Cruaud, P., Culley, A.I., Couture, R.M., Lovejoy, C., Vincent, W.F., 2021. Genomic

evidence for sulfur intermediates as new biogeochemical hubs in a model aquatic microbial ecosystem. Microbiome 9, 1–14. https://doi.org/10.1186/s40168-021-00999-x

Vitousek, P.M., Howarth, R.W., 1991. Nitrogen limitation on land and in the sea: How can it occur? Biogeochemistry 13, 87–115. https://doi.org/10.1007/BF00002772

Vollmers, J., Wiegand, S., Lenk, F., Kaster, A.K., 2022. How clear is our current view on microbial dark matter? (Re-)assessing public MAG & SAG datasets with MDMcleaner. Nucleic Acids Res. 50, E76. https://doi.org/10.1093/nar/gkac294

Walters, K.E., Martiny, J.B.H., 2020. Alpha-, beta-, and gamma-diversity of bacteria varies across habitats. PLoS One 15, 1–17. https://doi.org/10.1371/journal.pone.0233872

Warren, L.A., Kendra, K.E., Brady, A.L., Slater, G.F., 2016. Sulfur Biogeochemistry of an Oil Sands Composite Tailings Deposit. Front. Microbiol. 6, 1–14. https://doi.org/10.3389/fmicb.2015.01533

West, K.N., Wheeler, C., McCarney, J.P., Griffith, K.N., Bush, D., Liotta, C.L., Eckert, C.A., 2001. In situ formation of alkylcarbonic acids with CO2. J. Phys. Chem. A 105, 3947–3948. https://doi.org/10.1021/jp003846y

White, K.B., Liber, K., 2020. Chronic Toxicity of Surface Water from a Canadian Oil Sands End Pit Lake to the Freshwater Invertebrates Chironomus dilutus and Ceriodaphnia dubia. Arch. Environ. Contam. Toxicol. 78, 439–450. https://doi.org/10.1007/s00244-020-00720-3

Wolfe, A.L., Wilkin, R.T., 2017. Evidence of Sulfate-Dependent Anaerobic Methane Oxidation within an Area Impacted by Coalbed Methane-Related Gas Migration. Env. Sci Technol. 51,

1901–1909. https://doi.org/10.1021/acs.est.6b03709

Wu, Y.W., Simmons, B.A., Singer, S.W., 2016. MaxBin 2.0: An automated binning algorithm to recover genomes from multiple metagenomic datasets. Bioinformatics 32, 605–607. https://doi.org/10.1093/bioinformatics/btv638

Xiong, B., Loss, R.D., Shields, D., Pawlik, T., Hochreiter, R., Zydney, A.L., Kumar, M., 2018. Polyacrylamide degradation and its implications in environmental systems. npj Clean Water 1. https://doi.org/10.1038/s41545-018-0016-8

Yu, X., 2019. Improving cap water quality in an oil sands end pit lake with microbial applications. University of Alberta.

Zander, A., Bersier, L.F., Gray, S.M., 2017. Effects of temperature variability on community structure in a natural microbial food web. Glob. Chang. Biol. 23, 56–67. https://doi.org/10.1111/gcb.13374

Zhang, X., Niu, J., Liang, Y., Liu, X., Yin, H., 2016. Metagenome-scale analysis yields insights into the structure and function of microbial communities in a copper bioleaching heap. BMC Genet. 17, 1–12. https://doi.org/10.1186/s12863-016-0330-4

Zhao, T., Chen, P., Zhang, Lijie, Zhang, Lei, Gao, Y., Ai, S., Liu, H., Liu, X., 2021. Heterotrophic nitrification and aerobic denitrification by a novel Acinetobacter sp. TAC-1 at low temperature and high ammonia nitrogen. Bioresour. Technol. 339, 125620. https://doi.org/10.1016/j.biortech.2021.125620

Zhu, Y.G., Zhao, Y., Zhu, D., Gillings, M., Penuelas, J., Ok, Y.S., Capon, A., Banwart, S., 2019.

Soil biota, antimicrobial resistance and planetary health. Environ. Int. 131, 105059. https://doi.org/10.1016/j.envint.2019.105059

APPENDIX

Table A1: Average of microbial abundance for sulfur biogeochemical cycling over the experimental period

	Capping water				
Treatment			**Control**		
Taxa	Abundance	Percentage	Taxa	Abundance	Percentage
Sulfuritalea	367409	89.51	*Sulfuritalea*	340942	82.35
Ferritrophicum	30723	7.48	*Chlorobium*	28639	6.92
Immundisolibacter	3536	0.86	*Immundisolibacter*	17342	4.19
Pseudomonas	3203	0.78	*Desulfurivibrio*	6298	1.52
uncultured	1320	0.32	*Pseudomonas*	3379	0.82
Not_Assigned	1200	0.29	*Pseudoxanthobacter*	2839	0.69
Geobacter	751	0.18	*Geobacter*	2660	0.64
Thiobacillus	572	0.14	*uncultured*	2222	0.54
Pseudoxanthobacter	490	0.12	*Acinetobacter*	1585	0.38
Sulfuricurvum	486	0.12	*Not_Assigned*	1543	0.37
Desulfuromonas	309	0.08	*Syntrophus*	1320	0.32
Desulfatirhabdium	167	0.04	*Desulfovirga*	1233	0.3
Acinetobacter	156	0.04	*Desulfovibrio*	941	0.23
Desulfovirga	92	0.02	*Desulfatiglans*	859	0.21
Syntrophus	63	0.02	*Desulfobacca*	740	0.18
			Desulfatirhabdium	674	0.16
			Desulfomonile	452	0.11
			Sulfuricurvum	213	0.05
			Desulfuromonas	150	0.04
	Tailings				
Treatment			**Control**		
Taxa	Abundance	Percentage	Taxa	Abundance	Percentage

uncultured	78996	18.61	*Chlorobium*	138420	22.72
Desulfatiglans	64664	15.24	*Desulfatiglans*	112373	18.44
Sulfuritalea	53264	12.55	*uncultured*	85372	14.01
Not_Assigned	29347	6.92	*Sulfuritalea*	47846	7.85
Syntrophus	29074	6.85	*Desulfurivibrio*	41693	6.84
Desulfurivibrio	25640	6.04	*Syntrophus*	34332	5.63
Thiobacillus	17179	4.05	*Not_Assigned*	27917	4.58
Geothermobacter	16205	3.82	*Thiobacillus*	16433	2.7
Pseudomonas	15925	3.75	*Pseudomonas*	14270	2.34
Ferritrophicum	14479	3.41	*Geothermobacter*	13833	2.27
Sulfuricurvum	10834	2.55	*LCP_80*	12545	2.06
Desulfuromonas	8281	1.95	*Immundisolibacter*	8637	1.42
Desulfuromonadaceae	7145	1.68	*Desulfuromonas*	6527	1.07
Immundisolibacter	6588	1.55	*Desulfatirhabdium*	5885	0.97
LCP_80	5801	1.37	*Desulfuromonadaceae*	5628	0.92
Sulfurimonas	5617	1.32	*Desulfobacca*	5179	0.85
Desulfatirhabdium	5063	1.19	*Sulfuricurvum*	4197	0.69
Geobacter	5059	1.19	*Sulfurimonas*	4064	0.67
Sulfuricella	4468	1.05	*Desulfobacteraceae*	4026	0.66
Acinetobacter	3571	0.84	*Acinetobacter*	3445	0.57
Desulfobacteriumcatecholicumgroup	3069	0.72	*Desulfovirga*	3324	0.55
Desulfobacca	2756	0.65	*Geobacter*	3105	0.51
Desulfobacteraceae	2449	0.58	*Desulfobacteriumcatecholicumgroup*	2275	0.37
IncertaeSedis	2269	0.53	*IncertaeSedis*	1478	0.24
Desulfobulbus	890	0.21	*CandidatusDeferrimonas*	917	0.15
Desulfomicrobium	863	0.2	*Smithella*	848	0.14
Desulfovirga	677	0.16	*SEEP_SRB1*	766	0.13
SEEP_SRB1	670	0.16	*Syntrophorhabdus*	603	0.1
CandidatusDeferrimonas	668	0.16	*Desulfomicrobium*	482	0.08
Desulfovibrio	622	0.15	*KCM_B_112*	352	0.06

Caldimicrobium	544	0.13	*Desulfobulbus*	292	0.05
KCM_B_112	504	0.12	*Desulfopila*	253	0.04
Sva1033	372	0.09	*Sva1033*	250	0.04
Desulfopila	285	0.07	*Syntrophobacter*	250	0.04
Dethiosulfatibacter	148	0.03	*Desulfovibrio*	232	0.04
Geobacteraceae	126	0.03	*Geobacteraceae*	213	0.03
Desulfitibacter	121	0.03	*Dethiobacter*	207	0.03
Smithella	116	0.03	*Caldimicrobium*	206	0.03
Desulfobacula	25	0.01	*Sulfuricella*	197	0.03
			Desulfurispora	145	0.02
			Desulfatitalea	134	0.02
			Cavicella	112	0.02
			Desulfitibacter	39	0.01

Table A2: Average of microbial abundance for carbon biogeochemical cycling over the experimental period

Capping water					
Treatment			**Control**		
Taxa	Abundance	Percentage	Taxa	Abundance	Percentage
Brevundimonas	46104	24.8	Xanthobacter	97599	36
Xanthobacter	45227	24.33	Brevundimonas	73350	27.06
Sphingobium	24942	13.42	Methyloversatilis	31486	11.61
CyanobiumPCC_6307	24840	13.36	Sphingobium	24633	9.09
Magnetospirillum	11458	6.16	CyanobiumPCC_6307	13102	4.83
Methylovulum	8194	4.41	Methylovulum	7977	2.94
Oceanibaculum	7428	4	Oceanibaculum	6005	2.22
Methyloversatilis	5262	2.83	Magnetospirillum	4738	1.75
Methylobacterium_Methylorubrum	3299	1.77	Pseudomonas	3345	1.23
Pseudomonas	2809	1.51	Pseudoxanthobacter	2839	1.05
Methylotenera	2464	1.33	Novosphingobium	1456	0.54
Novosphingobium	2163	1.16	Acinetobacter	1382	0.51
uncultured	487	0.26	Desulfovirga	1292	0.48
Syntrophus	329	0.18	Syntrophus	1200	0.44
Not_Assigned	305	0.16	Methylobacterium_Methylorubrum	326	0.12
Pseudoxanthobacter	205	0.11	Ancylobacter	258	0.1
Ancylobacter	204	0.11	Methylobacillus	112	0.04
Acinetobacter	156	0.08			

Tailings					
Treatment			**Control**		
Taxa	Abundance	Percentage	Taxa	Abundance	Percentage
Syntrophus	28593	34.12	*Syntrophus*	34279	40.24
Pseudomonas	16059	19.16	*Pseudomonas*	14896	17.48
Magnetospirillum	14993	17.89	*Methyloversatilis*	9801	11.5

Not_Assigned	4042	4.82	*Not_Assigned*	3823	4.49
Acinetobacter	3852	4.6	*Acinetobacter*	3445	4.04
uncultured	3533	4.22	*Desulfovirga*	3238	3.8
Methyloversatilis	3117	3.72	*Methylotenera*	2627	3.08
Methylotenera	2954	3.52	*uncultured*	2508	2.94
CyanobiumPCC_6307	1961	2.34	*Methylovulum*	2167	2.54
Methylobacter	1133	1.35	*Magnetospirillum*	2000	2.35
Desulfovirga	832	0.99	*Methanolobus*	1337	1.57
Brevundimonas	680	0.81	*Smithella*	848	1
Novosphingobium	621	0.74	*Novosphingobium*	692	0.81
Sphingobium	335	0.4	*CyanobiumPCC_6307*	679	0.8
Oceanibaculum	327	0.39	*Brevundimonas*	669	0.79
Methanolobus	173	0.21	*Sphingobium*	455	0.53
Xanthobacter	158	0.19	*Xanthobacter*	447	0.52
Methyloparacoccus	153	0.18	*Methylophilaceae*	302	0.35
Clostridiumsensustricto13	106	0.13	*Syntrophorhabdus*	291	0.34
Pseudothermotoga	98	0.12	*Syntrophobacter*	250	0.29
Methylovulum	90	0.11	*Cavicella*	181	0.21
			Sh765B_TzT_35	146	0.17
			Clostridiumsensustricto13	113	0.13

Table A3: Average of microbial abundance for iron biogeochemical cycling over the experimental period

Capping water					
Treatment			**Control**		
Taxa	Abundance	Percentage	Taxa	Abundance	Percentage
Ferritrophicum	30723	43.93	*Sediminibacterium*	21032	42.31
Magnetospirillum	11458	16.38	*Acidovorax*	5017	10.09
Sediminibacterium	9023	12.9	*Magnetospirillum*	4738	9.53
Acidovorax	7951	11.37	*Ferrovibrio*	4097	8.24
Pseudomonas	2752	3.93	*Pseudomonas*	3401	6.84
Rhodoferax	2285	3.27	*Pseudoxanthobacter*	3400	6.84
Hydrogenophaga	2073	2.96	*Geobacter*	2597	5.22
Ferrovibrio	1511	2.16	*Hydrogenophaga*	2397	4.82
uncultured	1113	1.59	*Acinetobacter*	1585	3.19
Pseudoxanthobacter	490	0.7	*Sideroxydans*	598	1.2
Geobacter	213	0.3	*Aquabacterium*	582	1.17
Thiobacillus	192	0.27	*Rhodoferax*	268	0.54
Acinetobacter	156	0.22			

Tailings					
Treatment			**Control**		
Taxa	Abundance	Percentage	Taxa	Abundance	Percentage
Thiobacillus	17360	14.61	*Thiobacillus*	16872	21.28
Geothermobacter	16205	13.63	*Pseudomonas*	14726	18.57
Pseudomonas	15925	13.4	*Geothermobacter*	13833	17.45
Ferritrophicum	14479	12.18	*Rhodoferax*	7075	8.92
Magnetospirillum	9918	8.34	*Acidovorax*	5671	7.15
Rhodoferax	9713	8.17	*Acinetobacter*	3445	4.35
Acidovorax	8083	6.8	*Geobacter*	2977	3.75
Hydrogenophaga	5097	4.29	*Hydrogenophaga*	2975	3.75

Geobacter	4916	4.14	*uncultured*	2939	3.71
Not_Assigned	4815	4.05	*Not_Assigned*	2076	2.62
Acinetobacter	3571	3	*Deferrisoma*	2009	2.53
uncultured	2611	2.2	*Magnetospirillum*	2000	2.52
Sideroxydans	2203	1.85	*CandidatusDeferrimonas*	704	0.89
Deferrisoma	1808	1.52	*Hydrogenophilus*	555	0.7
CandidatusDeferrimonas	668	0.56	*Sideroxydans*	398	0.5
Hydrogenophilus	495	0.42	*KCM_B_112*	352	0.44
KCM_B_112	360	0.3	*Hydrogenobacter*	222	0.28
Geobacteraceae	229	0.19	*Dethiobacter*	207	0.26
Hydrogenobacter	169	0.14	*Cavicella*	112	0.14
Clostridiumsensustricto13	106	0.09	*CandidatusNitrotoga*	93	0.12
Aquabacterium	65	0.05	*Geobacteraceae*	45	0.06
CandidatusNitrotoga	60	0.05			

Table A4: Average of microbial abundance for nitrogen biogeochemical cycling over the experimental period

Capping water					
Treatment			**Control**		
Taxa	Abundance	Percentage	Taxa	Abundance	Percentage
CyanobiumPCC_6307	24840	48.96	*CyanobiumPCC_6307*	12722	26.78
Magnetospirillum	11458	22.59	*Magnetospirillum*	5779	12.16
Not_Assigned	4204	8.29	*Obscuribacteraceae*	5513	11.6
Pseudomonas	3072	6.06	*Azospirillum*	4812	10.13
Azospirillum	2126	4.19	*Vampirovibrionales*	3614	7.61
Novispirillum	1699	3.35	*Pseudoxanthobacter*	3400	7.16
Obscuribacteraceae	1146	2.26	*Pseudomonas*	3387	7.13
Niveispirillum	669	1.32	*Niveispirillum*	2738	5.76
Vampirovibrionales	480	0.95	*Not_Assigned*	1773	3.73
Pseudoxanthobacter	415	0.82	*Acinetobacter*	1382	2.91
DSSD61	270	0.53	*DSSD61*	1257	2.65
uncultured	196	0.39	*Novispirillum*	469	0.99
Acinetobacter	156	0.31	*Bradyrhizobium*	382	0.8
			CandidatusOmnitrophus	168	0.35
			Methylobacillus	112	0.24

Tailings					
Treatment			**Control**		
Taxa	Abundance	Percentage	Taxa	Abundance	Percentage
Thauera	19313	21.06	*uncultured*	19686	24.8
uncultured	18274	19.93	*Thauera*	17937	22.59
Thiobacillus	17360	18.93	*Thiobacillus*	16872	21.25
Pseudomonas	15925	17.37	*Pseudomonas*	15136	19.06
Magnetospirillum	9126	9.95	*Acinetobacter*	3445	4.34
Acinetobacter	3571	3.89	*Magnetospirillum*	2000	2.52

Rhizobium	2013	2.2	*Rhizobium*	963	1.21
Not_Assigned	1996	2.18	*CyanobiumPCC_6307*	801	1.01
CyanobiumPCC_6307	1658	1.81	*CandidatusOmnitrophus*	761	0.96
Ellin6067	976	1.06	*GOUTA6*	755	0.95
GOUTA6	824	0.9	*Ellin6067*	402	0.51
Aquaspirillumarcticumgroup	326	0.36	*Not_Assigned*	381	0.48
4_29_1	160	0.17	*Cavicella*	112	0.14
Clostridiumsensustricto13	106	0.12	*CandidatusNitrotoga*	93	0.12
CandidatusNitrotoga	60	0.07	*Nitrosomonas*	50	0.06

Table A5: Concentrations of elements in capping water and tailings

	Capping water (mg/L)		Tailings (mg/Kg)	
Elements	Treatment	Control	Treatment	Control
Al	0.002	0.001	118.8	85.17
B	2.253	2.341	0.177	0.166
Ca	31.34	27.8	4.176	4.5
Cu	0.415	0.249	0.198	1.524
Fe	0.006	0.001	32.18	34.06
K	11.95	11.57	16.19	13.72
Mg	12.79	11.8	6.747	6.438
Mo	0.055	0.062	0.503	0.541
Mn	0.049	0.06	0.003	0.003
Na	511.5	535.9	4.331	4.985
Ni	0.044	0.024	0.327	0.483
P	0.032	0.027	0.345	0.361
S	103.5	112.5	12.82	14.08
Zn	0.988	0.321	0.68	1.561
Total C	153.7	141.7	7.81	7.90

Table A6: CheckM2 bin quality report

Bins	Completeness	Contamination	N50	Genome size	GC content
bin_1	88.52	1.02	21361	6259106	0.57
bin_10	96.63	3.67	21625	3800770	0.55
bin_100	76.24	2.06	18304	1691150	0.41
bin_101	99.91	1.17	20930	3162328	0.6
bin_102	99.84	1.64	34326	7190928	0.59
bin_103	78.75	8.92	6834	2804357	0.53
bin_104	98.38	2.1	23067	2782183	0.65
bin_105	83.02	3.15	3162	2875134	0.4
bin_106	81.56	0.87	28222	3038824	0.64
bin_107	74.94	1.25	3666	2714037	0.71
bin_108	78.98	1.2	10376	1471807	0.65
bin_109	84.25	2.12	4034	3935458	0.43
bin_11	95.64	6.74	21400	3796874	0.62
bin_110	96.55	7.92	36719	735050	0.31
bin_111	79.09	9.1	4879	2127888	0.54
bin_112	74.29	2.19	2124	1885738	0.42
bin_113	81.5	9.49	3933	5549853	0.66
bin_12	99.93	2.27	50571	3499225	0.61
bin_13	91.25	9.11	3285	3480638	0.7
bin_14	84.21	1.86	5057	2261608	0.44
bin_15	88.49	3.83	19852	2691227	0.67
bin_16	68.35	0.44	59154	1224046	0.43
bin_17	96.59	3.37	9840	4321095	0.54
bin_18	88.75	7.98	20112	3660598	0.65
bin_19	91.25	1.66	3355	2891962	0.46
bin_2	91.77	10.22	8264	1982275	0.36
bin_20	97.4	1.26	22066	1079734	0.36
bin_21	79.48	2.61	4405	2972776	0.63
bin_22	97.61	6.6	17096	2666554	0.55
bin_23	96.72	1.32	21076	4787596	0.62
bin_24	97.92	0.03	132899	3687821	0.4
bin_25	92.26	5.12	8968	3300008	0.64
bin_26	100	4.27	292227	3128948	0.55
bin_27	92.77	4.87	12815	5758229	0.68
bin_28	83.36	7.26	8360	3253928	0.64
bin_29	95.8	1.67	8622	3957255	0.42
bin_3	91.94	7.23	31738	3546103	0.42
bin_30	80.82	2.8	5016	2320211	0.6
bin_31	86.75	0.03	173009	598672	0.34
bin_32	72	5.73	3682	2978954	0.6
bin_33	99.9	0.06	45572	6162505	0.61
bin_34	94.54	0.91	57367	3759179	0.5
bin_35	78.66	4.73	6919	3072796	0.68

bin_36	79.55	1.4	10814	1298958	0.34
bin_37	71.42	4.84	5170	4007034	0.7
bin_38	94.26	11.91	11751	3022727	0.69
bin_39	87.51	4.61	8866	5468431	0.69
bin_4	92.19	0.07	142537	916798	0.41
bin_40	74.8	4.77	6363	3541549	0.64
bin_41	84.3	0.92	7260	3687183	0.5
bin_42	100	1.04	28274	2374873	0.42
bin_43	97.01	0.46	43828	5916574	0.6
bin_44	98.26	4.54	14550	3204399	0.67
bin_45	98.74	3.54	16247	1241803	0.4
bin_46	70.08	9.02	4001	2790951	0.36
bin_47	86.62	1.14	416241	769474	0.32
bin_48	88.31	1.69	12509	5926142	0.6
bin_49	99.21	0.97	95227	1124301	0.43
bin_5	95	0	64520	1324419	0.39
bin_50	99.32	0.39	98621	2068656	0.32
bin_51	100	1.17	23637	7949933	0.65
bin_52	99.97	0.19	153508	2500532	0.55
bin_53	86.54	4.98	5387	4859748	0.61
bin_54	88.78	4.14	4379	1601199	0.54
bin_55	87.37	1.87	7217	2258114	0.39
bin_56	85.09	2.08	3750	1333349	0.44
bin_57	99.96	2.8	73233	2852136	0.54
bin_58	76.14	6.6	5582	2738999	0.64
bin_59	77.33	4.22	4001	3696302	0.65
bin_6	100	3.62	20574	4406543	0.65
bin_60	100	0.88	129893	4566015	0.64
bin_61	99.95	1.1	16930	4235876	0.66
bin_62	98.52	6.48	38378	763352	0.34
bin_63	83.46	2.98	3679	1757232	0.43
bin_64	75.18	7.15	4931	2484360	0.64
bin_65	100	7.03	10270	3081351	0.64
bin_66	100	4.4	105124	3596690	0.51
bin_67	94.58	4.42	244221	1892709	0.6
bin_68	99.94	1.07	38899	7118858	0.58
bin_69	89.41	3.49	7032	2664394	0.65
bin_7	96.11	5.24	14296	3429466	0.39
bin_70	85.68	5.12	5859	4339163	0.69
bin_71	92.01	3.34	6570	2316257	0.67
bin_72	99.97	3.93	15820	5645079	0.65
bin_73	96.36	1.34	47849	2541116	0.62
bin_74	60.86	1.48	10205	4049740	0.59
bin_75	98.82	7.8	45864	5633528	0.67
bin_76	88.77	0.17	54606	1435254	0.48
bin_77	98.98	0.29	70179	718724	0.34

bin_78	89.54	5.51	20184	5172080	0.67
bin_79	93.11	5.32	24690	3804089	0.41
bin_8	97.98	5.03	181184	6273195	0.47
bin_80	89.51	9.09	8434	2497332	0.45
bin_81	85.48	4.31	28812	1620737	0.63
bin_82	99.7	1.12	47735	3098365	0.62
bin_83	100	5.07	26804	3459433	0.67
bin_84	90.16	6.95	5763	3845102	0.65
bin_85	86.47	3.13	4765	2219724	0.67
bin_86	99.98	0.62	911438	2607029	0.56
bin_87	97.86	0.15	373043	998445	0.45
bin_88	100	5.12	27233	1100176	0.42
bin_89	90.87	13.11	11102	4586924	0.63
bin_9	93.45	2.4	9393	1804414	0.54
bin_90	90.07	2.09	24848	2628723	0.57
bin_91	99.67	1.05	40406	2454411	0.65
bin_92	83.11	5.98	12710	2982878	0.67
bin_93	79.41	1.5	9826	2370078	0.57
bin_94	97.52	2.68	25212	2987972	0.68
bin_95	84.38	1.68	4530	2225503	0.6
bin_96	92.06	0.61	68483	6716421	0.63
bin_97	93.15	3.57	8053	3647332	0.67
bin_98	98.18	5.93	7561	2814012	0.41
bin_99	97.78	0.06	58742	957850	0.37

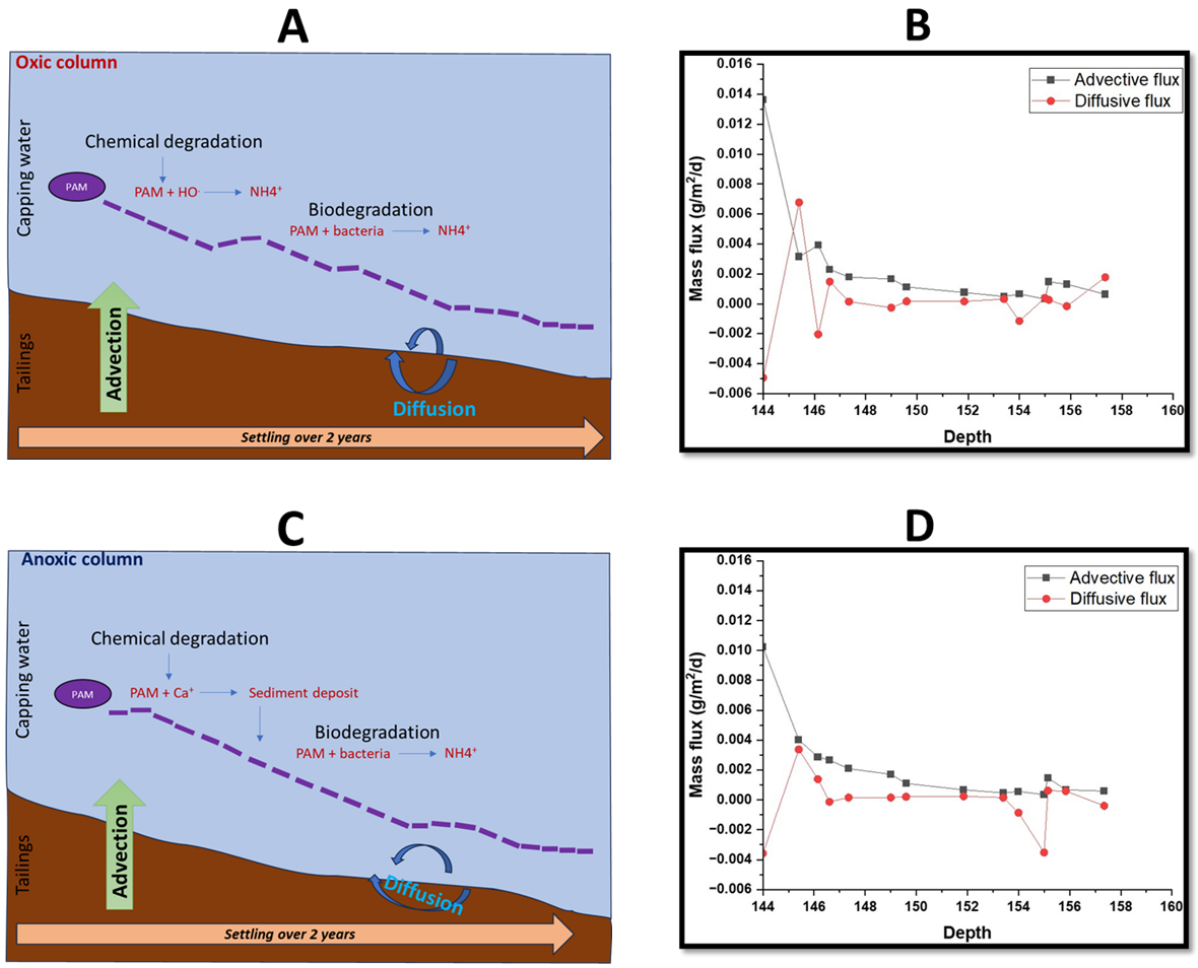

Figure A1: (A) Fate of PAM in Oxic columns (B) Mass flux of PAM in Oxic columns (C) Fate of PAM in Anoxic columns (D) Mass flux of PAM in Anoxic columns. PAM = polyacrylamide

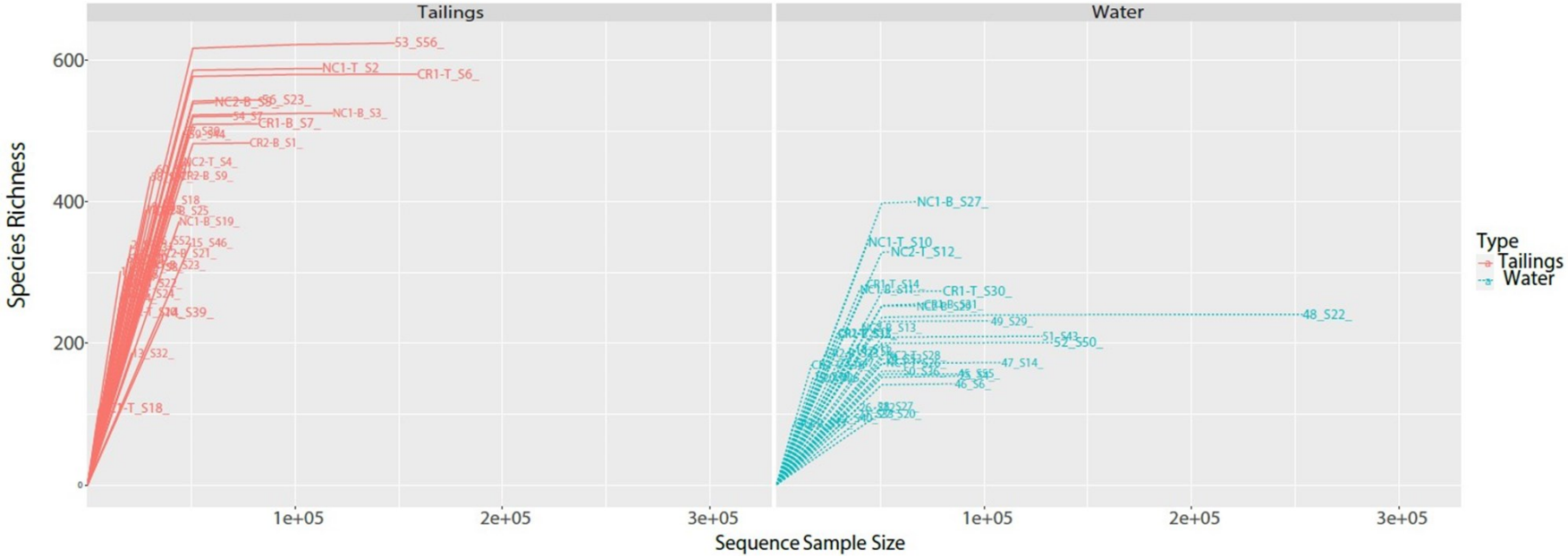

Figure A2: Rarefraction curve comparing species richness in tailings against capping water

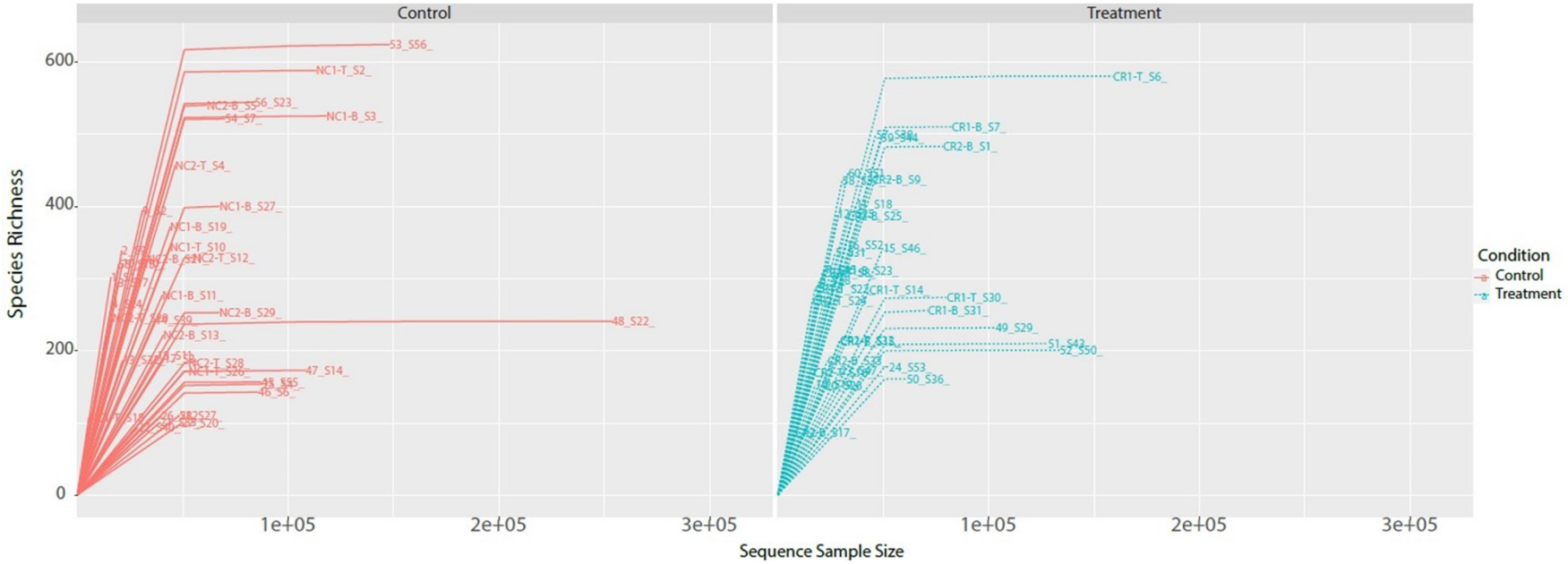

Figure A3: Rarefraction curve comparing species richness in control columns against treatment columns

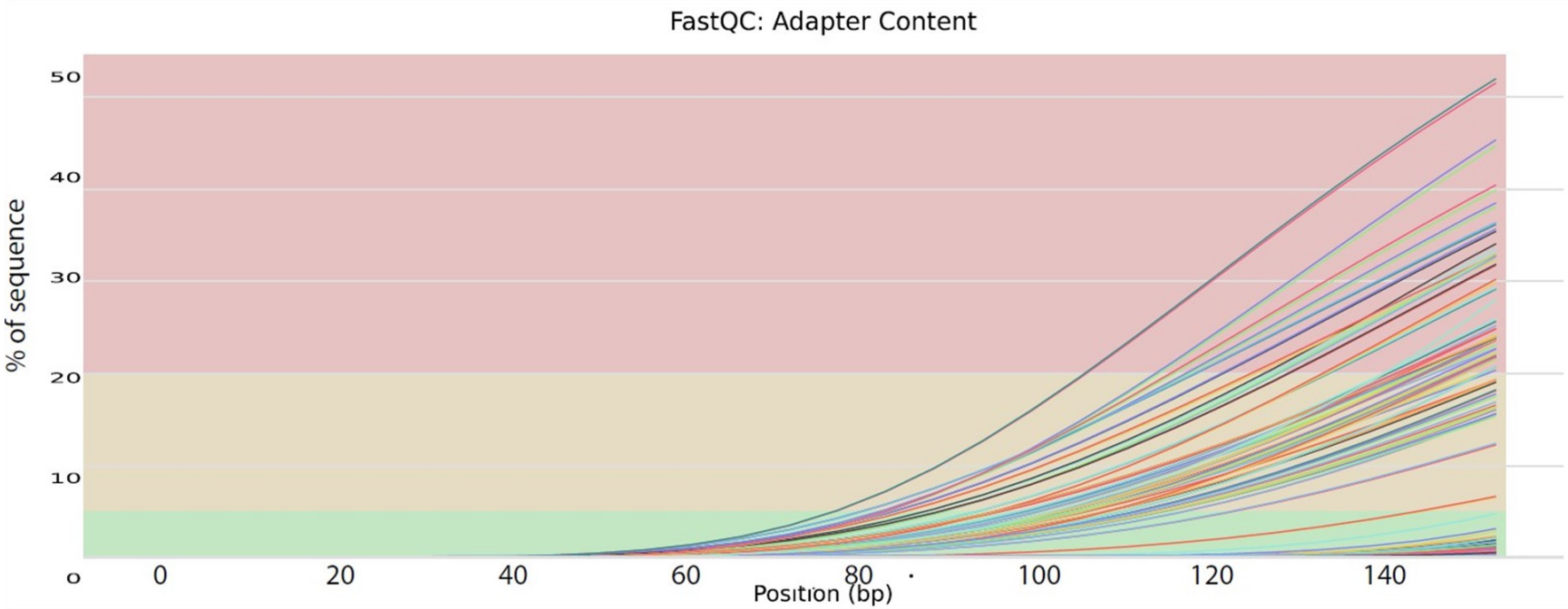

Figure A4: FastQC plot showing adapter content before trimming with Trimmomatic and fastp

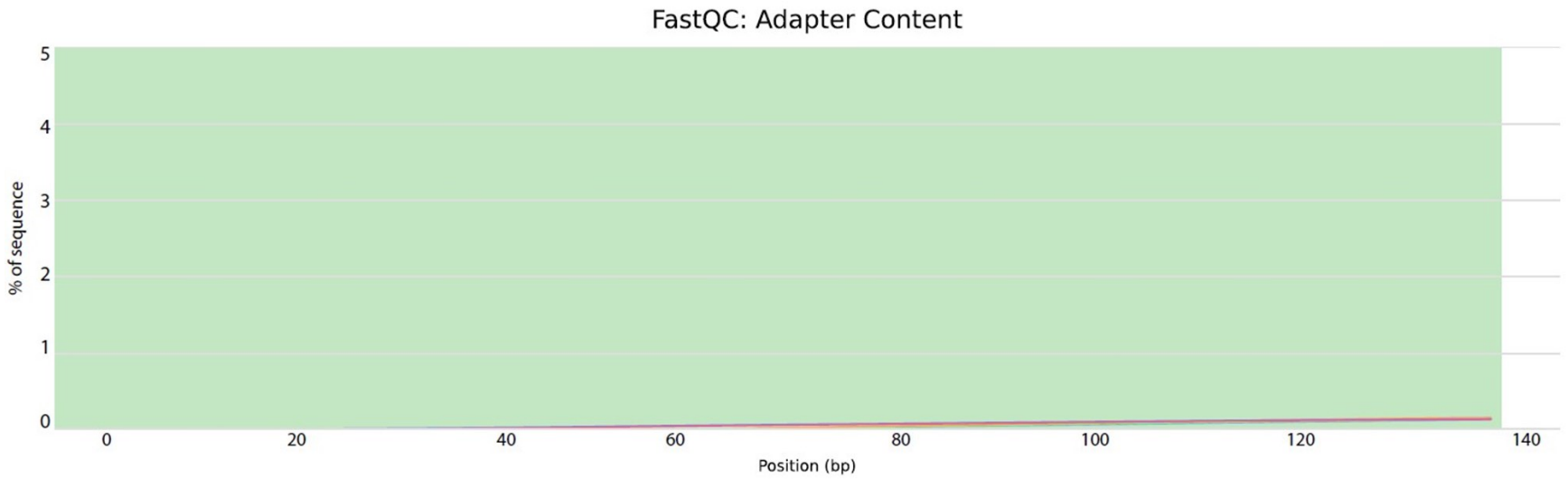

Figure A5: FastQC plot showing adapter content after trimming with Trimmomatic and fastp